TNF reverse signalling in the developing peripheral nervous system

A thesis submitted to Cardiff University for the degree of PhD in Integrative Neuroscience

2015

Clara Erice Jurecky

Cardiff School of Biosciences
Cardiff University

“Mientras el cerebro sea un misterio, el universo continuará siendo un misterio.”

Santiago Ramón y Cajal

Dedicado a mis padres,

Jane y Ricardo.

ACKNOWLEDGEMENTS

I would first like to thank Prof. Alun Davies for allowing me to carry out the research I wanted and giving me the opportunity to do so, when all the odds seemed against such a prospect. In addition, I would like to thank him for his mentorship and guidance throughout my PhD. A special thank you to Dr. Sean Wyatt for his scientific guidance and feedback and to Dr. Laura Howard for helping me with my introduction.

A very big thank you goes out to Dr. Lilian Kisiswa and Dr. Catarina Osório who had a great impact on my research. This project would not have been possible without Lilian, to her I owe my initial training and all her input to my project. I thank Catarina for giving me the chance to discuss my ideas about science during her stay at the lab and her friendship which was critical during my “second year blues”.

A very warm and special thank you goes to Chris Laurie who not only provided me with invaluable help in the lab but with his “light hearted” grumpiness made this whole process enjoyable and got me through late nights of writing in the office and stopped me from having various breakdowns.

Thank you to Dr. Pedro Chacon who was always willing to lend me a hand and advice, as well as to all past and present members of the Davies and Wyatt lab.

To my family away from home, Virginie, Amie, Baker and Laura, there is no thank you that will do for all your love and support and all our in-promptu dinner parties at 74 Mackintosh Place, a period of my life I will always cherish. To all my friends in Cardiff, Ewa, Jakub, Mike, Lisa, Rebecca and Marianna, you have given me 4 years full of memories: the pub, dancing and trips, but most of all, your company.

The biggest thank you in the world to my dearest Jimena, Leonor and Konstantinos, for not letting me forget and reminding me every day of my love for science. It has been the greatest of pleasures to see you grow into incredible scientists and I am extremely lucky to have been able to learn so much from you, and for creating a life-long friendship. This thesis would not have been possible without your encouragement and belief in my capabilities and our exchange of daily messages of our adventures and misfortunes. I look forward to co-owning our bakery/bar/jazz/science café.

Most importantly, I would like to remember my beautiful family. My parents who always taught me never to give up and pursue my dreams, I thank you for your constant support, understanding and unconditional love. To my sisters Teresa and Ana, thank you for being the best role models I could have ever asked for, I will always look up to you.

ABSTRACT

Tumour necrosis factor (TNF) is an extensively well characterised proinflammatory cytokine. It is expressed as a type two membrane glycoprotein that is active both as a membrane-integrated ligand and as a soluble ligand following proteolytic release of the ectodomain from the cell membrane. TNF signals via two receptors, TNFR1 and TNFR2. In the immune system, it has been shown that these receptors can function as ligands for membrane-integrated TNF and initiate TNF reverse signalling. I was a member of a team that discovered, characterised and evaluated the physiological significance of TNF reverse signalling in the nervous system. We showed that TNFR1 is expressed in tissues innervated by sympathetic neurons and that this initiates TNF reverse signalling in postnatal sympathetic axons, which in turn enhances their growth and branching locally. Using a tissue whole mount method to visualize sympathetic fibres, I found that the innervation of multiple tissues that receive their innervation exclusively or predominantly from the paravertebral sympathetic chain is defective both in mice lacking TNF and mice lacking TNFR1. Sympathetic fibres reach these tissues in these mice but fail to grow and branch extensively in these tissues. In contrast, tissues that receive their sympathetic innervation predominantly from prevertebral ganglia are either unaffected, in mice lacking TNF and TNFR1, or hyperinnervated. Using live calcium imaging, pharmacological blockers of calcium channels and shRNA gene knockdown, I obtained evidence that T-type calcium channels are required for the effects of TNF reverse signalling on axon growth. I also showed that TNF reverse signalling enhances the growth of sensory axons, during an earlier stage in development than sympathetic neurons. This work establishes that TNF reverse signalling is widely involved in regulating axon growth in the developing peripheral nervous system.

ABBREVIATIONS

Ab- antibody

Akt/PKB- Ak transforming/protein kinase B

AP-1- activator protein 1

APRIL- a proliferation-inducing ligand

ATP- adenosine triphosphate

BABB- 1 part benzyl alcohol: 2 parts benzyl benzoate

BAD- Bcl2-associated agonist of cell death

BAFF– B-cell-activator factor

BAFFR– BAFF receptor

BAK- Bcl2-antagonist/killer

BAX- Bcl2-Associated X Protein

Bcl-2- B-cell lymphoma-2

BCMA- B-cell maturation antigen

BDNF- brain-derived neurotrophic factor

BID- BH3-interacting domain death agonist

BIM- Bcl-2-interacting mediator of cell death

BMP- bone morphogenetic protein

BOK- Bcl2-related ovarian killer

bp– base pair

BSA- bovine serum albumin

°C- degree Celcius

Ca^{2+}- calcium

$CaCl_2$- calcium chloride

CAMs- cell-adhesion molecules

CaSR- calcium-sensing receptor

Cav3.1- gene encoding t-type calcium channel CACNA1G

Cav3.2- gene encoding t-type calcium channel CACNA1H

Cav3.3- gene encoding t-type calcium channel CACNA1I

CD30- cluster of differentiation 30

CD40- cluster of differentiation 40

cDNA- complementary DNA

CG- celiac ganglion

Ch- chicken

CKI- casein kinase I

cm- centimetre

CNS- central nervous system

CNTF- ciliary neurotrophic factor

CO_2- carbon dioxide

CRD- cysteine-rich domain

Ct value– cycle threshold value

CT-1- cardiotrophin-1

DBH- dopamine β-hydroxylase

DcR- decoy receptor

DD- death domain

DMEM– Dulbecco's modified Eagle's medium

DMSO- dimethyl sulfoxide

DNA- deoxyribonucleic acid

dNTPs- deoxynucleotide triphosphates

DR– death receptor

DRG- dorsal root ganglion

E- embryonic day

EDAR- ectodysplasin A receptor

EMT- epithelial to mesenchymal transition

End3- endothelin-3

ERK- Ras/extracellular signal regulated kinase

FADD- FAS-associated death domain

FasL– Fas ligand

FoxD3- forkhead box D3

FRET- fluorescence resonance energy transfer

FRS2- fibroblast receptor substrate-2

Fwd– forward

g– gram

GAPDH- glyceraldehyde 3-phosphate dehydrogenase

GC base pairing– Guanine and Cytosine base pairing

GDNF- glial cell-derived neurotrophic factor

GFP- green fluorescent protein

GITR- glucocorticoid-induced tumour necrosis factor-related protein

GITRL- glucocorticoid-induced tumour necrosis factor-related protein ligand

Gt- Goat

GTP- guanosine triphosphate

h- hour

H_2O_2- hydrogen peroxide

HBSS- Hanks balanced salt solution

HCl– hydrochloric acid

Het- heterozygous

HFc- human Fc fragment

HGF- hepatocyte growth factor

HRP- horse radish peroxidase

HPRT1- hypoxanthine phosphoribosyltransferase 1

HSD- honest significant difference

HVA- high-voltage activated calcium channel

IgM- immunoglobulin M

IL-6- interleukin-6

IMG- inferior mesenteric ganglion

IML- intermediolateral column

JNK- Jun N-terminal kinase

K^+- potassium

KCl- potassium chloride

kDa- kilodalton

KO- knock out

LB- Luria Bertani

LIF- leukaemia inhibitory factor

LIGHT- lymphotoxin-related inducible ligand that competes for glycoprotein D binding to herpesvirus entry mediator on T cells

LPS- lipopolysaccharide

LT-α- lymphotoxin-alpha

LVA- low-voltage activated calcium channel

M- molar

MAPK- mitogen activated protein kinase

MASH1- mammalian achaete scute homolog-1

MEK- mitogen-activated kinase/extracellular signal-regulated kinase kinase

MeOH- methanol

mg– milligram

Mg^{2+}- magnesium

$MgCl_2$- magnesium chloride

min- minute

ml- millilitre

mm– millimetre

mM- millimolar

MMP-7- metalloproteinase-7

MOMP- mitochondrial outer membrane permeabilization

mRNA- messenger RNA

MSP- macrophage-stimulating protein

mTNF- membrane-integrated TNF

Na^+- sodium

NaCl- sodium chloride

NaOH- sodium hydroxide

NC- neural crest

NF-κB– nuclear factor- κB

ng- nanogram

NGF- nerve growth factor

NK- natural killer cells

nM- nanomolar

NRIF- neurotrophin receptor-interacting factor

NS- not significant

NT- nasal turbinate

NT-3- neurotrophin-3

NT-4/5- neurotrophin-4/5

OCT- optimal cutting temperature

OPG - osteoprotegerin

OSM- oncostatin-M

P- postnatal day

p- p-value

p75^{NTR}- p75 neurotrophin receptor

PBS- phosphate saline buffer

PCD- programmed cell death

PCR- polymerase chain reaction

PDGF- platelet-derived growth factor

PFA- paraformaldehyde

PG- pineal gland

Phox2a- paired-like homeobox protein 2a

PI3K- phosphoinositide 3-kinase

PKC- protein Kinase C

PLAD– pre-ligand assembly domain

PLC-γ- phospholipase C-gamma

PNS- peripheral nervous system

qPCR- quantitative real-time PCR

RANKL- receptor-activator of NF-κB ligand

Ras– rat sarcoma

Rb- Rabbit

Rev– reverse

RhoA– Ras homolog gene family, member A

RING- really interesting new gene

RIP– receptor-interacting protein

RNA- ribonucleic acid

rpm– rotations per minute

RT- room temperature

RT-qPCR- reverse transcription-quantitative PCR

s- second

s.e.m.- standard error mean

SCG- superior cervical ganglion

SDHA- succinate dehydrogenase complex

Sema3A– Semaphorin- 3A

SG- stellate ganglion

Shc- Src homology 2 domain containing

shRNA- short hairpin RNA

SMG- submandibular salivary gland

SMG- superior mesenteric ganglion

SOX10- sex determining region Y-box

SPPL2b- signal peptide peptidase-like 2B

sTNF- soluble TNF

Ta– annealing temperature

TACE- TNF converting enzyme

TACI– transmembrane activator and cyclophilin ligand interactor

TD- TRAF domain

TGF-β- transforming growth factor-β

TH- tyrosine hydroxylase

THD- TNF homology domain

TIM- TRAF-interacting motif

Tm– melting temperature

TNF- tumour necrosis factor-α

Tnfα- gene encoding TNF

TNFR- TNF receptor

TNFR1-Fc- TNFR1-Fc chimera

TNFR2-Fc- TNFR2-Fc chimera

TNFSF- tumour necrosis factor superfamily

TNRSF- tumour necrosis receptor superfamily

Tnfrsf1a- gene encoding TNFR1

Tnfrsf1b- gene encoding TNFR2

TRADD- TNFR-associated death domain

TRAF- TNF-receptor associated factor

TRAIL- TNF-related apoptosis-inducing ligand

TrK- tropomyosin receptor kinase

TWEAK– TNF-like weak inducer of apoptosis

V- volts

-ve- negative

VEGF– vascular endothelial growth factor

VEGI– vascular endothelial cell growth inhibitor

Wnt- Wingless

WT- wild type

XEDAR- X-linked EDA receptor

µg- microgram

µl- microlitre

µm- micrometre

µM- micromolar

LIST OF FIGURES

Chapter 1

Chapter 2

Chapter 3

Chapter 4

Chapter 5

Chapter 6

Chapter 7

LIST OF TABLES

Chapter 2

Chapter 5

TABLE OF CONTENTS

Preface

Chapter 1: General Introduction

Chapter 2: Materials and Methods

Chapter 3: TNF mediated reverse signalling in developing sympathetic neurons *in vitro*

Chapter 1
General Introduction

The development of any organ is a fascinating process involving the integration of multiple signals which are recycled at many levels and interpreted depending on the context they are found in. Development of the nervous system, in addition, requires both the guidance of extending axons to their target fields, often over long distances, and the correct regulation of innervation density once these axons reach their specific targets. This is a precise and refined process, and depends upon a series of tightly regulated and evolutionarily conserved mechanisms which ultimately result in the formation of a functional nervous system supporting cognitive, sensory and motor function.

My main research interests include the concept of signal recycling: how one single protein can facilitate multiple outcomes and have particular roles depending on its cellular and environmental setting. As well as how neurons with extending axons make their correct connections with their target fields during development. This thesis uses the mouse peripheral nervous system (PNS) as a model to study the involvement of tumour necrosis factor-α (TNF)-mediated reverse signalling during target field innervation, exemplifying and expanding on the mechanism of signal recycling during development.

In this section, I will give an overview of PNS structure and development followed by a description of autonomic development concentrating in particular on sympathetic neuronal survival and outgrowth. I will focus on the superior cervical ganglion (SCG), one of the three cervical paravertebral ganglia found in vertebrates. The SCG contains the cell bodies of those neurons that provide sympathetic innervation to rostral targets in the head and neck, and are an accessible, well-studied and experimentally tractable

neuronal population, and are used as model ganglia in this study. Lastly the tumour necrosis factor superfamily (TNFSF) will be reviewed focusing specifically on TNF and its receptors.

1.1 Organisation and early development of the peripheral nervous system

The nervous system is comprised of the central nervous system (CNS) and the peripheral nervous system (PNS). The CNS consists of the brain and spinal cord and the PNS of the somatic and autonomic nervous systems (Fig.1). The PNS essentially serves as a relay system of information between the CNS and the body's extremities, the limbs and organs, allowing integration, processing and coordination of sensory information and motor commands (Kandel et al., 2000).

The CNS and PNS are anatomically separate systems with distinct functions. However, there is extensive crosstalk between them as they act in conjunction to maintain cognitive, sensory and motor functions. In addition, they share basic cellular and developmental processes which include cell identity specification, neuronal migration and outgrowth and synaptogenesis (Gilbert, 2006). Special attention will be given to sympathetic neuronal survival and outgrowth in the following sections in order to put into context the results presented in this thesis.

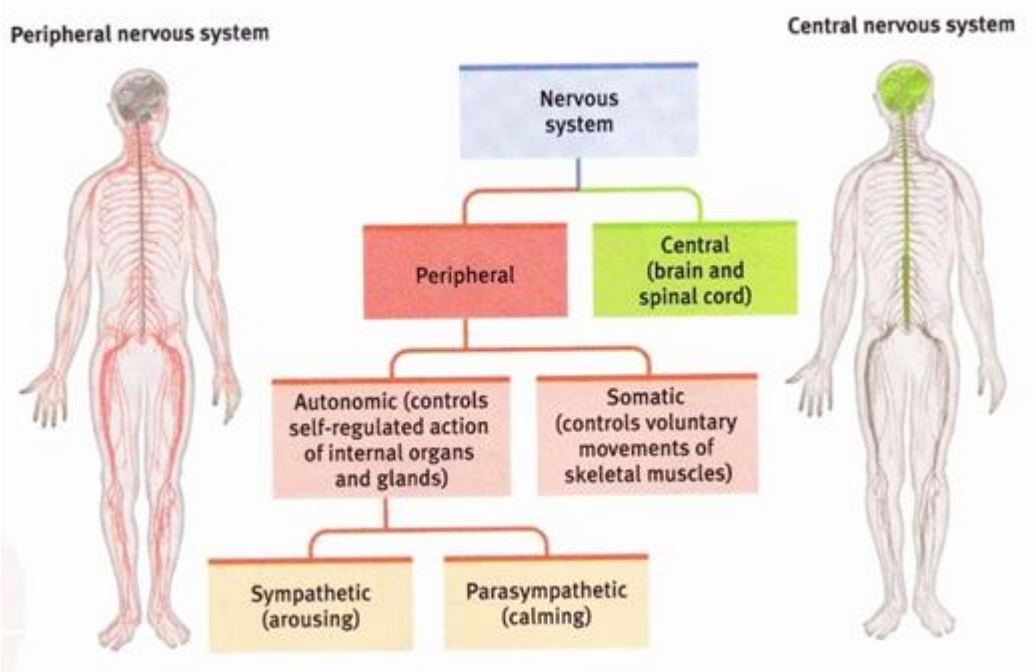

Figure 1: Organisation of the nervous system. The nervous system is divided into the CNS and PNS. The CNS is composed of the brain and spinal cord (green), The PNS is composed of and sub-divided into the somatic and autonomic system (red). From (Myers, 2013).

1.1.1 Overview of PNS organisation and early development

The somatic system is responsible for the voluntary movement of our bodies in response to changes in our environment. It is divided into the cranial and spinal nerves which are comprised of afferent (travelling into the CNS) sensory and efferent (travelling away from the CNS) motor neurons (Kandel et al., 2000).

The autonomic system, in contrast, is involved in controlling the involuntary movements of an organism and hence maintaining its internal homeostasis. Therefore, the autonomic system regulates many physiological processes of the deep organs, controlling; circulation, respiration, body temperature, sweating, digestion and metabolism (Rohrer, 2011). It is made up of the sympathetic, parasympathetic and enteric nervous systems. The sympathetic and parasympathetic systems are both anatomically and functionally distinct, although they generally innervate the same

organs, functioning in a “pull-push” relationship. For example, sympathetic neurons stimulate the heart while parasympathetic neurons decrease heart rate (Zigmond, 1999, Purves, 2008). The enteric nervous system’s main function is to govern the function of the gastrointestinal tract and, although it receives input from the parasympathetic and sensory nervous system, it predominantly operates autonomously (Zigmond, 1999, Purves, 2008).

All neurons and glial cells of the PNS, except for some neurons of certain cranial nerve sensory ganglia that are derived from neurogenic placodes, originate from neural crest (NC) cells, a population of transient cells with both migratory and pluripotent capabilities (Dupin et al., 2006). Germ layers are the building blocks of any organism, as they are the initial embryonic layers from which tissues and organs originate. Hence, the neural crest has been referred to as ‘the 4th germ layer’ as it gives rise to multiple cell types and in turn these migrate very long distances in the developing embryo (Hall, 2000). Furthermore, it is thought that the appearance of the NC allowed the evolution of the vertebrate organism and its diversification (Gans and Northcutt, 1983, Simoes-Costa and Bronner, 2015).

The NC forms dorsal to the neural tube in the developing vertebrate embryo. This occurs after the fusion of the neural folds and subsequent detachment from the ectoderm (Fig.2). During neural tube closure the presumptive NC starts to express genes characteristic of the NC lineage such as *FoxD3* and *SOX10* (Southard-Smith et al., 1998, Dottori et al., 2001). After complete neural tube closure these cells are ready to exit the CNS, and do this via an epithelial to mesenchymal transition (EMT), becoming the multipotent progenitor migratory NC cells (Simoes-Costa and Bronner, 2015).

The NC is a transient structure of highly invasive cells that give rise to a wide variety of cell types. In addition to the cells of the PNS, NC cells contribute to melanocytes, facial cartilage, bone and connective tissue (Douarin and Kalcheim, 1999). The fate of NC cells is greatly dependent on the migratory pathway they undertake through the developing embryo (Dupin et al., 2006). Although a transient structure, NC cells can be classified into four sub-divisions which are defined by the function and type of cell they will become: cranial neural crest, trunk neural crest, vagal and sacral crest and the cardiac neural crest (Gilbert, 2006).

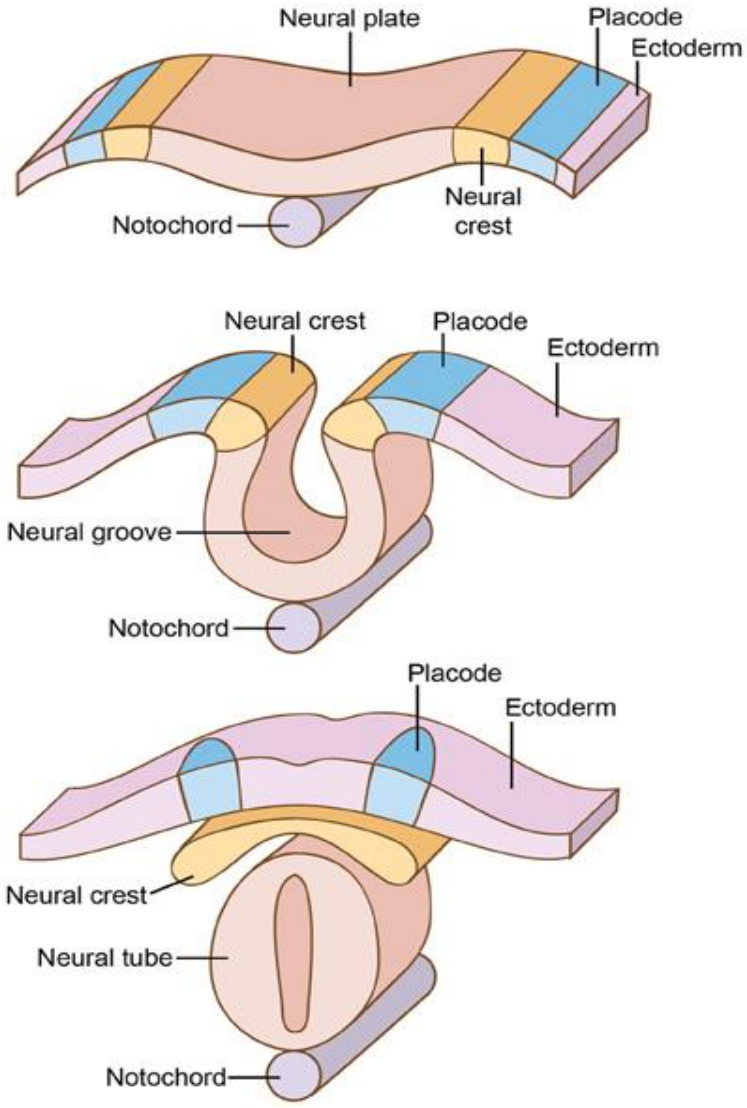

Figure 2: The neural crest and neurogenic placodes. Formation of the neural crest and neurogenic placodes arising from the fusion of the neural folds/neural plate. These structures will give rise to neurons and glial cells of the PNS. From (Feinberg and Mallatt, 2013).

1.1.2 Early development of the sympathetic nervous system

The sympathetic system arises from the sub-division of the NC termed the trunk neural crest. These cells have two migratory pathways which will largely define their fate. Those that start their migration early on will take a ventral route in relation to the neural tube and will eventually form the sensory dorsal root ganglia (DRG), sympathetic ganglia, adrenomedullary cells, and Schwann cells. NC cells that will form the sensory neurons of the DRG, arrest their migration earlier on and remain near the paraxial mesoderm,

which will form the somites and eventually dermomyotome, thus following a more ventrolateral route. On the other hand, those cells that continue their ventral migration beyond the dermomyotome, will become sympathetic ganglia, the adrenal medulla and nerve clusters surrounding the aorta (Gilbert, 2006). The second flow of migratory cells will take a dorsolateral pathway into the epidermis and give rise to melanocytes (Gilbert, 2006). Enteric ganglia arise from migrating NC cells from the trunk, vagal and sacral divisions (Gilbert, 2006), (Fig.3).

Specifically, those NC cells which will form the sympathetic nervous system travel to the mesenchyme lateral to the dorsal aorta (Britsch et al., 1998, Simoes-Costa and Bronner, 2015). Neuregulin-1 is one of the proposed factors that aid in this ventral migration (Britsch et al., 1998). A variety of bone morphogenetic proteins (BMPs) (BMP 2/4/7), which belong to the transforming growth factor-β (TGF-β) family of proteins, are in charge of instructing these NC cells to differentiate into sympathetic neurons (Reissmann et al., 1996, Shah et al., 1996). These cells can be identified by the expression of specific transcription factors such as *MASH1* and *Phox2a* (Guillemot and Joyner, 1993). In turn, these sympathetic-defined cells start to produce enzymes necessary for the biosynthesis of catecholamines, such as tyrosine hydroxylase (TH) and dopamine β-hydroxylase (DBH) (Ernsberger et al., 1995, Groves et al., 1995, Tiveron et al., 1996).

Postganglionic sympathetic neurons originate as a column of sympathetic ganglion primordia located near the dorsal aorta. Once these neuroblasts undergo specification and start to acquire noradrenergic characteristics, they conjoin to form the final sympathetic ganglia (Glebova and Ginty, 2005). Sema3A is thought to be involved in regulating arrest and aggregation of these cells in their specific sites (Kawasaki et al.,

2002). Some neuroblasts will migrate rostrally to form the SCG and others ventrally to establish the prevertebral ganglia, while those that remain in the column will become the sympathetic chain. Cells of the sympathetic ganglia start to elaborate axons and dendrites once proliferation and differentiation are complete (Glebova and Ginty, 2005).

Ultimately, the proliferation, migration and differentiation of NC cells into sympathetic ganglia requires the coordinated action of a number of specific proteins, transcription factors and the regulation of cell type-specific genes. Some of these are illustrated in Fig. 4, but this list is by no-means exhaustive.

The development of postganglionic sympathetic neurons and peripheral sensory neurons has been extensively studied due to their accessibility and well defined target fields, making them a good model for addressing questions on initial axonal growth and final target field innervation. Therefore, my research focuses on neurons within the developing sympathetic system, and in particular those of the SCG (Davies and Lumsden, 1990, Glebova and Ginty, 2005).

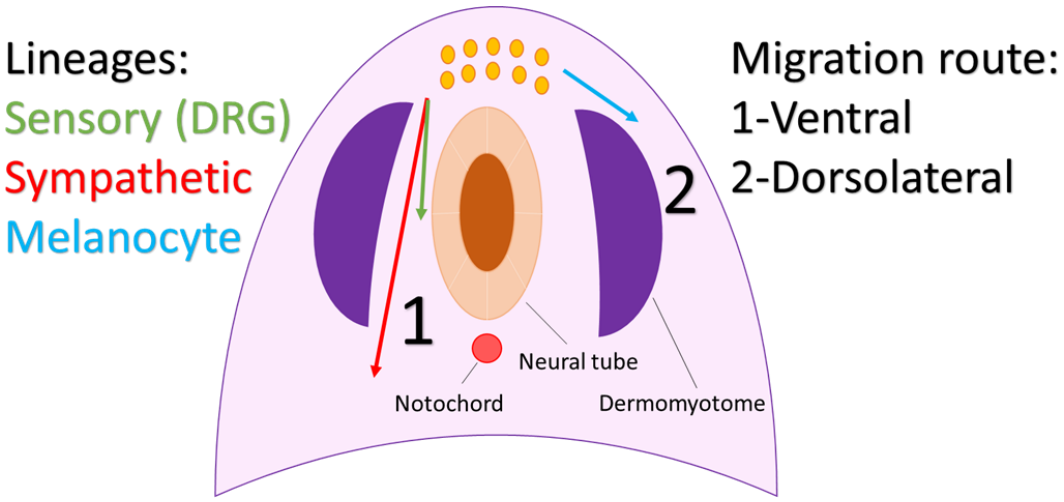

Figure 3: Trunk neural crest cell migration routes. NC cells migrating ventrally (1) will form the DRG, sympathetic ganglia and adrenal medulla. Those destined to become DRG cells take a more ventrolateral route (green arrow), while those that migrate further down the ventral path (red arrow) will form autonomic ganglia, including the sympathetic ganglia, and the adrenal medulla. An alternative dorsolateral migration route (2) into the ectoderm, will give rise to melanocytes (blue arrow). Original figure based on (Marmigere and Ernfors, 2007).

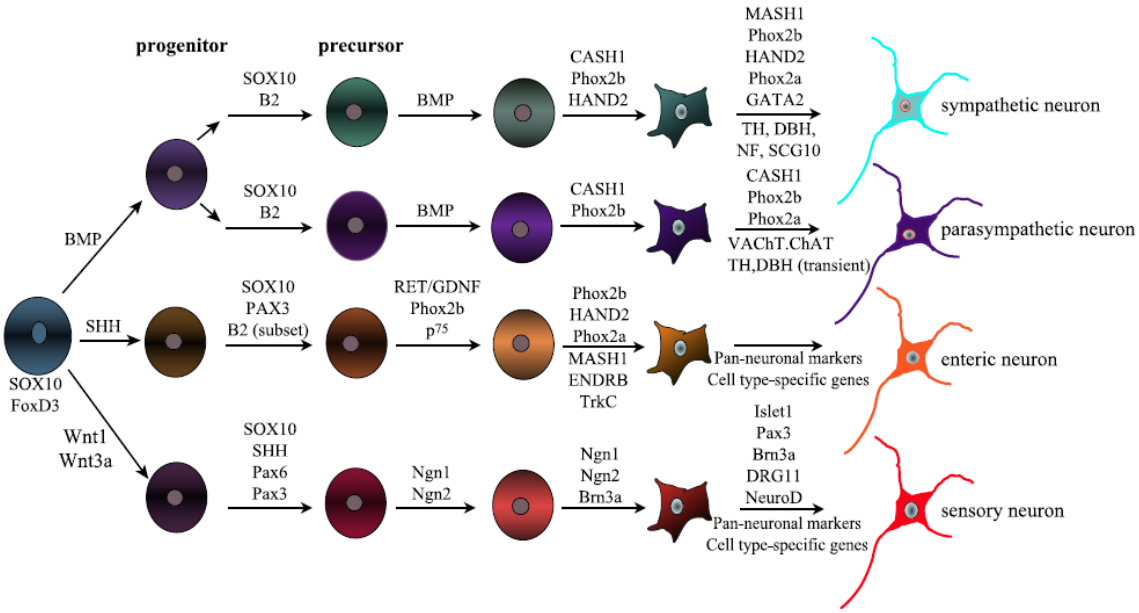

Figure 4: Neural crest differentiation. Schematic showing the key events in the development of autonomic, enteric and sensory neurons from neural crest cells. NC cells at the dorsal neural tube are identified by FoxD3 and SOX10. BMPs are involved in instructing NC cells towards an autonomic fate. MASH1 and Phox2a are markers for noradrenergic sympathetic neurons. From (Howard, 2005).

1.1.3 Organisation of the sympathetic nervous system

The sympathetic nervous system consists of paired ganglia that run from the skull to the coccyx and are sub-divided into: paravertebral ganglia that form the sympathetic trunk, and prevertebral ganglia, which are concerned with innervation of abdominopelvic viscera. Paravertebral ganglia include the cervical ganglia; the SCG, the middle cervical ganglion (sometimes absent) and the stellate ganglion (SG), and the sympathetic chain; which includes ganglia along spinal cord segments T1-L2. The prevertebral ganglia are constituted by the celiac ganglion (CG), the superior mesenteric ganglion (SMG), and the inferior mesenteric ganglion (IMG). Preganglionic neurons reside in the lateral grey horn of the spinal cord, in the intermediolateral column at the thoracic and upper lumbar levels (T1-L2); hence, the sympathetic system has a thoracolumbar organisation. The fibres of these preganglionic neurons will exit through the respective anterior nerve root and then branch off as white rami (myelinated) and invade the sympathetic chain;

postganglionic fibres will then exit through adjacent nerve roots as grey rami (unmyelinated) and form connections with target organs (Shields, 1993, Glebova and Ginty, 2005, FitzGerald et al., 2012), exemplified in a simplified schematic in Fig.5.

Preganglionic neuron fibres entering the sympathetic chain and making connections with its ganglia will synapse onto the closest ganglion from segments T1-L2. Postganglionic neurons of the sympathetic chain will innervate blood vessels, sweat glands and erector pili muscles in the vicinity of T1-L2 (FitzGerald et al., 2012). In other instances fibres will travel upwards through the chain synapsing on the SCG, middle cervical ganglion or the stellate ganglion. These ganglia extend axons to innervate the head, neck, upper limbs and heart. Alternatively, preganglionic fibres entering the sympathetic chain will descend and form connections with lumbar or sacral ganglia which in turn will send out processes to innervate blood vessels and skin of the lower limbs. Lastly, some preganglionic fibres will travel along the chain and exit it as splanchnic nerves which reach the abdomen and connect with the prevertebral ganglia; the celiac and superior mesenteric ganglia. Alternatively the nerves enter the pelvis in order to synapse with the IMG. The first two ganglia provide innervation to the gastrointestinal tract, liver, pancreas, and kidneys whilst the IMG ganglion send out postganglionic axons to the genitourinary tract (Glebova and Ginty, 2004, FitzGerald et al., 2012). Fig.6 shows a diagram of the mouse sympathetic ganglia.

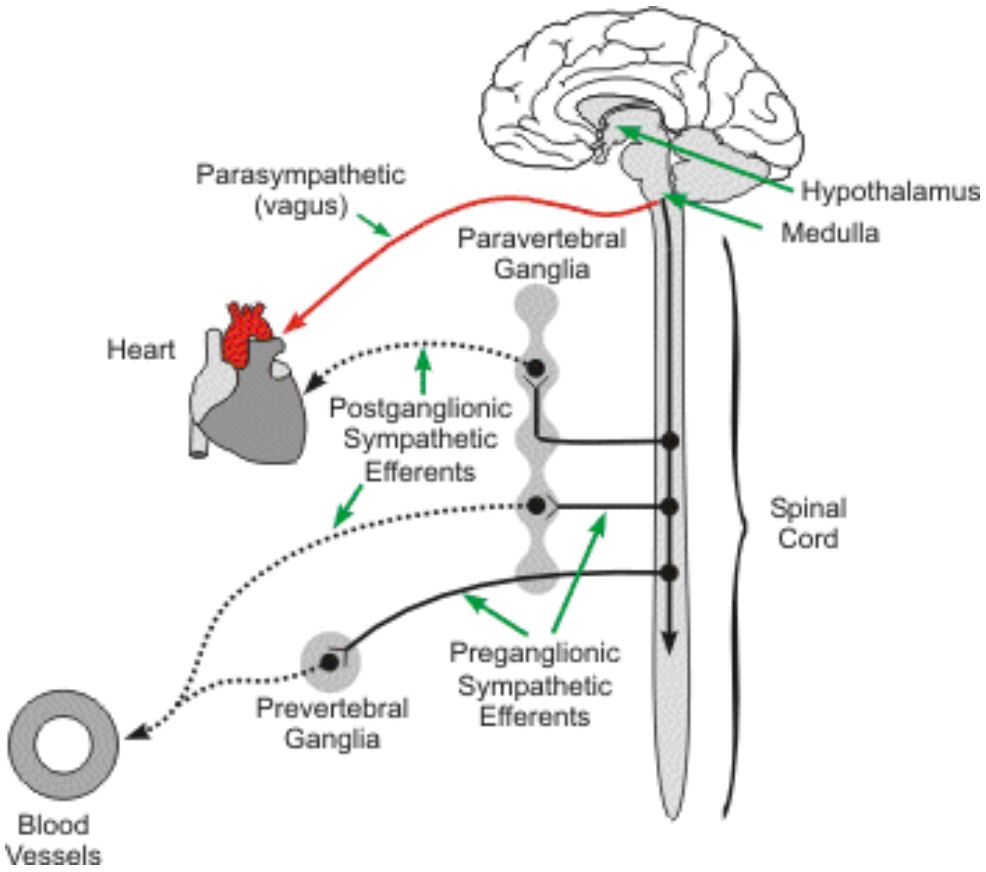

Figure 5: Sympathetic nervous system. Simplified schematic of the sympathetic system. Preganglionic fibres, solid line, synapse on paravertebral ganglia or exit the sympathetic trunk to form connections with prevertebral ganglia. Postganglionic fibres, dashed line, innervate target fields. From (Klabunde, 2005).

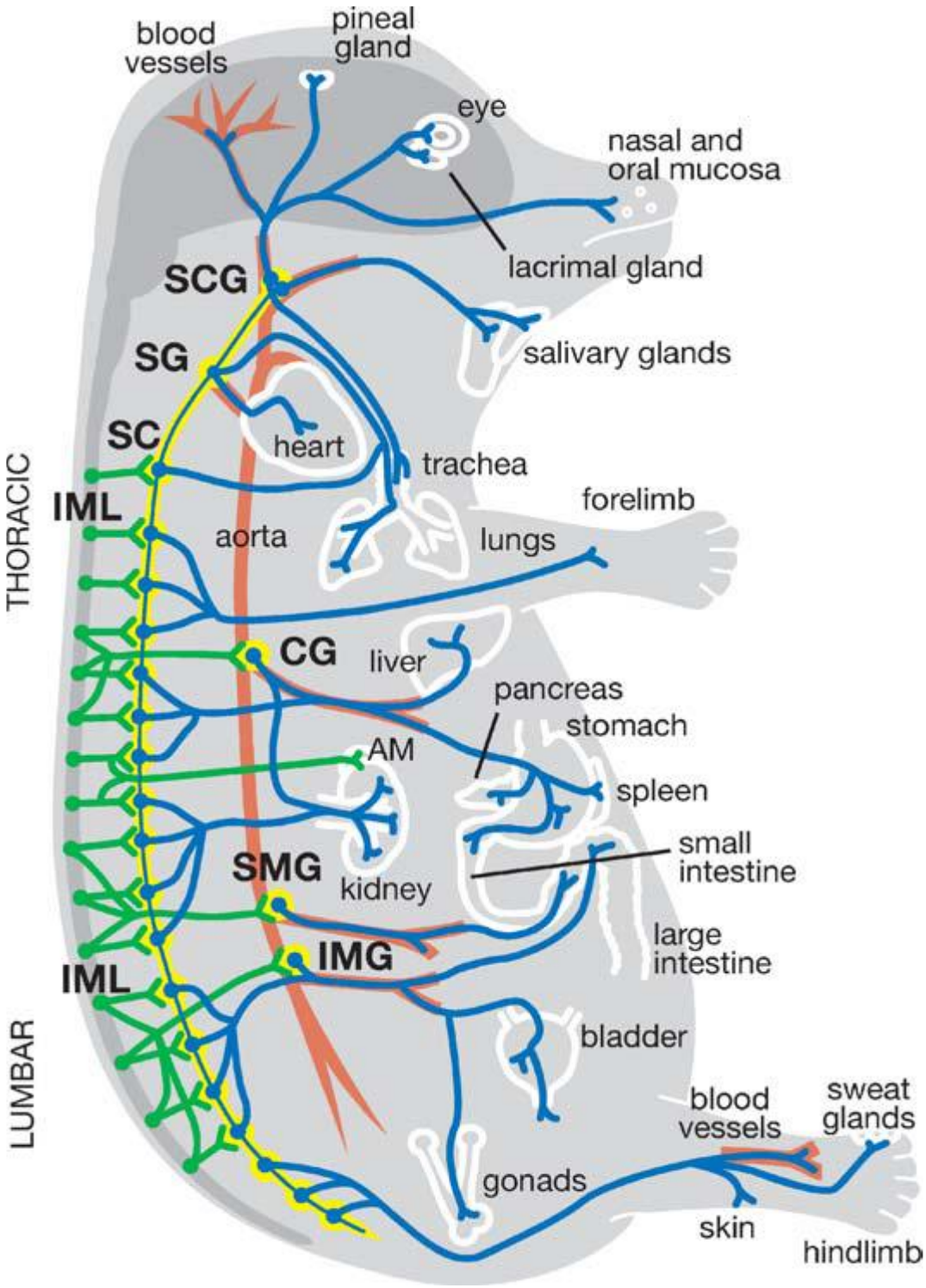

Figure 6: Mouse sympathetic nervous system. Diagram of the mouse sympathetic system. Preganglionic neurons (green) residing in the intermediolateral column (IML) make connections with paravertebral and prevertebral ganglia (yellow). Postganglionic fibres (blue) synapse with target fields (white). From (Glebova and Ginty, 2005).

1.2 Neuronal survival and the neurotrophic hypothesis

During development neurons are generated in excess, and those that are not required are eliminated in a phase of cell death that occurs shortly after they begin to innervate their target organs (Oppenheim, 1991, Davies, 2003). This mechanism is thought to have evolved to ensure that neurons with inappropriate synaptic connections are removed and that only those which exactly match the innervation requirements of the specific targets survive (Marmigere and Ernfors, 2007, Davies, 2009). This occurs via a process known as programmed cell death (PCD), or apoptosis, and it is not restricted to developing neurons. Apoptosis is an essential physiological mechanism of multicellular organisms with key roles in development, morphogenesis, controlling cell number and removal of mutated and damaged cells (Vaux and Korsmeyer, 1999). Hence, all cell types share basic apoptotic programmes (Yuan and Yankner, 2000).

Apoptosis is mediated by a family of cysteine proteases, known as caspases, and it mainly follows two pathways, either the intrinsic (mitochondrial) pathway or the extrinsic (death receptor) pathway (Fig.7). The intrinsic pathway is tightly regulated by members of the B-cell lymphoma-2 (Bcl-2) protein family. In contrast, the extrinsic pathway is Bcl-2-independent and is induced by the activation of death receptors (reviewed in (Elmore, 2007)).

Bcl-2 members can be classified into three sub-groups; pro-apoptotic (BAX, BAK, BOK), anti-apoptotic (Bcl-2, Bcl-X_L, Bcl-W) and those that regulate anti-apoptotic members in order to increase apoptosis (BAD, BIK, BIM and NOXA) (reviewed in (Czabotar et al., 2014)). Pro-apoptotic members will initialise mitochondrial outer membrane

permeabilization (MOMP), which results in the release of proteins from the mitochondrial intermediate space (such as cytochrome C), which in turn activate the caspase cascade, resulting in PCD. Anti-apoptotic members bind to pro-apoptotic Bcl-2 members to prevent MOMP (Tait and Green, 2010).

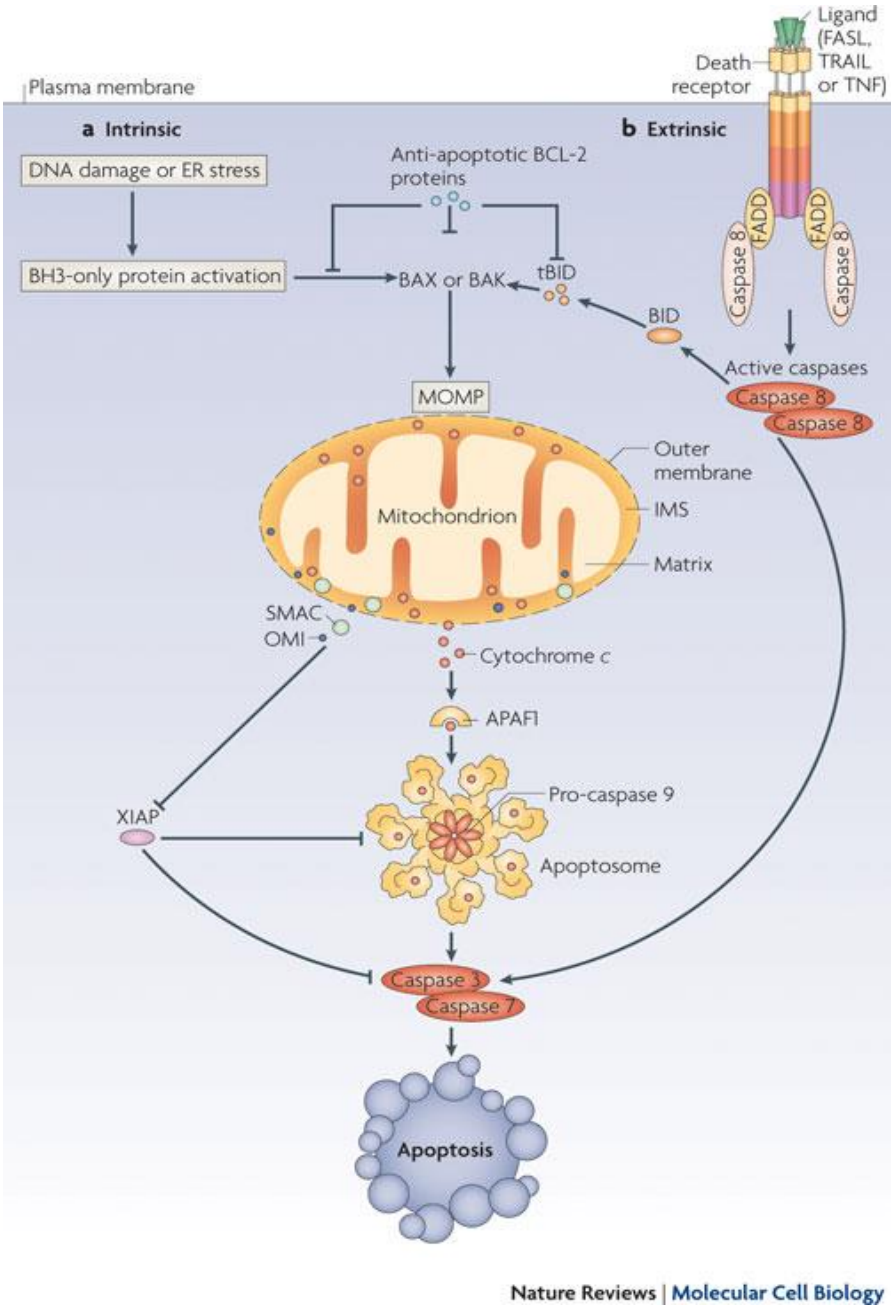

Figure 7: Programmed cell death. A) Intrinsic apoptotic pathway. Pro-apoptotic Bcl-2 proteins such as BAX or BAK can initiate MOMP which results in the release of proteins such as cytochrome C which trigger the initiation of the caspase cascade. **B)** Extrinsic apoptotic pathway. Activation of death receptors triggers the caspase cascade. From (Tait and Green, 2010).

1.2.1 The neurotrophic hypothesis

The balance between cell survival and death to ensure correct PNS development is largely orchestrated by a family of functionally and structurally closely related secreted proteins, the neurotrophins, which belong to a larger group of neurotrophic factors that promote neuronal survival, target field innervation and function (Davies, 1996, Davies, 2003, Davies, 2009).

Nerve growth factor (NGF), the founding member of the family, is the best characterized neurotrophin. Classic experiments by Viktor Hamburger, Rita Levi-Montalcini and Stanley Cohen leading to the discovery of NGF, and the subsequent demonstration that NGF promotes the survival of developing sympathetic and some sensory neurons *in vitro*, together with the observation that target tissue ablation results in neuronal death, helped formulate the neurotrophic hypothesis (Levi-Montalcini and Angeletti, 1968, Thoenen and Barde, 1980, Hamburger and Yip, 1984, Levi-Montalcini, 1987, Purves et al., 1988). The neurotrophic hypothesis postulates that target fields produce limiting amounts of neurotrophic factors which function as survival signals. Consequently, only the neurons that reach target fields first and obtain sufficient amounts of neurotrophic factors will survive (Levi-Montalcini, 1987, Davies, 2003). The neurotrophic hypothesis has been further supported by *in vivo* studies showing that the addition of anti-NGF antibodies during the period of target field innervation eliminates population of neurons which are dependent on NGF for survival, while the addition of exogenous NGF results in the rescue of neurons that would normally die during target field innervation due to a lack of trophic support. Moreover, sensory and sympathetic ganglia of mice that have a null mutation in either the NGF gene or the NGF receptor, tropomyosin receptor kinase (TrkA) gene, contain dramatically reduced numbers of neurons compared to wild type

mice (Levi-Montalcini and Angeletti, 1968, Johnson et al., 1980, Hamburger and Yip, 1984, Crowley et al., 1994, Smeyne et al., 1994, Davies, 1996, Davies, 2003).

During the late 1980's and early 1990's, the other neurotrophin family members; brain derived neurotrophic factor (BDNF), neurotrophin-3 (NT-3) and neurotrophin-4/5 (NT-4/5) were identified and characterised (Barde et al., 1982, Huang and Reichardt, 2001). Subsequent studies on these proteins helped refine the neurotrophic hypothesis, as well as elucidate that it was more complex than initially thought. For example, one single neurotrophic factor does not support the survival of a specific population of neurons; rather, different neurotrophic factors are able to cooperate and regulate the survival of certain neuronal populations (Davies, 1994b, Davies, 1997, Forgie et al., 2003). PNS populations are able to survive independently of trophic support at different stages of development, and this period usually correlates with the distance their axons need to travel to reach target fields (Davies, 1989, Vogel and Davies, 1991). On the other hand, some peripheral neurons are dependent on neurotrophic factors before they start to innervate their target fields (Francis and Landis, 1999, Davies, 2009). In addition, neurotrophic factors are not only secreted from target organs, but can be secreted by the intermediate environment, such as the vasculature, in a paracrine manner and even by neurons themselves, thus exerting an autocrine effect (Fig.8) (Skaper, 2012). Furthermore, neurotrophins not only promote neuronal survival, but also regulate neuroblast proliferation, neuronal differentiation, axonal guidance and growth and synaptic plasticity (Bibel and Barde, 2000, Davies, 2000, Thoenen, 2000, Glebova and Ginty, 2005, Davies, 2009, Cunha et al., 2010). Together, this highlights the concept of signal recycling, depending on the spatio-temporal context in which a neurotrophin is

found, it can have different effects on neuronal physiology as well as regulation of survival.

Besides neurotrophins, several members of other protein families have been shown to be implicated in promoting the survival of particular neuronal populations at different developmental ages as well as regulating differentiation, growth, maturation and function. These include: glial cell-derived neurotrophic factor (GDNF), neurturin and artemin from the GDNF family; ciliary neurotrophic factor (CNTF), leukaemia inhibitory factor (LIF), oncostatin-M (OSM), cardiotrophin-1 (CT-1) and interleukin-6 (IL-6) from the neurotrophic cytokine family; and the related proteins hepatocyte growth factor (HGF) and macrophage-stimulating protein (MSP) (Davies, 1994a, Lewin and Barde, 1996, Maina and Klein, 1999, Airaksinen and Saarma, 2002, Forgie et al., 2003, Bauer et al., 2007).

This thesis uses the SCG as a model to study target innervation, hence special attention will be given to the neurotrophins regulating SCG survival and axonal outgrowth. In the next sections I will first provide an overview of neurotrophins, their receptors and their downstream signalling in order to contextualise SCG survival and axonal outgrowth.

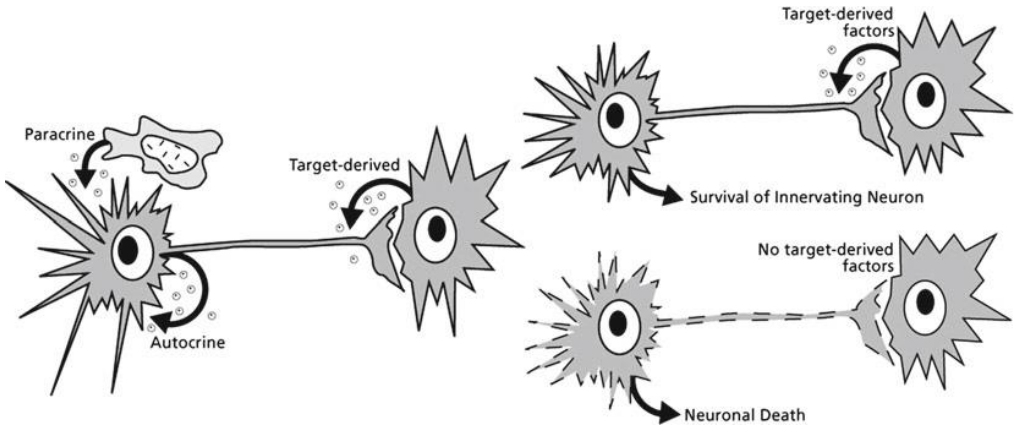

Figure 8: Neurotrophin presentation. Neurotrophins are presented to innervating neurons by target field cells, but they can also be secreted in a paracrine manner by cells of the intermediate environment, such as the vasculature, as well as be secreted in an autocrine mode. Neurons that do not receive enough neurotrophins during development die. From (Skaper, 2012).

1.2.2 Neurotrophins and their receptors

It is most likely that neurotrophins arose from gene duplication events as they share homologies both in sequence and structure (Mowla et al., 2001). Neurotrophins are secreted proteins that are synthesized with a pro-domain and have to be proteolytically cleaved to give rise to the mature protein. Both Furin and pro-convertases, which recognise a highly conserved cleavage site, intracellularly cleave the neurotrophins to release the mature protein (Seidah et al., 1996, Chao, 2003, Skaper, 2012). Furthermore, after secretion, pro-neurotrophins can also be cleaved by extracellular plasmin or matrix metalloproteinase-7 (MMP-7) (Bruno and Cuello, 2006). Mature neurotrophins are low molecular weight proteins which form non-covalent homodimers. They form part of a larger superfamily of growth factors with whose members they share a particular tertiary fold and cysteine knot. Some growth factors sharing this characteristic are TGF-β and platelet-derived growth factor (PDGF) (Skaper, 2012).

Neurotrophins bind to two non-related classes of receptors, the p75 neurotrophin receptor ($p75^{NTR}$) and the tropomyosin receptor kinase (Trk) family that comprises TrkA, TrkB and TrkC (Chao, 2003, Skaper, 2012).

$p75^{NTR}$ was initially described as a low-affinity receptor for NGF. However, it was later elucidated that all members of the neurotrophins bind with equal efficiency to $p75^{NTR}$ (Rodriguez-Tebar et al., 1990, Frade and Barde, 1998, Reichardt, 2006). This receptor belongs to the tumour necrosis receptor super family (TNFRSF) and is a single transmembrane protein containing a death domain in the cytoplasmic portion (Reichardt, 2006).

Trk receptors form part of the larger family of receptor tyrosine kinases. Each receptor contains a tyrosine kinase domain in their intracellular domain which is surrounded by tyrosine residues which function as phosphorylation-dependent binding sites. These receptors cross the membrane once and contain two cysteine rich domains in their extracellular portion as well as two immunoglobulin-like domains (Reichardt, 2006).

TrkA was the first of the three receptors to be discovered followed by TrkB and TrkC. Each neurotrophin displays specificity for an individual Trk receptor. Neurotrophins bind to the immunoglobulin domain closest to the membrane and crystallography studies have elucidated some of the residues conferring ligand-receptor specificity (Ultsch et al., 1999, Wiesmann et al., 1999). NGF binds to TrkA, BDNF and NT-4/5 bind to TrkB (Soppet et al., 1991, Squinto et al., 1991, Klein et al., 1992) while NT-3 preferentially activates TrkC (Lamballe et al., 1991, Chao, 2003, Reichardt, 2006, Skaper, 2012) (Fig. 9). In the absence of $p75^{NTR}$ expression, NT-3 is also able to interact with and activate TrkA and

TrkB but has a low affinity for them. In accordance with receptor specificity, knockout (KO) mice for Trk receptors show similar losses in neuronal populations as with those KO mice for their corresponding neurotrophin partner (Klein et al., 1993, Smeyne et al., 1994). Interestingly, it has been shown both *in vitro* and *in vivo* that TrkA and TrkC induce neuronal cell death. The expression of these proteins by developing peripheral neurons, instructs these cells towards apoptosis. Therefore, suggesting a possible explanation for the dependence of developing peripheral neurons on soluble factors for survival. It must be mentioned that TrkB does not possess this ability, suggesting that cell death is mediated by other mechanisms in peripheral neurons dependent on BDNF for survival (Nikoletopoulou et al., 2010).

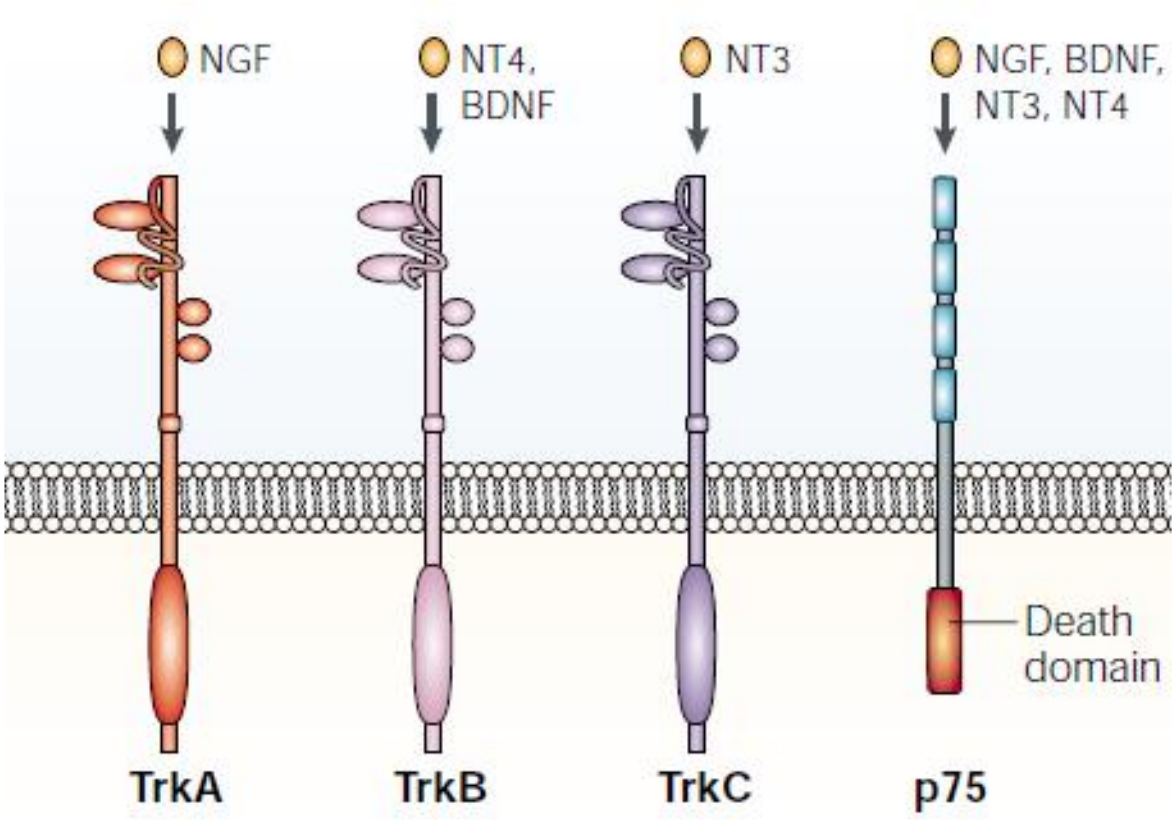

Figure 9: Neurotrophins and their Trk receptors. Neurotrophins bind to Trk receptors with specificity: NGF binds to TrkA, NT-4/5 and BDNF bind to TrkB while NT-3 binds to TrkC. $p75^{NTR}$ is able to bind to all neurotrophins. From (Chao, 2003).

NGF

NGF plays a crucial role in the development of sympathetic neurons, hence, a brief overview of its structure and expression during development will be given in the next section.

Like all neurotrophins NGF is produced as a precursor pro-protein, proNGF, which is subsequently cleaved, giving the mature NGF. NGF is active as a homodimer, composed by two subunits of 118 amino acids each (Angeletti and Bradshaw, 1971, Berger and Shooter, 1977). As mentioned above it contains a conserved cysteine-knot and, in addition, it is characterised by two anti-parallel β-strands (Mcdonald et al., 1991, Bradshaw et al., 1994).

NGF is widely expressed during development both in the CNS and PNS as well as by non-neuronal cells. Regions of NGF expression in the CNS include the basal forebrain and the hippocampus (Korsching et al., 1985, Johnston et al., 1987). In the PNS, target organs innervated by NGF-dependent peripheral neurons are the main source of NGF. Some examples include the pineal gland, submandibular salivary gland, nasal turbinate tissue, the iris and whisker pads (Heumann et al., 1984). Furthermore, NGF expression is not restricted to the developing nervous system; the immune, reproductive and endocrine systems all express this neurotrophin. However, the role of NGF during the development of these tissues is not well characterised (Tessarollo, 1998).

1.2.3 Neurotrophin signalling

Upon binding of a neurotrophin, Trk receptors dimerise and are activated by transphosphorylation of intracellular tyrosine residues (Chao, 2003, Reichardt, 2006,

Skaper, 2012). Activated Trk receptors contain phosphorylated tyrosine residues in the cytoplasmic domain that act as docking sites for adaptor proteins, resulting in the activation of various downstream signalling cascades (Kaplan and Stephens, 1994). A specific example is that of tyrosine residue 490, which binds to the adaptor proteins Src homology 2 domain containing (Shc) and fibroblast receptor substrate-2 (FRS2). This event can initiate various signalling cascades including the Ras/extracellular signal regulated kinase (ERK) and phosphoinositide 3-kinase (PI3K)/Ak transforming/protein kinase B (Akt/PKB) pathways (Fig.10) (Chao, 2003, Skaper, 2012). Activation of these pathways modulates neuronal survival, differentiation and maturation, and promotes target field innervation and regulation of the functional properties of neurons (Reichardt, 2006) (Fig.10).

Growth and branching of axon terminals, regulation of ion channel gating and exocytosis is mediated by local Trk-mediated activation of phospholipase C-gamma (PLC-γ) (Campenot and MacInnis, 2004). In contrast, activated Trks must be retrogradely transported to the cell soma via signalling endosomes to mediate functions involving gene expression such as neurotrophin-promoted neuronal differentiation, survival, and regulation of functional phenotypes, as this is dependent upon the signal reaching the nucleus (Ye et al., 2003, Campenot and MacInnis, 2004).

Retrograde signalling is an essential mechanism in the developing PNS, as neurons extend axons over long distances to target fields that express neurotrophins. Retrograde signalling uses the endocytotic pathway, where activated receptors are internalised, at times with intermediate signalling molecules, via clathrin-coated pits. Signalling endosomes are then trafficked to the cell body (Zweifel et al., 2005).

In the absence of cognate Trk expression, $p75^{NTR}$-mediated neurotrophin signalling induces apoptosis by activating a number of intracellular signalling pathways. These pathways include TNF-receptor associated factor 6 (TRAF6)-mediated activation of Jun N-terminal kinase (JNK), and nuclear translocation of a complex consisting of the cleaved, soluble $p75^{NTR}$ intracellular domain bound to the transcription factor neurotrophin receptor interacting factor (NRIF). In some cell types, neurotrophin binding to $p75^{NTR}$ can also induce the generation of ceramide by membrane sphingomyelinase, leading to ceramide-mediated inhibition of PI3K/Akt survival signalling. Conversely, the binding of neurotrophins to $p75^{NTR}$ in the presence of cognate Trk receptors can promote neuron survival or process outgrowth by either inducing TRAF6-mediated activation of nuclear factor-κB (NF-κB) signalling or modulating the activity of the small GTPase RhoA, respectively (Reichardt, 2006, Chen et al., 2009) (Fig.10).

More recently, it has become evident that pro-NGF can bind to $p75^{NTR}$ in the absence of mature neurotrophins, resulting in the induction of apoptosis (Chen et al., 2009). Furthermore, the receptor sortilin can form a high affinity pro-neurotrophin receptor complex with $p75^{NTR}$, which can induce cell death more efficiently than $p75^{NTR}$ by itself (Teng et al., 2010). Pro-NGF is also able to selectively promote postnatal SCG neurite outgrowth via $p75^{NTR}$ *in vitro* (Howard et al., 2013).

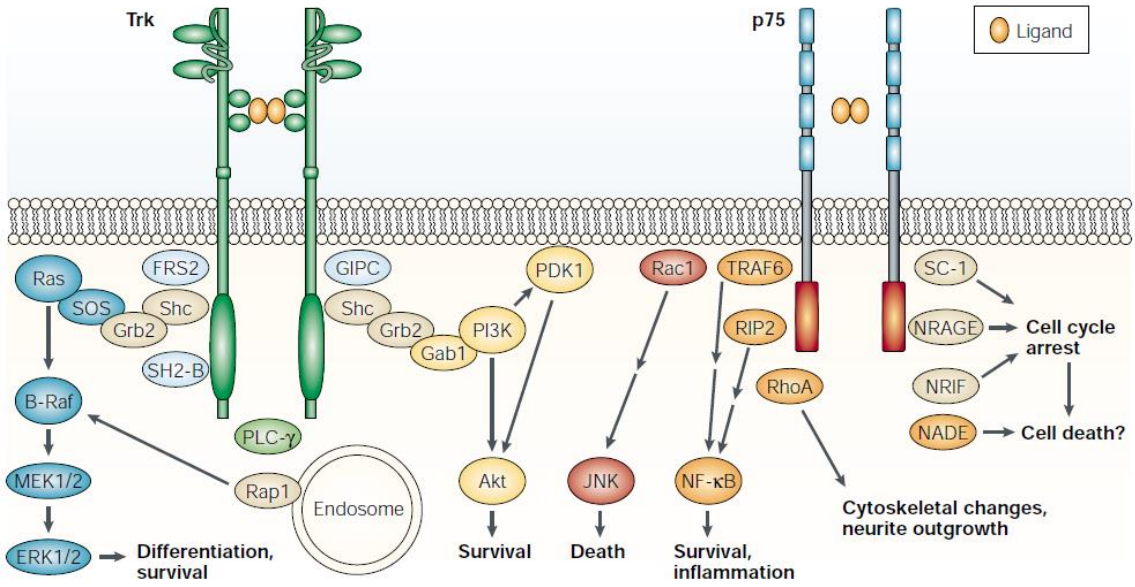

Figure 10: Neurotrophin signalling. Downstream signalling mechanisms for Trk and $p75^{NTR}$ receptors. From (Chao, 2003).

1.2.4 Neurotrophin requirement for SCG survival

NGF is the main survival-promoting factor for developing SCG neurons (Crowley et al., 1994, Fagan et al., 1996). SCG cells start responding to NGF from around embryonic day 14 (E14) and subsequently become dependent on NGF for survival until early postnatal ages (Wyatt and Davies, 1995). Nonetheless, SCG neurons also respond to a variety of neurotrophins and neurotrophic factors at different developmental ages. During early development SCG cells are able to survive *in vitro* independently of neurotrophic factors (Ernsberger et al., 1989). However, various studies suggest that HGF is involved in sustaining sympathetic neuroblast survival, promoting neuroblast differentiation and initiating axonal growth during this period (Maina et al., 1998). In addition, artemin also seems to play a role during early development, promoting initial axonal extension. Artemin is expressed by the intermediate environment, along the vasculature, and not only promotes sympathetic axonal growth *in vitro* but is also able to attract sympathetic axons in *vivo* (Honma et al., 2002, Yan et al., 2003). Interestingly, artemin and HGF can

both promote the survival of SCG neurons much later in their postnatal development (Andres et al., 2001, Thompson et al., 2004). NT-3 appears to support the survival of a subset of mouse NGF-dependent SCG neurons from E16 (Wyatt et al., 1997, Francis et al., 1999). However, a later study suggests that NT-3 is required for proximal target field innervation by developing SCG neurons, and that the death of a sub-population of SCG neurons in the NT-3 null mutant mouse is the result of reduced access of these neurons to target field NGF (Kuruvilla et al., 2004). Together with artemin and HGF, the neurotrophic factors CNTF and LIF also seem to have a role during later development, as late postnatal SCG neurons are able to respond to them *in vitro* (Kotzbauer et al., 1994). Fig.12 summarised SCG development and some of the events described above.

1.3 Neuronal outgrowth in the nervous system

In order to achieve a functioning nervous system, developing neurons with extending axons must travel long distances to their target field, in particular within the developing PNS, and must therefore be both precisely guided to and then instructed to correctly innervate these specific targets. This is a tightly regulated and precise process, and although the nervous system is composed of highly diverse populations of neurons which in turn innervate very different targets, axonal outgrowth, guidance and branching share common mechanisms throughout the developing nervous system (Kolodkin and Tessier-Lavigne, 2011).

At the end of every neuron, with extending neurites/processes towards target fields, is a highly dynamic and motile structure, the growth cone. This structure allows the extension of the axon and serves as an environment “sensor” to the neuron, interpreting

cues and signals that will direct it correctly. The growth cone is characterised by many thin extensions termed filopodia, which consist of F-actin, and lamellipodia which web the filopodia together and are comprised of an actin mesh. Growth cones also contain individual and stable microtubules. F-actin dynamics allow the forward movement of this structure whilst microtubules enable it to steer around the environment (Lowery and Van Vactor, 2009). Importantly, the growth cone functions as the sensor and motor unit of the extending axon by integrating and adapting extrinsic cues (Kandel et al., 2000).

Neurite outgrowth and the signals regulating this mechanism have been investigated extensively over the past 100 years since Santiago Ramón y Cajal first described the growth cone (Gibson and Ma, 2011). These studies have revealed some common characteristics which are applicable to most neurons extending axons (Kolodkin and Tessier-Lavigne, 2011). The first events in axonal outgrowth are activity independent, they then depend on signals from the intermediate environment to reach targets, when axons reach targets and subsequently innervate them, electrical signals are then used to refine these connections. Guidance cues, which are the signals that tell axons in which direction to grow, can be found both at long and short ranges. In addition, they can function as diffusible signals or exert their effects via a contact-mediated mechanism. Secreted diffusible signals allow guidance cues to influence axons at long ranges, however, these secreted signals can also stay in the vicinity, exerting local effects. On the other hand, membrane-bound guidance cues are dependent on cell to cell contact, hence, restricting their actions to specific locations (Fig.11). These signals can instruct axons to bundle together into nerves and fascicles in order to follow a common predetermined path to reach target organs where they can then separate. Additionally,

guidance signals influence how axons interact with the surrounding environment, with either intermediate targets or final targets, by being chemorepulsive or chemoattractive (Fig.11). These signals, furthermore, are multifunctional and can influence growth cones in diverse ways depending on the context and the environment they are found in, emphasizing once again the recurring theme of signal recycling during development; one same signal can have multiple functions depending on the context it is found in. In addition, many of these guidance cues and their roles and functions are evolutionarily conserved (Dickson, 2002), highlighting the importance of tightly regulating neurite outgrowth in the generation of a functioning nervous system. Guidance cues can be classified into four protein families which have well-defined roles during axonal outgrowth and are sometimes referred to as the "canonical cues", consisting of the netrins, slits, semaphorins and ephrins (Kolodkin and Tessier-Lavigne, 2011). Both netrins and slits function as secreted molecules and hence, can exert their effects at very long ranges. Semaphorins can either be secreted or membrane-bound. On the other hand, ephrins are membrane-bound hence, are dependent on contact-mediated interactions. However, many different types of signalling molecules are involved in the complex process of regulating neurite outgrowth and correct final target innervation and these include morphogens, growth factors, cell-adhesion molecules (CAMs) and the immunoglobulin (Ig) and cadherin super families (Kolodkin and Tessier-Lavigne, 2011).

Neurotrophic factors play a crucial role during correct final target innervation. As target-derived molecules, they have a great influence on incoming axonal processes and this is not restricted to cell survival. The neurotrophic hypothesis not only postulates that target-derived factors regulate the survival of neurons innervating target fields but that they also promote the growth and branching of their axons within the target field

(Davies, 2009). In addition, it is becoming apparent that they also play roles during early-mid axonal guidance, more specifically influencing axonal outgrowth, as they are expressed by the intermediate environment, like the vasculature.

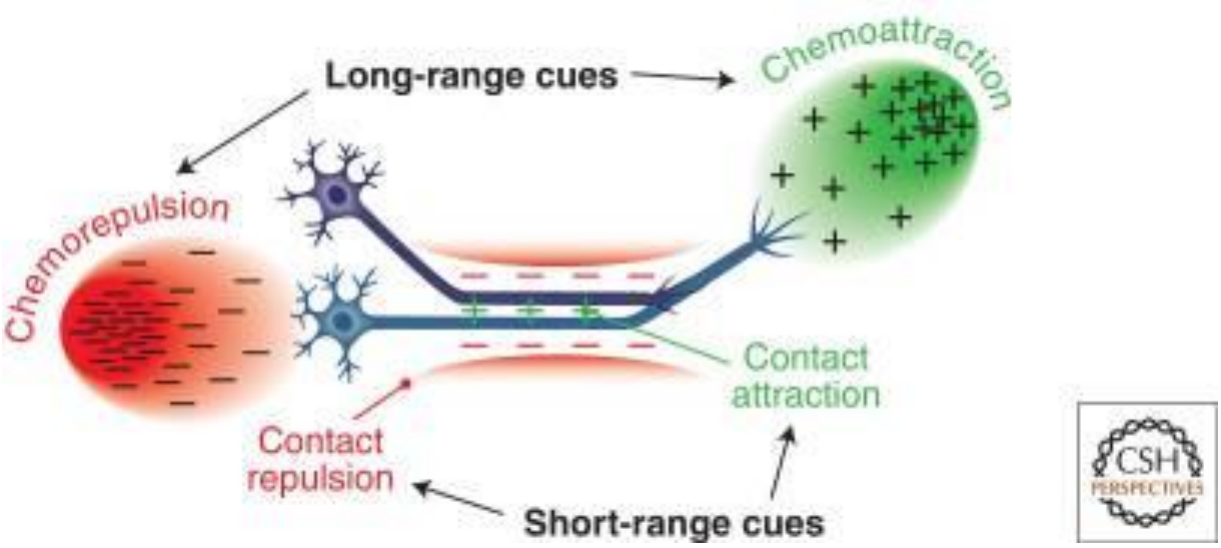

Figure 11: Simplified schematic of axon guidance. Extending axons can be influenced by positive or negative cues that can be either long or short range and secreted, diffusible or membrane-bound molecules. From (Kolodkin and Tessier-Lavigne, 2011).

1.3.1 The roles of neurotrophic factors in regulating sympathetic peripheral target field innervation

Neurotrophic factors not only regulate survival but also peripheral neuronal growth and final target field innervation. Sympathetic outgrowth towards peripheral targets incorporates the common mechanisms outlined in the above section which include axonal elongation, fasciculation, defasciculation, changes in axon morphology, cross-talk with intermediate targets, followed by axonal growth and branching within final target fields (Rubin, 1985).

Sympathetic neurons follow the vasculature in order to reach their final targets, hence, the intermediate environment is responsible for both expressing and secreting guidance cues and growth promoting signals, to guide these advancing axons. These interactions

therefore, can be contact-mediated or carried out by diffusible molecules. This section concentrates on the roles of neurotrophic factors during this process, which are secreted molecules. As mentioned in previous sections artemin is one of these proposed factors, together with endothelins and NT-3 (Davies, 2009).Therefore, these factors have roles during early-mid guidance, before processes reach their targets, acting as short-range diffusible factors. Artemin is expressed and secreted along the vasculature, and Ret and GFRα3, which form the receptor complex for artemin, are expressed by the sympathetic chain at the time when they start to extend axons (Pachnis et al., 1993, Baloh et al., 1998, Honma et al., 2002). Artemin is able to promote sympathetic axonal growth *in vitro* and is able to attract sympathetic axons in *vivo.* This is highlighted by the fact that KO mice for either artemin, Ret or GFRα3 all have defective sympathetic axonal processes. These mice have both abnormal sympathetic axonal migration patterns and projections (Enomoto et al., 2001, Honma et al., 2002, Yan et al., 2003). Endothelin-3 (End3) is thought to be an intermediate growth cue for a subset of sympathetic axons as it is also expressed and secreted along the vasculature, particularly near the external carotid artery. Its receptor is expressed by SCG cells. End3 is able to promote sympathetic axon growth *in vitro* and *in vivo* (Makita et al., 2008). Similarly, NT-3 is expressed by blood vessels during the time sympathetic axons are growing towards their targets (Scarisbrick et al., 1993) and in accordance with this, NT-3 is able to promote sympathetic axonal growth *in vitro* (Belliveau et al., 1997), and mice lacking NT-3 have impaired sympathetic growth along the vasculature (Kuruvilla et al., 2004). NT-3 is able to activate TrkA but unlike NGF it fails to promote retrograde signalling. This emphasises NT-3s role as an intermediate guidance cue, promoting axonal growth locally. On the other hand, NGF is able to promote survival by retrograde signalling (Ye et al., 2003, Kuruvilla et al., 2004, Davies, 2009).

The potent growth-promoting effects of NGF *in vitro* have been known since the 1950s (Cohen et al., 1954). Studies overexpressing NGF showed that both sensory and sympathetic nerves were hypertrophic in these mice (Edwards et al., 1989, Albers et al., 1994). In addition, *in vitro* studies using compartmentalised cultures showed that NGF had local effects on axonal growth and branching (Campenot, 1987). However, due to the survival dependence of developing sympathetic peripheral neurons on NGF, until recently it was not possible to assess exactly the extent to which NGF is involved in axonal growth and guidance.

The experimental approach to cross NGF deficient mice with BAX KO mice has allowed researchers to circumvent this issue (Glebova and Ginty, 2004). These mice are able to survive without NGF, as neurons do not undergo apoptosis as they lack BAX, a pro-apoptotic Bcl-2 family member. Accordingly it has been shown that mice that do not express BAX do not undergo the period of PCD that is characteristic of sympathetic development (White et al., 1998), a phenomenon which is consistent in BAX and NGF double KO mice (Middleton and Davies, 2001). This experimental paradigm therefore allows for the study of NGF-promoted axonal growth *in vivo* independently of its role in promotion of neuronal survival. In addition, these experiments suggest that NGF functions as a growth promoting signal, during late axonal guidance and during terminal arborisation of target fields.

In vivo studies using BAX/NGF double KO mice and the analysis on sympathetic innervation of a variety of sympathetic target organs via whole mount staining showed that the requirement of NGF for sympathetic target innervation during development is heterogeneous. Furthermore, NGF is not required for axonal guidance to target organs,

as axonal bundles reached target organs in these mice. What was impaired was axonal growth into target organs or branching within target fields, therefore placing NGF as a factor important for final target field innervation and arborisation. Some organs have an extreme reduction in innervation in the absence of NGF, for example salivary glands and the heart, while others, like the kidney and stomach have sympathetic innervation but it is incomplete. In stark contrast some target organs, like the trachea, were completely unaffected in these mice (Glebova and Ginty, 2004). These observations suggest that there are other target-derived factors necessary for sympathetic final target innervation. Fig.12 summarises the events of sympathetic development described in this section and 1.2.4.

Further studies have exploited this method of using BAX double KO mice to study the role of TrkA and other neurotrophic factors like NT-3, which has allowed the elucidation of further roles of NGF and neurotrophic factors in sensory target field innervation independently of their role in neuronal survival. For example, one study looked into sensory innervation from the DRG. Two double null mice line strains were used: both lacked BAX and either NGF or TrkA. In these mice, superficial cutaneous innervation was absent and the rescued sensory neurons lacked biochemical markers for nociceptive phenotypes. Therefore, NGF/TrkA signalling is necessary for both sensory target field innervation and for full phenotypic differentiation (Patel et al., 2000). Furthermore, overexpression experiments for NT-3 and *in vivo* studies of NT-3 null mice have linked NT-3 to both sensory and sympathetic axonal growth and guidance (Albers et al., 1996, Kuruvilla et al., 2004). MSP has also been reported to promote sensory and sympathetic axonal growth at different developmental stages (Forgie et al., 2003). The survival dependence of sensory ganglia on neurotrophic factors and their roles during sensory

target field innervation, together with key experiments, will be addressed in more detail in Chapter 6.

In addition to neurotrophic factors of the GDNF and neurotrophin families, a large number of secreted and membrane-associated proteins have been implicated in controlling the growth, branching and guidance of neural processes in the developing nervous system, including extracellular matrix proteins, netrins, semaphorins, cell adhesion molecules, ephrins and Wnts (Davies, 2009). Furthermore, even Ca^{2+} ions have the ability to modulate NGF-promoted sympathetic axonal growth. Activating the extracellular calcium-sensing receptor (CaSR) in sympathetic cultures with high concentrations of Ca^{2+}, enhances the growth of axons (Vizard et al., 2008).

Together, this has expanded the concept of what type of signals can be considered neurotrophic factors. For instance, the discovery that multiple members of the TNF superfamily (TNFSF) are potent positive or negative regulators of neurite growth in the developing CNS and PNS has opened up a new exciting area of research in developmental biology (Barker et al., 2001, Neumann et al., 2002, Desbarats et al., 2003, Zuliani et al., 2006, Gutierrez et al., 2008, O'Keeffe et al., 2008, Takei and Laskey, 2008, Gavalda et al., 2009, Gutierrez et al., 2013, Wheeler et al., 2014, McWilliams et al., 2015). This thesis focuses on the possible roles of TNF, a member of this family, on sympathetic neuronal survival and outgrowth during development, hence the following section provides an in depth description of the TNFSF, in particular TNF and its receptors.

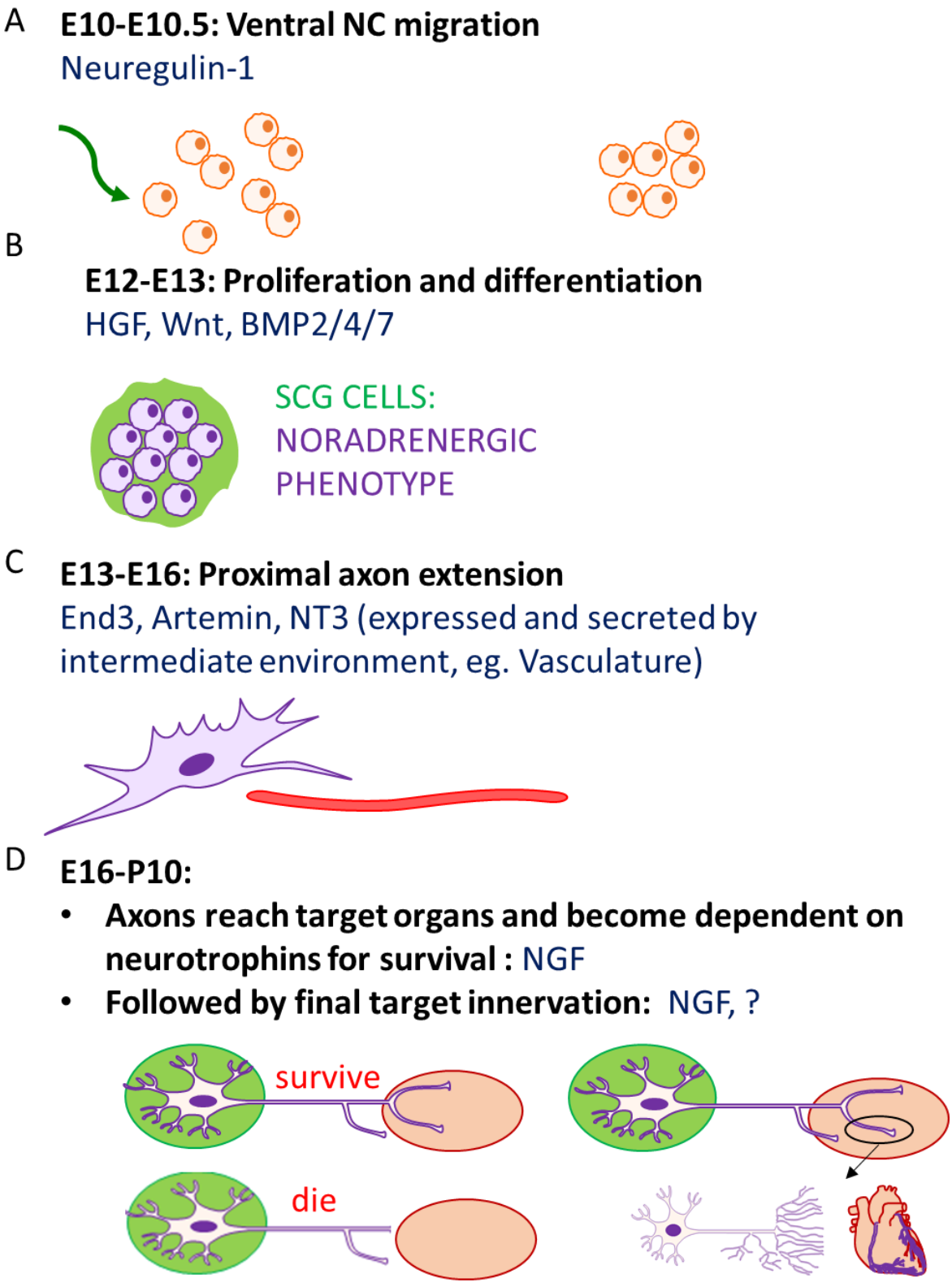

Figure 12: Summary timeline of sympathetic neuron development and main factors involved .A-B) Early development. **C)** Proximal axon extension. **D)** Final target innervation.

1.4 TNFSF and TNFRSF

TNF, tumour necrosis factor, is the founding member of the TNFSF, and thus gives the name to this protein family. This nomenclature arose from the observation that a factor isolated from the serum of mice infected with bacteria had anti-tumour activity, as it was able to kill cancer line cells *in vitro* and to reduce or even eliminate transplanted sarcomas (Carswell et al., 1975). Extensive research during the following 25 years has facilitated the discovery and establishment of the different members of the TNFSF and the TNF receptor super family (TNFRSF). The TNFSF and their receptors were first identified and described as cytokines and their role as immunological mediators has been lengthily investigated, overshadowing focus on their other functions. However, over the past decade it has become clear that they exert pleiotropic effects. They not only have critical roles in the development, homeostasis and adaptive responses of the immune system, but are also involved in bone homeostasis, mammary gland development, hair follicle and sweat gland development (Feng, 2005). In addition, they have roles in mediating CNS development, function and homeostasis under normal physiological conditions (Twohig et al., 2011) and, as mentioned above, have been found to be involved in PNS development (Barker et al., 2001, Desbarats et al., 2003, Zuliani et al., 2006, Gutierrez et al., 2008, O'Keeffe et al., 2008, Takei and Laskey, 2008, Gavalda et al., 2009, Gutierrez et al., 2013, Wheeler et al., 2014, McWilliams et al., 2015).

The TNFSF comprises 19 members to date, most of which are type II transmembrane glycoproteins, with the exception of LT-α and VEGI. Therefore, they have an intracellular N terminus and an extracellular C terminus, and span the membrane once (Aggarwal, 2003, Hehlgans and Pfeffer, 2005). These proteins share approximately 20-30%

homology within their C terminal domains, a region accordingly named the TNF homology domain (THD). TNFSF members are active as non-covalent homotrimers and some can be preoteolytically cleaved by metalloproteases to generate functional soluble cytokines. LT-α is the only member able to form heterotrimers with LT-βR (Aggarwal, 2003). It is the characteristic conserved THD that forms the interface of the tertiary trimeric structure, while the exterior non-homologous surfaces account for receptor specificity (Hehlgans and Pfeffer, 2005).

Twenty-nine members of the TNFRSF have been identified so far, most of which are type I transmembrane proteins (with an extracellular N terminus and intracellular C terminus) which are functional as homotrimers. However, some TNFRSF members are type III proteins (BCMA, TACI, BAFFR, and XEDAR) or soluble proteins (DcR3 and OPG) and TRAIL-R3 is a membrane protein attached by a glycolipid (Twohig et al., 2011). These receptors are characterised by a cysteine-rich domain (CRD) in the extracellular domain, the number of which varies (1-6) between different members (Bodmer et al., 2002, Hehlgans and Pfeffer, 2005). Most members of the TNFSF ligands are promiscuous and bind to more than one receptor and vice versa (Fig. 13). The individual receptor-ligand systems formed have non-redundant functions, resulting in a complex signalling system (Tansey and Szymkowski, 2009).

The TNFRSF can be classified into three sub-groups depending on their intracellular sequences. The first sub-group of TNFSF receptors contain an intracellular death domain (DD) (Bodmer et al., 2002, Hehlgans and Pfeffer, 2005, Tansey and Szymkowski, 2009) . Upon activation, these receptors recruit the adaptor proteins FAS-associated death domain (FADD) or TNFR-associated death domain (TRADD) to the DD. These adaptors

induce apoptosis by activating the caspase cascade. Nine members of the TNFRSF have been identified containing a DD; TNFR1, Fas, DR3, DR4, DR5, DR6, $p75^{NTR}$, EDAR and DcR2 (Aggarwal, 2003). Alternatively, if the receptor contains TNF-receptor associated factor (TRAF)- interacting motifs (TIMs) in its cytoplasmic domain, it belongs to the second TNFRSF sub-group. These receptors do not contain a DD, but their activation leads to the recruitment of TRAF family members and the initiation of various signalling pathways including those involving NF-κB, JNK, p38, ERK and PI3K. To date, six TRAFs have been identified in mammals (TRAFS 1-6) which share common structural features. They are characterised by having a C-terminal TRAF domain (TD) and RING finger and zinc finger domains (Chung et al., 2002). TRAFs can also bind to the DD, but this is via other adaptor proteins. The third TNFRSF sub-group comprises those receptors that lack intracellular signalling motifs. Since they act as competitors for the other two groups by sequestering their ligands, they are also known as decoy receptors (DcR). TNFRSF members classified as DcR include; DcR1, DcR2, DcR3 and OPG (Aggarwal, 2003). (Extensively reviewed in (Bodmer et al., 2002, Aggarwal, 2003, Feng, 2005, Hehlgans and Pfeffer, 2005, Tansey and Szymkowski, 2009)).

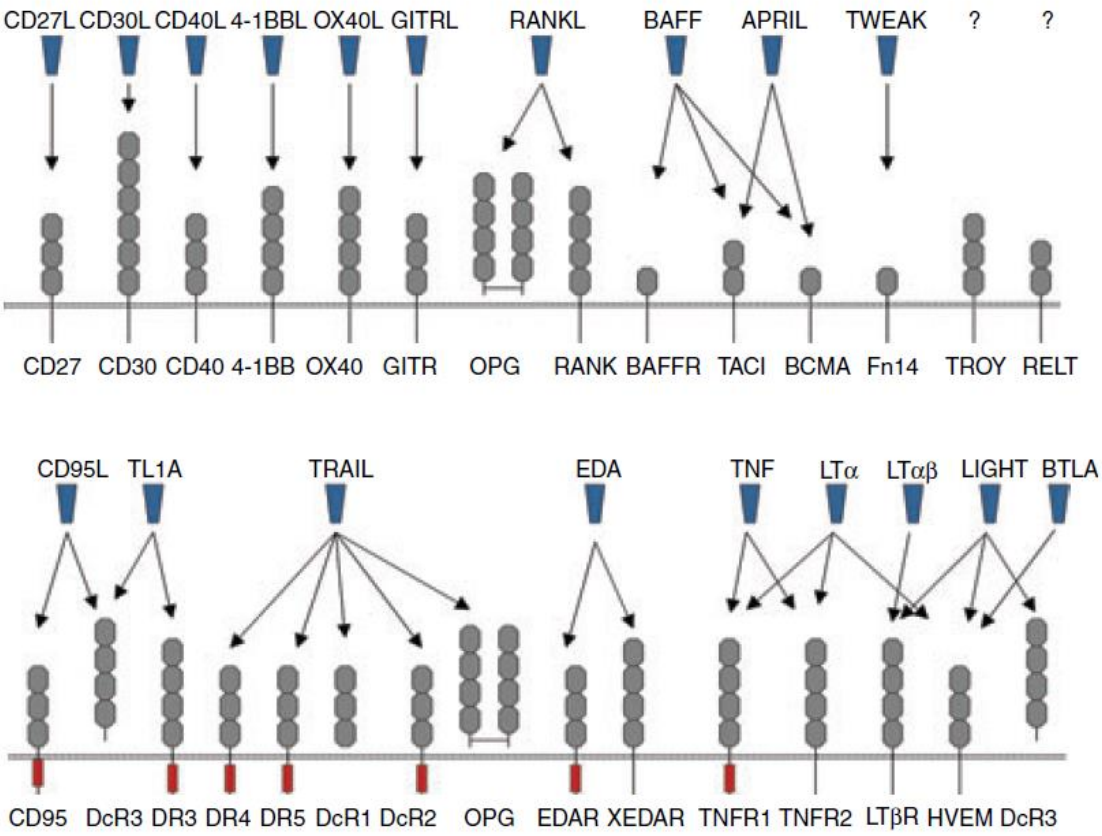

Figure 13: The TNF and TNFR superfamily. Ligands are depicted by blue boxes, ligand-receptor interactions by arrows, receptor CRD by grey circles and receptor DD by red rectangles. Receptors with DDs sequester proteins containing TRADDS and FADDS; receptors with no DD bind TRAF adaptor proteins and those with no cytoplasmic domain act as decoys. From (Hehlgans and Pfeffer, 2005).

1.4.1 Reverse signalling

Interestingly, some membrane-integrated TNFSF ligands are able to transduce signals when their cognate receptors bind to them, a phenomenon which is referred to as reverse signalling or bi-directional signalling (Eissner et al., 2004, Sun and Fink, 2007). The possibility of bi-directional signalling was proposed due to the observation that TNFSF ligands have highly conserved intracellular domains across species, indicating that they might have some type of function (Smith et al., 1994). Indeed, reverse signalling by TNFSF members is now well accepted, and although not much is known about the downstream molecular mechanisms of reverse signalling, there are extensive studies

describing the cellular responses to reverse signalling mediated by different members of the TNFS family during the immune response. In general reverse signalling will have an opposite effect than the forward signal from the same pair of proteins. For example, one signalling pathway will attenuate the immune response, whilst the other will intensify it (Juhasz et al., 2013). TNFSF members that have been identified with the capability of mediating reverse signalling include TNF, CD30L, TRAIL, FasL, CD40L, 4-1BBL, RANK and LIGHT (Sun and Fink, 2007). Reverse signalling during the immune response by membrane-integrated TNFSF ligands has been shown to regulate cell proliferation, cytokine secretion, oxidative burst, class switch and T-cell maturation (Sun and Fink, 2007) (Fig.14). Furthermore, reverse signalling is accompanied by an influx of extracellular calcium in the immune system (Watts et al., 1999) The level of intracellular free Ca^{2+} is controlled by a variety of pumps and channels, voltage gated calcium channels playing a major role (Perez-Reyes, 2003).). Hence, it can be speculated that calcium channels might be involved in the downstream effects of bi-directional signalling. TNF reverse signalling will be addressed in detail in Chapter 3. Reverse signalling highlights once again the concept of signal recycling; reverse signalling adds another layer to the dynamic roles of the TNFSF members, by introducing an additional mechanism to enable one single protein to have multiple outcomes and roles depending on the context in which it is found.

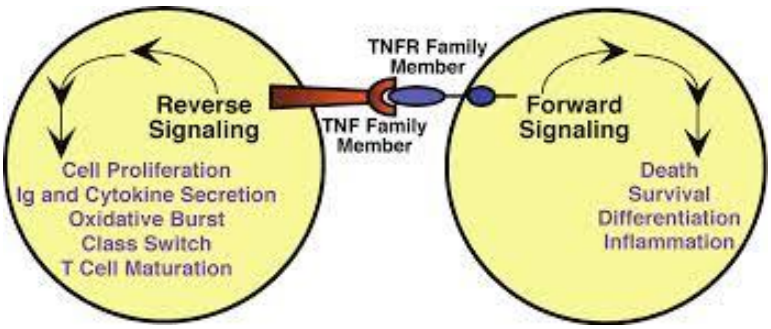

Figure 14: TNFSF reverse signalling during the immune response. Some membrane-integrated TNFSF ligands are able to transduce signals from their cognate receptors, which is known as bi-directional or reverse signalling. From (Sun and Fink, 2007).

1.4.2 TNFSF and TNFRSF in peripheral nervous system development

The Davies group, in an attempt to identify new regulators of sympathetic and sensory neuron development, carried out comprehensive qPCR-based expression screens of known families of transmembrane receptors in developing sympathetic and sensory ganglia and their target organs. Various members of the TNFRSF appeared to be highly expressed in developing PNS neurons and were later proven to play a role in regulating axonal growth (Barker et al., 2001, Gutierrez et al., 2008, O'Keeffe et al., 2008, Gavalda et al., 2009, Gutierrez et al., 2013, McWilliams et al., 2015) . In addition, other research groups have reported roles for TNFSF members in PNS development (Desbarats et al., 2003, Takei and Laskey, 2008, Wheeler et al., 2014). Interestingly the involvement of $p75^{NTR}$ during PNS development as a neurotrophin receptor (refer to 1.2.2.) has been known for many years, giving the first hints that the TNFSF might play a role during neuronal development.

For example, it was found that the ligands TNF, LIGHT (lymphotoxin-related inducible ligand that competes for glycoprotein D binding to herpesvirus entry mediator on T cells) and RANKL (receptor-activator of NF-kB ligand), decrease neurite outgrowth from

developing mouse PNS neurons in culture (Gavalda et al., 2009, Gutierrez et al., 2013). In cultures of E18 and P0 nodose sensory neurons, the overexpression of LIGHT inhibits BDNF-promoted neurite growth. Accordingly, nodose neurons in cultures established from neonatal mice lacking LIGHT display greater neurite growth compared to neurons in cultures established from wild type neonates (Gavalda et al., 2009). Similarly, overexpressing the RANKL receptor, RANK, or supplementing cultures with soluble RANKL inhibits neurotrophin-promoted neurite outgrowth from both sensory and sympathetic neurons (Gutierrez et al., 2013). In addition, enhancing NF-κB transcriptional activity by adding soluble TNF to neonatal SCG cultures also results in a strong inhibition of neurite growth (Gutierrez et al., 2008). In contrast, another study showed that TNF is able to enhance NGF-promoted survival of rat postnatal DRG neurons *in vitro* (Takei and Laskey, 2008). Fas is also able to enhance early postnatal sensory neuronal outgrowth *in vitro* (Desbarats et al., 2003).

Furthermore, autocrine signalling by some TNFSF members has been shown to modulate sympathetic survival and target field innervation. TNF and TNF receptor 1 (TNFR1), via a suggested autocrine loop, induce the death of NGF-dependent sympathetic neurons that do not receive sufficient neurotrophic factor during the initial stages of target field innervation (Barker et al., 2001). Moreover, glucocorticoid-induced tumour necrosis factor receptor-related protein (GITR) and its ligand GITRL increase NGF-promoted neurite growth. In culture, addition of GITRL enhances neurite growth from neonatal sympathetic neurons. In addition, disrupting GITRL-GITR signalling or knocking down GITR inhibits NGF-promoted growth, and mice lacking GITR have reduced sympathetic innervation compared to wild type mice. It has been suggested that these effects are also mediated by autocrine signalling (O'Keeffe et al., 2008). A

recent study has demonstrated that CD40 (cluster of differentiation 40) autocrine signalling is able to enhance sympathetic axonal growth and branching. Moreover, this observation is physiologically relevant as CD40 deficient mice have decreased sympathetic innervation density in only those target organs that express low levels of NGF, which is in accordance with observations that NGF negatively regulates CD40 expression (McWilliams et al., 2015).

Several members of the TNFSF, including TNF, are able to reverse signal. TNF has also been linked to PNS development (Barker et al., 2001, Gutierrez et al., 2008, Takei and Laskey, 2008) and CNS development (reviewed in(Twohig et al., 2011)) but never in the context of reverse signalling until recently. In addition, TNF is highly expressed during PNS development, particularly in the SCG. Therefore, making it an interesting candidate to study its effects during PNS development. In 2013 a study from the Davies group, to which results from this thesis contributed extensively, reported a role for TNF reverse signalling during sympathetic development (Kisiswa et al., 2013). These results will be referred to in detail in following chapters. In addition, another investigation carried out after the aforementioned study linked TNF reverse signalling to sensory neuron development (Wheeler et al., 2014), which is also addressed in subsequent chapters. Hence, this project focuses on TNF reverse signalling in the developing peripheral nervous system and the next sections outline the biochemistry of TNF and its receptors together with their roles during nervous system development. It must be mentioned that LTα is also able to bind to TNFR1 and TNFR2, the cognate receptors for TNF, reflecting ligand promiscuity of the TNFSF. However, in the qPCR screen LTα was not highly expressed during development in SCG ganglia and its target organs. Furthermore

LTα is not able to induce reverse signalling in the immune response. Thus this project concentrated on TNF.

1.4.3 TNF

TNF is first expressed in its membrane bound state, consisting of a 233 amino acid polypeptide (26 kDa) (Horiuchi et al., 2010). It is active as a homotrimer, both in its membrane bound state (mTNF) and soluble form (sTNF). The metalloprotease, TNF converting enzyme (TACE) cleaves TNF between residues alanine (76) and valine (77) to release a soluble homotrimer consisting of 157 amino acid residue (17 kDa) monomers (Black et al., 1997, Moss et al., 1997) (Fig. 15). After cleavage by TACE, the remaining cytoplasmic domain is further processed by signal peptide peptidase-like 2B (SPPL2b) and translocates back to the nucleus of the TNF expressing cells (Horiuchi et al., 2010). TNF is palmitoylated at a cysteine residue located between the transmembrane and cytoplasmic domains. The intracellular domain contains a casein kinase I (CKI) motif as well as three serine residues that are conserved across species and are phosphorylated (Fig.15). Both of these features are thought to be important for reverse signalling (reviewed in (Horiuchi et al., 2010)).

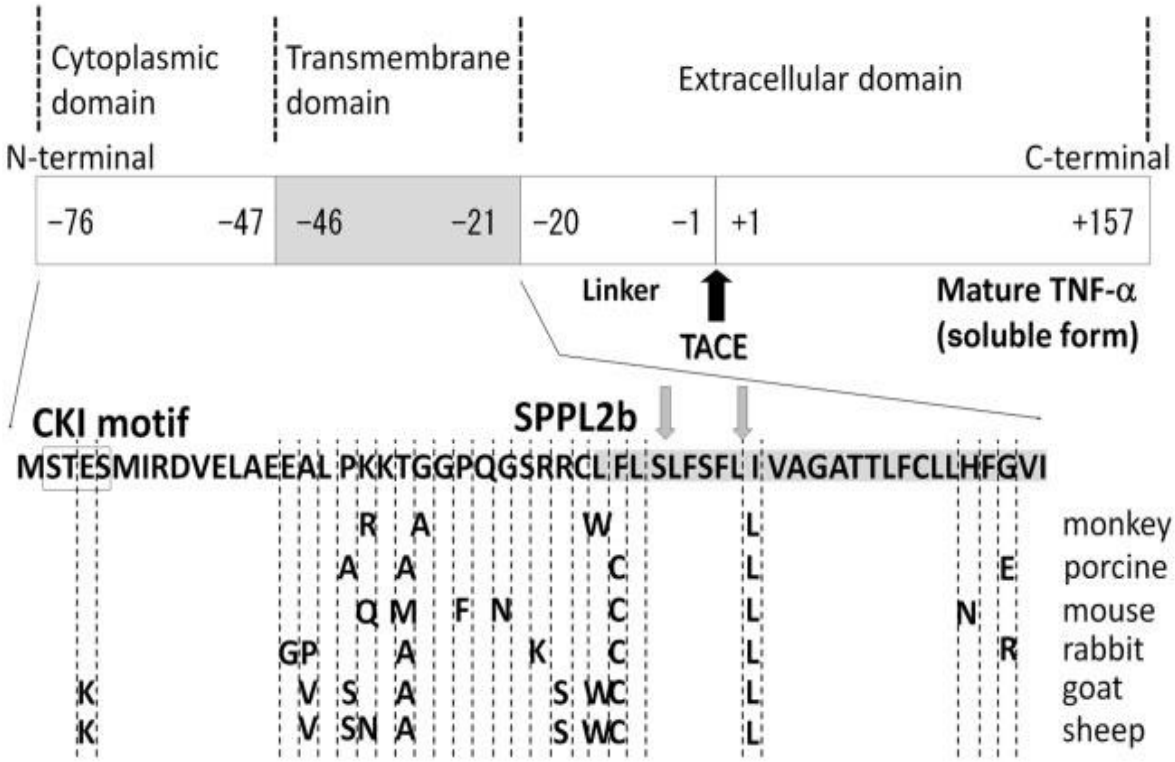

Figure 15: TNF structure. Structure of TNF protein showing its different domains. The black arrow indicates TACE cleavage site and the grey arrows, SPPL2b cleavage site. The intracellular domain contains a CKI motif (boxed) and three serines (S) which are conserved among species. The serines are thought to be crucial for reverse signalling. From (Horiuchi et al., 2010).

1.4.4 TNF receptors

TNF exerts its biological functions via two receptors: TNF receptor 1 (TNFR1) and TNF receptor 2 (TNFR2) (Grell, 1995, Horiuchi et al., 2010). TNFR1 can be activated by both sTNF and mTNF and is functional as a homotrimer consisting of 55 kDa monomers (Fig. 16). TNFR1 contains a DD in its intracellular domain, and has 4 CRDs in its extracellular domain. TNFR1 is expressed in almost all cell types. In contrast, TNFR2 is preferentially activated by mTNF, does not contain a DD and has restricted expression. TNFR2 is also functional as a homotrimer, consisting of 75 kDa monomers and containing 4 CRDs in its extracellular domain. Both receptors contain proteolytic cleavage sites.

Metalloproteases, such as TACE, can cleave these proteins resulting in the release of their respective extracellular domains (reviewed in (Cabal-Hierro and Lazo, 2012)).

Activation of TNFR1 by binding of TNF recruits the adaptor protein, TRADD to the DD (Cabal-Hierro and Lazo, 2012). This results in the binding of other adaptor proteins including TRAF2 and RIP1. If this protein association remains attached to the plasma membrane, it is referred to as complex I. This complex triggers various cellular signalling pathways culminating with the activation of the transcription factors NF-κB and activator protein 1 (AP-1) and the promotion of cytokine expression, cell proliferation and survival (Cabal-Hierro and Lazo, 2012). However, if this association of protein moieties is endocytosed after TNFR1 activation, there is a change in receptor conformation which alters the adaptor proteins that can interact with it, thereby leading to the formation of Complex II. Complex II includes TRADD and FADD, as well as procaspase-8, and its formation induces apoptosis. TNFR2 activation mediates transcriptional activation of genes involved in cell proliferation and survival by activation of NF-κB and AP-1 via TRAF2 (Fig. 17) (reviewed in (Cabal-Hierro and Lazo, 2012)).

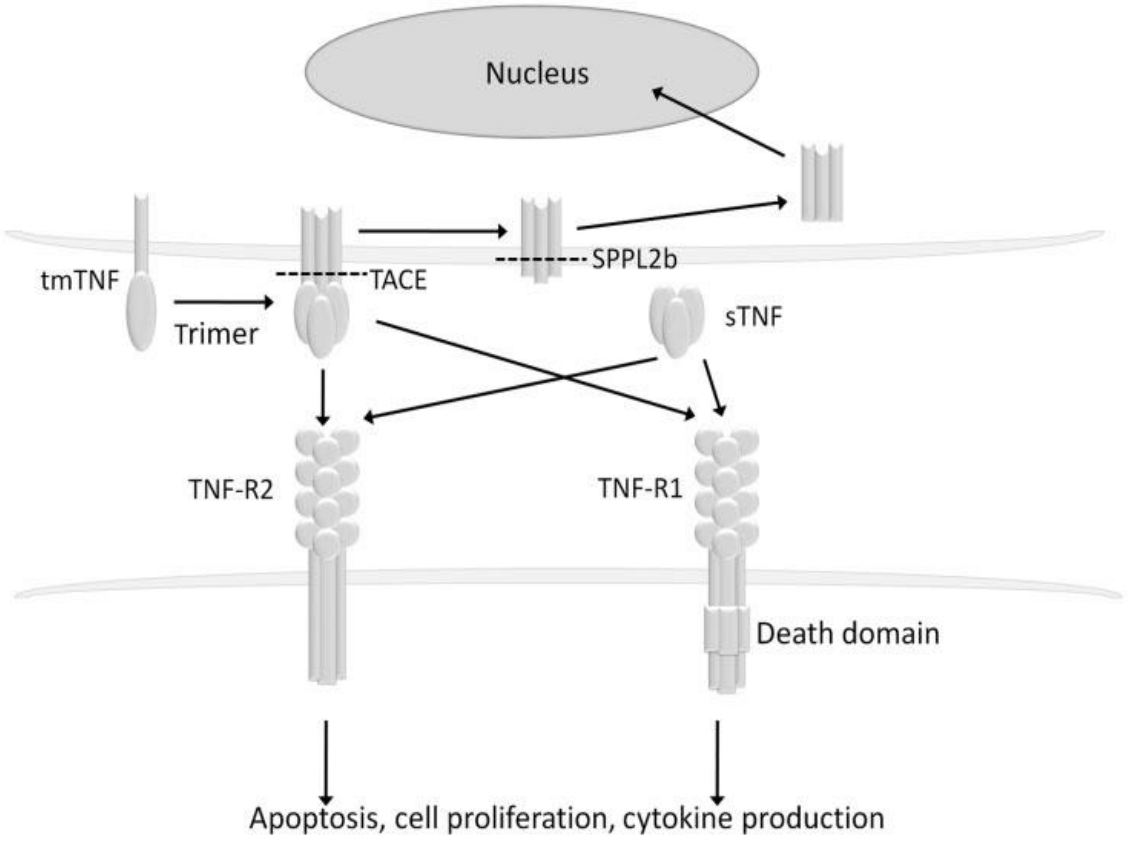

Figure 16: Proteolytic processing of TNF. TNF homotrimers and interactions of sTNF and mTNF with TNFR1 and TNFR2. TNFR1 is activated by both sTNF and mTNF; TNFR2 can bind both forms, but is only efficiently activated by mTNF. From (Horiuchi et al., 2010).

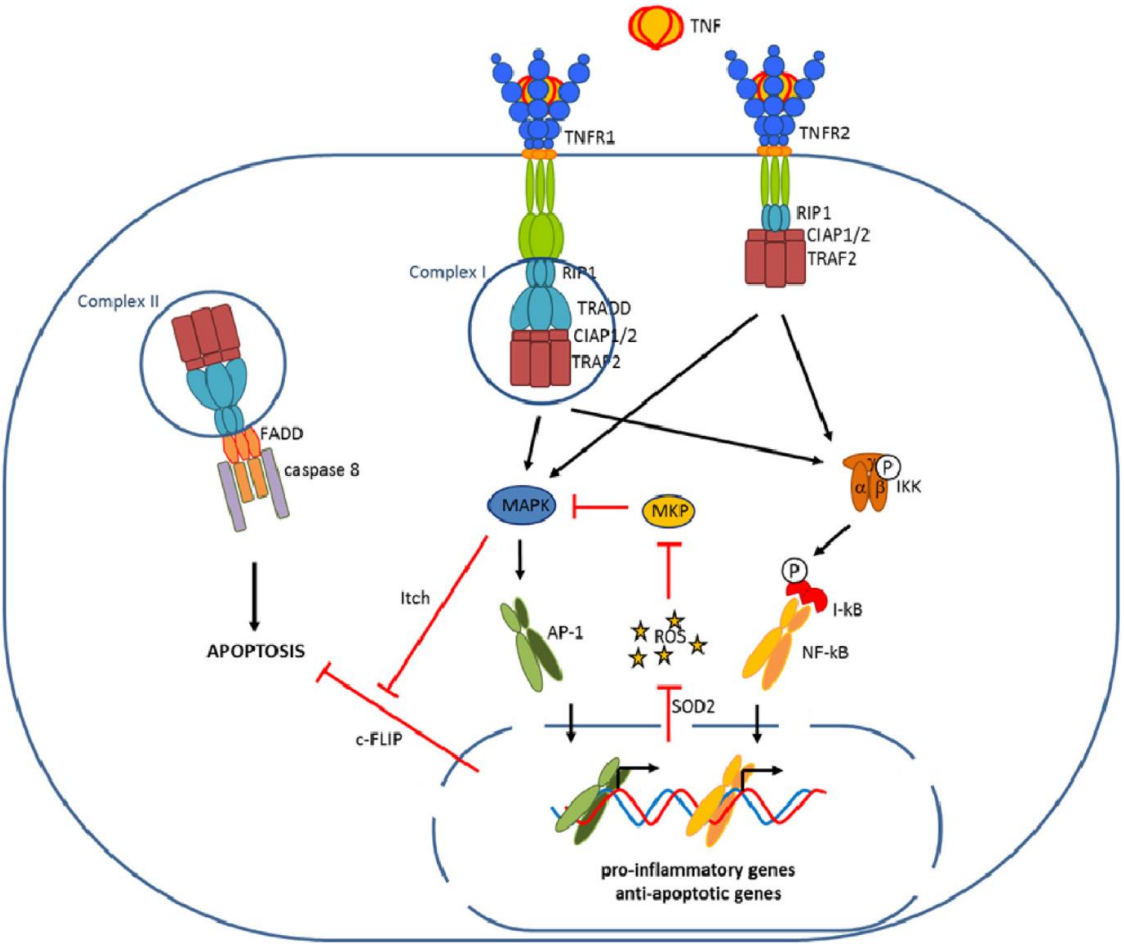

Figure 17: Downstream signalling via TNF receptors. TNFR1 Complex I and Complex II and TNFR2. From (Puimege et al., 2014).

1.4.5 TNF in the developing nervous system

TNF is expressed in both the PNS and CNS during development (Park and Bowers, 2010, Twohig et al., 2011). With regards to CNS development, TNF has been most studied in the hippocampus (reviewed in (Park and Bowers, 2010, Twohig et al., 2011)). To date, most data has suggested that TNF exerts a negative influence on hippocampal development. For example, the absence of TNF in transgenic mice leads to accelerated dentate gyrus development and improved spatial learning and memory by a mechanism that is thought to involve the loss of TNF-mediated suppression of NGF synthesis (Golan et al., 2004). In support of this, overexpression of TNF reduces hippocampal NGF expression and leads to deficits in spatial learning and memory (Fiore et al., 2000).

Moreover, *in vitro* studies have observed that the addition of TNF to hippocampal neuron cultures leads to a reduction in neurite length and branching (Neumann et al., 2002). However, discrepancies exist regarding the hypothesis that TNF is a negative regulator of hippocampal development and function, as CA1 and CA3 pyramidal neurons display less complex dendritic arborisation in TNF null mutant mice compared to wild type mice (Golan et al., 2004). Furthermore, TNF signalling via TNFR2 promotes the survival of hippocampal neurons *in vitro* (Yang et al., 2002). However, it must be stressed that the data obtained from studies investigating the roles of TNF in hippocampal development were only interpreted in the context of TNF forward signalling, and implications of effects resulting from the more recently discovered concept of reverse signalling should also be considered.

1.5 Concluding remarks

It is obvious that the TNFSF members are pleiotropic in nature, carrying out a plethora of roles in the developing and mature organism. Furthermore, the fact that some members of the family are able to reverse signal provides further opportunity for their versatility. Therefore they exemplify in many ways the concept of signal recycling.

With regard to TNF it is clear that it plays essential roles during nervous system development. In addition, it has the ability to reverse signal. Investigation into the roles of TNF reverse signalling in the development of a functional sympathetic nervous system therefore allows us to pose a number of interesting research questions.

1.6 Hypothesis and aims

In an attempt to identify novel regulators of PNS development, the Alun Davies group carried out a comprehensive qPCR screen on the TNFSF members, in sympathetic and sensory PNS ganglia. TNF was found to be highly expressed in the SCG at a developmental period coinciding with final target innervation. In addition, TNF is able to reverse signal during the immune response. These findings, together with the fact that various members of the TNFSF are positive or negative regulators of axonal growth during development, make TNF an interesting candidate to study its role during PNS development. This thesis sets out to establish whether TNF reverse signalling occurs and plays a role during SCG development, hypothesizing that it will positively or negatively regulate sympathetic survival and/or growth during final target innervation. The main aims of this project are outlined below.

1) Determine if TNF reverse signalling regulates either positively or negatively sympathetic survival and/or axon growth and target innervation during SCG development, using both an *in vitro* and *in vivo* approach.

2) Investigate the mechanism of TNF reverse signalling in sympathetic neurons and the possible resemblance with TNF reverse signalling in the immune response. Does extracellular calcium influx play a role in TNF reverse signalling during development?

3) Establish whether TNF reverse signalling operates in other kinds of neurons in the developing nervous system, specifically in sensory neurons.

Chapter 2
Materials and Methods

2.1 Animal husbandry

All animal work was conducted according to the regulations of the Home Office Animals (Scientific Procedures) Act, 1986. Embryonic and postnatal wild type CD1 mice and transgenic mice were obtained from timed matings. The presence of vaginal plugs was used for breeding confirmation. Embryonic day 1 (E1) was considered to be the day of fertilization and the day of birth postnatal day zero (P0). All animals were fed rodent global diet pellets (Harlan) and given water *ad libitum.*

In this study, three transgenic mice strains were used, all originating from C57BL/6 backgrounds. All transgenic mice were genotyped by polymerase chain reaction (PCR) (for details see Appendix I). Wild type (WT) and knock out (KO) mice for each strain were generated by crossing heterozygote (Het) females with Het males.

B6:129S6-*Tnf*$^{tm1Gkl/J}$ mice, from now on referred to as *Tnfα*$^{-/-}$, were kindly donated by K. Fox from Cardiff University. These mice were generated by a targeted deletion of the *Tnfα* gene that removes exon one (Pasparakis et al., 1996) and hence lack the expression of TNF. Tnfrsf1a^{tm1Imx} mice, from now on referred to as *Tnfrsf1a*$^{-/-}$, were generated by the targeted replacement of exons 2 to 5 of *Tnfrsf1a* with a neomycin resistance cassette (Peschon et al., 1998). This gene encodes the functional TNFR1 protein, therefore these mice lack TNFRI. B6.memTNF$^{\Delta/\Delta}$ mice, from now on referred to as *mTNF*$^{\Delta/\Delta}$, were generated by targeted replacement of exons 2 and 3 of the endogenous *Tnfα* gene, which encodes the TNF protein, with exons 2 and 3 of a genomic clone in which the TACE binding sites in these exons had been mutated using a PCR based mutagenesis approach (Ruuls et al., 2001). Therefore, *mTNF*$^{\Delta/\Delta}$ mice only express membrane-integrated TNF.

Tnfrsf1a$^{-/-}$ and *mTNF*$^{\Delta/\Delta}$ mice were obtained from D. Copland and A. Dick, University of Bristol and from G. Chaudhri, Australian National University, respectively.

All mouse lines survive until adulthood and have no obvious defects, therefore making them useful tools for the study of these genes and their functional proteins during sympathetic development. However, although not recorded, it has was observed along the course of this project that mice lacking either TNF or TNFR1 tend to develop glaucomas more frequently than their WT littermates. In addition, various studies on TNF and TNFR1 KO mice, have reported phenotypes which implicate these proteins in lymphatic tissue development and organisation, as well as, the immune response (Rothe et al., 1993, Pasparakis et al., 1996, Korner et al., 1997, Peschon et al., 1998). The splenic microarchitecture of TNF KO mice is abnormal. Specifically, the demarcation of T and B cell zones is compromised in these mice. Furthermore, TNF seems to also play a role in the organisation of Peyer´s patches (PP) zones in the spleen. It must be highlighted, that these roles seem to be restricted to the more advanced stages of development of lymphoid tissue, which are involved in specific cellular localisation (Pasparakis et al., 1996, Korner et al., 1997). TNFR1 KO mice also have abnormal lymphoid tissue structure and function. In addition, these mice are highly susceptible to infection caused by intracellular pathogens, in accordance with their role during the host defence mechanism against microorganisms (Rothe et al., 1993, Peschon et al., 1998). Mice that only express mTNF, have abnormal lymphoid tissue structure, but these defects are different to those observed in TNF KO mice, indicating distinct roles for sTNF and mTNF in lymphoid tissue structure development and organisation. These mice are also deficient in chemokine induction, in accordance with the role of their receptor, TNFR1, in the host defence mechanism against pathogens (Ruuls et al., 2001).

2.2 Primary neuronal cultures

Primary neuronal culture was used to define protein expression profiles of neurons under defined conditions and to determine the effects of soluble recombinant TNFR1-Fc, the knock down of specific genes and the inhibition of T-type calcium channels on the normal physiology and biochemistry of peripheral neurons. Dissociated SCG, nodose and trigeminal neurons from embryonic or P0 CD1 mice were cultured in a defined serum-free medium on a Poly-DL-ornithine/laminin substratum, a protocol developed and well established in the Davies lab (Davies et al., 1993). These cultures also contained non-neuronal cells, such as glia cells.

2.2.1 Culture dishes

Neurons were grown on a Poly-DL-ornithine/laminin substratum. 35 mm culture dishes (Greiner bio-one) were pre-coated with 1 ml of 0.5 mg/ml Poly-DL-ornithine (Sigma) and incubated overnight at room temperature (RT). The next day, Poly-DL-ornithine was aspirated and the dishes were washed twice with sterile water (Sigma) before being left to air dry, for 2 h, in a laminar flow hood. The centre of poly-DL-ornithine treated culture dishes were coated with 100 µl of 20 µg/µl laminin (Sigma) in Hanks Balanced Salt Solution (HBSS) (Sigma) and incubated at 37°C, for at least 25 min, prior to seeding the dishes with a dissociated neuron suspension.

2.2.2 Media

Following trypsin treatment, PNS neurons were washed to inactivate trypsin using F-12 washing media. Dissociated neurons were cultured in F-14 media.

Washing media (F-12)

50 ml of heat-inactivated horse serum (Gibco) was added to 500 ml of F-12 (Gibco). F-12 culture medium was sterile-filtered using a bottle top filter (Nalgene).

Culture Media (F-14)

294 mg of sodium hydrogen bicarbonate was added to 250 ml of sterile distilled water. 25 ml of this solution was discarded and replaced with 25 ml of 10X F-14 (JRH Biosciences). 2.5 ml of 200 mM glutamine (Gibco), 5 ml of albumax (Gibco) and 5 ml of penicillin(10000 units/ml)-streptomycin (10 mg/ml) (Sigma) were added to the F-14. Albumax, a bovine serum albumin (BSA) solution, was previously supplemented with progesterone (60 µg/ml), putrescine (16 µg/ml), L-thyroxine (400 ng/ml), sodium selenite (38 ng/ml) and tri-iodothyronine (340 ng/ml) (all from Sigma). F-14 culture medium was sterile-filtered using a bottle top filter.

2.2.3 Tungsten needles

Tungsten needles allow for precise, clean cuts and are ideal for cleaning dissected ganglia to remove adherent nerve roots and non-neuronal connective tissue. 5 cm long, 0.5 mm diameter tungsten wire (InterFocus) was bent at the tip at a 90 degree angle. The tungsten wires were then connected to the cathode of a variable, low voltage AC power supply. The anode of the power supply was immersed in a 2 M NaOH solution in a glass beaker. Next, tungsten needle tips were immersed in the NaOH solution and a 3-12 V AC current was passed through the solution. The tungsten tips were electrolytically sharpened by vertically dipping them in an out of the NaOH.

2.2.4 Dissections and plating neurons

Dissection tools (InterFocus) were sterilised with 70% ethanol before and after each use. Dissections were carried out in laminar flow hoods, in petri-dishes containing sterile

phosphate buffered saline (PBS) (Sigma). For embryonic ages, pregnant females were sacrificed by cervical dislocation at gestation periods E16 and E18. Embryos were isolated by laparotomy, placed in petri-dishes and staged using the Theiler mouse atlas of embryonic development (Westphal and Theiler, 2014) to confirm their developmental age. P0 pups were culled by decapitation. Peripheral ganglia dissections were carried out using scissors and forceps followed by tungsten needles to remove all connective tissue.

Dissections were carried out as described by Alun Davies in chapter 12 of Neural cell cultures: a practical approach (Cohen and Wilkin, 1995). Briefly, ganglia were visualised by bisection of the head along the medial sagittal plane followed by the removal of brain tissue and the occipital bone. This exposes the SCG and nodose ganglia which are located at the mouth of the jungular foramen. The SCG is oval in shape and is seen at the junction between the internal and external carotid arteries. The nodose ganglion is circular and smaller than the SCG and is found attached to the vagus nerve. The trigeminal ganglion is found adjacent to the hindbrain at the base of the skull.

Ganglia were enzymatically digested in 1 ml of Ca^{2+}/ Mg^{2+}-free HBSS (Gibco) containing 0.05% trypsin (Worthington), for 25 min at 37°C. After digestion, ganglia were washed twice with F-12 washing media before being mechanically dissociated, by passing through a 200 µl pipette tip several times, to produce a high density single cell suspension.

Dissociated neurons were appropriately diluted in F14 media (10 µl of cell suspension per 2 ml media) and plated onto 35 mm dishes that had been pre-treated with Poly-DL-

ornithine and laminin. Neuronal cultures were typically incubated at 37°C, for 18-24 h, in 5% $C0_2$.

2.3 Immunocytochemistry/Immunohistochemistry

Immunohistochemistry uses antibodies against specific proteins in order to visualise the location of these proteins in tissue or cells. Visualisation of targeted proteins is achieved by either chromogenic or fluorescence detection. In the first instance, antibodies are conjugated to enzymes that produce coloured deposits at the site of antibody-antigen binding when they are incubated with an appropriate substrate. In the second case, antibodies are conjugated to fluorophores and thus can be visualised by fluorescence (Javois, 1994).

2.3.1 Immunocytochemistry

For *in vitro* studies, primary neuronal cultures were fixed for 20 min with either ice-cold methanol or 4% paraformaldehyde (PFA) (Sigma), washed with PBS and blocked with 5% BSA, 0.1% Triton X-100 (Sigma) in PBS, for 1 h at RT. Fixed neurons were incubated, overnight at 4°C, with primary antibodies that had been appropriately diluted in 1% BSA (Table 1). Next day, the fixed cultures were washed with PBS and incubated with the appropriate Alexa-Fluor-labelled (Invitrogen) secondary antibody, diluted 1:500 in 1% BSA, for 2 h at RT. After a brief wash in PBS, to remove non-bound secondary antibody, protein expression was examined by confocal microscopy (Zeiss LSM 510).

2.3.2 Immunohistochemistry

For *in vivo* protein localisation studies, tissues (nasal turbinates and submandibular salivary glands at P0, P5 and P10) were dissected and fixed in 4% PFA, overnight. Fixed

tissues were washed with PBS and cryoprotected by incubating overnight, at 4°C, in 30% sucrose in PBS. The next day, cryoprotected tissues were embedded in OCT (Tissue-Tek) before snap freezing in 2-methylbutane/iso-Pentane (Fisher scientific) in a metallic crucible surrounded by dry ice. Embedded tissues were stored at -80°C until sectioning. Serial cryostat sections were cut at 15 µm, mounted onto glass slides and stained using the same protocol as outlined above for immunocytochemistry, with the exception that P10 sections were blocked in 5% BSA, 0.5% Triton X-100 in PBS. Fig.1 illustrates how sections looked and highlights the areas imaged, which correspond to the areas with the highest sympathetic innervation in each target organ. For the submandibular salivary gland, one lobe was selected for sectioning and imaging was concentrated on the gland tubules. While in the nasal turbinates, sectioning and imaging focused on the connective tissue of the core of the turbinates (Kisiswa et al., 2013).

Table 1: Primary Antibodies used for protein localisation

Antibody target	Source	Company	Dilution
β-III tubulin	Mouse	R&D Systems	1:500
TH	Sheep	Millipore	1:200
TNF	Rabbit	Abcam	1:200
TNFR1	Rabbit	Abcam	1:200
TNFR2	Goat	R&D Systems	1:20
CACNA1I/Cav3.3	Rabbit	Abcam	1:100
CACNA1H/Cav3.2	Goat	Santa Cruz	1:200
CACNA1G/Cav3.1	Goat	Santa Cruz	1:200

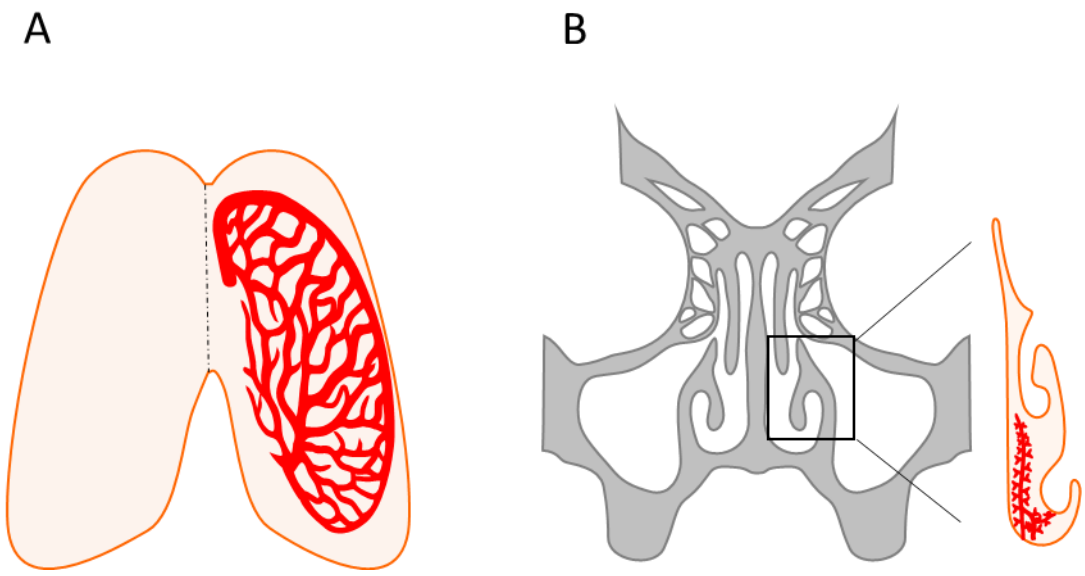

Figure 1: Schematic of sectioning and staining of target organs .Sectioning and imaging was focused on the areas of highest sympathetic innervation. **A)** Salivary submandibular gland, the area of interest was the gland tubules. **B)** Nasal turbinates, the area of interest was the connective tissue of the core turbinates. Red areas illustrate sympathetic innervation.

2.4 Neuronal growth and survival

Dissociated primary neuronal cultures were used to investigate TNF reverse signalling *in vitro*. Embryonic or P0 cultures were set up from SCG, nodose and trigeminal ganglia and in most cases were supplemented with either 10 ng/ml NGF (R&D Systems), in the case of SCG and trigeminal neurons, or 10 ng/ml BDNF (R&D Systems), in the case of nodose neurons, to promote neuron survival and process outgrowth and branching. In these type of cultures dendrites and axons are not distinguishable, hence process/neurite branching and growth is assessed. However, in short-term cultures, such as these, processes are almost exclusively axons. Cultures were incubated overnight with different combinations of neurotrophic factors, 10 ng/ml TNFR1-Fc chimera (R&D Systems) and 200 nM of the selective T-type calcium channel blockers, TTA-A2 and TTA-P2 (Alomonelabs). Some experiments were carried out without the addition of

neurotrophic factors. In these cases, 1 µg/ml of the cell-permeant broad-spectrum caspase inhibitor Q-VD-OPh (R&D Systems) was added to cultures in order to inhibit apoptosis.

For experiments designed to determine the effect of exogenous reagents on the extent of neuronal process outgrowth and branching, neuronal cultures were stained after 18-20 h by adding 100 ng/ml of the vital dye, calcein-AM (Invitrogen) to cultures and incubating at 37°C for 30 min. Calcein-AM is a cell-permeant, non-fluorescent dye that is metabolised within living cells by intracellular esterases. Once metabolised, calcein-AM becomes non-cell permeant and fluoresces strongly green, thereby enabling neurons and their processes to be imaged using a fluorescent microscope (Zeiss Axiovert 200). In order to asses neuronal growth and branching *in vitro,* a modified and automated Sholl analysis was used, as described in (Gutierrez and Davies, 2007), to analyse imaged neurons. In this analysis, virtual concentric rings of increasing radii are centred at the neuron soma and the number of neurites intersecting each of the rings are counted (Fig.2). Sholl profiles are graphical representations of neuritic morphology and represent the number of intersections that neurites make with each of the virtual centric rings vs the radial distance of the rings from the cell soma (Sholl, 1953). The improved Sholl analysis method increases the efficiency of analysis, by reducing the number of data inputs (Gutierrez and Davies, 2007), and runs on the statistical analysis programme, MATLAB. The output from MATLAB is in the form of an Excel spreadsheet that not only allows the plotting of a Sholl profile for each experimental condition, but also allows mean total neurite length and mean number of branch points per condition to be ascertained. At least 50 images were taken from individual neurons for each

experimental condition in each experiment. Each experiment was repeated at least three times.

For experiments designed to analyse the effect of exogenous reagents on neuron survival, neuron survival was estimated as follows. 2 hours after plating, 35 mm culture dishes were placed on top of a larger petri dish that had a 12 X 12 mm grid scored onto it, so that the grid was under the centre of the culture dish, and the number of neurons within the grid were counted using a phase contrast microscope. The number of surviving neurons within the grid was counted after 24 h of culture and expressed as a percentage of the neuron count at 2 h.

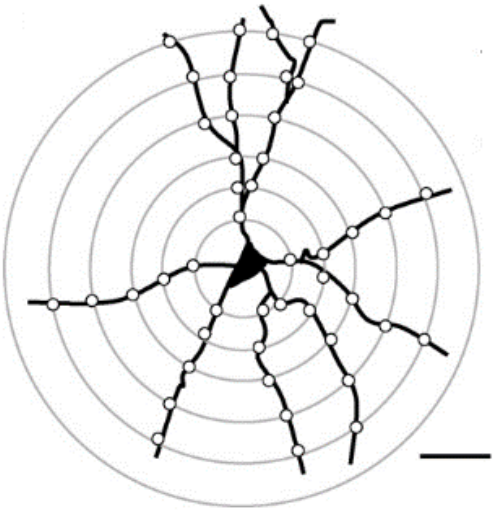

Figure 2: Sholl analysis. Rings of increasing radii are centred at the cell soma and the neurites intersecting the rings are counted. Adapted from (Gutierrez and Davies, 2007).

2.5 Microfluidic compartment cultures

During development, extending axons are subjected to different environments compared to their cell bodies as they grow towards and reach their targets. Microfluidic devices mimic this *in vitro*, as they are able to expose the soma and processes of

individual neurons to separate fluid micro-environments. This allows the effects of adding reagents to either the soma or processes, on the extent of process outgrowth, to be individually assessed. Microfluidic devices are made up of two chambers connected by a series of small micro-channels that are just wide enough to allow processes to grow through them (Fig.3). Therefore, if neurons are seeded into one chamber they can extend processes across the micro-channel barrier into the other chamber. The media in the two chambers is fed from two wells, one at the top and one at the bottom of each chamber (Fig. 3). The volumes of media in the two chambers can be adjusted to establish a small hydrostatic pressure differential between the chambers. This ensures that reagents added to one chamber do not leak into the other chamber through the micro-channels (microfluidics, 2009).

Microfluidic devices (Xona) were placed on polyornithine treated 35 mm culture dishes and the right and left chambers and micro channels were coated with laminin by adding 100 µl and 80 µl of 10 ug/ml laminin in HBSS to the left and right wells, respectively. After 25 min, the laminin in the right well was aspirated. A very high density, P0 SCG neuronal cell suspension was established from CD1 neonates as described above (2.2) and 10 µl was slowly pipetted into the opening of the right hand side chamber of each microfluidic device through the top and bottom right hand wells, thereby filling the right chamber with the neuronal cell suspension. After incubating for 30 min, at 37°C in 5% CO_2, to allow the neurons to attach to the substratum in the right chamber, the right (soma) and left (axon) chambers were filled with F14 culture media containing the desired combination of experimental reagents, by slowly pipetting 100 µl of F14 into the right hand wells and 90 µl of F14 into the left hand wells. Cultures were incubated for 24 h, at 37°C, in 5% CO_2. After 24 h, 1 µl of a 1:10 dilution of calcein-AM in F14 was added

to the top and bottom left hand wells that feed the neuronal process chamber. The microfluidic chambers were then covered and left to incubate at 37°C for 30 min. The regions of the right and left chambers that are proximal to the micro-channels were imaged in a series of non-overlapping sections, in a methodical top to bottom manner, using a fluorescent microscope. Images were analysed by a stereological based method, as described in (Ronn et al., 2000), to determine mean process length. Briefly a grid with 200 µm squares was superimposed on the images. The number of times processes of neurons that grew across the micro-channel barrier crossed the 200 µm grid line was recorded, as well as the total number of neurons that had processes that crossed the micro-channel barrier. Length was determined by the formula: πDI/2, where D is the interline interval (200) and I the mean number of intersections (I=number of intersections/number of cell bodies).

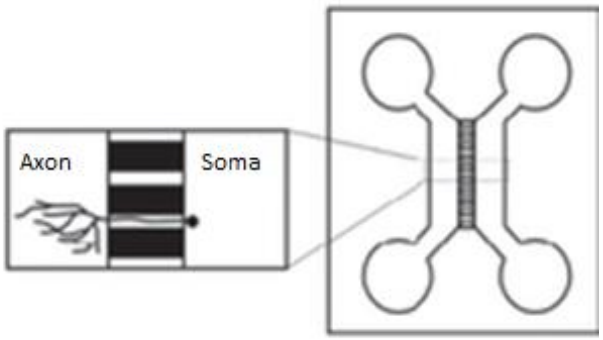

Figure 3: Schematic of microfluidic compartment cultures. Neurons are plated into the right chamber through upper and lower right side wells. Processes are able to grow through a micro-channel barrier into the left side chamber. The fluid environments that fill each chamber are effectively isolated by the creation of a hydrostatic gradient between the chambers, enabling the soma and axons to be exposed to different experimental conditions. Adapted from (Kisiswa et al., 2013).

2.6 Whole mount staining

Whole mount staining, which allows the staining of intact organs and structures, was used to analyse sympathetic innervation of the submandibular salivary gland, pineal gland, trachea, heart, spleen, kidney and stomach of P10 *Tnfrsf1a*$^{-/-}$, *Tnfα*$^{-/-}$ and *mTNF*$^{\Delta/\Delta}$ mice and their wild type littermates. Whole mount staining follows the same principles as immunohistochemistry, but requires some modifications to the immunohistochemistry protocol described above. In this thesis, the DAB-HRP method of antigen detection was used, whereby secondary antibodies were conjugated to horseradish peroxidase (HRP). HRP catalyses the oxidation of the chromogenic substrate, DAB, producing a brownish product that remains in the vicinity of the secondary antibody.

The submandibular salivary glands, pineal glands, tracheae, hearts, spleens, kidneys and stomachs of P10 mice were fixed in 4% PFA, at 4°C, for 24 h. Milk was removed from the stomachs by making a sagittal incision on the ventral mesentery of the stomach before fixation. Following fixation, the PFA was aspirated, replaced with fresh 4% PFA and incubated at RT for 1 h. Next, tissues were dehydrated in 50% methanol (MeOH), for 1 h at RT, and 80% MeOH for a further 1 h at RT. After dehydration, endogenous peroxidase activity was quenched by placing organs in 80% MeOH/20%DMSO/3%H_2O_2, overnight at 4°C. The next day, tissues were rehydrated by sequential incubations in; 50% MeOH for 1 h at RT, 30% MeOH for 1 h at RT, PBS for a further 1 h at RT. Rehydrated tissues were blocked by incubating, overnight at 4°C, with PBS containing 4% BSA and 1% Triton X-100 (blocking solution). Organs were then incubated, for 72 h at 4°C, with rabbit polyclonal anti-TH antibody (1:200, Millipore) in blocking solution. Next, samples

were washed three times, at RT for 2 h each, in PBS containing 1% Triton X-100 before being washed a fourth time, overnight at 4°C, in this solution. Washed tissues were incubated, overnight at 4°C, with HRP conjugated anti-rabbit secondary antibody (Promega), diluted 1:300 in PBS containing 4% BSA plus 1% Triton X-100. Samples were then washed three times, at RT for 2 h each, with PBS containing 1% Triton X-100. All previous steps were carried out on a shaker.

TH-positive fibres were visualized by HRP- DAB staining. Target tissues were incubated with 1X DAB for 20 min at RT and then with DAB containing 0.006% H_20_2 for less than 5 min to develop staining. The developing step was followed by two quick PBS washes and an overnight incubation, at 4°C, in PBS. BABB (1 part benzyl alcohol: 2 parts benzyl benzoate, both Sigma) was used as a clearing solution. Tissue was placed in 50% MeOH for 10 min at RT and then washed 3 times with 100% MeOH (1X 30min, 2X 15min) at RT. Following this, tissues were incubated in 1 part MeOH: 1 part BABB for 5 min, at RT, and finally placed in 100% BABB.

Samples were imaged by phase contrast light microscopy (Nikon Diaphot). The same orientation and area was imaged, for each animal and for each tissue, by using anatomical landmarks. Confocal microscopy and z-stacking were not a possibility. Therefore, anatomical landmarks were also used as guidelines for focusing and acquiring images on the same plane for each target organ. The axonal bundles entering submandibular salivary glands, pineal glands and hearts and the lateral axonal bundle entering the tracheae were used as guides. For the heart, the images were concentrated on the axon bundles entering the left ventricle. It was difficult to maintain the structural integrity of the stomach after removal of milk, therefore the most intensely innervated

area closest to the ventral incision was imaged. The axon bundles entering the renal plexus around the renal artery were used as anatomical landmarks for the kidney, and the bundles following the splenic arteries were used as guides for the spleen. Fig.4 illustrates the areas chosen for imaging based on anatomical landmarks.

To compare the extent of sympathetic nerve branching, a modified line-intercept method was used. Using ImageJ, a grid of 24 squares (4 X 6 squares, 158 µm side length per square) was aligned in a standard orientation on images of the submandibular salivary gland, trachea, heart, spleen, kidney and stomach. For the smaller pineal gland, the grid consisted of 6 X 6 squares of side length 50 µm per square. The number of fibre bundles intersecting the sides of squares in the grid was scored blind for each of the organs from each animal. Fibre density was estimated using the formula $\pi DI/2$, where D is the interline interval (158 or 50) and I the mean number of intersections along one side of each square in the grid. For the placement of the grid in each target organs refer to Fig.4.

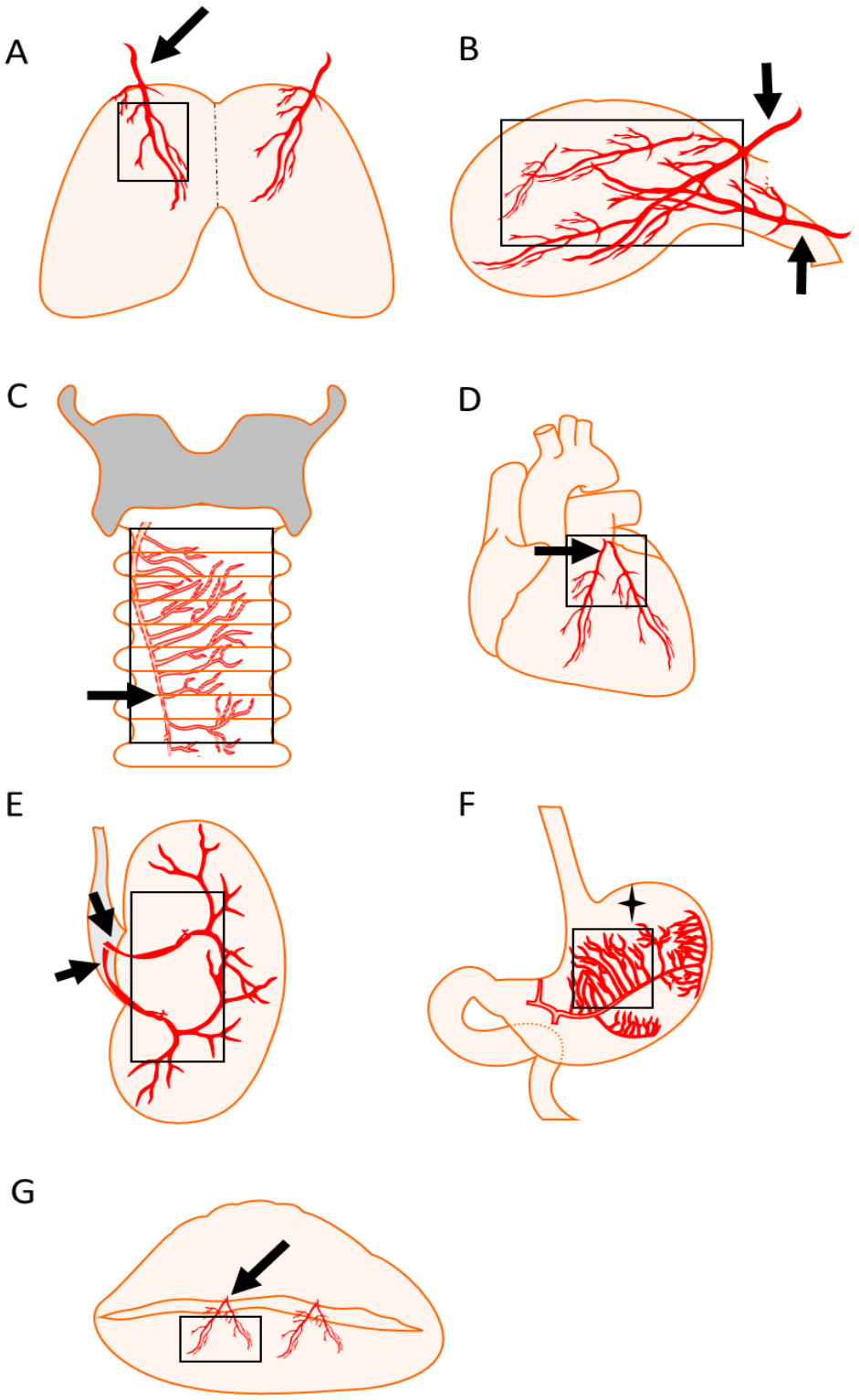

Figure 4: Schematic of areas imaged and anatomical landmarks used in whole mount staining. A) Salivary submandibular gland, **B)** pineal gland,**C)** trachea, **D)** heart, **E)** kidney, **F)** stomach and **G)** spleen. Black arrows indicate anatomical landmarks and star indicates that no anatomical landmark was available. Red areas depict sympathetic innervation and black squares indicate the placement of grids for quantification.

2.7 Transfections

Transfections allow the introduction of desired foreign nucleic acids into cells. In this study, I took advantage of this technique in order to knockdown gene expression via small hairpin RNA (shRNA). The expression of the genes for the three types of T-type calcium channels, *Cav3.1, Cav3.2* and *Cav3.3*, was reduced using this method.

2.7.1 Transfection vectors

For shRNA experiments, plasmids were obtained from Origene. shRNAs (refer to Table 2 for shRNA sequences) were cloned into the vector pGFP-V-RS, which allows for expression of green fluorescent protein (GFP) in transfected cells as well as the shRNA.

Table 2: ShRNA construct sequences

CACNA1G/Cav3.1	CACNA1H/Cav3.2	CACNA1I/Cav3.3
CGTCACATTAACTGCTGGATACC TTGCCTA	CGCTGGAGATAAGCAACATCGT GTTCACC	TCAACCTGTGCCTCGTTGTCATAG CGACC
TAACCTGCTTGTCGCCATTCTCGT GGAGG	CTGCGGAACCGATGCTTCCTGGA CAGCGC	CACGGTGTCTAACTACATCTTCAC AGCCA
GCCTCTGAACACCAAGACTGTAA TGGCAA	TCATCTTCCTCAACTGTATCACCA TTGCC	CATCTTCCTCAACTGTATCACCAT TGCTC
CAGTCAGGCTCCATCTTGTCTGTT CACTC	GTATCTGTGTCCAGGATGCTCTC GCTACC	CGTTGGAGGCGACACTGAGAGC CACCTGT

Table 3: Plasmid description

Plasmid	Company	Resistance gene	Sequence of interest
p-GFP-shRNA-V-RS	Origene	Kanamycin	Refer to Table 2

2.7.2 Bacterial transformation and plasmid preparation

Competent *E.coli* H107 cells (Promega) were thawed on ice. 50 ng of cold plasmid DNA was added to 100 µl of bacteria, mixed carefully and incubated on ice for 30 min.

Subsequently, bacteria were heat shocked, by placing in a 42°C water bath for 90 s and returned to ice for 5 min. 900 µl of Luria Bertani (LB) medium (Fisher Scientific) without antibiotics was then added and the mixture was incubated at 37°C for 1 h with agitation. LB agar (Fisher Scientific) plates containing 50 µg/ml kanamycin (Sigma) were prepared beforehand. 100 µl of the LB mixture was spread onto an agar plate with a sterile spreader and the rest was centrifuged, resuspended in 100 µl LB and spread onto a different agar plate. Agar plates were incubated at 37°C overnight. The following day, several colonies were selected randomly and grown in 3 ml LB containing antibiotics for 8 h, at 37°C, with agitation. 1 ml of the 8 h culture was added to 200 ml of LB with antibiotics and incubated overnight, at 37°C, in a shaking incubator. The next day, plasmid DNA was isolated and purified from the bacterial culture using a Highpure Plasmid Filter Midiprep kit (Invitrogen) according to the manufacturer's instructions.

2.7.3 Transfection of neurons by electroporation

Primary neuronal cultures from P0 CD1 mice were set up as above up to the stage of trypsinization (2.2). After trypsin incubation, ganglia were washed once with F-12 and twice with PBS, before being mechanically dissociated in 30-60 µl electrolytic buffer (Invitrogen). 2.5 µg of desired plasmid was added to 12 µl of dissociated neuron suspension and the suspension was electroporated using a microporator (Digital Bio) (2X 30 ms pulses at 900 V).

2.8 Calcium imaging

Calcium (Ca^{2+}) can act as a secondary messenger during signal transduction and plays a vital role in the normal physiology and biochemistry of cells. Therefore, Ca^{2+} imaging is a key tool in order to understand many cellular mechanisms. Ca^{2+} imaging exploits Ca^{2+}

indicator molecules whose fluorescent properties change after binding Ca^{2+}. Two types of Ca^{2+} indicators are used; chemical indicators and genetically encoded Ca^{2+} sensors. This thesis utilises the chemical indicator, Fura-2.

2.8.1 Fura-2 calcium imaging

Fura-2, a ratiometric fluorescent dye that binds to intracellular Ca^{2+}, was used to visualise Ca^{2+} entry into SCG neurons. SCG neurons were cultured for 12 h at high density in the presence of 10 ng/ml NGF. The culture media was then changed to Ringer's solution (125 mM NaCl, 4 mM KCl, 1.2 mM $CaCl_2$, 0.5 mM $MgCl_2$, 10 mM glucose and 10 mM HEPES, pH 7.4) containing 0.1% BSA and 1 mg/ml Fura-2 AM (Invitrogen). Neurons were incubated in this media for 30 min at RT and then washed twice, for 10 min each time, with Ringer's solution. Neurons were then exposed to Ringer's solution containing either 5 µg/ml TNFR1-Fc or TNFR1-Fc plus 1 µM of the relatively non-selective calcium channel blocker, mibefradil. Time-lapse imaging of the 340/380 nm ratio was carried out using a Zeiss Axiovert 200 fluorescence microscope. The mean percentage change in the 340/380 nm ratio (minus background) was calculated.

2.9 Gene expression analysis

Reverse transcription-quantitative PCR (RT-qPCR) is a powerful tool to measure the amount of a specific mRNA sequence present in an RNA sample. Following reverse transcription of mRNAs into cDNA, qPCR amplification of specific target cDNA sequences is based on the classical PCR reaction, but the amount of DNA that accumulates at each cycle of amplification is quantified by using either a fluorescent intercalating dye or fluorescent probes.

In this thesis, dual-labelled hybridization probes were used to detect the exponential increase in PCR products during qPCR cycling. Dual-labelled hybridization probes are sequence-, and hence template-specific. The probes anneal to one of the template strands during the annealing step of PCR, just 3' to one of the primers. The 5' end of the probe is labelled with a FAM fluorophore. The 3' end of the probe is labelled with a quencher molecule that is close enough to the FAM to stop it fluorescing as a result of fluorescence resonance energy transfer (FRET). As the PCR primer that is close to the probe is extended to reach the probe during the extension phase of the PCR reaction, the inherent 5' to 3' exonuclease activity of Taq polymerase cuts the probe into single nucleotides, thereby releasing the FAM fluorophore into solution. Since the free FAM can no longer be quenched by BHQ1, it fluoresces. The amount of free, unquenched, fluorescent FAM increases exponentially on a cycle by cycle basis. Because dual-labelled hybridization probes are template specific, they significantly increase the specificity of the PCR reaction compared to Sybr Green incorporation, the most commonly used qPCR product detection method. The amount of amplified products of the qPCR reaction are directly proportional to the fluorescence signal detected by the qPCR thermal cycler once the fluorescence exceeds the threshold detection level of the thermal cycler. Since the number of qPCR reaction cycles that have been completed when threshold detection has been reached (Ct value) is inversely proportional to the amount of initial target cDNA, the greater the amount of initial target cDNA the lower the Ct value.

2.9.1 RNA extraction

Peripheral ganglia target organs were dissected and incubated, overnight at 4°C, in 10 volumes of RNA-later (Ambion), after which they were stored at -80°C. Desired tissue was dissected from three embryos or pups from the same litter and this was repeated

for at least three different litters. The RNeasy Lipid Mini extraction kit (Qiagen) was used to extract and purify total RNA according to the manufacturers' instructions.

2.9.2 Reverse transcription

40 µl reverse transcription reactions were carried out containing; 10 µl of RNA sample, 2 µl AffinityScript reverse transcriptase (Agilent technologies), 1X manufacturer's buffer, 5 mM dNTPs (Roche) and 10 µM random hexamers (Fermentas). Reverse transcription was carried out for 1 h at 45°C.

2.9.3 qPCR

2 µl of the resulting cDNA was amplified in a 20 µl reaction using Brilliant III ultrafast qPCR master mix reagents (Agilent). Dual labelled (FAM/BHQ1) hybridisation probes (Eurofins) specific to each of the cDNAs of interest were used to detect PCR products. The sequences of primers and probes can been seen in Table 4. Forward and reverse primers were used at 225 nM, and dual-labelled probes were used at a concentration of 500 nM. Primers and probes were designed using Beacon Designer software (Premier Biosoft). qPCR was carried out on the Stratagene MX3000P thermal cycler. Cycling conditions were: 30 s at 95°C; followed by 45 cycles consisting of 10 s at 95°C and 30 s at 60°C. Standard curves were generated for every PCR run with each primer/probe set using: either serial five-fold dilutions of reverse transcribed adult mouse spleen RNA (Zyagen) for quantification of *Tnfrsf1a*, *Tnfrsf1b* and *Tnfα* mRNAs and reference mRNAs or serial five-fold dilutions of reverse transcribed adult mouse brain RNA (Zyagen) for quantification of *Cav3.1*, *Cav3.2* and *Cav3.3* mRNAs and reference mRNAs. *Tnfrsf1a*, *Tnfrsf1b*, *Tnfα, Cav3.1*, *Cav3.2* and *Cav3.3* mRNA levels were expressed relative to the geometric mean of the reference mRNAs; *Gapdh*, *Sdha* and *Hprt1*.

Table 4: qPCR primer and probe sets

Gene	Oligo	Sequence (5' to3')
Tnfα	Forward	CTC CCT CTC ATC AGT TCT AT
	Reverse	CTA CAG GCT TGT CAC TCG
	Probe	FAM-CCC AGA CCC TCA CAC TCA GAT-BHQ1
Tnfrsf1a	Forward	TTC CCA GAA TTA CCT CAG
	Reverse	AAC TGG TTC TCC TTA CAG
	Probe	FAM-CAC CGT GTC CTT GTC AGC-BHQ1
Tnfrsf1b	Forward	CTC CAA GCA TCC TTA CAT
	Reverse	GTC CTA ACA TCA GCA GAC
	Probe	FAM-ATG TCA CTC CAA CAA TCA GAC CAA T-BHQ1
Cav3.1	Forward	CTG GTT ATT CTC CTC AAC T
	Reverse	TTC CCA AAG ATA CCC AAA
	Probe	FAM-CGA CCA TCT TCA CCA CCA-BHQ1
Cav3.2	Forward	TGC TTC TTC GTC TTC TTC
	Reverse	CAG ATG AAT GGG TTC TCC
	Probe	FAM-CCT CCT CTG TCT GGT AGT ATG GC-BHQ1
Cav3.3	Forward	CAT TGG AAA CAT TGT CCT C
	Reverse	CAG TGA TAG AAC TTG CCT
	Probe	FAM-CGC CTT CTT CAT CAT CTT CGG T-BHQ1
Gapdh	Forward	GAG AAA CCT GCC AAG TAT G
	Reverse	GGA GTT GCT GTT GAA GTC
	Probe	FAM-AGA CAA CCT GGT CCT CAG TGT-BHQ1
Sdha	Forward	GGA ACA CTC CAA AAA CAG
	Reverse	CCA CAG CAT CAA ATT CAT
	Probe	FAM-CCT GCG GCT TTC ACT TCT CT-BHQ1
Hprt1	Forward	TTA AGC AGT ACA GCC CCA AAA TG
	Reverse	AAG TCT GGC CTG TAT CCA ACA C
	Probe	FAM-TCG AGA GGT CCT TTT CAC CAG CAA G-BHQ1

2.10 Statistics

If data was normally distributed, pair-wise comparisons were analysed by two tailed student T-tests. If data was not normally distributed, the non-parametric Mann-Whitney-U test was used. One-way ANOVA followed by *post-hoc* analysis with Tukey's honest significant difference (HSD) was carried out for statistical analyses of data from three or more experimental conditions.

Chapter 3
TNF mediated reverse signalling in developing sympathetic neurons *in vitro*

3.1 Introduction

TNFSF members are active either as soluble trimeric or membrane-integrated ligands. Several membrane-integrated TNFSF members can additionally function as receptors for their respective TNFRSF partners and mediate reverse signalling. It has been demonstrated in cell lines and a variety of cells of the immune system that at least ten TNFSF members are capable of mediating reverse signalling (Sun and Fink, 2007). In the case of membrane-integrated TNF (mTNF), reverse signalling has been shown to stimulate T-cells to express cytokines and adhesion molecules (Ferran et al., 1994, Higuchi et al., 1997, Harashima et al., 2001) and to differentially regulate T cell activity against allogenic endothelial cells (Vudattu et al., 2005). TNF reverse signalling can be induced experimentally by soluble TNFR1 and TNFR2, resulting in the desensitization of monocytes and macrophages to lipopolysaccharide (LPS) (Eissner et al., 2000, Kirchner et al., 2004b), activation and apoptosis of monocytic cells (Waetzig et al., 2005, Xin et al., 2006) and sensitization of natural killer (NK) cells to activating stimuli by increasing their cytotoxicity *in vitro* (Yu et al., 2009). Interestingly, the N-terminal cytoplasmic domains of TNFSF proteins are conserved across species but vary between family members, which is consistent with conserved biological functions mediated by reverse signalling. Furthermore, the cytoplasmic domains of six (TNF among them) of the ten TNFSF members that have been shown to mediate reverse signalling contain a CKI binding site, raising the possibility that this motif may be involved in reverse signalling (Sun and Fink, 2007).

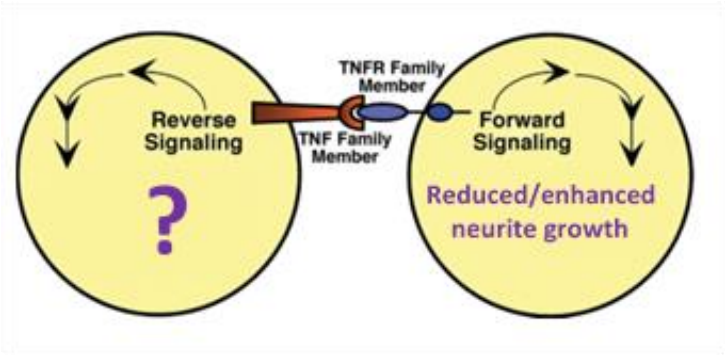

Figure 1: TNFSF forward and reverse signalling. Schematic representation of TNFSF forward and reverse signalling and its effect in the developing PNS. Adapted from (Sun and Fink, 2007).

This chapter reports my contributions to a recently published study from the Davies laboratory (Kisiswa et al., 2013) together with related unpublished work. This study reported for the first time the occurrence of TNF reverse signalling in the nervous system and demonstrated its physiological relevance. The investigation showed that TNF reverse signalling enhances the growth and branching of axons from developing sympathetic neurons in culture and plays an important role in establishing sympathetic innervation *in vivo*. The aims of the work reported in this chapter were to ascertain the expression and localisation of TNF and TNFR1 in SCG neurons and their targets during development and to characterise the effects of TNF reverse signalling on sympathetic axon growth *in vitro.*

RESULTS

3.2 Localisation of TNF and TNFR1 in SCG neurons and target organs

Work by others in the Davies group showed that *Tnfα* and *Tnfr1sf1a* transcripts are expressed in the developing SCG (Appendix II, Fig.1.A) (Kisiswa et al., 2013). These transcripts encode the TNF and TNFR1 proteins respectively. The highest levels of expression of both transcripts (between P0 and P10) coincides with the period when SCG neurons require target field-derived NGF for survival and SCG axons are arborizing within target fields and establishing their final pattern of innervation. To determine the cellular localisation of TNF and TNFR1, I used immunocytochemistry in dissociated SCG cultures and immunohistochemistry in tissue sections.

Dissociated cultures of P0 SCG neurons were grown overnight in the presence of NGF to sustain their survival and promote neurite growth. Neurons were positively identified by β-III tubulin staining. Cultures were double labelled with anti-β-III tubulin and anti-TNF and with anti-β-III tubulin and anti-TNFR1 (Fig.2). These studies demonstrated that all P0 SCG neurons in these cultures expressed both proteins. Whereas TNF immunostaining was observed at the cell bodies and along the full extent of axons, TNFR1 immunostaining was restricted to the cell bodies. Cultures incubated with secondary antibody alone exhibited no background immunofluorescence.

The expression of TNF and TNFR1 were studied in sections of the submandibular salivary gland (SMG) and nasal turbinates (NT) of P0, P5 and P10 CD1 pups. Refer to section 2.3.2 for illustrations depicting areas imaged and sectioned. In order to validate the specificity

of the antibodies used both in immunocytochemistry (Fig.2) and immunohistochemistry (Fig.4) sections from target organs from both TNF and TNFR1 KO mice were used as negative controls. Sympathetic fibres were recognised in these sections by double labelling the sections with anti-tyrosine hydroxylase (TH) antibodies. TH catalyses the rate-limiting step in catecholamine biosynthesis and is an established marker for sympathetic fibres (Flatmark, 2000, Glebova and Ginty, 2004).Tissue sections from Tnfα$^{-/-}$ (Fig.3A) and *Tnfrsf1a*$^{-/-}$ (Fig.3B) animals were not stained with anti-TNF and anti-TNFR1, respectively, demonstrating the specificity of these antibodies. TH staining is present (red) while TNF and TNFR1 staining is absent (green) (Fig.3).

Following the validation of antibodies the expression of TNF and TNFR1 were studied in CD1, wild type, mice. TH-positive fibres were doubled labelled with anti-TNF but not with anti-TNFR1.in both target organs. TH staining shows localisation of transversed axons, as the samples are sectioned Intense TNFR1 immunoreactivity was, however, evident in the surrounding tissue of both the submandibular salivary gland and nasal turbinates (Fig.4). The areas imaged and the tissue with high TNFR1 immunoreactivity correspond to the areas where sympathetic innervation is concentrated in both targets. In the salivary submandibular gland these are the gland tubules and in the nasal turbinates the connective tissue found in the core of the nasal turbinates (Kisiswa et al., 2013). This staining pattern was observed at all ages studied and is consistent with the axonal localisation of TNF but not TNFR1, as observed in cultured SCG neurons. Sections incubated with secondary antibody alone exhibited no background immunofluorescence (Fig.4).

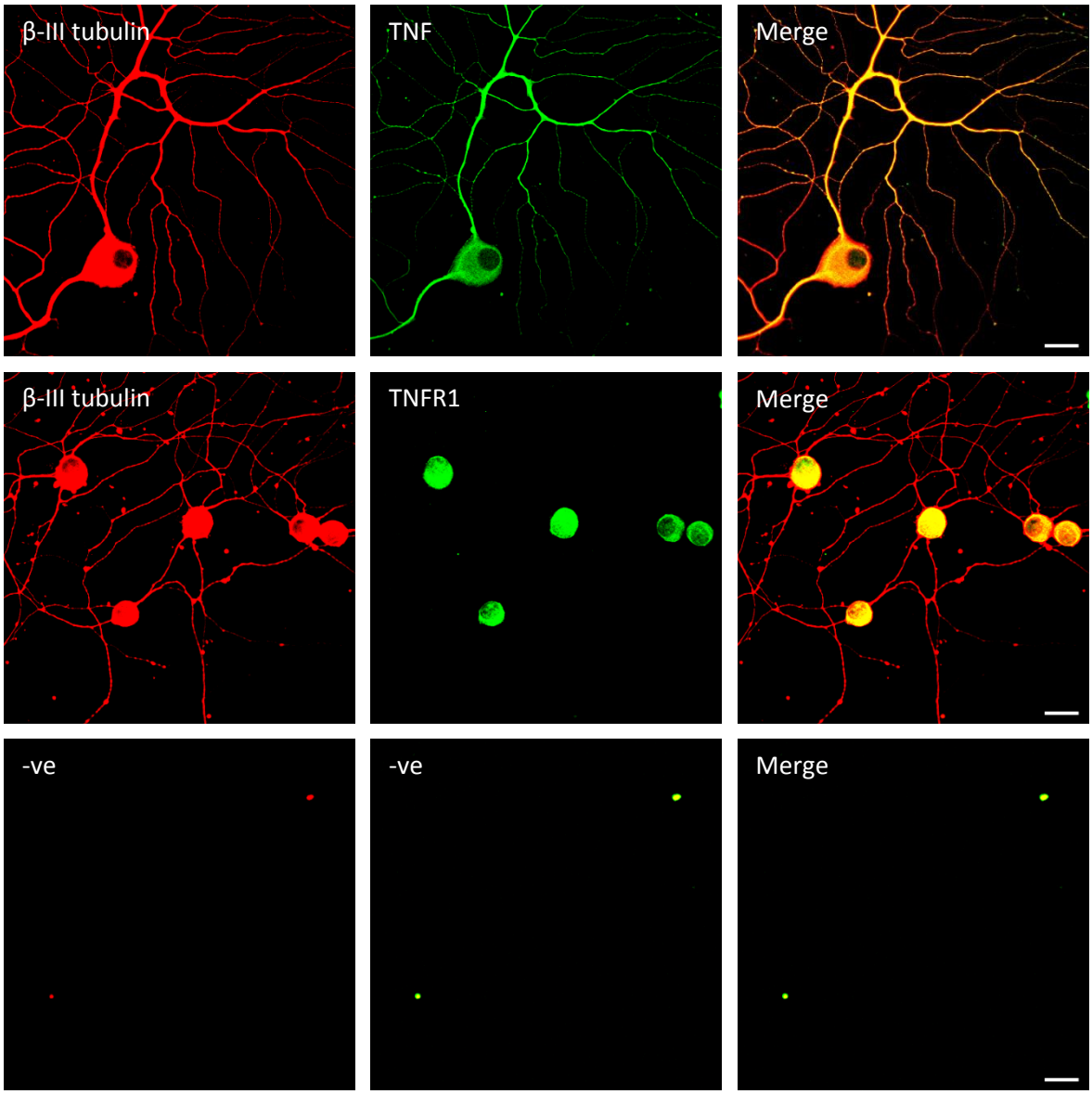

Figure 2: TNF and TNFR1 are expressed by developing SCG neurons. Dissociated P0 SCG neurons were cultured overnight in the presence of 10 ng/ml NGF and stained the next day with specific antibodies for TNF and TNFR1. The cultures were double labelled with anti-β-III tubulin to positively identify neurons and outline the full extent of their processes. The lower panels show cultures in which the primary antibodies were omitted from the staining protocol. Scale bar, 20µm, n=3.

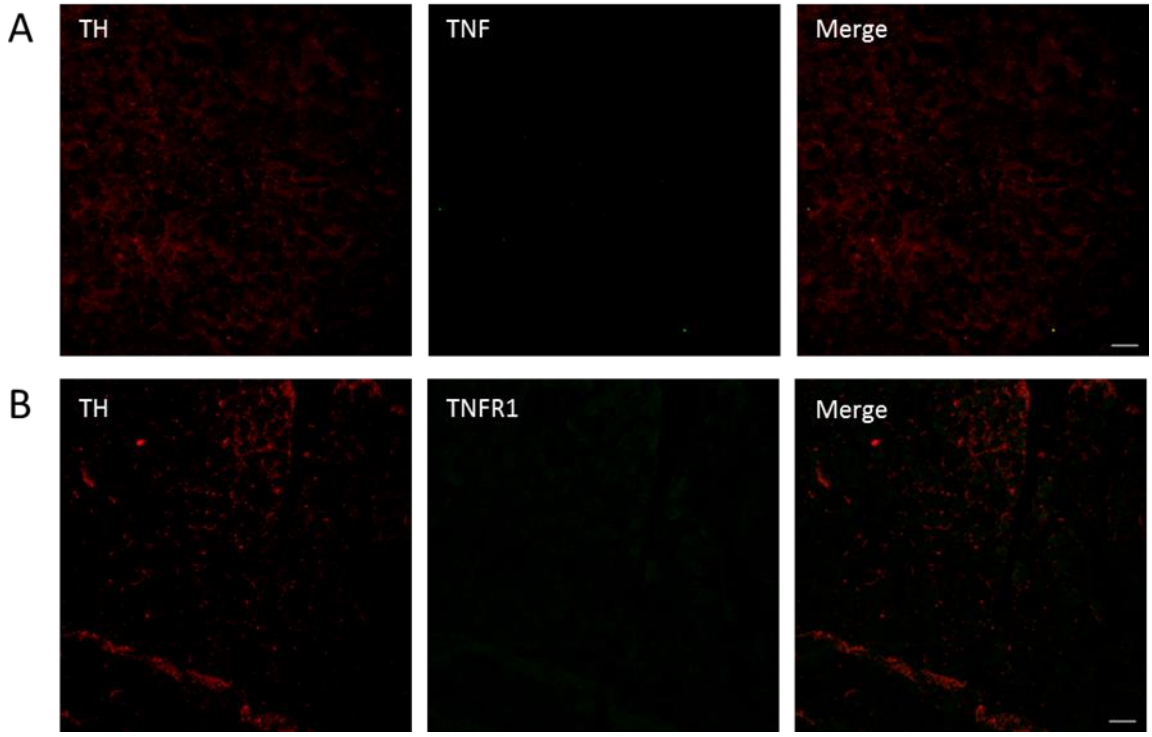

Figure 3: TNF and TNFR1 are not expressed in the submandibular salivary gland (SMG) at P10 of *Tnfα* and *Tnfrsf1a* deficient mice. Representative sections of the SMG double labelled for TH and TNF and for TH and TNFR1. **A)** TH and TNF staining in *Tnfα* deficient mice. **B)** TH and TNFR1 staining in *Tnfrsf1a* deficient mice. Scale bar = 50µm.

A

P0- SMG

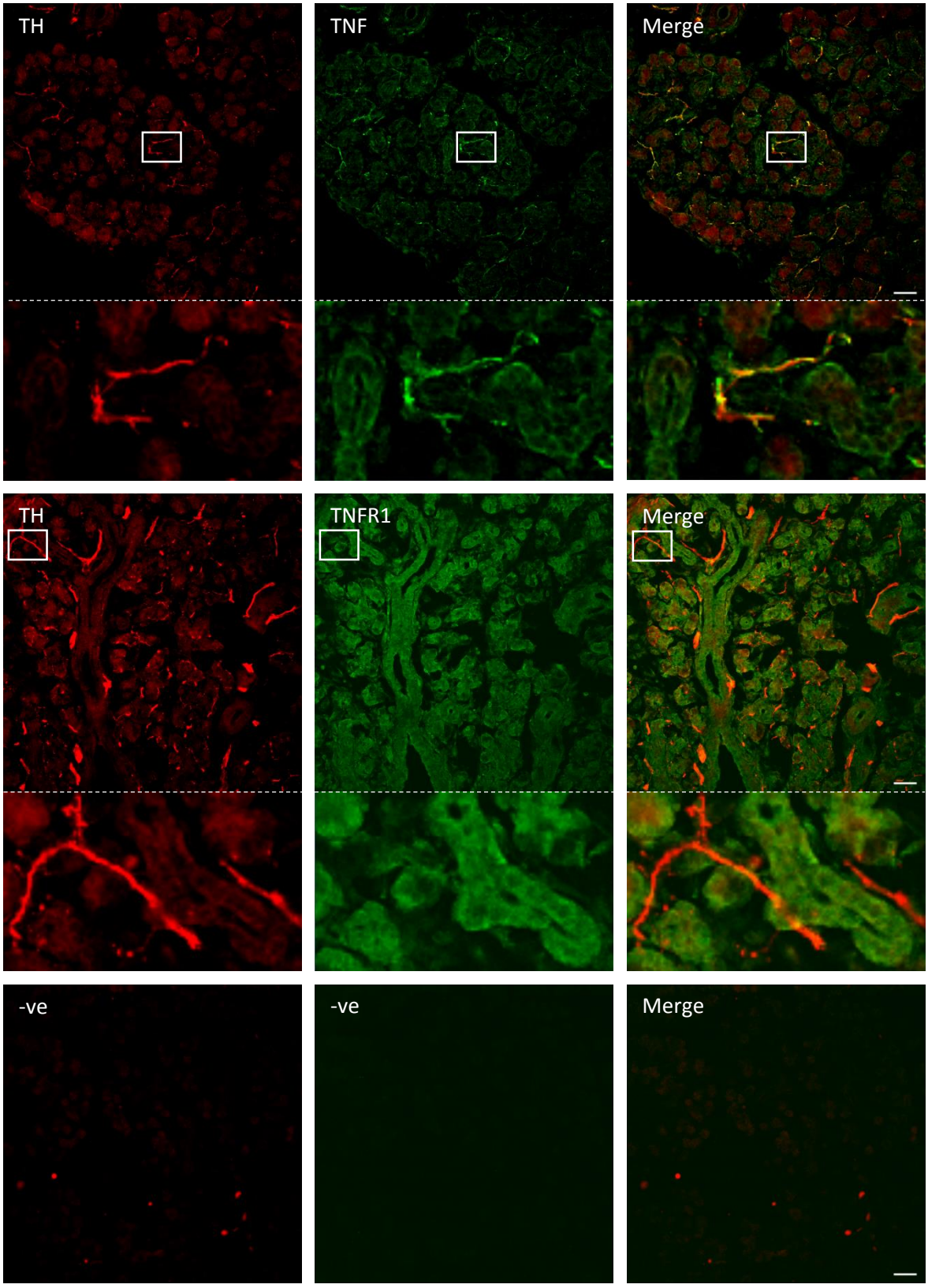

B

P0- NT

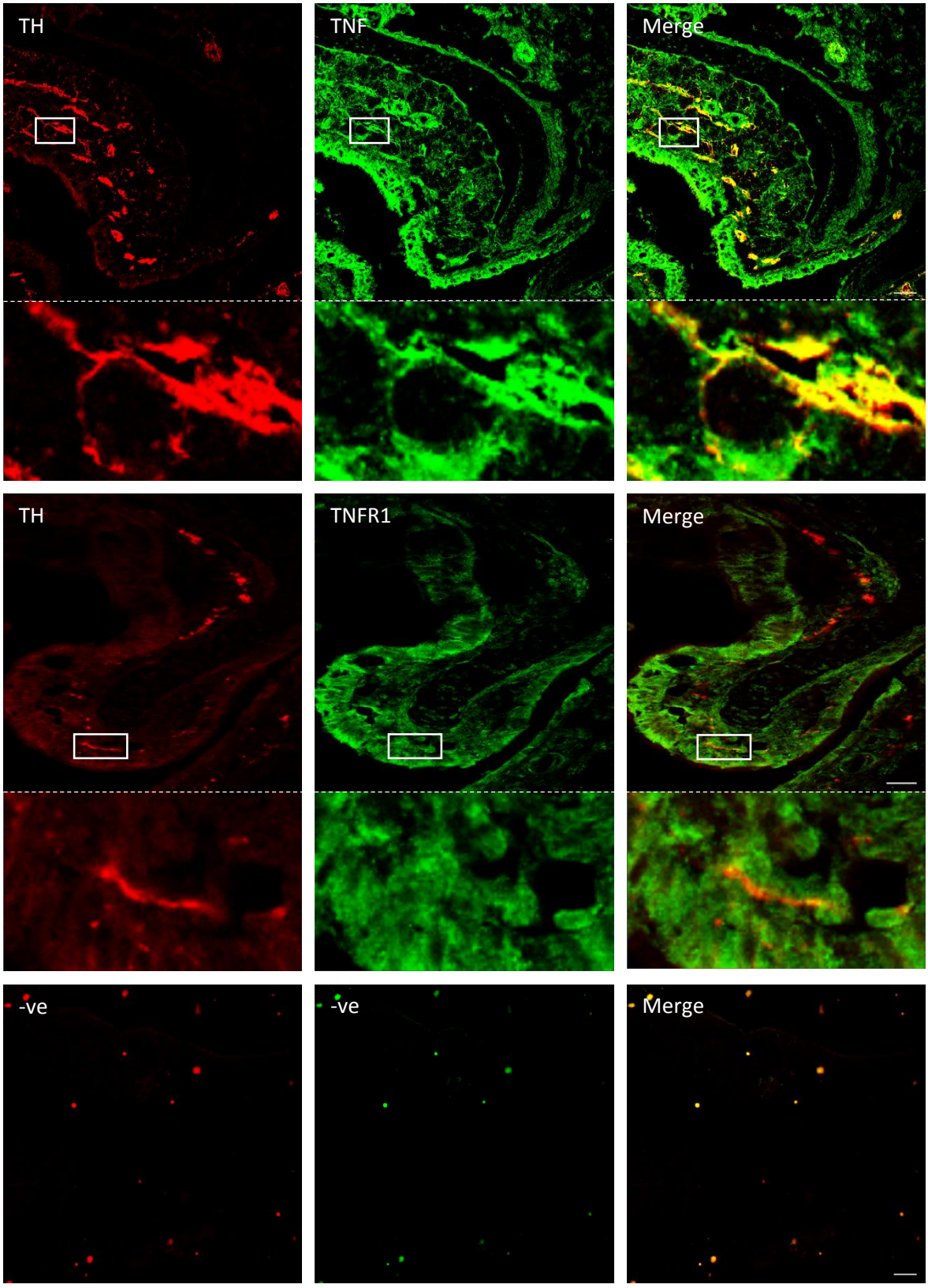

C

P5- SMG

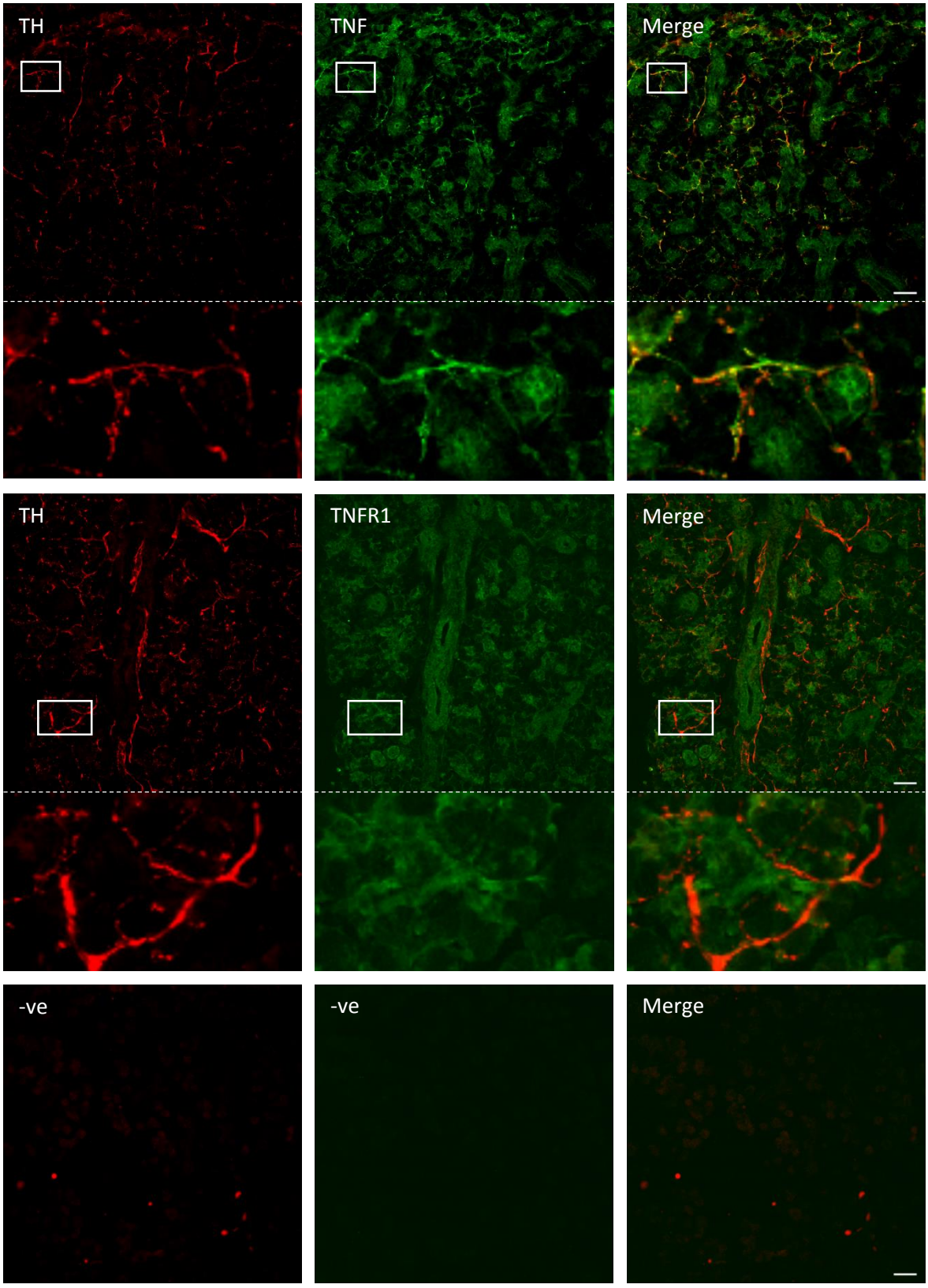

D

P5- NT

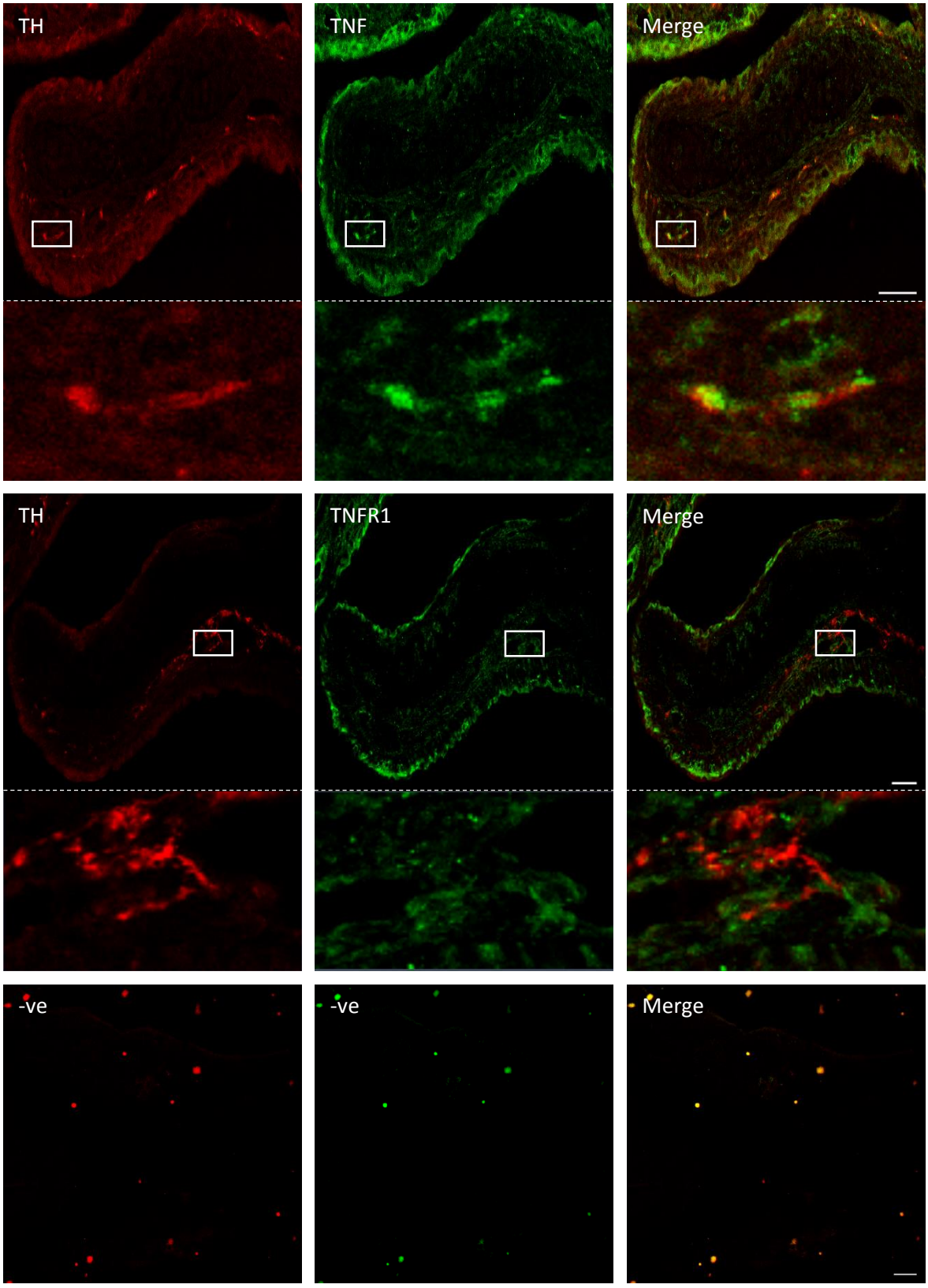

E

P10- SMG

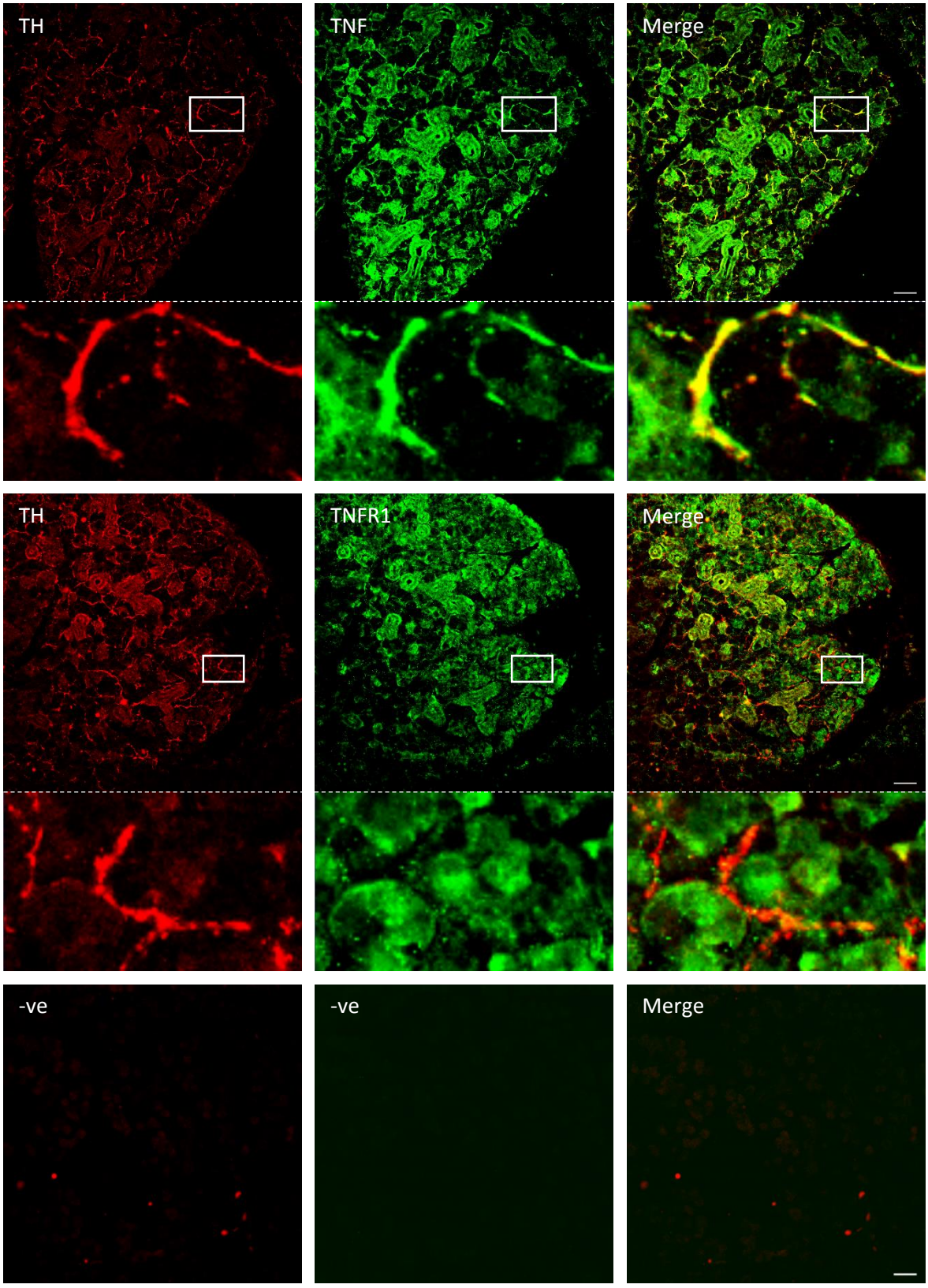

F

P10- NT

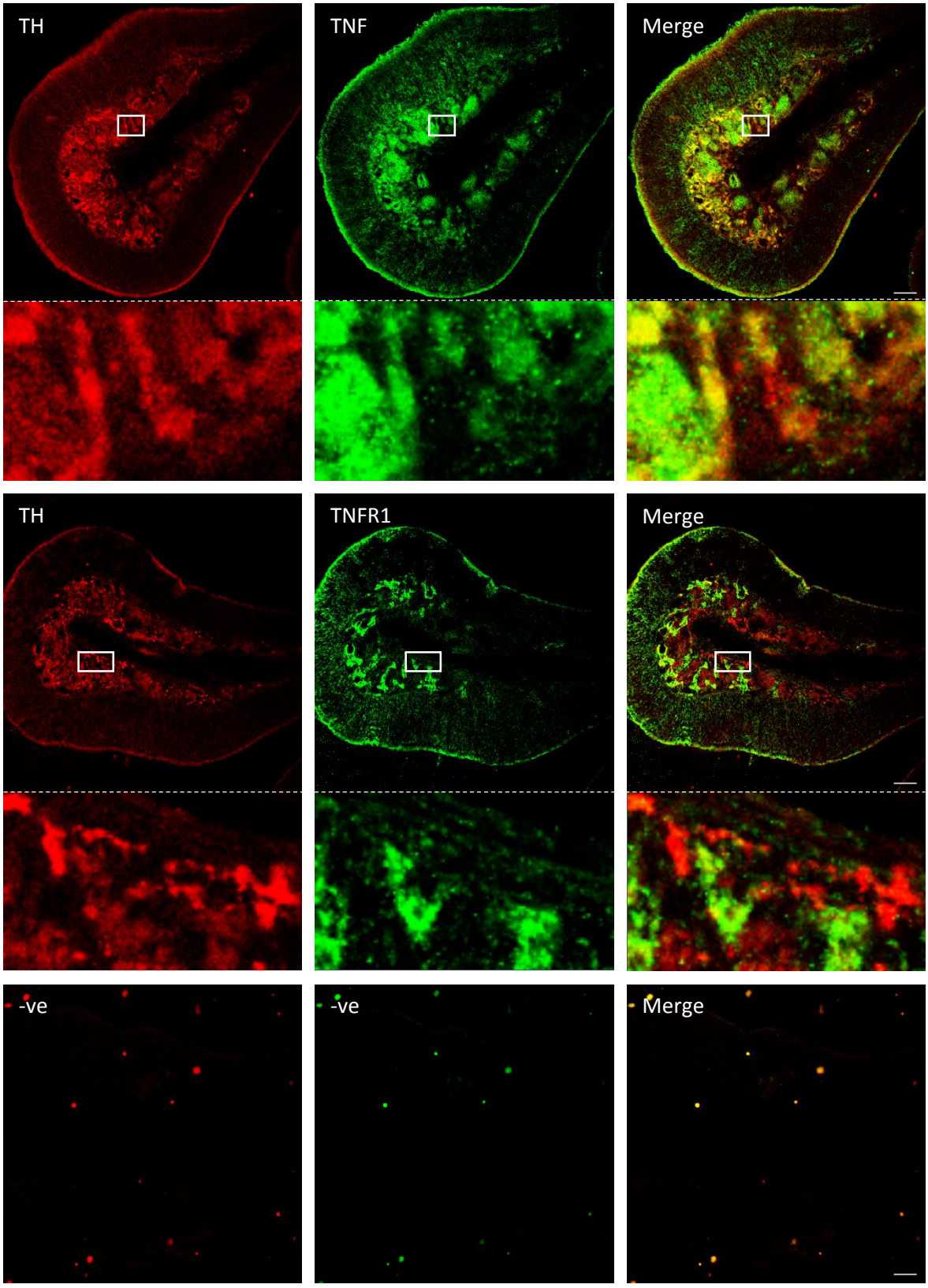

Figure 4, legend on following page.

Figure 4: Expression patterns of TNF and TNFR1 in the submandibular salivary gland (SMG) and nasal turbinates (NT) at P0, P5 and P10. Representative sections of the SMG (**A, C** and **E**) and NT (**B, D** and **F**) at P0 (**A** and **B**), P5 (**C** and **D**) and P10 (**E** and **F**) double labelled for TH and TNF and for TH and TNFR1. The white boxes indicate the areas of the sections shown at high magnification. Scale bar, 50µm, n=3. The lower panels in each set show sections in which the primary antibodies were omitted from the staining protocol.

3.3 TNF reverse signalling enhances sympathetic neurite growth and branching

The finding that TNF is expressed by postnatal sympathetic axons at the time when they are ramifying within targets that express TNFR1, raised the possibility that target-derived TNFR1 might act as a reverse signalling ligand for TNF. To investigate this possibility and ascertain how TNF reverse signalling might affect developing sympathetic neurons, I activated TNF reverse signalling in cultured NGF-dependent SCG neurons and studied whether it might affect NGF-promoted neurite growth and/or NGF-promoted survival. TNF reverse signalling was activated by treating the neurons with a TNFR1-Fc chimera (TNFR1-Fc) which consists of two TNFR1 extracellular domains linked to the Fc part of human IgG1 antibody. This chimera, which is commercially available, has been shown to be a potent reverse signalling ligand for TNF (Eissner et al., 2000).

To investigate whether TNF reverse signalling influences NGF-promoted neurite growth and/or NGF-promoted survival, dissociated cultures of P0 SCG neurons were grown for 24 hours with 10 ng/ml NGF with and without 10 ng/ml TNFR1-Fc. As illustrated in the representative images and camera lucida drawings shown in Fig. 5A, neurons grown with TNFR1-Fc plus NGF were larger and more branched than neurons grown with NGF alone. In SCG dissociate cultures it is not possible to distinguish between axons and dendrites, hence processes are referred to as neurites. Although, in short-term cultures, such as the ones presented here, processes are almost exclusively axons. Neurons have the typical morphology of dissociate cultures, but *in vivo* they consist of a single axon that branches extensively within their target organs. Sholl analysis (Fig. 5B) and quantification of neurite arbor branch point number (Fig. 5C) and length (Fig. 5D)

revealed that the neurite arbors of neurons cultured with TNFR1-Fc plus NGF were significantly more complex and larger than those of neurons cultured with NGF alone. Over 70% of the neurons survived in these cultures and there was no significant difference in survival in cultures containing TNFR1-Fc plus NGF and cultures containing NGF alone (Fig. 5E). These results suggest that TNFR1-Fc significantly enhances NGF-promoted axon growth and branching without affecting the magnitude of NGF-promoted survival of newborn SCG neurons.

To control for any effect of the Fc component of the TNFR1-Fc chimera on axon growth and branching, an additional set of experiments were carried out in which P0 SCG neurons were cultured with 10 ng/ml NGF alone, NGF plus 10 ng/ml of a human Fc fragment (HFc) and NGF plus 10 ng/ml TNFR1-Fc. In these cultures, there was no significant difference in the size and complexity of the neurite arbors of neurons grown with NGF alone and NGF plus HFc (Fig.5F-H). This suggests that the enhancement of NGF-promoted growth by TNFR1-Fc is due to the TNFR1 component.

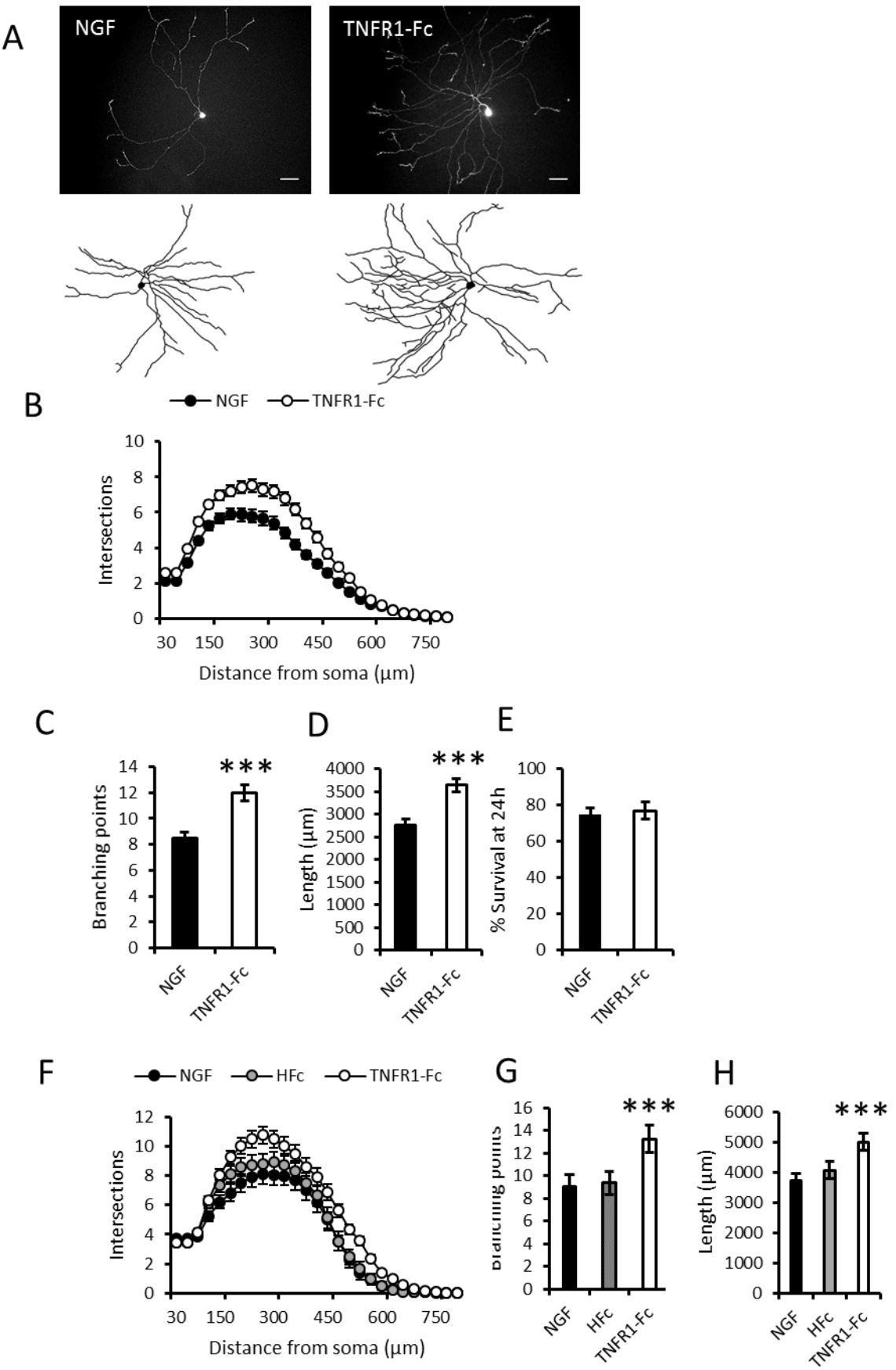

Figure 5, legend on following page.

Figure 5: TNF reverse signalling enhances axonal growth from cultured sympathetic neurons without affecting survival. Dissociated cultures of P0 SCG neurons were grown overnight in the presence of either 10 ng/ml NGF alone or NGF plus 10 ng/ml TNFR1-Fc or NGF plus 10 ng/ml HFc **A)** Representative micrographs depicting the difference in morphology of P0 SCG neurons grown for 24 hours with and without TNFR1-Fc. Scale bar, 20µm. **B)** Sholl profiles, **C)** branch point number, **D)** neurite length and **E)** percent survival in the neurite arbors of neurons grown with NGF alone or NGF plus TNFR1-Fc. **F)** Sholl profiles, **G)** branch point number and **H)** neurite length in the neurite arbors of neurons grown with NGF alone or NGF plus HFc or NGF plus TNFR1-Fc. Mean ± s.e.m of the data from 3 separate experiments are plotted. More than 50 neurons analysed per condition in each experiment; statistical comparison with control, NGF, ***p<0.001, student T-test and one-way ANOVA *post hoc* Tukey's HSD.

3.4 TNFR1-Fc acts locally on sympathetic axons

The demonstration that TNF reverse signalling enhances the growth of sympathetic neurites *in vitro,* together with the expression of TNFR1 by target field tissue and TNF on axon branches within the target field *in vivo,* implies that TNFR1-activated TNF reverse signalling might act locally on sympathetic axonal terminals *in vivo,* to enhance axon growth. To examine whether TNFR1 can act locally on sympathetic axon terminals to promote growth, SCG neurons were cultured in microfluidic devices in which the cell soma and growing axon terminals are cultured in different compartments separated by a barrier. SCG neurons were plated in one compartment (the soma compartment) of a two-compartment device that contained 10 ng/ml NGF in both compartments to sustain neuronal survival and encourage axon growth from the soma compartment into the axon compartment. 10 ng/ml TNFR1-Fc was added to either the soma or axon compartment. 10 ng/ml HFc was used as an internal control and added to axonal compartments. After 24 h incubation, the axons in the axon compartment were labelled with the fluorescent vital dye calcein-AM by adding it to the axon compartment. This also retrogradely labelled the cell bodies of the neurons that projected axons into the axon compartment. A stereological method was used to quantify the extent of axon

growth in the axon compartment relative to the number of neurons projecting axons into this compartment, thus, controlling for number of neurons plated. Addition of TNFR1-Fc to the axon compartment resulted in a marked and highly significant increase in axon growth within this compartment compared with NGF-treated axons, whereas HFc-treated axons showed no significant increase when compared to NGF-treated axons. Addition of TNFR1-Fc to the soma compartment had no significant effect on axon growth in the axon compartment (Fig. 6B). Quantification only takes into account axonal length. However, representative images show how addition of TNFR1-Fc to axonal compartments not only make axons grow longer but they seem more branched and complex as well (Fig.6A). These results suggest that TNFR1 expressed in sympathetic targets is capable of acting locally on sympathetic terminals to enhance their growth and ramification within these tissues.

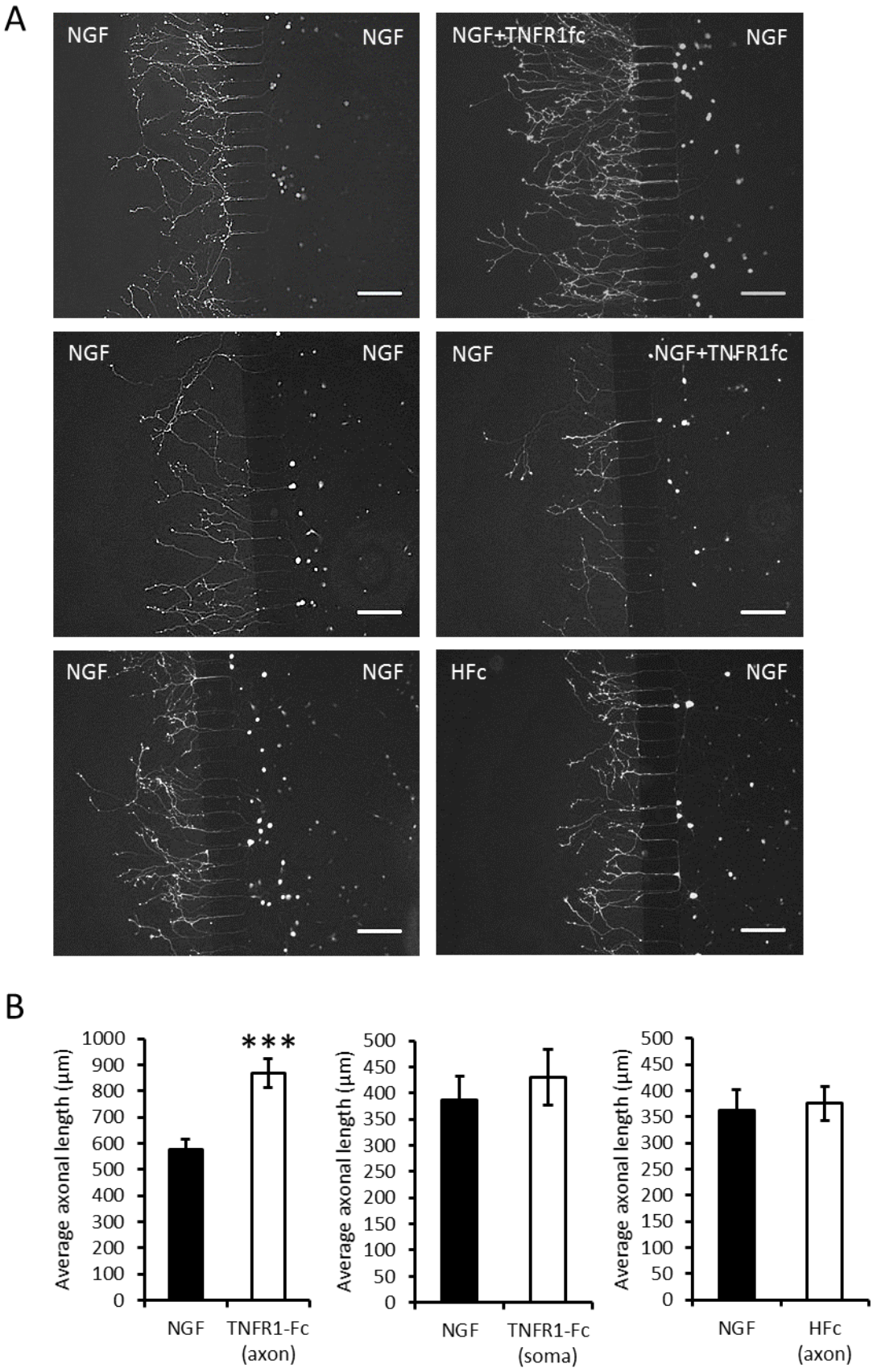

Figure 6, legend on following page.

Figure 6: TNFR1-Fc acts locally on axons to enhance their growth. A) Representative images of calcein-AM labelled P0 SCG neurons that were cultured for 24 h in a two-compartment microfluidic device containing 10 ng/ml NGF in both compartments, with either 10 ng/ml TNFR1-Fc in the axon compartment or soma compartment or 10 ng/ml HFc in the axon compartment. Scale bar, 200 μm. **B)** Bar charts (mean ± s.e.m) of average axonal length from 3 separate experiments of each type. Statistical comparison with control (NGF), ***P<0.001, student T-test.

3.5 Discussion

The occurrence of reverse signalling via multiple membrane-integrated members of the TNFSF has been demonstrated in a variety of cells of the immune system (Sun and Fink, 2007). Although there is increasing evidence that the TNFSF plays important roles in the nervous system in development, physiology and pathology (Desbarats et al., 2003, Gutierrez et al., 2008, O'Keeffe et al., 2008, Gavalda et al., 2009, Park and Bowers, 2010, Gutierrez et al., 2013), this has been interpreted from the perspective of forward signalling. My work and that of others in the Davies laboratory has provided for the first time evidence that TNFSF reverse signalling can occur in the nervous system. I have shown that a divalent TNFR1-Fc chimera, a protein that has been demonstrated to initiate TNF reverse signalling in a variety of TNF-expressing cell lines and cells of the immune system (Eissner et al., 2000, Kirchner et al., 2004b) enhances NGF-promoted axon growth and branching from TNF-expressing postnatal SCG neurons in culture without affecting NGF-promoted neuronal survival.

While postnatal SCG neurons co-express TNF and TNFR1, these proteins exhibit different spatial patterns of expression in the neurons. Whereas TNF is distributed along the axons both *in vitro* and *in vivo*, TNFR1 expression is restricted to the soma. The expression of TNFR1 by cells in tissues innervated by SCG neurons, together with the demonstration in compartment cultures that TNFR1-Fc enhances axon growth when

applied to the axon terminals, but not to the cell soma, raises the possibility that TNFR1 acts by a target-derived mechanism *in vivo* and suggests that target-derived TNFR1 acts locally on axons to enhance growth. The co-expression of TNF and TNFR1 by the neurons at the cell body raises the possibility that autocrine signalling might additionally affect axon growth. However, this seems unlikely because it has been shown by other members in the Davies group, that the magnitude of NGF-promoted neurite growth from cultured postnatal SCG neurons lacking either TNFR1 or TNF is not significantly different from that of wild type neurons (Kisiswa et al., 2013). The function of TNFR1 expressed at the cell body is unclear. While activating TNF forward signalling in postnatal SCG neurons using soluble TNF reduces the extent of NGF-promoted neurite growth (Gutierrez et al., 2008), the finding that the sympathetic innervation density of multiple tissues is significantly reduced in *Tnfα*$^{-/-}$ and *Tnfrsf1a*$^{-/-}$ mice, data presented in chapter 4, suggests that TNF forward signalling, if it does play a role in regulating sympathetic axon growth *in vivo*, this is minor in comparison with the axon growth-promoting effects of TNF reverse signalling *in vivo*. In future work, it would be interesting to establish whether preganglionic sympathetic neurons express TNF, as a potential source of TNF for postganglionic sympathetic neurons.

It would be interesting to ascertain whether TNFR1 is acting as a soluble ligand or as membrane bound ligand in target tissue *in vivo*. Interestingly, although TNFRSF members can be proteolytically cleaved and soluble receptors can initiate reverse signalling *in vitro*, it is thought that during the immune response, reverse signalling most likely occurs in a cell-to-cell contact manner, allowing spatial and functional resolution of the immune response by restricting reverse signalling to specific compartments and cell types (Eissner et al., 2004). Neurotrophic factors, which promote survival and axon

growth, are secreted molecules. A membrane bound, immobilised axon growth-promoting molecule in target tissue, would in principle provide a more specific mechanism, via contact-mediated interactions, for governing the disposition of axons in the target field, allowing a determined path to be followed rather than a concentration gradient. To start to understand this, stripe assays (Knoll et al., 2007) could be used to assess if SCG neurons grow exclusively on stripes containing bound TNFR1-Fc using HFc fragment stripes as controls. Alternatively, cells, such as cardiomyocytes or fibroblasts from wild type and *Tnfrsf1a* deficient mice could be co-cultured with SCG neurons to see if the axons of these neurons grow preferentially on TNFR1-expressing cells. In addition, it would be of interest to analyse the exact disposition of TNFR1 in target tissue and how this is related to the pattern of TH-positive fibres. Indeed, my results suggest that TNFR1 expression in target tissue and organs is concentrated around TH-positive fibres. It would be specifically interesting to determine if the disposition of TNFR1 varied between tissues, as different types of cells are innervated by sympathetic fibres, depending on the target organ, and if only a sub-set or type of cell expressed TNFR1 within target organs. For example the disposition of TNFR1 in secretory cells of the submandibular tubules versus its disposition in the connective tissue of the core of the nasal turbinates and if it was expressed by other types of cells in these respective tissues. One would predict TNFR1 expression to follow closely that of TH fibres. In addition to TNFR1, the expression of TNFR2 was also examined in dissociated SCG cultures and in tissue sections. A low level of TNFR2 immunostaining was evident at the cell bodies and along axons that co-localized with TH staining *in vivo* (data not shown). A low level of TNFR2 immunostaining was also evident in target tissues. However, the significance of this low level of TNFR2 immunoreactivity was unclear as TNFR2-Fc did not enhance axonal growth in dissociated SCG cultures (data not shown). These preliminary results

do not provide support for TNFR2 activating TNF reverse signalling in developing SCG neurons.TNFR2-Fc is able to activate reverse signalling in cells of the immune system. This suggests that TNFR2 mediated-reverse signalling does not play a role during sympathetic innervation, rather than, TNFR2-Fc not being able to induce reverse signalling experimentally.

Lilian Kisiswa expanded the results presented in this chapter carrying out key experiments to support the idea that the observed increased length and branching of sympathetic neuritic processes after the addition of TNFR1-Fc was due to TNF -mediated reverse signalling. First, she showed that TNFR1-Fc effects were restricted to a developmental window between P0 and P5, coinciding with peak expression of *Tnfα* and *Tnfrsf1a* transcripts in the SCG (Appendix II, Fig 1.B) and the developmental period when sympathetic axons are ramifying extensively in their targets. Furthermore, in SCG cultures from *Tnfα* deficient mice, addition of TNFR1-Fc had no effect on axonal branching and length, however in cultures from *Tnfrsf1a* deficient mice, there was an increase in branching and length (Appendix II Fig 2. A-B). In accordance with this, addition of TACE, the metalloprotease that cleaves mTNF, to wild type cultures, abrogated the growth enhancing effects of TNFR1-Fc on SCG processes (Appendix II, Fig.2C). Experiments carried out on cultures of SCG neurons obtained from BAX-deficient mice, which survive without NGF, showed that TNFR1-Fc increased axonal length and branching in the absence of NGF (but not as greatly as NGF alone), suggesting that TNF-mediated reverse signalling is able to enhance axon growth independently of NGF (Appendix II, Fig.2D).

In conclusion, the results reported in this chapter, together with those of Lilian Kisiswa, provide the first evidence for TNF reverse signalling in the nervous system. The data suggest that TNFR1-activated TNF reverse signalling in sympathetic axons enhances their growth during the stage of development when these axons are ramifying in their target tissues under the influence of target-derived NGF. The target tissue appears to be the source of TNFR1 and raises the possibility of a new mechanism for promoting the growth and disposition of sympathetic axons in target tissue. The physiological relevance of these *in vitro* observations is evaluated in chapter 4.

Chapter 4
TNF reverse signalling is required for establishing appropriate sympathetic innervation *in vivo*

4.1 Introduction

In chapter 3, I provided *in vitro* evidence showing that TNF reverse signalling enhances sympathetic axonal growth during the stage in development when these axons are ramifying within their target fields. This chapter outlines evidence for the physiological relevance of these *in vitro* findings.

These studies were based on assessing sympathetic innervation density of a variety of tissues in wild type mice and mice that are heterozygous and homozygous for null mutations in the *Tnfα* and *Tnfrsf1a* genes. Sympathetic fibres were recognised by staining with TH, either in tissue sections or in tissue whole mount preparations. These studies were carried out at P10, by which time sympathetic innervation is well established. Quantification of TH immunofluorescence in tissue sections was restricted to three SCG targets (iris, submandibular salivary gland and nasal tissue) and was carried out by other members of the Davies group (Kisiswa et al., 2013) and showed significant reductions in innervation density in $Tnf\alpha^{-/-}$ and $Tnfrsf1a^{-/-}$ mice compared with wild type littermates (Appendix III Fig.1).

While these studies demonstrated the physiological relevance of the *in vitro* findings, the analysis of tissue sections does not provide clear information about the three dimensional disposition of sympathetic fibres within tissues. For this reason, I carried out the whole mount studies reported in this chapter. These studies included additional SCG innervation targets and innervation targets of more caudal ganglia of the paravertebral sympathetic chain as well as innervation targets of the prevertebral ganglia. I show that the sympathetic innervation of tissues innervated by paravertebral

ganglia is reduced in *Tnfα*$^{-/-}$ and *Tnfrsf1a*$^{-/-}$ mice compared with wild type littermates and that the sympathetic innervation of tissues mainly or exclusively innervated by prevertebral ganglia is either unaffected in *Tnfα*$^{-/-}$ and *Tnfrsf1a*$^{-/-}$ mice or is increased. Moreover, in tissues with reduced innervation in *Tnfα*$^{-/-}$ and *Tnfrsf1a*$^{-/-}$ mice, sympathetic fibres reach the tissue but fail to branch and ramify adequately in the tissue.

My studies not only complement and expand studies of sympathetic innervation carried out on tissue sections but provide a clearer understanding of the role played by TNF reverse signalling in establishing sympathetic innervation during development. Some of my findings were reported in (Kisiswa et al., 2013).

RESULTS

4.2 The targets of paravertebral sympathetic neurons of *Tnfα* and *Tnfrsf1a* deficient mice have disrupted sympathetic innervation

TH whole mount staining was conducted on tissues innervated by the SCG, stellate ganglion and thoracic ganglia of the paravertebral sympathetic chain of P10 *Tnfα*$^{-/-}$ and *Tnfrsf1a*$^{-/-}$ mice and their heterozygous and wild type littermates. The submandibular salivary gland, pineal gland and trachea receive their innervation from the SCG, with the trachea receiving a small part of its innervation from the stellate ganglion (Kappers, 1960, Smith and Satchell, 1985, Smith and Satchell, 1986, Kummer et al., 1992, Moller et al., 1996, Glebova and Ginty, 2004, Ferreira and Hoffman, 2013). The heart receives most of its innervation from the stellate ganglion and a small percentage from the SCG and mid-thoracic paravertebral ganglia (Pardini et al., 1989, Glebova and Ginty, 2004). A modified line-intercept method was used to quantify innervation density, using defined anatomical landmarks to standardise quantification between specimens (refer to 2.6 for more details on methodology). All imaging and quantification was carried out blind.

The submandibular salivary gland showed statistically-significant decreases in innervation density in *Tnfα*$^{-/-}$ and *Tnfrsf1a*$^{-/-}$ mice compared to wild type littermates (Fig.1). There were no statistically significant decreases in innervation density in heterozygous mice relative to wild type mice. The pineal gland showed highly significant decreases in innervation density in *Tnfα*$^{-/-}$ and *Tnfrsf1a*$^{-/-}$ mice compared to wild type littermates. In contrast to the submandibular salivary gland, statistically significant decreases in innervation density were also observed in heterozygous mice compared to

wild type littermates, which is indicative of a gene dosage effect (Fig. 2). There were statistically-significant decreases in innervation density of the trachea in *Tnfα*$^{-/-}$ and *Tnfrsf1a*$^{-/-}$ mice compared to wild type littermates. A statistically-significant reduction in innervation density was observed in *Tnfrsf1a*$^{+/-}$ mice compared to wild type littermates, but not in *Tnfα*$^{+/-}$ mice (Fig.3). Highly significant reductions in sympathetic innervation density were observed in the hearts of *Tnfrsf1a*$^{-/-}$ and *Tnfrsf1a*$^{+/-}$ mice compared to *Tnfrsf1a*$^{+/+}$ littermates. However, while the sympathetic innervation density of the heart of *Tnfα*$^{-/-}$ mice was less than that of *Tnfα*$^{+/+}$ mice, this reduction was not statistically significant (Fig.4).

In addition to the reduction in innervation density observed in the submandibular salivary gland, pineal gland, trachea and heart of *Tnfα*$^{-/-}$ and *Tnfrsf1a*$^{-/-}$ mice compared to wild type littermates, a consistent and striking qualitative observation in all tissues was a marked reduction in TH-positive nerve fibre branching within these tissues. Whereas TH-positive nerves branched into multiple finer branches after reaching these tissues in wild type mice, TH-positive nerves of *Tnfα*$^{-/-}$ and *Tnfrsf1a*$^{-/-}$ mice did not give off as many branches, and the main nerve trunk had a tapped appearance, suggesting that whereas sympathetic nerves reach these tissues during development, many fibres failed to grow into and ramify within these tissues (Figs. 1A, 2A, 3A and 4A). Although, each organ is comprised of different tissues and cells and hence the pattern of sympathetic innervation differs from one another as seen in the representative images, they all follow the trend of having impaired branching in target organs of KO mice.

The submandibular salivary gland is extensively innervated by sympathetic fibres as they project to the gland tubules, which make up a large percentage of this organ (Kisiswa et

al., 2013). Arrows in Fig.1A show how in KO mice this extensive innervation is stunted. The pineal gland is also densely innervated by the SCG, with most sympathetic innervation concentrating around the pinealocyte cells, which are the hormone producing cells (Moller and Baeres, 2002). Arrows in Fig.2A show how, like in the submandibular salivary gland, the extensive innervation of the target organ is stunted in KO mice. The trachea has a very distinctive pattern of sympathetic innervation, almost like a ladder. This is due to the fact that sympathetic axons project to the smooth muscle of this organ, which is located on the cartilage rings thus, creating this ladder-like pattern (Pack et al., 1984, Davis and Kannan, 1987). Fig.3A shows how in KO mice these sections of innervation are diminished in number, and those present, have less complex TH staining, fibres seem to branch less within these areas of dense sympathetic innervation. Imaging of the heart concentrated on the left ventricle (refer to section 2.6). Sympathetic innervation of the ventricles concentrates on the myocardium. As can be appreciated in the representative images, innervation in KO mice fails to reach the bottom of the ventricles (Fig.4A).

In summary, all tissues innervated by paravertebral sympathetic neurons analysed to date by TH staining in whole mount preparations (this chapter) and in histological sections (Appendix III) (Kisiswa et al., 2013), have decreased sympathetic innervation density in TNF-deficient and TNFR1-deficient mice by P10, a stage in development by which time sympathetic innervation is normally well established.

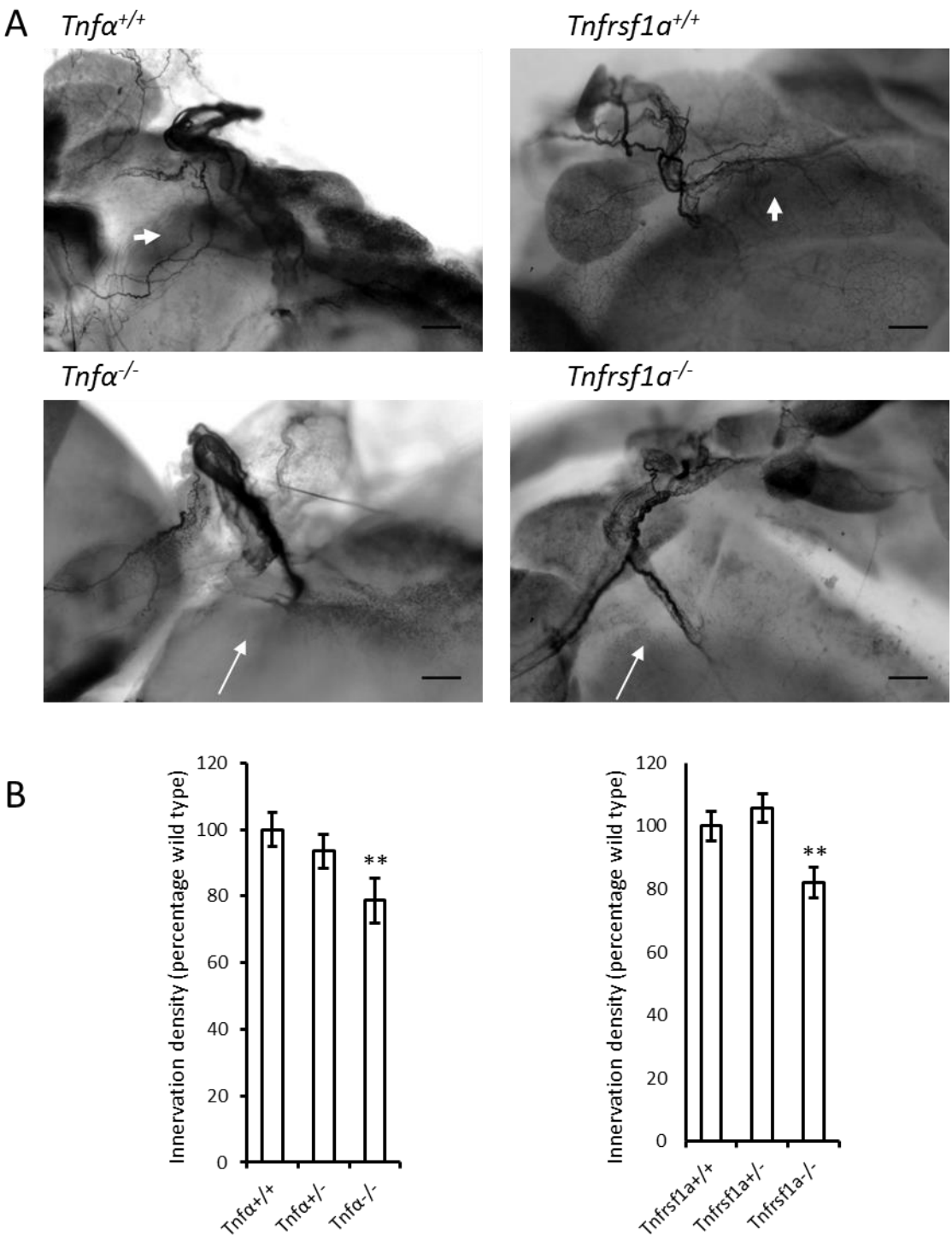

Figure 1: Sympathetic nerve fibre branching in P10 submandibular salivary gland (SMG) *Tnfα*$^{-/-}$ and *Tnfrsf1a*$^{-/-}$ mice. A) Representative images of TH labelled whole mount preparations of the submandibular salivary gland hilus of P10 T*nfα*$^{+/+}$, T*nfα*$^{-/-}$, T*nfrsf1a*$^{+/+}$ and *Tnfrsfa1*$^{-/-}$ mice. Small arrows indicate areas of normal innervation, long arrows indicate areas of decreased innervation. Scale bars, 100 µm. **B)** Relative length per unit area of fibres of *Tnfα*$^{+/+}$, *Tnfα*$^{+/-}$, *Tnfα*$^{-/-}$, *Tnfrsf1a*$^{+/+}$, *Tnfrsf1a*$^{+/-}$ and *Tnfrsf1a*$^{-/-}$ mice expressed as a percentage of the mean level in *Tnfα*$^{+/+}$ or *Tnfrsf1a*$^{+/+}$ mice. Mean ± s.e.m of data from 6 or 7 animals of each genotype are shown. Statistical comparison with wild type, **P < 0.01, one-way ANOVA *post-hoc* Tukey's HSD.

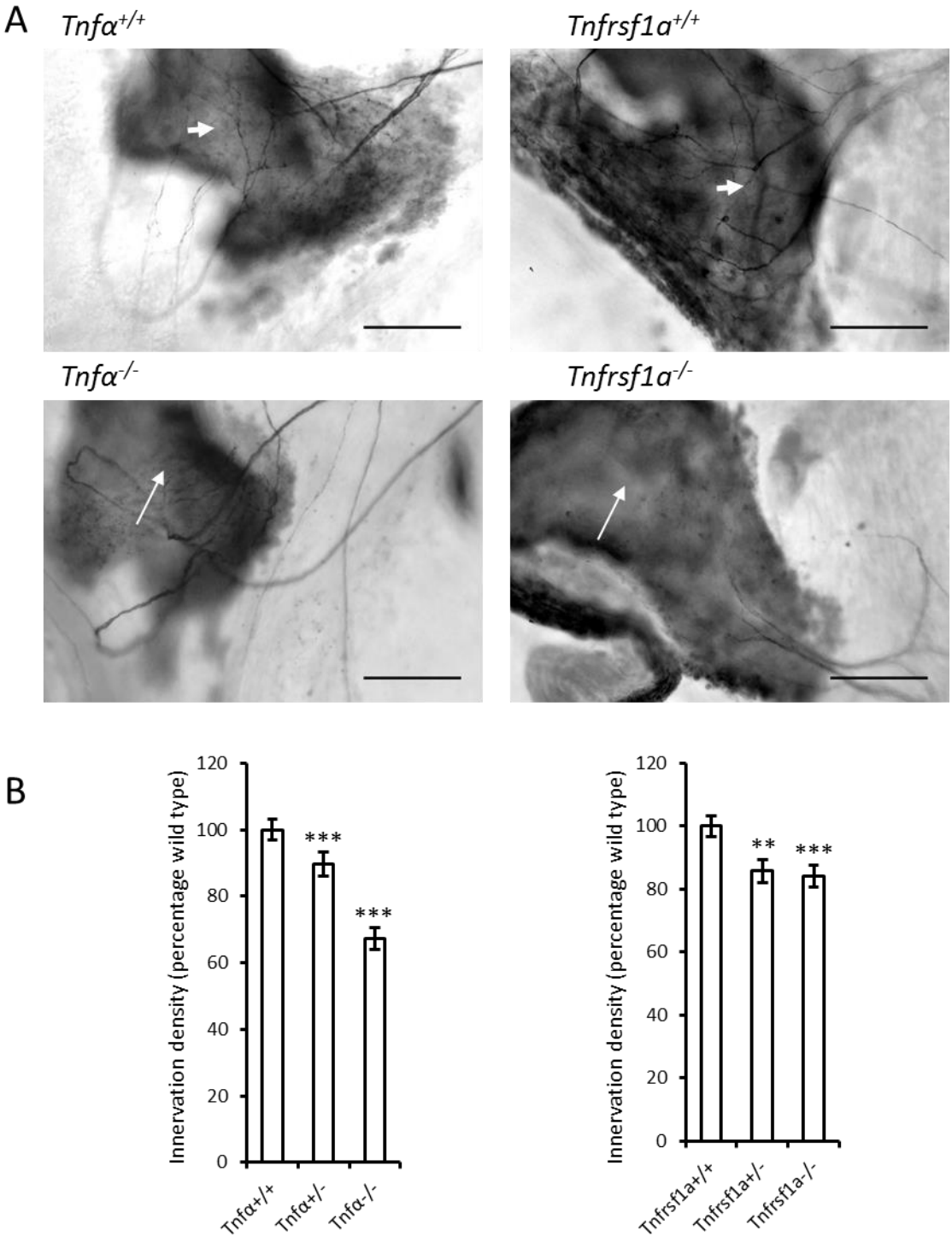

Figure 2: Sympathetic nerve fibre branching in P10 pineal gland (PG) *Tnfα*$^{-/-}$ and *Tnfrsf1a*$^{-/-}$ mice. A) Representative images of whole mount staining preparations of the pineal gland of P10 *Tnfα*$^{+/+}$, *Tnfα*$^{-/-}$, *Tnfrsf1a*$^{+/+}$ and *Tnfrsf1a*$^{-/-}$ mice labelled with anti-TH. Small arrows indicate areas of normal innervation, long arrows indicate areas of decreased innervation. Scale bars, 100 µm. **B)** Relative length per unit area of fibres of *Tnfα*$^{+/+}$, *Tnfα*$^{+/-}$, *Tnfα*$^{-/-}$, *Tnfrsf1a*$^{+/+}$, *Tnfrsf1a*$^{+/-}$ and *Tnfrsf1a*$^{-/-}$ mice expressed as a percentage of the mean level in *Tnfα*$^{+/+}$ or *Tnfrsf1a*$^{+/+}$ mice. Mean ± s.e.m of data from 6 to 8 animals of each genotype are shown. Statistical comparison with wild type, **P < 0.01, *** P < 0.001, one-way ANOVA *post-hoc* Tukey's HSD.

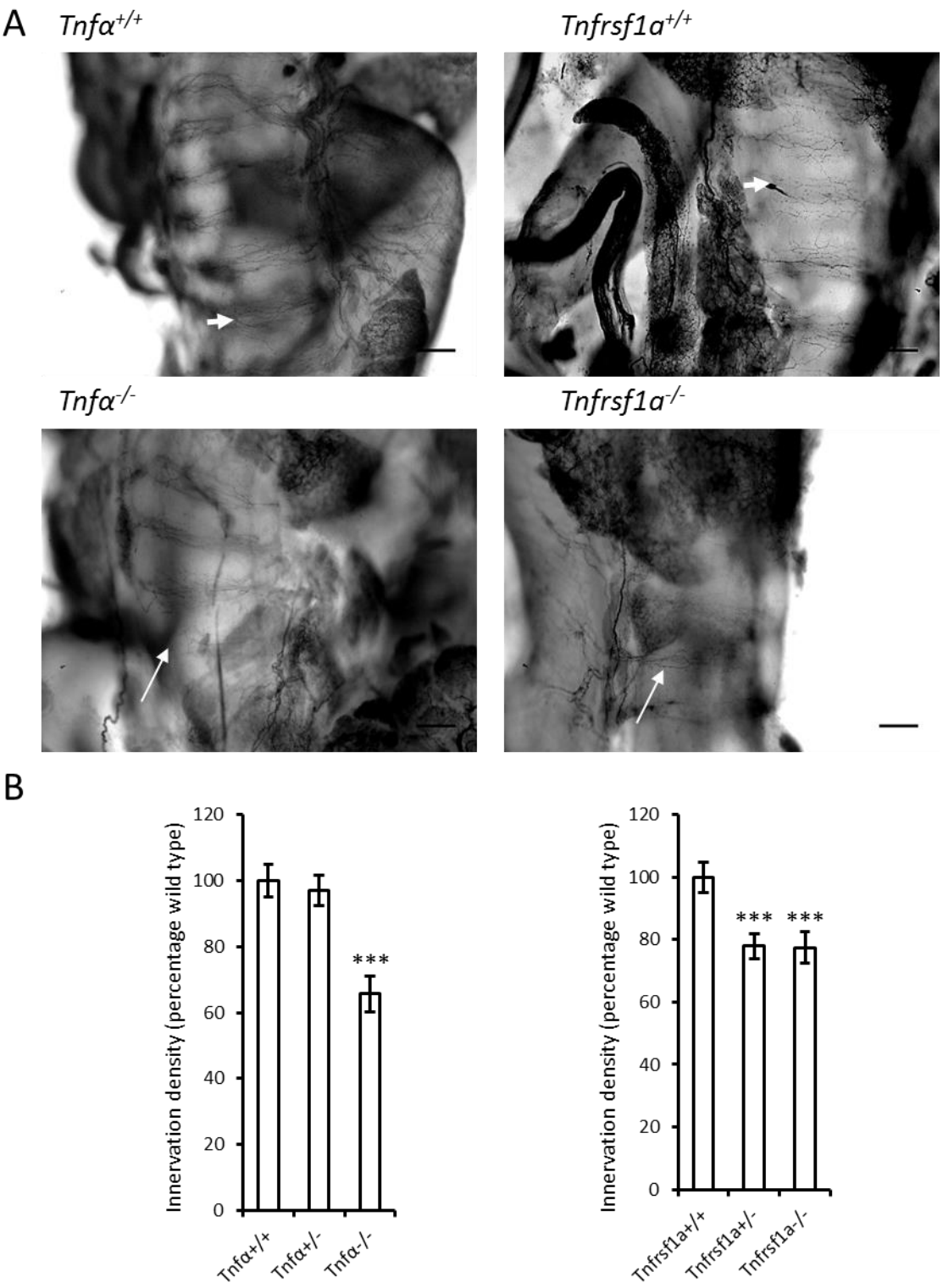

Figure 3: Sympathetic nerve fibre branching in P10 trachea *Tnfα*$^{-/-}$ and *Tnfrsf1a*$^{-/-}$ mice. A) Representative images of whole mount staining preparations of the trachea of P10 *Tnfα*$^{+/+}$, *Tnfα*$^{-/-}$, *Tnfrsf1a*$^{+/+}$ and Tnfrsf1a$^{-/-}$ mice labelled with anti-TH. Small arrows indicate areas of higher innervation, long arrows indicate areas of decreased innervation. Scale bars, 100µm. **B)** Relative length per unit area of fibres of *Tnfα*$^{+/+}$, *Tnfα*$^{+/-}$, *Tnfα*$^{-/-}$, *Tnfrsf1a*$^{+/+}$, *Tnfrsf1a*$^{+/-}$ and *Tnfrsf1a*$^{-/-}$ mice expressed as a percentage of the mean level in *Tnfα*$^{+/+}$ or *Tnfrsf1a*$^{+/+}$ mice. Mean ± s.e.m of data from 5 to 7 animals of each genotype are shown. Statistical comparison with wild type, *** $P < 0.001$, one-way ANOVA *post-hoc* Tukey's HSD.

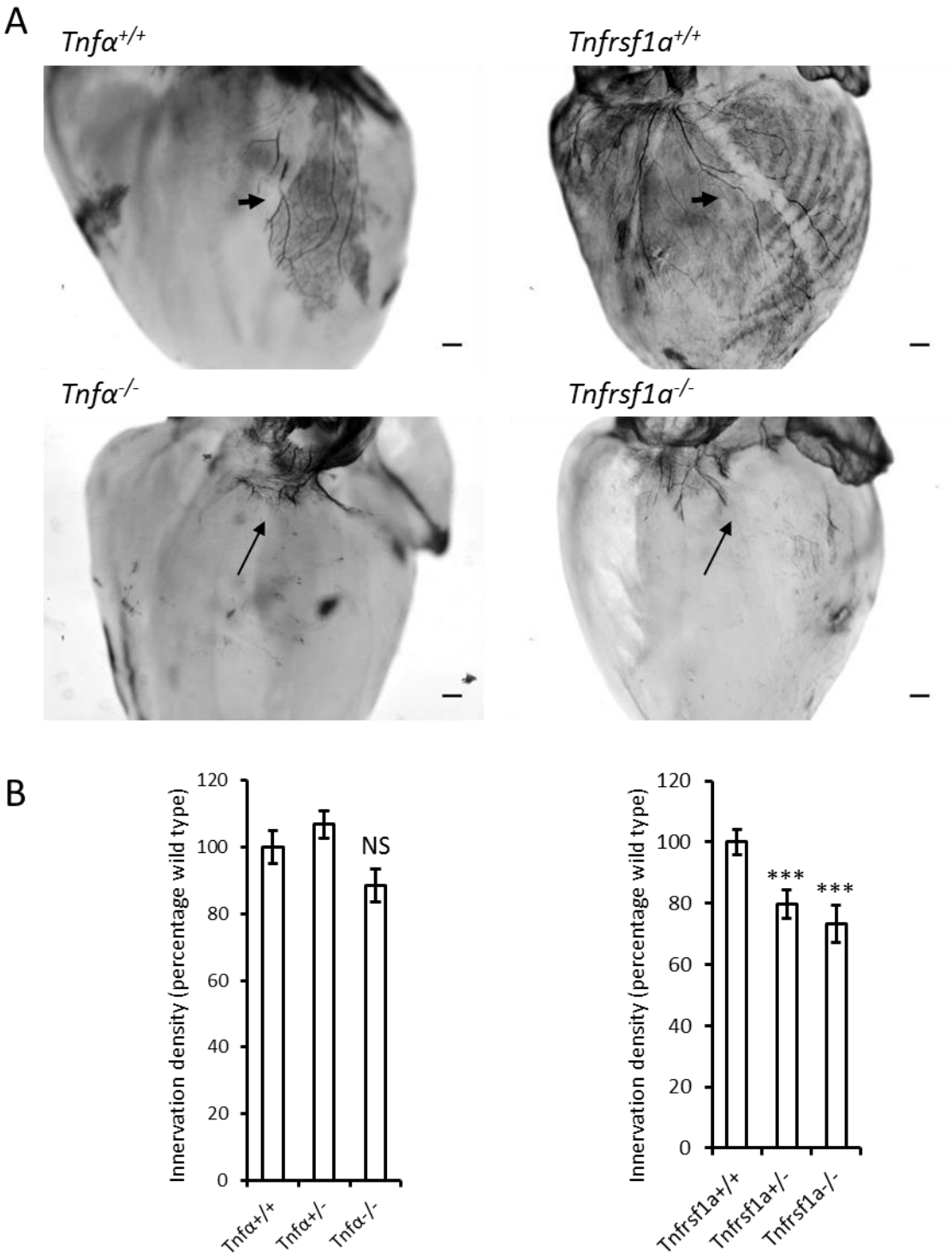

Figure 4: Sympathetic nerve fibre branching in P10 heart *Tnfα*$^{-/-}$ and *Tnfrsf1a*$^{-/-}$ mice. A) Representative images of whole mount staining preparations of the heart of P10 *Tnfα*$^{+/+}$, *Tnfα*$^{-/-}$, *Tnfrsf1a*$^{+/+}$ and *Tnfrsf1a*$^{-/-}$ mice labelled with anti-TH. Small arrows indicate areas of higher innervation, long arrows indicate areas of decreased innervation. Scale bars, 100 µm. **B)** Relative length per unit area of fibres of *Tnfα*$^{+/+}$, *Tnfα*$^{+/-}$, *Tnfα*$^{-/-}$, *Tnfrsf1a*$^{+/+}$, *Tnfrsf1a*$^{+/-}$ and *Tnfrsf1a*$^{-/-}$ mice expressed as a percentage of the mean level in *Tnfα*$^{+/+}$ or *Tnfrsf1a*$^{+/+}$ mice. Mean ± s.e.m of data from 6 to 8 animals of each genotype are shown. Statistical comparison with wild type, *** $P < 0.001$, NS= not significant, one-way ANOVA *post-hoc* Tukey's HSD.

4.3 Normal sympathetic innervation in mice possessing a non-cleavable form of TNF

To gain further insight into the role of TNF in the establishment of sympathetic innervation, I investigated the innervation of SCG target tissues in mice which possess mutated TACE binding sites (Ruuls et al., 2001). These mice express a non-cleavable, membrane integrated form of TNF that retains the ability to mediate reverse signalling and is capable of initiating forward signalling only when TNF-expressing cells are in direct contact with TNFR1-expressing cells. TH whole mount staining was conducted on the submandibular salivary gland, pineal gland and trachea of these mice ($mTNF^{\Delta/\Delta}$) and wild type littermates at P10. Analysis of innervation density revealed no significant differences between $mTNF^{\Delta/\Delta}$ mice and wild type littermates (Figs.5–7). Also, there were no apparent differences between the overall arrangement of TH-positive nerve fibre bundles in these tissues of $mTNF^{\Delta/\Delta}$ and wild type mice. This suggests that TNF forward signalling by soluble TNF plays no role in the establishment of the sympathetic innervation of these tissues.

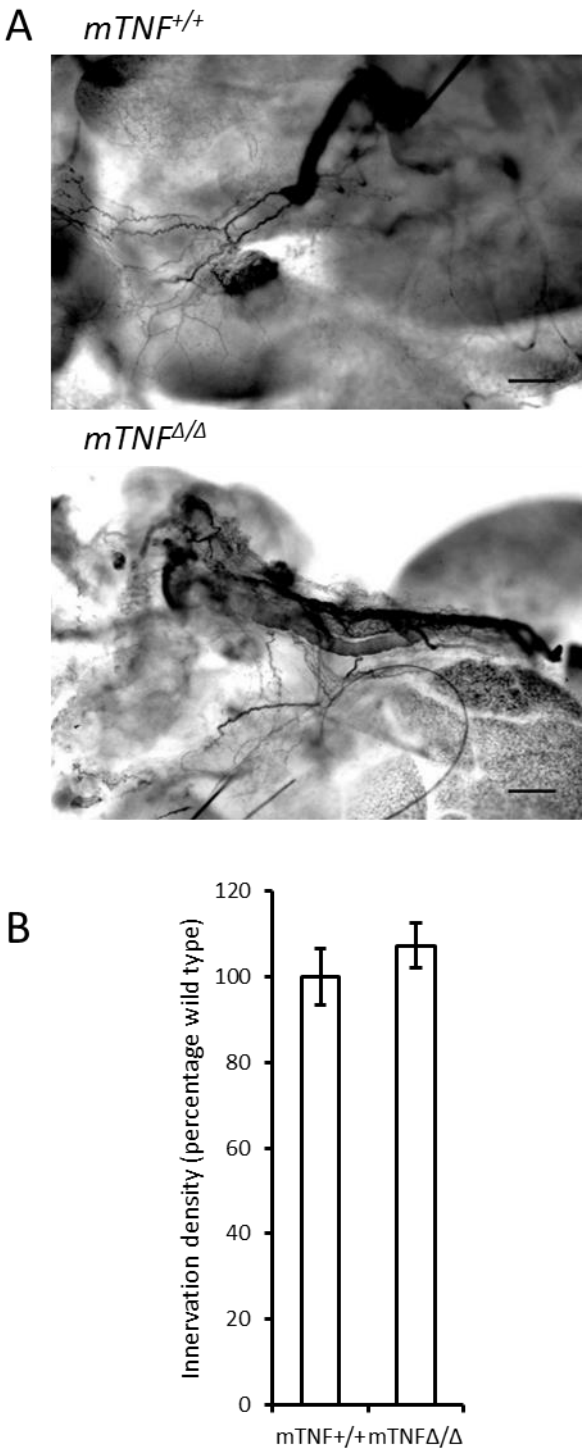

Figure 5: Sympathetic nerve fibre branching in P10 submandibular salivary gland *mTNF*$^{\Delta/\Delta}$ mice. A) Representative images of whole mount staining preparations of the submandibular salivary gland of P10 *mTNF*$^{+/+}$ and *mTNF*$^{\Delta/\Delta}$ mice labelled with anti-TH. Scale bars, 100 µm. **B)** Relative length per unit area of fibres of *mTNF*$^{+/+}$ and *mTNF*$^{\Delta/\Delta}$ mice expressed as a percentage of the mean level in *mTNF*$^{+/+}$ mice. Mean ± s.e.m of data from 4 animals of each genotype are shown. Statistical comparison with wild type, no significant differences, student T-test.

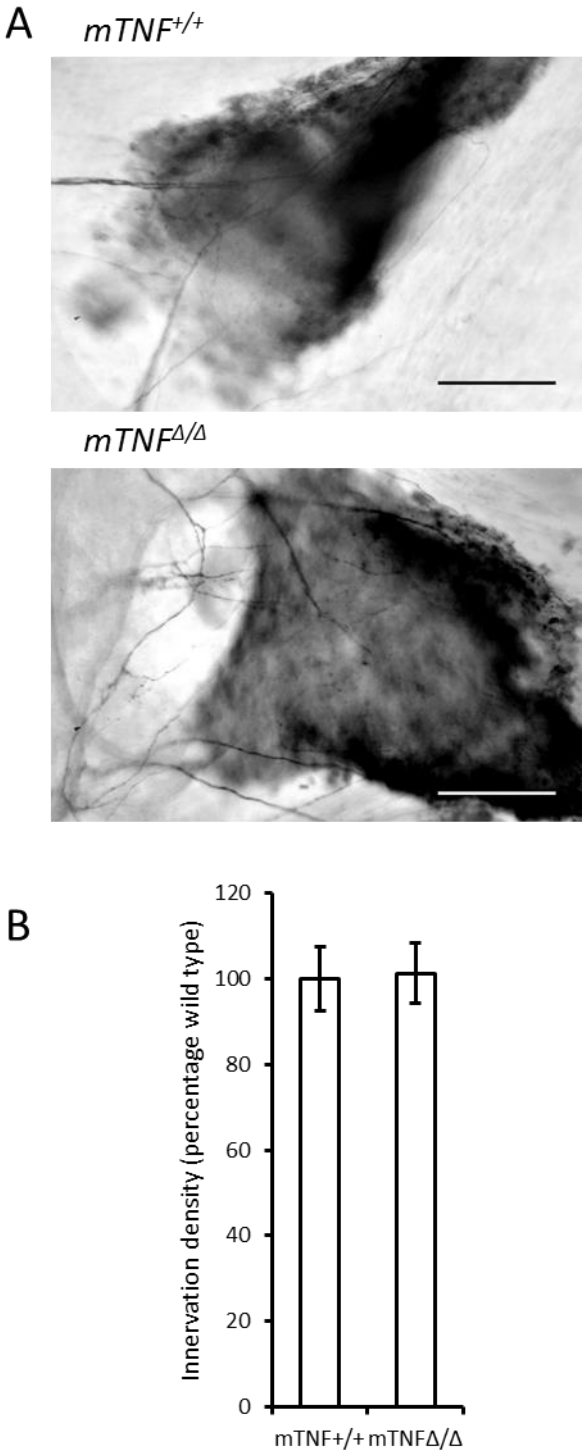

Figure 6: Sympathetic nerve fibre branching in P10 pineal gland *mTNF$^{\Delta/\Delta}$* mice. A) Representative images of whole mount staining preparations of the pineal gland of P10 *mTNF$^{+/+}$* and *mTNF$^{\Delta/\Delta}$* mice labelled with anti-TH. Scale bars, 100 µm. **B)** Relative length per unit area of fibres of *mTNF$^{+/+}$* and *mTNF$^{\Delta/\Delta}$* mice expressed as a percentage of the mean level in *mTNF$^{+/+}$* mice. Mean ± s.e.m of data from 4 animals of each genotype are shown. Statistical comparison with wild type, no significant differences, student T-test.

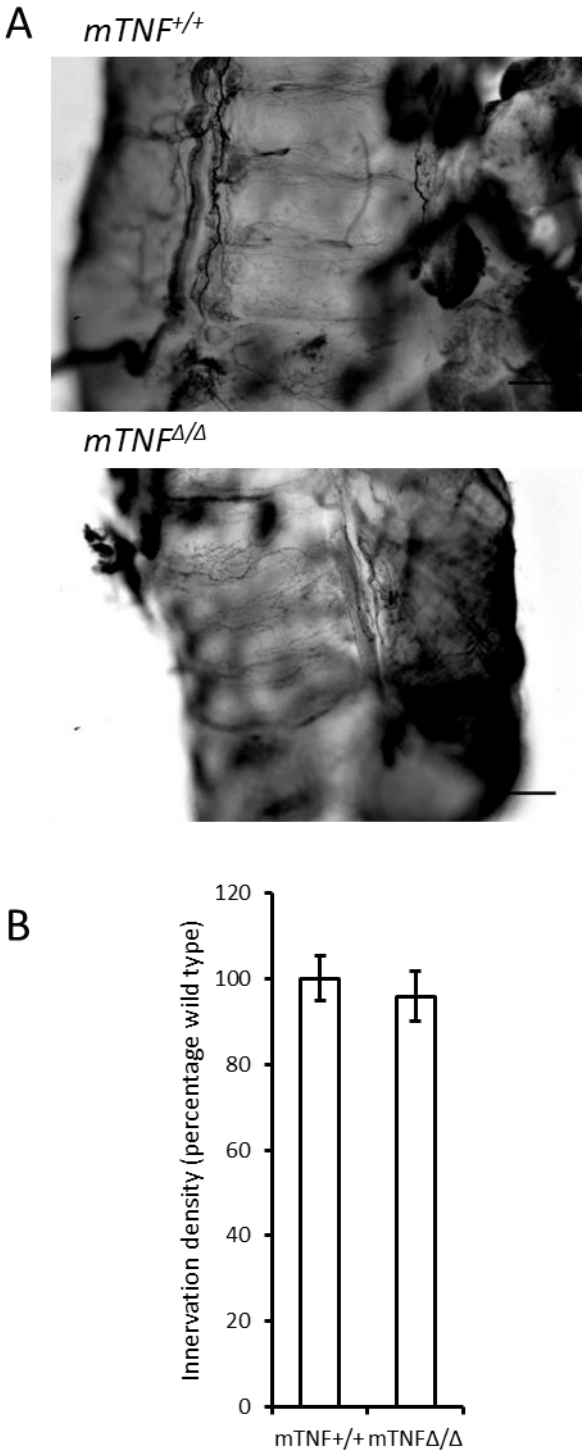

Figure 7: Sympathetic nerve fibre branching in P10 trachea *mTNF$^{\Delta/\Delta}$* mice. A) Representative images of whole mount staining preparations of the trachea, P10 *mTNF$^{+/+}$* and *mTNF$^{\Delta/\Delta}$* mice labelled with anti-TH. Scale bars, 100 µm. **B)** Relative length per unit area of fibres of *mTNF$^{+/+}$* and *mTNF$^{\Delta/\Delta}$* mice expressed as a percentage of the mean level in *mTNF$^{+/+}$* mice. Mean ± s.e.m. of data from 4 animals of each genotype are shown. Statistical comparison with wild type, no significant differences, student T-test.

4.4 Prevertebral sympathetic target organs are affected to different degrees in *Tnfα* and *Tnfrsf1a* deficient mice

Sympathetic postganglionic ganglia of the autonomic nervous system consist of paravertebral ganglia but also of prevertebral ganglia. To see if the sympathetic innervation of target organs of prevertebral ganglia followed a similar pattern to that of paravertebral ganglia in *Tnfα* and *Tnfrsf1a* deficient mice, TH-whole mount staining was carried out on the kidney, stomach and spleen of P10 mice.

While the paravertebral ganglia (T10-L1) are the major source of sympathetic innervation for the mouse kidney, the prevertebral celiac ganglion makes a significant contribution to its innervation (Ferguson et al., 1986, Gattone et al., 1986, Chevendra and Weaver, 1991, Dehal et al., 1993, Glebova and Ginty, 2004). The kidney showed statistically significant decreases in innervation in $Tnf\alpha^{-/-}$ and $Tnfrsf1a^{-/-}$ mice compared to wild type littermates (Fig.8B). $Tnf\alpha^{+/-}$ mice also showed a statistically-significant decrease in innervation relative to wild type mice and while the innervation density of $Tnfrsf1a^{+/-}$ was less than that of wild type mice, this decrease was not significant (Fig.8B). Visual inspection of the kidney whole mount preparations revealed that, as in the case of SCG target organs, sympathetic axonal bundles reached the kidney in $Tnf\alpha^{-/-}$ and $Tnfrsf1a^{-/-}$ mice but failed to branch normally within the kidney (Fig.8A). The kidney receives a large amount of sympathetic innervation to various parts, including the vasculature, renal tubules and the juxtaglomerular cells (Johns et al., 2011). Imaging (refer to section 2.6) concentrated on the innervation of the renal vasculature. Fig.8A reflects how in WT mice sympathetic innervation mimics the vasculature path, where in

KO mice, as indicated by arrows, sympathetic innervation fails to follow the renal arteries into the organ.

Unlike the kidney, the stomach receives most of its sympathetic innervation from the celiac ganglion and a very small contribution from the thoracic paravertebral sympathetic chain (Trudrung et al., 1994, Glebova and Ginty, 2004). In marked contrast to the kidney and all tissues innervated by the SCG analysed, the innervation density of the stomach of *Tnfα*$^{-/-}$ and *Tnfrsf1a*$^{-/-}$ mice was not statistically significantly different from that of wild type mice and there were no apparent differences in the branching of sympathetic fibres in the stomach (Fig.9). Sympathetic fibres follow the gastric and gastroomental arteries and then enter the stomach where they innervate blood vessels and musculature (Site et al., 2008). Due to dissection techniques (refer to section 2.6) the areas imaged were a mixture of both blood vessel and muscle innervation, which seem to be not affected in mice lacking TNF and TNFR1.

Like the stomach, the spleen receives most of its sympathetic innervation from the celiac ganglion with only a minor contribution from the thoracic paravertebral sympathetic chain (Chevendra and Weaver, 1991, Quinson et al., 2001, Glebova and Ginty, 2004). Surprisingly, when analysing whole mount stainings of P10 spleen from both *Tnfα*$^{-/-}$ and *Tnfrsf1a*$^{-/-}$ mice there was an increase in innervation density compared to wild type mice (Fig.10A). This increase was statistically significant in *Tnfrsf1a*$^{-/-}$ mice compared with *Tnfrsf1a*$^{+/+}$ mice, but did not reach statistical significance in *Tnfα*$^{-/-}$ mice compared with *Tnfα*$^{+/+}$ mice, although the difference between *Tnfα*$^{-/-}$ and *Tnfα*$^{+/-}$ mice was statistically significant (Fig.10B). The spleen is less densely innervated by sympathetic fibres than other target organs analysed (Fig.10A). However, like in all target organs, the

sympathetic fibres follow the vasculature into the spleen, where they enter the white pulp and branch into the periarteriolar lymphatic sheath and marginal zone (Carlson et al., 1987, Madden et al., 1997). Arrows in Fig.10A show how in KO mice this branching within the periarteriolar plexus is more extended within the tissue when compared to WT littermates.

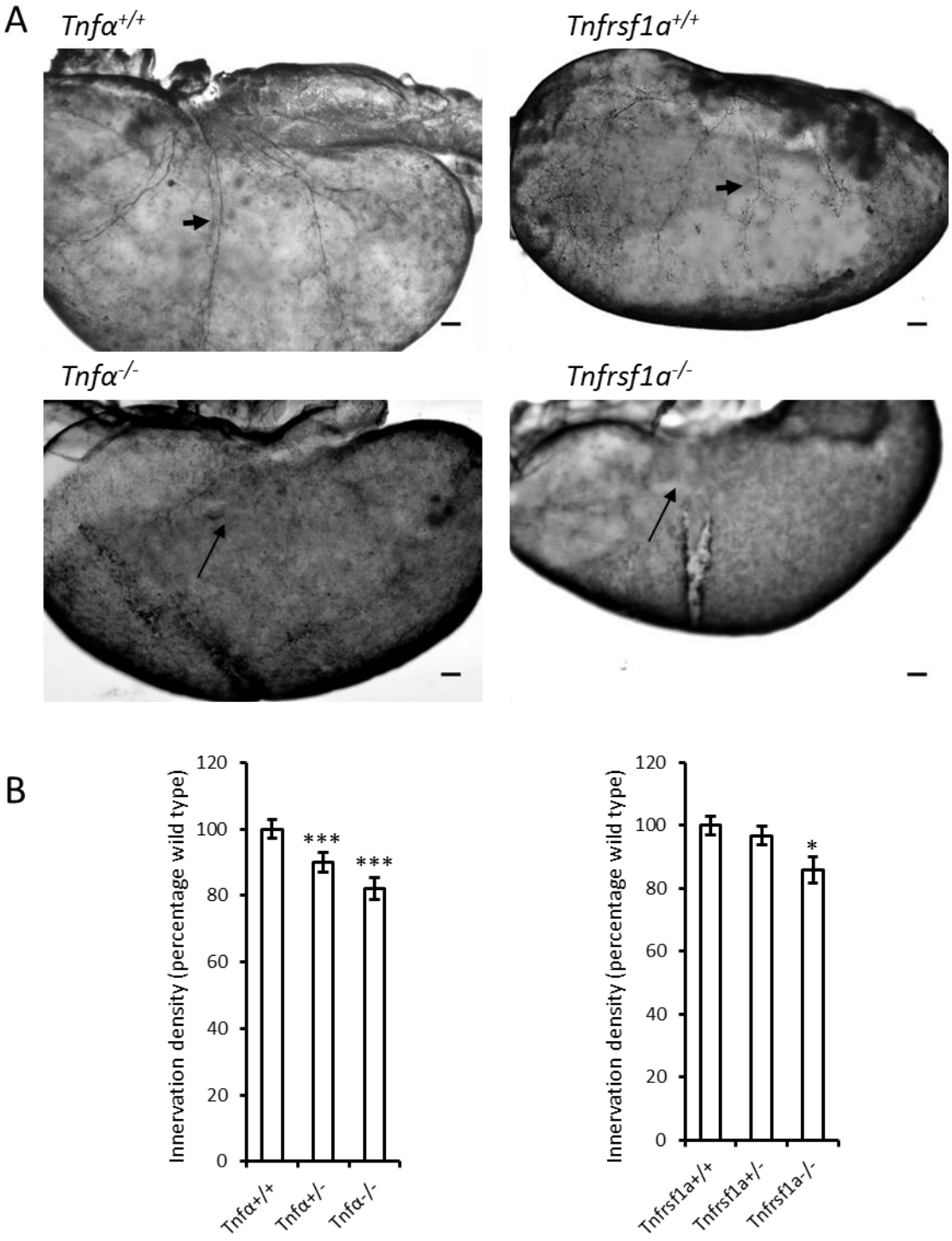

Figure 8: Sympathetic nerve fibre branching in P10 kidney *Tnfα*$^{-/-}$ and *Tnfrsf1a*$^{-/-}$ mice. A) Representative images of whole mount staining preparations of the kidney of P10 *Tnfα*$^{+/+}$, *Tnfα*$^{-/-}$, *Tnfrsf1a*$^{+/+}$ and *Tnfrsf1a*$^{-/-}$ mice labelled with anti-TH. Small arrows indicate areas of normal innervation, long arrows indicate areas of decreased innervation. Scale bars, 100 µm. **B)** Relative length per unit area of fibres of *Tnfα*$^{+/+}$, *Tnfα*$^{+/-}$, *Tnfα*$^{-/-}$, *Tnfrsf1a*$^{+/+}$, *Tnfrsf1a*$^{+/-}$ and *Tnfrsf1a*$^{-/-}$ mice expressed as a percentage of the mean level in *Tnfα*$^{+/+}$ or *Tnfrsf1a*$^{+/+}$ mice. Mean ± s.e.m of data from 4 to 8 animals of each genotype are shown. Statistical comparison with wild type, *P < 0.05, *** P < 0.001, one-way ANOVA *post-hoc* Tukey's HSD.

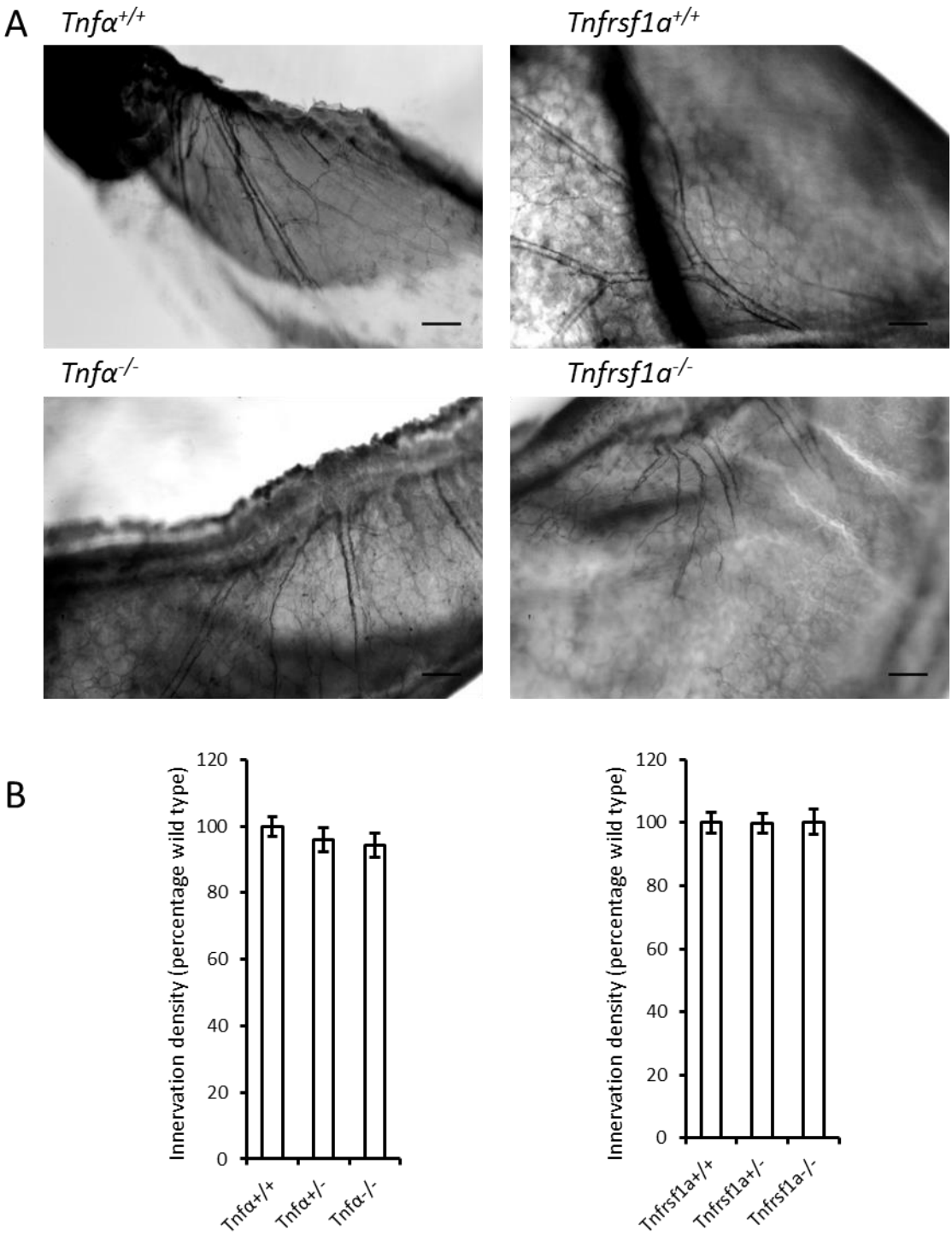

Figure 9: Sympathetic nerve fibre branching in P10 stomach *Tnfα*$^{-/-}$ and *Tnfrsf1a*$^{-/-}$ mice. A) Representative images of whole mount staining preparations of the stomach of P10 *Tnfα*$^{+/+}$, *Tnfα*$^{-/-}$, *Tnfrsf1a*$^{+/+}$ and *Tnfrsf1a*$^{-/-}$ mice labelled with anti-TH. Scale bars, 100 µm. **B)** Relative length per unit area of fibres of *Tnfα*$^{+/+}$, *Tnfα*$^{+/-}$, *Tnfα*$^{-/-}$, *Tnfrsf1a*$^{+/+}$, *Tnfrsf1a*$^{+/-}$ and *Tnfrsf1a*$^{-/-}$ mice expressed as a percentage of the mean level in *Tnfα*$^{+/+}$ or *Tnfrsf1a*$^{+/+}$ mice. Mean ± s.e.m of data from 5 to 8 animals of each genotype are shown. Statistical comparison with wild type, no significant differences were evident, one-way ANOVA *post-hoc* Tuckey's HSD.

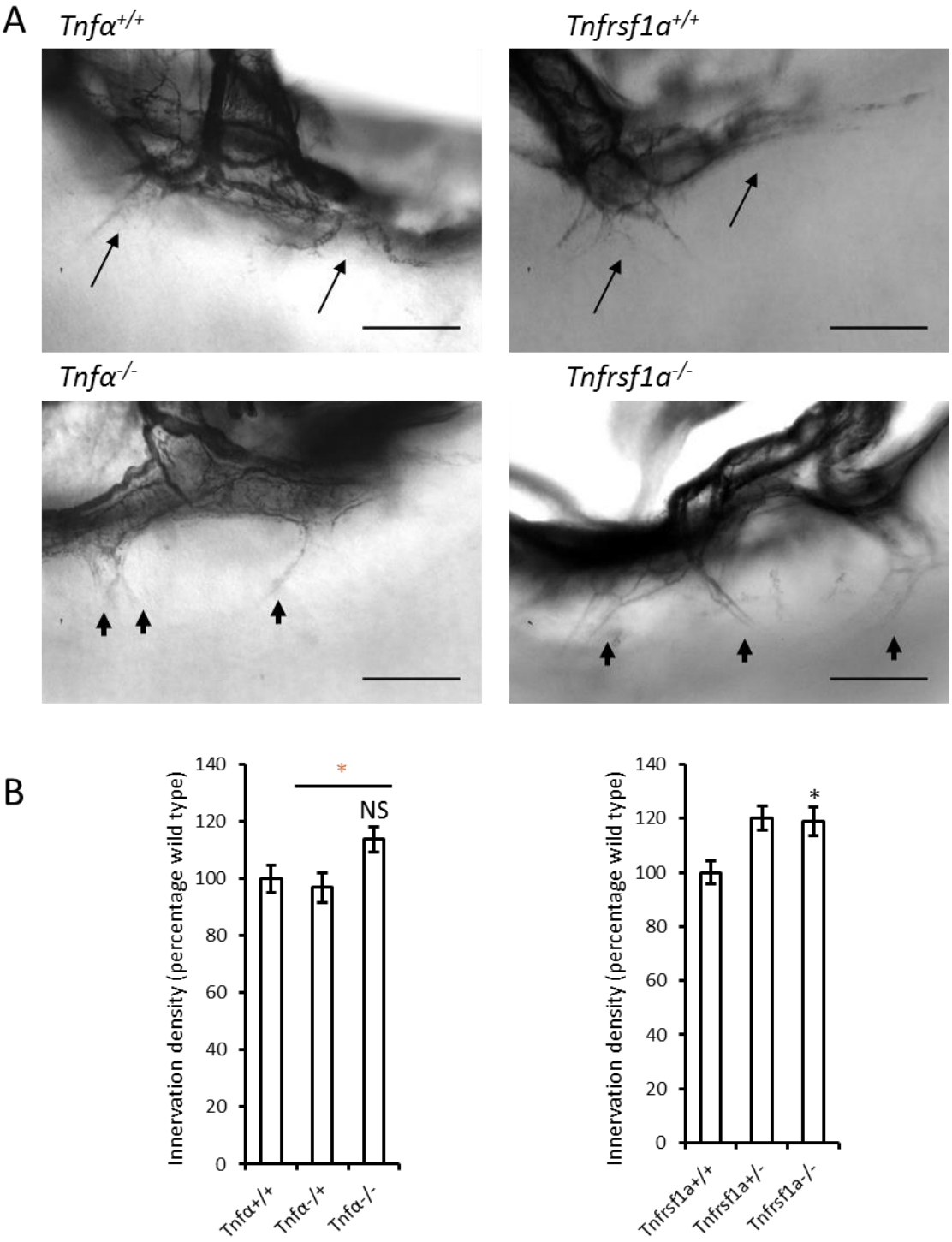

Figure 10: Sympathetic nerve fibre branching in P10 spleen *Tnfα*$^{-/-}$ and *Tnfrsf1a*$^{-/-}$ mice. A) Representative images of whole mount staining preparations of the spleen of P10 *Tnfα*$^{+/+}$, *Tnfα*$^{-/-}$, *Tnfrsf1a*$^{+/+}$ and *Tnfrsf1a*$^{-/-}$ mice labelled with anti-TH. Small arrows indicate areas of increased innervation, long arrows indicate areas of normal innervation. Scale bars, 100 µm. **B)** Relative length per unit area of fibres of *Tnfα*$^{+/+}$, *Tnfα*$^{+/-}$, *Tnfα*$^{-/-}$, *Tnfrsf1a*$^{+/+}$, *Tnfrsf1a*$^{+/-}$ and *Tnfrsf1a*$^{-/-}$ mice expressed as a percentage of the mean level in *Tnfα*$^{+/+}$ or *Tnfrsf1a*$^{+/+}$ mice. Mean ± s.e.m of data from 6 to 8 animals of each genotype are shown. Statistical comparison with wild type, *P < 0.05, NS= not significant; statistical comparison with *Tnfα*$^{+/-}$ mice, *P < 0.05, one-way ANOVA *post-hoc* Tukey's HSD.

4.5 mRNA expression levels of *Tnfα*, *Tnfrsf1a* and *Tnfrsf1b* transcripts in different sympathetic target organs

Whole mount data shows that the sympathetic innervation of prevertebral ganglion target organs is modulated in different ways and to different extents by TNF and TNFR1. To investigate whether these differences are related to differences in the expression of TNF and its receptors in these targets, I used quantitative real-time PCR (qPCR) to determine the relative levels of *Tnfα*, *Tnfrsf1a* and *Tnfrsf1b* mRNA in these target organs throughout the period when sympathetic fibres are branching and ramifying in these tissues during postnatal development. *Tnfrsf1b* is the transcript for TNFR2. Total RNA was extracted from P0, P5 and P10 target organs and the qPCR data for *Tnfα, Tnfrsf1a* and *Tnfrsf1b* transcripts were normalised to the levels of the mRNAs encoding the housekeeping proteins glyceraldehyde phosphate dehydrogenase (GAPDH) and succinate dehydrogenase (SDHA). For comparison, I included heart RNA and submandibular salivary gland RNA, as these organs are innervated exclusively by paravertebral sympathetic neurons and both depend on TNF and TNFR1 for the establishment of appropriate sympathetic innervation.

Tnfα mRNA was expressed in most target organs at very low levels, except in the spleen, where the levels were much higher throughout the period of development studied. The submandibular salivary gland also expressed much higher levels of *Tnfα* mRNA than the stomach, kidney and heart, but approximately half the level of the spleen (Fig.11A). The highest levels of *Tnfrsf1a* mRNA were expressed in the stomach and the submandibular salivary gland. Both organs displayed a similar developmental expression profile with similar levels at P0 and P5, dropping almost 1/3 by P10. The spleen showed high

expression, dropping by about a half at P5 and P10. The kidney and the heart maintained a low level of expression at all ages studied (Fig.11B). *Tnfrsf1b* mRNA is highly expressed in the spleen throughout the period studied. The stomach and submandibular salivary gland expressed much lower levels of *Tnfrsf1b* mRNA, and *Tnfrsf1b* mRNA was barely detectable in the kidney and heart. (Fig 11C).

In summary, these results indicate that the spleen, which is hyperinnervated in mice lacking either TNF or TNFR1, expressed the highest levels of TNF and TNFR2 of the organs analysed.

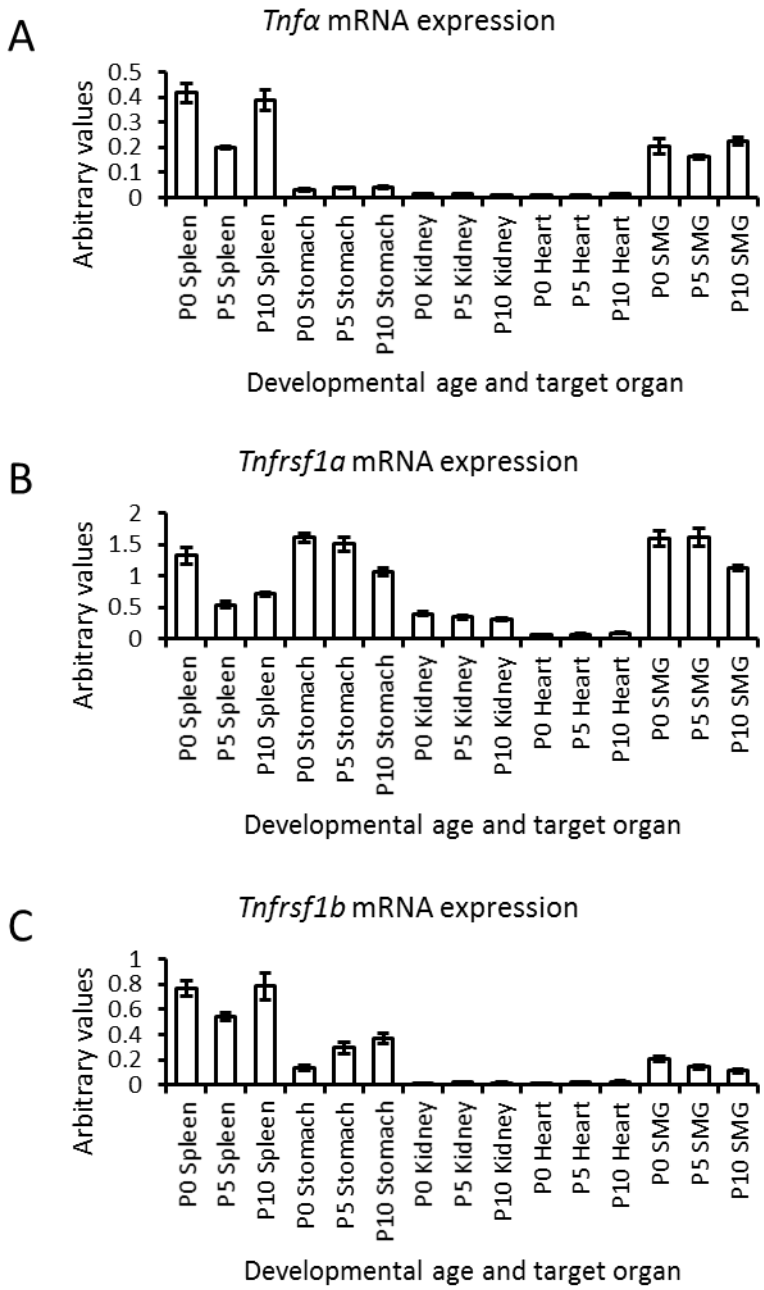

Figure 11: Relative expression of *Tnfα*, *Tnfrsf1a* and *Tnfrsf1b* mRNAs in the spleen, stomach, kidney, heart and submandibular salivary gland (SMG). mRNA levels are relative to the levels of housekeeping mRNAs at different developmental ages. **A)** *Tnfα* mRNA, **B)** *Tnfrsf1a* mRNA and **C)** *Tnfrsf1b* mRNA. Mean and s.e.m. of data from four separate samples (arbitrary units).

4.6 Discussion

In this chapter I have reported data that demonstrate the requirement for TNFR1 and TNF *in vivo* in the establishment of the sympathetic innervation of tissues that receive their sympathetic innervation from neurons of the paravertebral sympathetic chain. Using TH as a marker for sympathetic fibres in whole mount preparations, I found statistically-significant reductions in sympathetic innervation density in the submandibular salivary gland, pineal gland, trachea, heart, and kidney, tissues and organs that receive their sympathetic innervation either exclusively or predominantly from the paravertebral sympathetic chain, in TNF-deficient and TNFR1-deficient mice at P10. In several of these tissues, there were also statistically-significant reductions in sympathetic innervation density in heterozygous mice compared with wild type mice, although these reductions were not as great as those seen in homozygous mice. This implies a gene dosage effect for both genes. These results complement and confirm the results of the estimation of sympathetic innervation density in TNF-deficient and TNFR1-deficient mice by quantifying TH immunostaining in tissue sections (Appendix III) (Kisiswa et al., 2013). In this latter study, highly significant reductions in sympathetic innervation were observed in tissues innervated by the SCG, the submandibular salivary gland, iris and nasal turbinates. Furthermore, it was shown that decreases in sympathetic innervation density in TNF-deficient and TNFR1-deficient mice are not secondary to loss of sympathetic neurons or reduced neuronal staining for TH (Kisiswa et al., 2013). These results are consistent with the operation of TNFR1-activated TNF reverse signalling in establishing the innervation of multiple paravertebral sympathetic chain targets *in vivo.*

My work not only extends the analysis to more caudal ganglia of the paravertebral sympathetic chain, but by visualizing the topography of sympathetic fibres in whole mount preparations, I show that sympathetic fibres reach these target tissues, but the subsequent growth and branching of the fibres within these tissues is markedly impaired. This suggests that TNFR1-activated TNF reverse signalling plays no role in guiding sympathetic axons to these tissues, but plays a role in promoting the growth and ramification of sympathetic axons within target tissues. This corresponds nicely with the developmental window when TNF reverse signalling effects are seen *in vitro* (P0 to P5) as this coincides with the period of final target innervation, a point at which axons have already reached target organs and are starting to ramify within tissues.

Mice lacking TNF and TNFR1 survive normally until adulthood (refer to section 2.1 for description of KO mice) reflecting the subtle decreases in innervation observed. However, it is interesting to consider the possible physiological effects on the flight or fight-response of these animals, if left in the wild. An interesting approach would be to carry out behavioural studies on *Tnfα* and *Tnfrs1a* deficient mice to see to what extent target organ function is impaired. This is particularly feasible when considering heart innervation. Heart rate and myocardial contractility can be measured in catheterized wild type and KO mice, after recording baseline measurements, α_2-adrenergic receptor antagonist yohimbine (YOH) can be administered to the mice. This antagonist increases post-ganglionic sympathetic activity, hence, differences between genotypes can be assessed (described in (Eldredge et al., 2008)).

TNFR1-activated TNF reverse signalling contributes to the establishment of sympathetic innervation *in vivo*, as opposed to being an essential requirement. The stereological

method I employed revealed that the reduction in sympathetic innervation in whole mount preparations was approximately 20% in paravertebral sympathetic chain targets in TNF-deficient and TNFR1-deficient mice, except the heart, where the reduction was less. However, the restricted region chosen for stereological analysis in the heart, the densely-innervated region where sympathetic fibre bundles enter the left ventricle around the atrioventrical node and bundle of His (Kimura et al., 2012), may not be fully representative of the organ as a whole. Retrospective examination of the heart images after the images were unblinded (representative images shown in Fig.4A) indicates that sympathetic fibres do not reach the bottom of the ventricle in both TNF-deficient and TNFR1-deficient mice. Thus, choosing different anatomical regions for the stereological analysis might affect the magnitude of the innervation decrease. However, there was insufficient time to collect and analyse another batch of tissue blind using modified criteria.

Notwithstanding the latter caveat regarding the stereological analysis of heart innervation, the rather modest reductions in sympathetic innervation density in TNF-deficient and TNFR1-deficient mice contrast with the finding of the major contribution made by NGF to the terminal growth of sympathetic fibres in most tissues (Glebova and Ginty, 2004). NGF is the classic target-derived neurotrophic factor for sympathetic neurons that is required both for neuronal survival and the growth and ramification of sympathetic axons in target tissues. To study the contribution of NGF to terminal sympathetic fibre growth *in vivo*, independently of its requirement for survival, NGF/BAX double knockout mice were studied (Glebova and Ginty, 2004). BAX is a key protein in the cell death pathway, and in NGF/BAX double knockout mice NGF-dependent sympathetic neurons fail to die in the absence of NGF (White et al., 1998, Middleton and

Davies, 2001). Glebova and Ginty found that in these mice sympathetic neurons extended axons to their targets, but failed to ramify within many targets. While no quantification was carried out in this study, it is clear from the TH-labelled whole mount preparations illustrated in their study that many tissues were almost devoid of sympathetic fibres. Yet, despite the survival requirement of all sympathetic neurons for NGF, the sympathetic innervation of some tissues was only partially disrupted in NGF/BAX double knockout mice and the innervation of some tissues was unaffected. This suggests the operation of additional factors that regulate sympathetic axon growth and branching in certain targets independently of NGF (Glebova and Ginty, 2004). In this regard, it is interesting that the trachea was one such tissue whose sympathetic innervation was unaffected in NGF/BAX double knockout mice. However, I found that the sympathetic innervation of this tissue was significantly reduced in TNF-deficient and TNFR1-deficient mice, suggesting that target-derived TNFR1 contributes to establishing the sympathetic innervation of this tissue independently of NGF.

NGF and TNFR1 are but two of the factors that have been shown to be required for the establishment of sympathetic innervation *in vivo*. Not all such factors operate in a target-derived manner like NGF and TNFR1. Some factors influence the establishment of sympathetic innervation by an autocrine mode of action. Autocrine Wnt5a signalling has been shown, using mice that have a conditionally inactivated *Wnt5a* gene in sympathetic neurons, to be required for the growth and terminal arborization of sympathetic fibres in multiple tissues (Bodmer et al., 2009). Autocrine GITR signalling is required for establishing the sympathetic innervation of the two tissues examined in this study, the iris and nasal turbinates (O'Keeffe et al., 2008). Autocrine CD40 reverse signalling enhances NGF-promoted sympathetic axon growth and has a regional effect

on establishing sympathetic innervation *in vivo*. This is because NGF negatively regulates the expression of CD40 and its autocrine signalling partner CD40L, with the result that these proteins are only expressed at functionally relevant levels in low NGF-expressing tissues, which are those that are selectively hypoinnervated in *Cd40*$^{-/-}$ mice (McWilliams et al., 2015).

A notable finding of the analysis of TH whole mount staining in TNF-deficient and TNFR1-deficient mice was the different requirements of paravertebral and prevertebral sympathetic neuron targets for TNF and TNFR1 in establishing their innervation. Whereas the sympathetic innervation density of tissues that receive their innervation exclusively or predominantly from paravertebral ganglia was universally reduced in mice lacking TNF and TNFR1, as discussed above, tissues that receive their innervation predominantly from prevertebral ganglia were either unaffected or hyperinnervated. The stomach, which is predominantly innervated by the prevertebral celiac ganglion, retains normal innervation in mice lacking TNF or TNFR1, whereas the spleen, which is also predominantly innervated by the celiac ganglion, has increased sympathetic innervation in *Tnfα*$^{-/-}$ and *Tnfrsf1a*$^{-/-}$ mice. This contrasts with the findings in NGF/BAX double knockout mice (Glebova and Ginty, 2004) and mice in which *Wnt5a* is conditionally-inactivated in sympathetic neurons (Bodmer et al., 2009), where all target organs of prevertebral ganglia analysed had marked decreases in sympathetic innervation. The hyperinnervation of the spleen in mice lacking TNF or TNFR1 is particularly intriguing. One possible explanation for this may be a predominant role for TNF forward signalling in modulating sympathetic innervation of this organ. TNF forward signalling has been shown to reduce NGF-promoted sympathetic axon growth *in vitro* (Gutierrez et al., 2008). So if forward signalling, as opposed to reverse signalling, did

predominate in modulating the innervation of certain tissues *in vivo*, one would predict hyperinnervation of those tissues in mice lacking TNF. Indirect evidence, that is consistent with this possibility, comes from the quantification of the relative levels of *Tnfα*, *Tnfrsf1a* and *Tnfrsf1b* mRNAs in the spleen and other tissues during the period when sympathetic fibres are ramifying in these tissues. Of all tissues studied, the spleen had the highest levels of TNF mRNA, which is consistent with a predominant role for target-derived TNF forward signalling.

A recent study has reported that TNF forward and TNF reverse signalling have opposing actions on axon growth from sensory DRG neurons akin to those previously reported for sympathetic neurons (Gutierrez et al., 2008, Kisiswa et al., 2013). Neurite outgrowth from peptidergic nociceptors was negatively regulated by TNF-forward signalling, whilst neurite outgrowth from nonpeptidergic nociceptors was enhanced by TNF-reverse signalling. Furthermore, the target fields of peptidergic neurons were hyperinnervated in *Tnfα*$^{-/-}$ and *Tnfsrsf1a*$^{-/-}$ mice, whereas target fields for nonpeptidergic neurons were hypoinnervated (Wheeler et al., 2014).

While it will be essential to complement the qPCR data with western blot analysis to compare protein expression levels of TNF and its receptors in the spleen and other tissues, it is important to consider the significance of the expression of *Tnfα*, *Tnfrsf1a* and *Tnfrsf1b* mRNAs in the spleen may only have a minor role in regulating sympathetic innervation. The spleen is a secondary lymphoid organ, and TNFα, TNFR1 and TNFR2 have key roles in the development of the immune system. For example, it has been shown that TNF is essential for the development of spleen fibroblastic reticular cells (Zhao et al., 2015). Also it is important to consider that knocking out TNF or TNFR1 might

disrupt immune system development in the spleen that could affect its innervation in ways that do not directly involve TNF signalling. It would be of interest to examine the innervation of the thymus in mice deficient for *Tnfrsf1a* and *Tnfα* to see if they have a similar phenotype, for example. In addition, the thymus is innervated primarily by the SCG (Nance and Sanders, 2007), so this analysis would tell us whether ganglionic origin of sympathetic innervation (paravertebral versus prevertebral) or hematopoietic target organs versus non-hematopoietic target organs is the important defining characteristic for the sympathetic innervation phenotype in $Tnf\alpha^{-/-}$ and $Tnfrsf1a^{-/-}$ mice.

It is important to consider the possibility that there might be intrinsic differences in the response of paravertebral and prevertebral sympathetic neurons or subsets of neurons in these ganglia to TNFR1-activated TNF reverse signalling. Prevertebral sympathetic neurons tend to be more heterogeneous in nature than paravertebral neurons and it has been shown that there are distinct differences in gene expression between paravertebral and prevertebral ganglia (Carroll et al., 2004). This study identified 141 unique mRNA transcripts corresponding to prevertebral ganglia and 118 transcripts specific to the SCG (paravertebral ganglia). These transcripts coded for specific neurotransmitters and neurotransmitter receptors. It was also found that the different ganglia preferentially expressed different types of transcripts for particular proteins involved in synaptic structure, synaptic vesicle transport, fusion and membrane recovery (Carroll et al., 2004) This is in accordance with previous reports describing differences between both types of ganglia in biochemical, structural, functional electrophysiological and immunohistochemical characteristics (Szurszewski, 1981, Sejnowski, 1982, Janig and McLachlan, 1992, Elfvin et al., 1993, Carroll et al., 2004). Paravertebral ganglia tend to be more “simple” as their main function is to relay information. On the other hand,

prevertebral ganglia have to integrate the complex and varied visceral reflexes (Carroll et al., 2004). Hence, if not all sub-populations of sympathetic neurons respond to TNFR1, the effects of TNF reverse signalling might be diluted in a highly heterogeneous neuronal population. Several retrograde tracing studies on mice and rat SCGs propose that specific neuronal sub-populations innervate target organs preferentially and that they can be identified by their morphology and neuropeptide immunoreactivity (Wright and Luebke, 1989, Gibbins, 1991, Luebke and Wright, 1992). It would be of interest to determine if all sympathetic cells are capable of responding to TNFR1 or only a subset identified by their neuropeptide expression profile. Also, it would be of interest to compare the response of paravertebral and prevertebral sympathetic neurons to TNFR1-Fc *in vitro*.

In summary, I have presented data suggesting that paravertebral sympathetic target organs require TNF reverse signalling for correct final target innervation while prevertebral sympathetic target organs vary in their dependence. This may be due to the fact that the balance between forward and reverse signalling is different in these target organs or might be related to intrinsic differences in the response of paravertebral and prevertebral neurons to TNFR1.

Chapter 5
T-type calcium channels are required for enhanced sympathetic axon growth in response to TNF reverse signalling

5.1 Introduction

The results reported in the previous chapters show that TNF reverse signalling is a key regulator of sympathetic axonal growth, playing a crucial role in establishing the sympathetic innervation of paravertebral ganglion target organs during development. This chapter reports the results of studies that tackle the mechanistic link between TNF reverse signalling and enhanced sympathetic axonal growth.

The starting point of these studies was our published observation that treating cultured P0 SCG neurons with TNFR1-Fc causes a rapid and significant increase in cytosolic Ca^{2+}. This elevation in cytosolic Ca^{2+} failed to occur in Ca^{2+}-free medium and the intracellular Ca^{2+} chelator BAPTA prevented neurite growth enhancement by TNFR1-Fc (Appendix IV, Fig.1-2) (Kisiswa et al., 2013). This suggests that activation of TNF reverse signalling causes Ca^{2+} influx and elevation of cytoplasmic Ca^{2+} which is required for neurite growth enhancement. The main aim of the studies reported in this chapter was to identify the ion channel required for Ca^{2+} influx. I will first provide a brief overview of voltage gated calcium channels.

Calcium channels

Calcium is a key secondary messenger that plays crucial roles for correct cellular function. Its broad range of action includes: activation of Ca^{2+}-dependent enzymes, hormone and neurotransmitter secretion, cell proliferation, differentiation, apoptosis and cell death (reviewed in (Clapham, 2007, Iftinca and Zamponi, 2009, Zhang et al., 2013)).

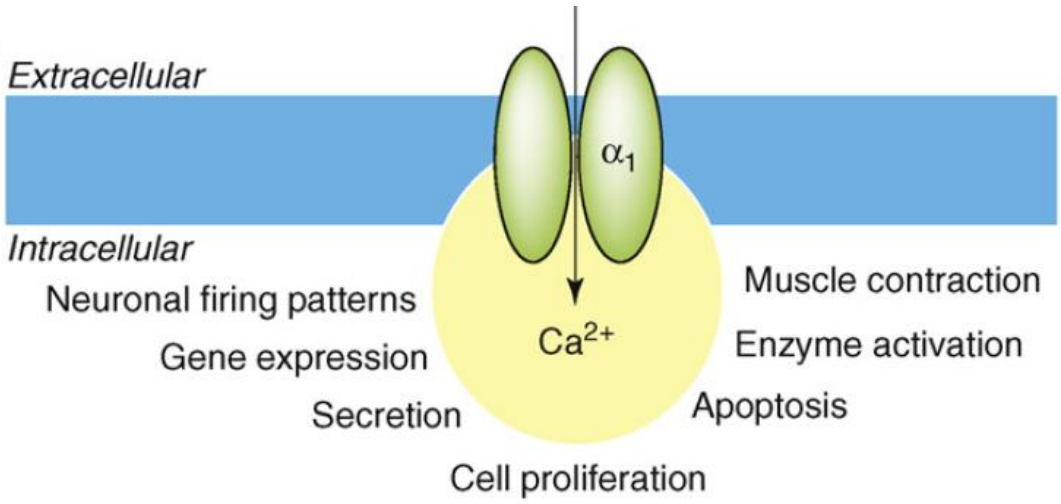

Figure 1: Ca^{2+} as a secondary messenger: Diagram depicting Ca^{2+} entry through a T-type calcium channel and its various physiological roles as a secondary messenger. From (Iftinca, 2011).

The level of intracellular free Ca^{2+} is controlled by a variety of pumps and channels, voltage-gated calcium channels playing a major role (Perez-Reyes, 2003). Voltage-gated calcium channels are broadly divided into two sub-groups; high-voltage activated (HVA) and low-voltage activated (LVA) calcium channels. As their name indicates, HVA channels rely on large membrane depolarizations to open, while LVA require much smaller membrane depolarizations. In addition LVA channels are characterised by faster gating kinetics than their counterparts and are known as transient or T-type calcium channels (reviewed in (Iftinca and Zamponi, 2009)).

The HVA channels are comprised by N-, P-, Q-, L- and R-types. These channels are heteromultimers, comprised of an α_1 subunit which forms the pore and hence ascribes what HVA sub-type the channel will be. The α_1 subunit is associated with β and α_2-δ subunits which modulate the functional properties of the channels (reviewed in (Iftinca and Zamponi, 2009)). Unlike HVA channels, T-type channels are only formed by a single functional α_1 subunit. In both categories of calcium channels α_1 subunits are comprised

by four homologous domains (I-IV). Each domain in turn has six transmembrane helices (S1 to S6) and a loop, the four loops come together and allow the selective passage of Ca^{2+} ions. The S4 segment of each domain come together to form the voltage sensor as they contain positively charged amino acid residues on every third position (Iftinca, 2011).

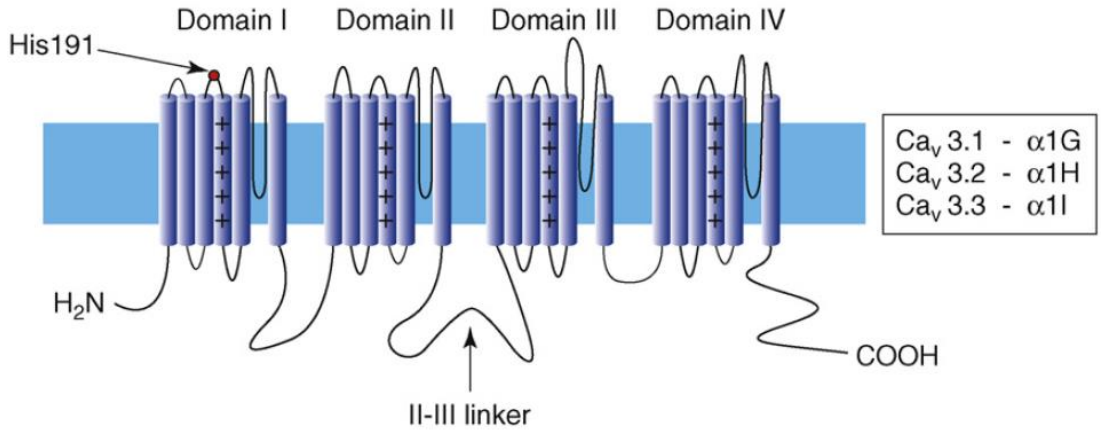

Figure 2: General structure of T-type calcium channels. Diagram depicting the α_1 subunit that comprises all three T-type calcium channels. They all contain 4 domains with one loop each that will come together to allow the selective passage of Ca^{2+}. Each domain is comprised of 6 segments. Segment 4 has positively charged amino acids on every third position which allows the detection of changes in membrane potentials. From (Iftinca and Zamponi, 2009).

Three types of T-type calcium channels are encoded by three separate genes: Cav3.1 or CACNA1G, Cav3.2 or CACNA1H and Cav3.3 or CACNA1I. These channels differ in their functional and pharmacological characteristics as well as cellular and subcellular localisations (Table 1). Furthermore, each isoform has multiple splice variants adding to their diversity, and it is thought that these splice variants have unique electrophysiological properties (Iftinca, 2011).

Table 1: Tissue distribution of T-type calcium channels. From (Iftinca and Zamponi, 2009)**.**

Table 1. Tissue distribution of T-type calcium channel isoforms .

Tissue	Isoform
Brain	Cav3.1, Cav3.2, Cav3.3
Peripheral nervous tissue (DRG, autonomic ganglia)	Cav3.1, Cav3.2, Cav3.3
Heart (myocytes, pacemaker cells)	Cav3.1, Cav3.2
Smooth muscle	Cav3.1, Cav3.2
Skeletal muscle	Cav3.2
Bone (osteoblasts)	Cav3.1
Endocrine cells (adrenal, pituitary, pancreas, thyroid)	Cav3.1, Cav3.2
Sperm	Cav3.1, Cav3.2

The studies reported in this chapter strongly suggest that T-type calcium channels are a key element in mediating the neurite growth-promoting effects of TNF reverse signalling in developing sympathetic neurons.

RESULTS

The experiments presented in sections 5.2 and 5.3 were carried out by Lilian Kisiswa and Lisa Kinnavane and are included in order to give a comprehensive framework to my results. My work focused mostly on the experiments with T-type calcium channels that followed on from these experiments.

5.2 Blocking calcium channels inhibits TNFR1-Fc promoted neurite growth

Given the demonstration that activation of TNF reverse signalling in postnatal sympathetic neurons causes Ca^{2+} influx, which is a necessary step for enhanced neurite growth (Kisiswa et al., 2013), we used a pharmacological approach to examine whether calcium channels participate in the neurite growth-promoting effect of TNF reverse signalling. Dissociated P0 SCG neurons were cultured for 24 h in the presence of 10 ng/ml NGF to sustain survival with 1 µM of the broad-spectrum voltage-gated calcium channel blocker dotarizine (Tejerina et al., 1993, Villarroya et al., 1995) for one hour before activating TNF reverse signalling with a divalent TNFR1-Fc chimera (Kisiswa et al., 2013). After 24 h axonal length and branching was assessed by Sholl analysis**.** Quantification of the size and complexity of the neurite arbors showed that the TNFR1-Fc chimera caused significant increases in neurite branch point number and length (Fig.3B-C). Accordingly, the Sholl profiles (Fig.3A) of neurons grown in the presence of TNFR1-Fc were clearly larger than those grown with NGF alone. Whereas the size and complexity of the neurite arbors of neurons treated with dotarizine or dotarizine plus TNFR1-Fc were not significantly different from those grown with NGF alone. Therefore, dotarizine completely prevented TNFR1-Fc-enhanced neurite growth (Fig.3). These studies suggest that calcium channels are required for the effect of TNF reverse signalling on axon growth.

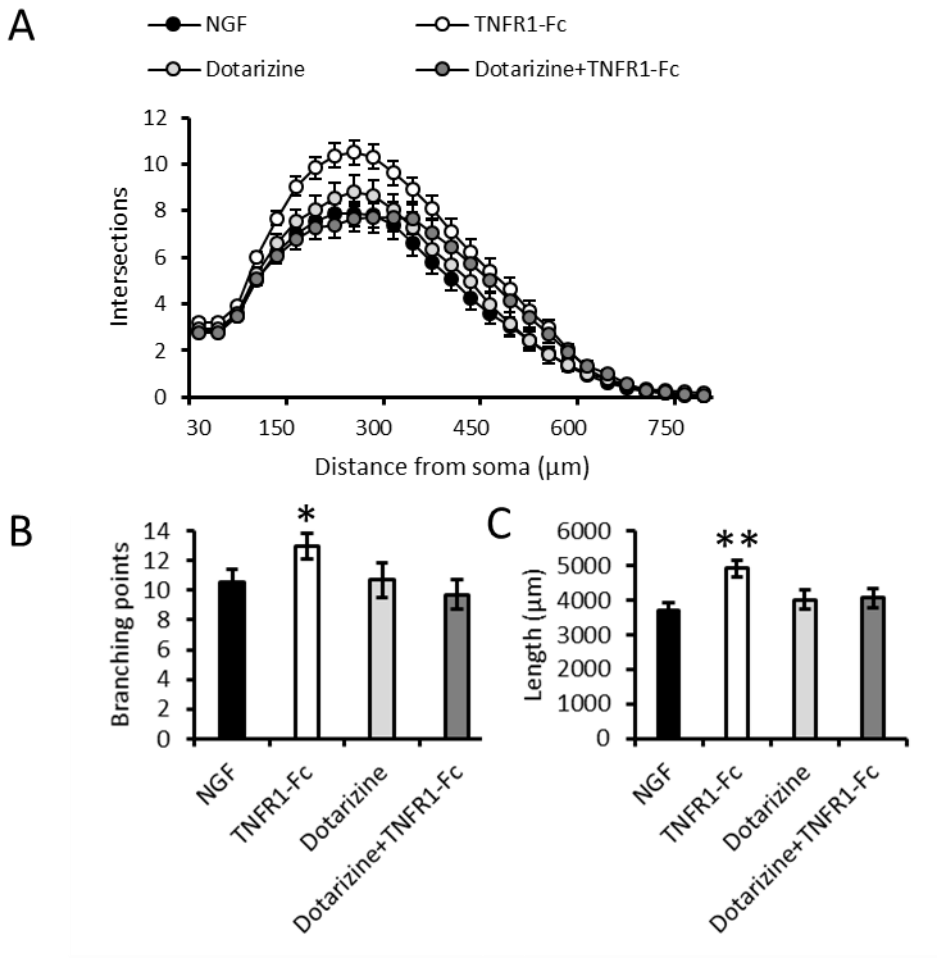

Figure 3: Voltage-sensitive calcium channels are required for TNFR1-Fc-promoted neurite growth. Dissociated cultures of P0 SCG neurons were grown overnight in the presence of 10 ng/ml NGF alone or NGF plus 10 ng/ml TNFR1-Fc or NGF plus 1 µM dotarizine either with or without TNFR1-Fc. **A)** Sholl profiles, **B)** branch point number and **C)** neurite length in the neurite arbors of the neurons grown under these conditions. Mean ± s.e.m. of the data from 3 separate experiments are plotted. More than 50 neurons analysed per condition in each experiment; statistical comparison with control (NGF), **p<0.01,*p<0.05, one-way ANOVA *post-hoc* Fischer's.

5.3 T-type calcium channels but not L, N, P/Q or R type are required for TNFR1-Fc-promoted neurite growth

To ascertain whether particular kinds of calcium channels are required for the neurite growth-promoting effect of TNF reverse signalling, we carried out a series of studies using sub-type selective calcium channel blockers. For these experiments we used 10 µM nifedipine which is a selective blocker of L-type channels (Vater et al., 1972), 100 nM ω-agatoxin TK which blocks P/Q-type channels (Teramoto et al., 1993), 10 nM ω-grammotoxin SIA which blocks N-type and P/Q-type channels (Lampe et al., 1993, Takeuchi et al., 2002), SNX 482 which blocks R-type channels (Newcomb et al., 1998), and 1 µM mibefradil which blocks T-type channels (Osterrieder and Holck, 1989, Mehrke et al., 1994, Massie, 1997). Dissociated P0 SCG neurons were cultured in the presence of 10 ng/ml NGF to sustain survival. The corresponding inhibitor was added at the time of plating, one hour before activating TNF reverse signalling with a divalent TNFR1-Fc chimera, and the cultures were examined 24 h later.

None of these calcium channel inhibitors had any significant effect on NGF-promoted survival (data not shown). Whereas neither nifedipine (Fig.4A), ω-agatoxin (Fig. 4B), ω-grammotoxin SIA (Fig.4C) nor SNX 482 (Fig.4D) had a significant effect on TNFR1-Fc-promoted neurite growth, mibefradil completely inhibited TNFR1-Fc-promoted neurite growth (Fig.4E). These results suggest the possible involvement of T-type calcium channels in mediating the effect of TNF reverse signalling on sympathetic axonal growth.

A

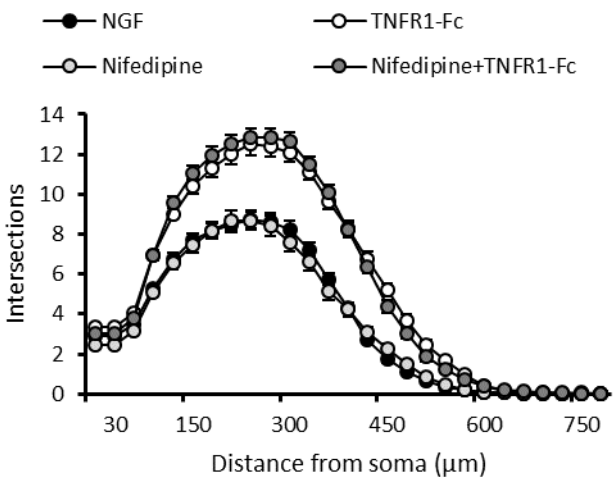
NGF
TNFR1-Fc
Nifedipine
Nifedipine+TNFR1-Fc
Intersections
0
2
4
6
8
10
12
14
30
150
300
450
600
750
Distance from soma (µm)

B

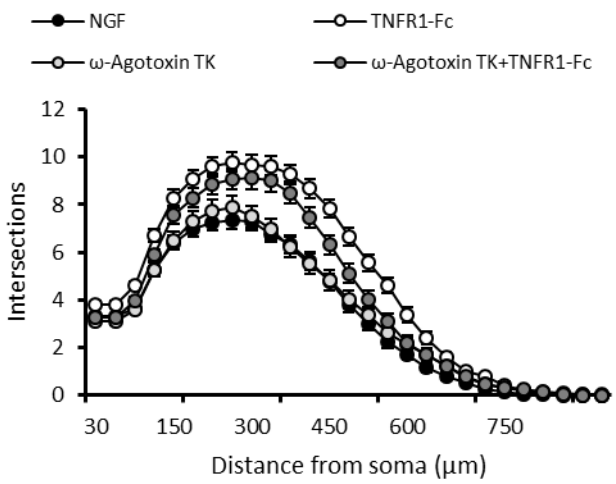
NGF
TNFR1-Fc
ω-Agotoxin TK
ω-Agotoxin TK+TNFR1-Fc
Intersections
0
2
4
6
8
10
12
30
150
300
450
600
750
Distance from soma (µm)

C

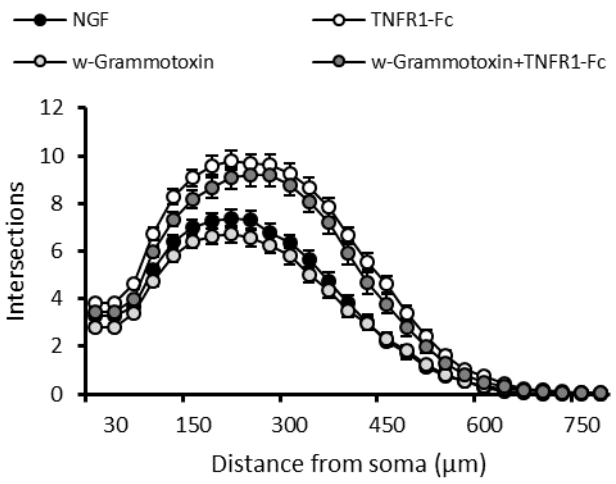
NGF
TNFR1-Fc
w-Grammotoxin
w-Grammotoxin+TNFR1-Fc
Intersections
0
2
4
6
8
10
12
30
150
300
450
600
750
Distance from soma (µm)

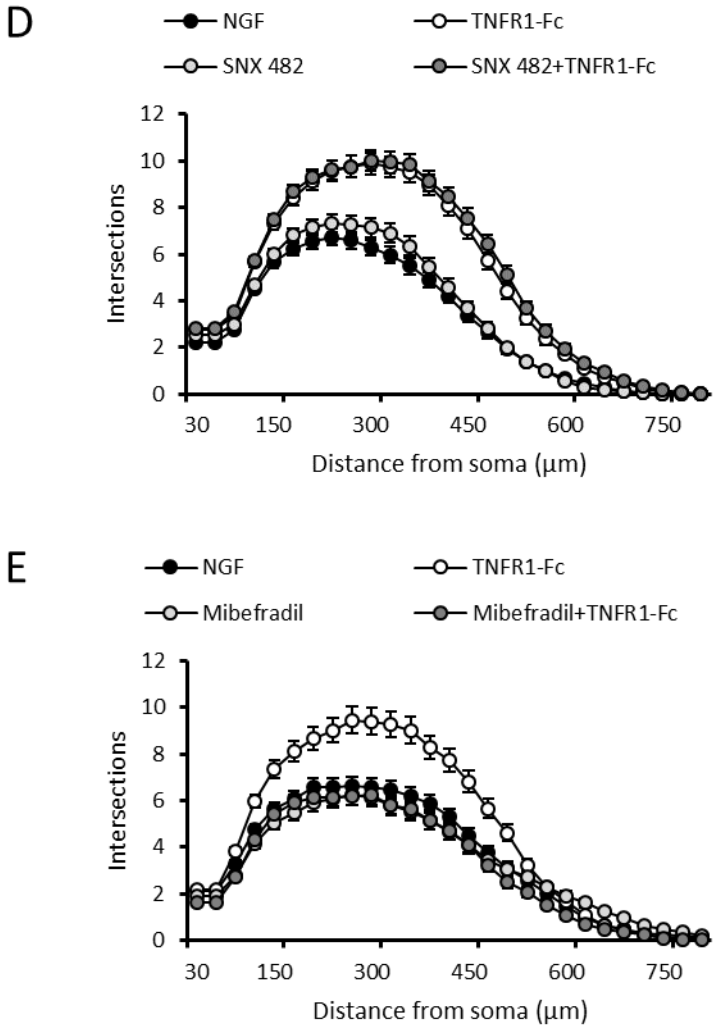

Figure 4: T-type calcium channels are required for TNFR1-Fc-promoted neurite growth. Sholl profiles of dissociated cultures of P0 SCG neurons which were grown overnight in the presence of 10 ng/ml NGF alone, NGF plus 10 ng/ml TNFR1-Fc, NGF plus a calcium channel blocker or NGF plus TNFR1-Fc and calcium channel blocker. **A)** 10 µM nifedipine **B)** 100nM ω-agatoxin TK **C)** 10nM ω-grammotoxin SIA **D)** SNX 482 **E)** 1 µM mibefradil. Mean ± s.e.m. of the data from 3 separate experiments are plotted. More than 50 neurons analysed per condition in each experiment.

5.4 Mibefradil prevents cytosolic calcium elevation by TNFR1-Fc

To provide direct evidence for the involvement of T-type calcium channels in mediating the Ca^{2+} influx in response to TNFR1-Fc, I carried out Ca^{2+} imaging studies on P0 SCG cultures treated with TNFR1-Fc with or without the T-Type calcium channel blocker, mibefradil. Dissociated SCG cultures were grown in the presence of 10 ng/ml NGF to sustain survival. The next day media was changed to Ringer's solution containing 1.2 mM Ca^{2+} and the Ca^{2+} indicator Fura-2 AM, and after washing with Ringer's, the neurons were treated with 5 µg TNFR1-Fc or with TNFR1-Fc plus 1 µM of the T-type channel inhibitor mibefradil. Ca^{2+} imaging revealed that whereas treatment with TNFR1-Fc alone caused rapid elevation of cytosolic Ca^{2+} within 5 min, mibefradil prevented the Ca^{2+} influx associated with TNFR1-Fc treatment (Fig.5A). Fig.5B depicts the field view of a calcium imaging experiment. Following the addition of TNFR1-Fc, cell bodies would flash red after 5min. However, it must be mentioned that not all cells were responsive. On the other hand, when mibefradil was added together with TNFR1-Fc, there was a noticeable and substantial decrease in the number of cells that would flash red after 5min. Accordingly, cytosolic Ca^{2+} was significantly higher in cultures treated with TNFR1-Fc alone compared to cultures treated both with TNFR1-Fc and mibefradil at 5, 10 and 15 min. These results suggest that Ca^{2+} entry into SCG neurons triggered by TNFR1-Fc is mediated by T-type channels.

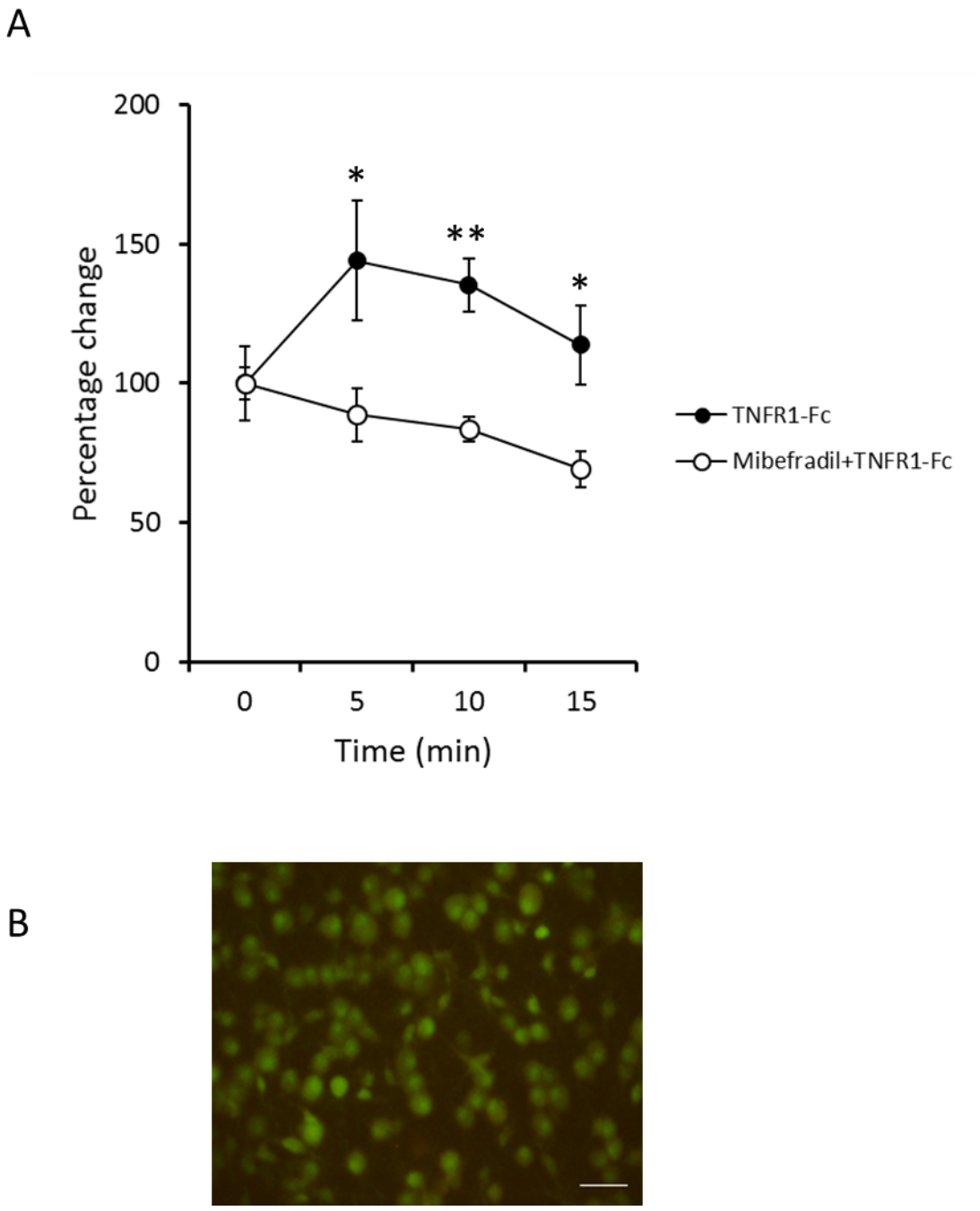

Figure 5: Mibefradil prevents cytosolic calcium elevation by TNFR1-Fc. **A)**Percentage change in cytosolic free-Ca^{2+} after addition of either 5 µg TNFR1-Fc alone or 1 µM mibefradil and TNFR1-Fc in medium containing 1.2 mM Ca^{2+}. Mean ± s.e.m. of data from 3 separate experiments are plotted. More than 20 neurons were analysed per condition in each experiment; * $P < 0.05$, ** $P < 0.01$, student T-test. **B)** Representative image of a typical field view during calcium imaging experiments.Scale bar, 20µm.

5.5 Specific T-type calcium channel blockers inhibit the effect of TNFR1-Fc on sympathetic axon growth

The observation that mibefradil inhibits both TNFR1-Fc promoted elevation of cytosolic free-Ca^{2+} and TNFR1-Fc promoted enhanced axon growth, provides substantial evidence for the involvement of T-type calcium channels in mediating the biological effects of TNF reverse signalling on developing sympathetic neurons. Although, mibefradil is a potent T-type calcium channel blocker, it is not specific for these channels as it also blocks voltage-dependent and ATP-sensitive K^+ channels and inhibits high-voltage Ca^{2+} and Na^+ currents (Lambert et al., 2014). Until recently, no specific T-type calcium channel inhibitors were available. However, in recent years there have been major advancements in developing specific T-type calcium channel blockers from piperidine derivatives. For example, TTA-A2 and TTA-P2 are potent and selective T-type calcium channels blockers that do not affect other voltage-dependent currents (Lambert et al., 2014). The difference between these two inhibitors is that TTA-A2 is a state-dependent inhibitor, its potency is dependent on the membrane potentials of the neurons, which does not affect our experimental paradigm.(Kraus et al., 2010).

For this reason, I repeated key experiments using these more specific inhibitors to provide more conclusive evidence for the involvement of T-type calcium channels in mediating the effects of TNF reverse signalling on sympathetic axon growth. Dissociated P0 SCG neurons were cultured for 24 h in the presence of 10 ng/ml NGF alone or NGF plus 10 ng/ml TNFR1-Fc with and without 200 nM of either of these inhibitors or NGF plus either inhibitor. Analysis of axonal length and branching by Sholl analysis showed that each inhibitor prevented the growth enhancing effects of TNFR1-Fc (Fig.6-7). These

observations confirm the results obtained with mibefradil and provide additional evidence that T-type calcium channels provide an essential link between TNF reverse signalling and axon growth.

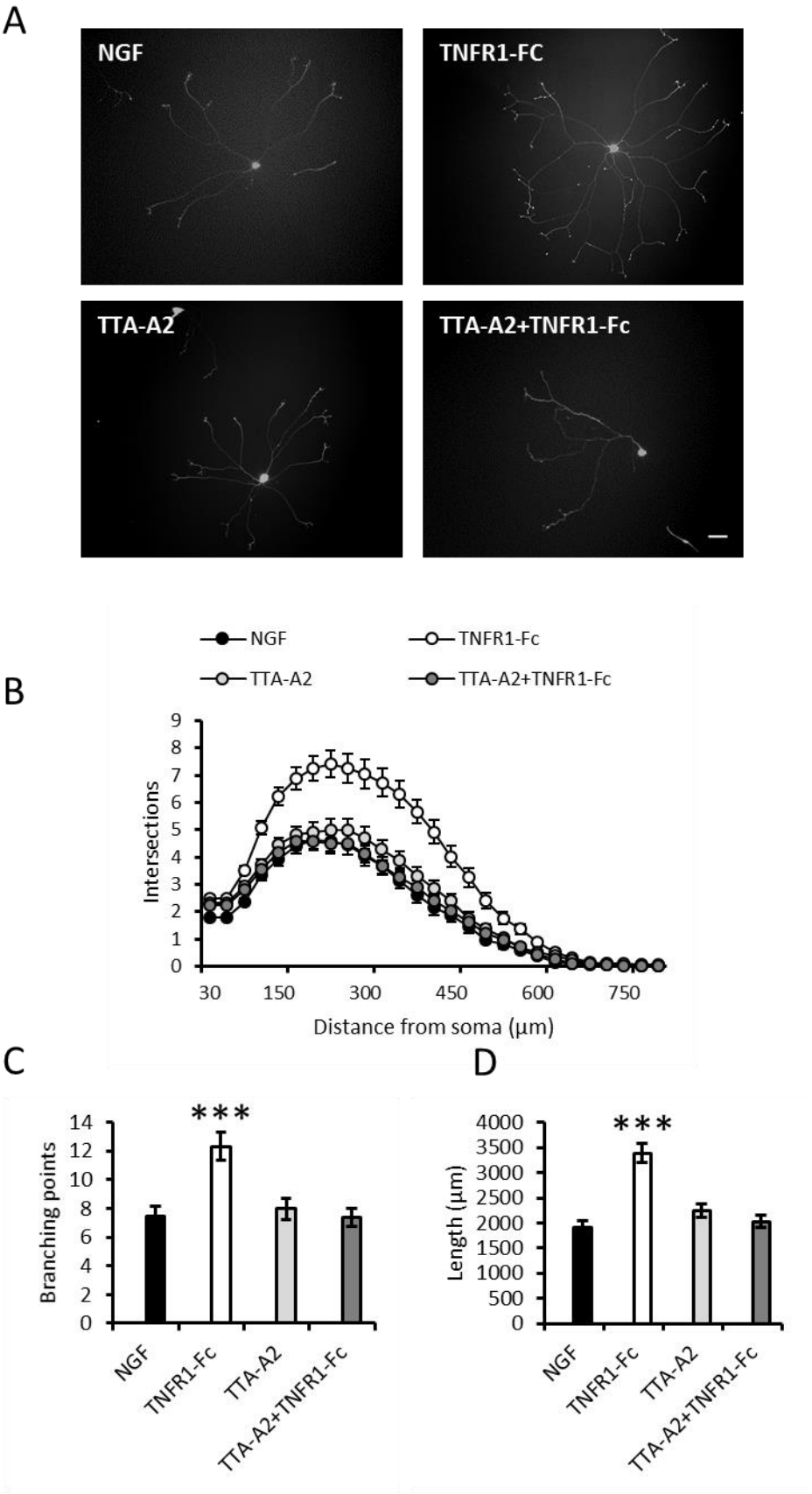

Figure 6, legend on following page.

Figure 6: TTA-A2 inhibits the enhancement of axon growth by TNFR1-Fc. Dissociated cultures of P0 SCG neurons were grown overnight in the presence of either 10 ng/ml NGF alone or NGF plus 10 ng/ml TNFR1-Fc with and without 200 nM TTA-A2 or NGF plus TTA-A2. **A)** Representative micrographs depicting the difference in neurite arbor morphology after 24 h incubation in the different experimental conditions. Scale bar, 20µm. **B)** Sholl profiles, **C)** branch point number and **D)** neurite length in the neurite arbors of the neurons grown under these conditions. Mean ± s.e.m. of the data from 2 separate experiments are plotted. More than 50 neurons analysed per condition in each experiment; statistical comparison with control (NGF), ***p<0.001, one-way ANOVA *post-hoc* Tukeys's HSD.

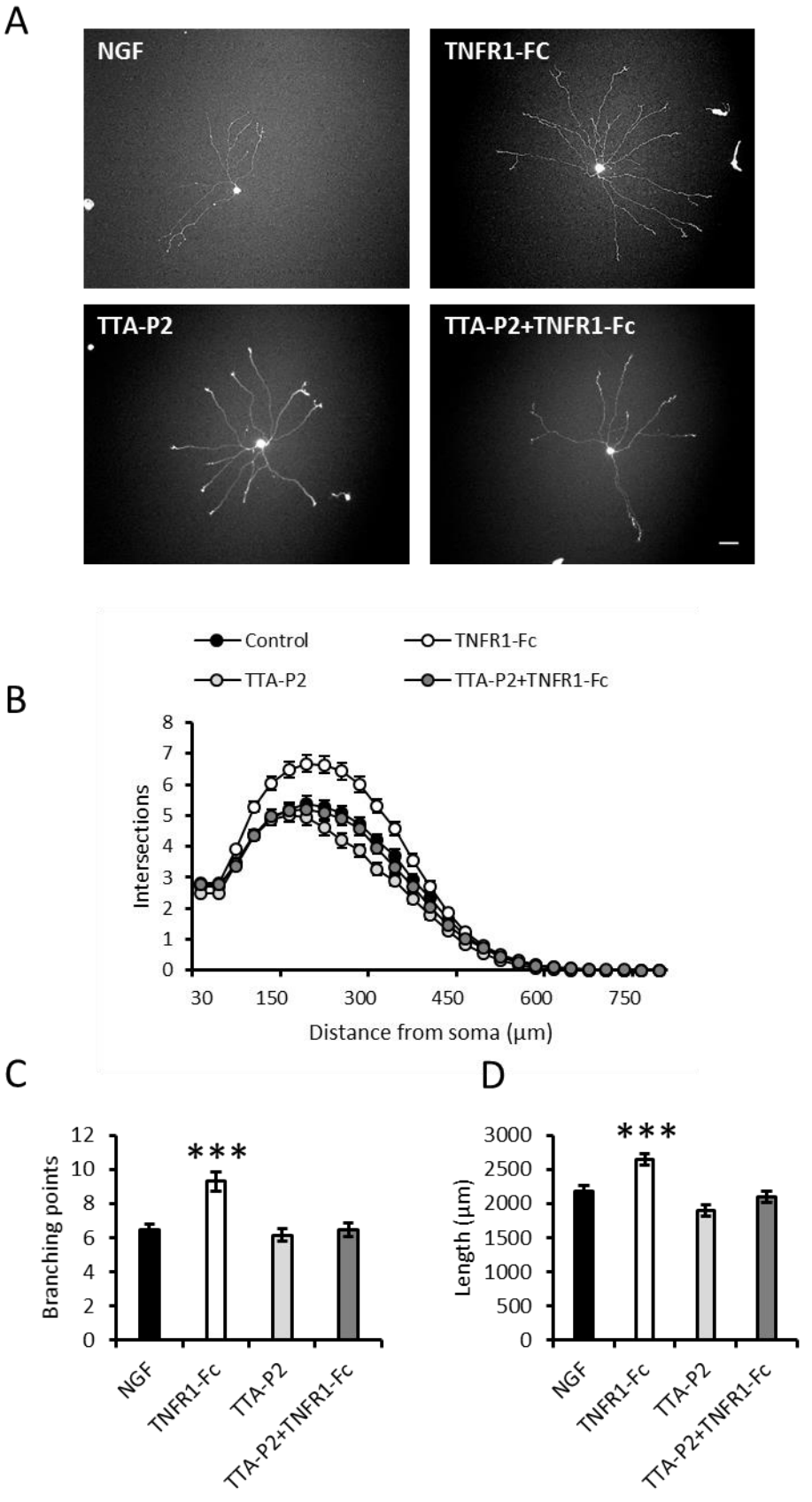

Figure 7, legend on following page.

Figure 7: TTA-P2 inhibits the enhancement of axon growth by TNFR1-Fc. Dissociated cultures of P0 SCG neurons were grown overnight in the presence of either 10 ng/ml NGF alone or NGF plus 10 ng/ml TNFR1-Fc with and without 200 nM TTA-P2 or NGF plus TTA-P2. **A)** Representative micrographs depicting the difference in neurite arbor morphology after 24 h incubation in the different experimental conditions. Scale bar, 20µm. **B)** Sholl profiles, **C)** branch point number and **D)** neurite length in the neurite arbors of the neurons grown under these conditions. Mean ± s.e.m. of the data from 3 separate experiments are plotted. More than 50 neurons analysed per condition in each experiment; statistical comparison with control (NGF), ***p<0.001, one-way ANOVA *post-hoc* Tukeys's HSD.

5.6 The specific T-type calcium channel blocker TTA-P2 locally inhibits TNFR1-Fc promoted axon growth

In chapter 3 I showed that TNFR1-Fc acts locally on sympathetic axons to enhance their length (section 3.4). Addition of TNFR1-Fc to cell bodies of P0 SCG neurons grown in microfluidic compartments had no effect on neurite length, whilst the addition of TNFR1-Fc to axon compartments enhanced neurite length. To test whether this local growth response to TNFR1-Fc is mediated by local activation of T-type calcium channels, I employed a similar experimental paradigm using the specific calcium channel blocker TTA-P2. TTA-P2 was used to block T-type channels at either the cell soma or growing axons. If TNFR1 is indeed acting like a target-derived factor and T-type calcium channels mediate this process, the addition of TTA-P2 to the axonal compartment should inhibit the growth enhancing effects of TNFR1-Fc.

P0 SCG neurons were seeded in the cell soma compartment of the microfluidic devices, and 10 ng/ml NGF was added to both the soma and axon compartments to sustain survival and encourage axon growth from the soma compartment into the axon compartment. 10 ng/ml TNFR1-Fc or 200 nM TTA-P2 or TTA-P2 plus TNFR1-Fc was either added to the soma or axon compartment. An extra condition was included where TTA-P2 was added to the soma compartment and TNFR1-Fc to the axonal compartment to

demonstrate the localised effects of TNF mediated reverse signalling. After 24 h incubation, axons were labelled in the axon compartment with the fluorescent vital dye calcein-AM, which retrogradely labels cell bodies of neurons that project axons into the axon compartment.

Addition of TTA-P2 to the axonal compartment inhibited the growth enhancing effects of TNFR1-Fc. However, when TTA-P2 was added to the soma compartment and TNFR1-Fc to axons, a significant increase in axonal length was still observed. TTA-P2 had no negative or positive effect on the normal growth promoting effects of NGF (Fig.8). This can be appreciated in the representative images of Fig. 8A. Axons grow longer when TNFR1-Fc is added to the axonal compartment, as well as when, TTA-P2 is present at the cell bodies and TNFR1-Fc in the axons, compared to all other conditions. This effect is not dependent on the number of neurons seeded as quantification takes into account the number of cell bodies that grow processes into the axon compartment.

These results highlight once again the localised effects of TNFR1-Fc on sympathetic axons and provide evidence for the involvement of T-type calcium channels in mediating the localised growth enhancing effects of TNF reverse signalling on SCG sympathetic neurons.

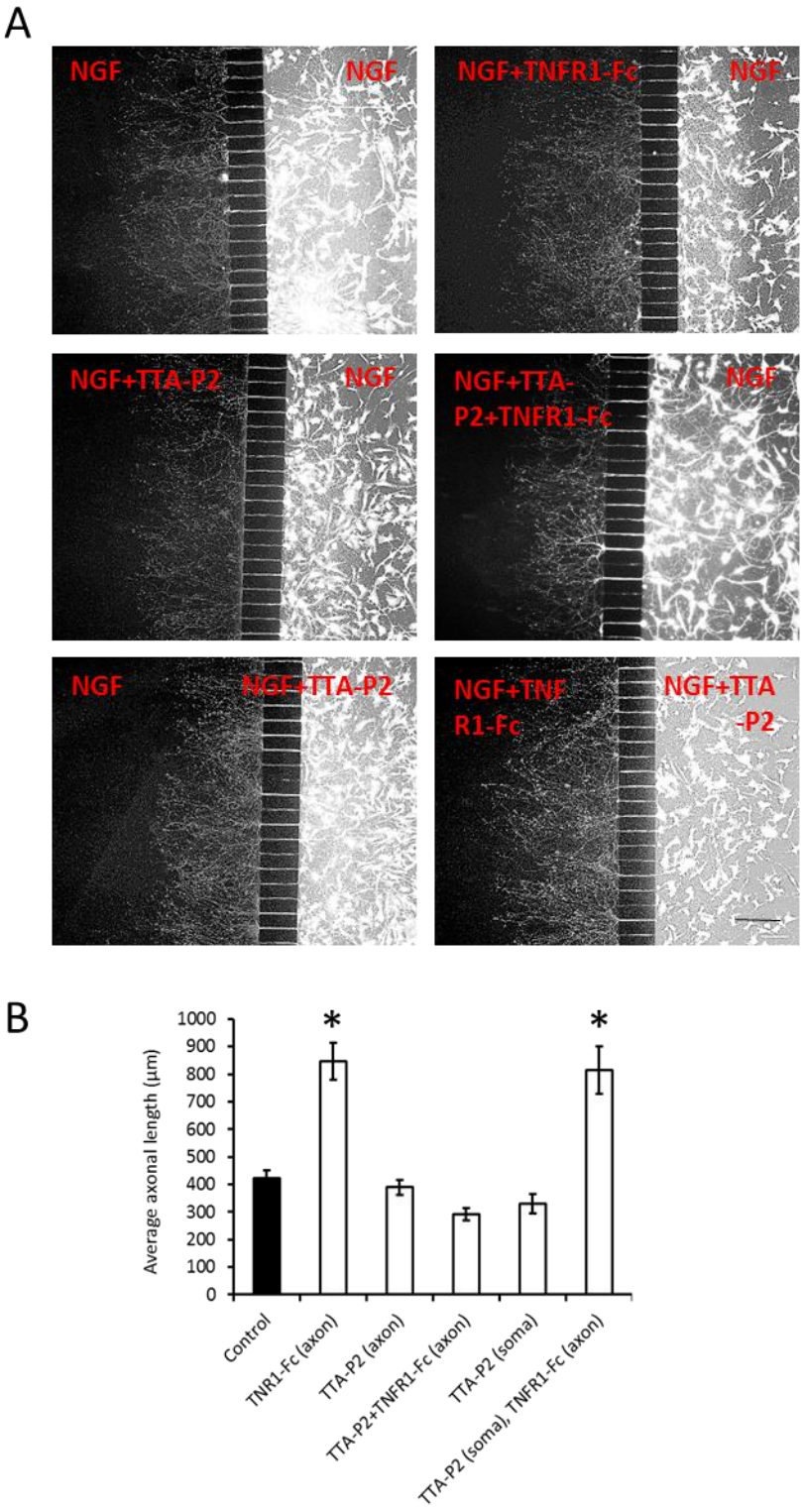

Figure 8, legend on following page.

Figure 8: The specific T-type calcium channel blocker TTA-P2 eliminates the localised effects of TNFR1-Fc on developing sympathetic axons to enhance their growth. A) Representative images of calcein-AM labelled P0 SCG neurons that were cultured for 24 h in a two-compartment microfluidic device containing 10 ng/ml NGF in both compartments with either 10 ng/ml TNFR1-Fc or 200 nM TTA-P2 or TNFR1-Fc plus TTA-P2 in the axon or soma compartment. TTA-P2 was also applied to cell bodies and TNFR1-Fc was applied to axons. Scale bar, 200 µm. **B)** Bar charts (mean ± s.e.m.) of average axonal length from 3 separate experiments of each type. Statistical comparison to control (NGF), * $p<0.05$, one-way ANOVA *post-hoc* Tukeys's HSD.

5.7 Expression of T-type calcium channel mRNAs in the developing SCG

The results presented in previous sections strongly suggest the involvement of T-type calcium channels in mediating the effect of TNFR1-Fc in enhancing axonal growth and branching in developing SCG neurons. To provide an indication of which sub-type or sub-types of T-type calcium channels are potentially capable of mediating this effect, I studied the expression of transcripts encoding the three types of T-type calcium channels, Cav3.1, Cav3.2 and Cav3.3, in developing SCG neurons. Total RNA was extracted from E18, P0, P5 and P10 SCG. qPCR was used to quantify the levels of *Cav3.1*, *Cav3.2* and *Cav3.3* transcripts and the qPCR data was normalised to the levels of the housekeeping genes *Gapdh* and *Sdha* mRNA.

Transcripts encoding *Cav3.1*, *Cav3.2* and *Cav3.3* were detected at all stages studied. The highest level of expression of all transcripts was at E18 and P0, with a drop in expression by P5. These expression patterns coincide with the effects of TNF reverse signalling *in vitro* observed in chapter 3 (P0-P5), as well as with the period of final target innervation (Fig.9). *Cav3.1* levels start out high at E18 dropping two-fold by P5 (Fig.9A). *Cav3.2* and *Cav3.3* transcripts display a similar developmental expression profile with peak

expression levels at P0. *Cav3.2* levels drop 4-fold by P5 (Fig.9B) and *Cav3.3* transcripts levels raise two-fold by P0, dropping back two-fold by P5 (Fig.9C).

In summary, the qPCR screen shows that the transcripts for all types of T-type calcium channels are expressed in the SCG with maximal expression levels occurring between E18 and P0, coinciding with the period of development when sympathetic axons are ramifying within their target organs and the period when enhanced sympathetic axonal growth by TNFR1 is maximal.

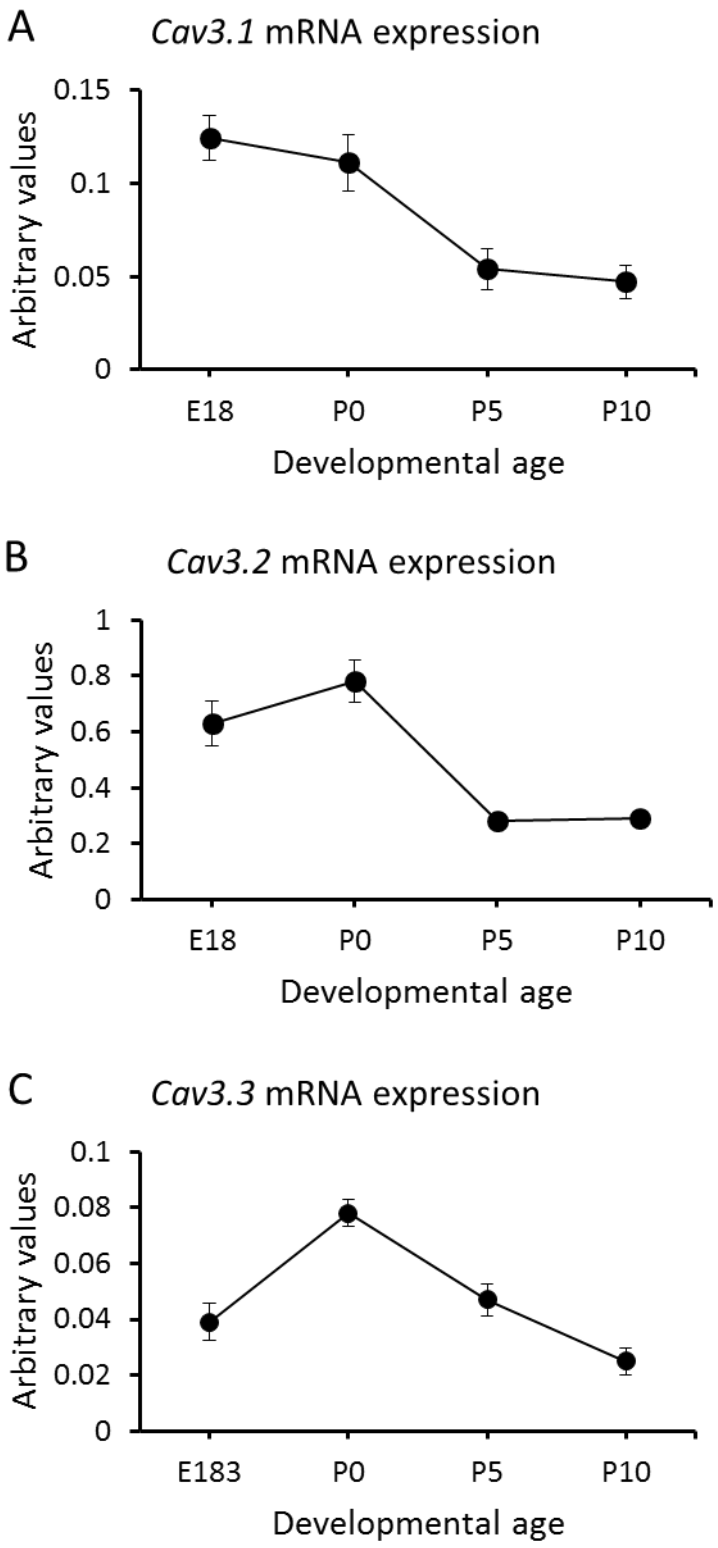

Figure 9: Relative expression of *Cav3.1*, *Cav3.2* and *Ca3.3* mRNAs in the SCG. mRNA levels are relative to the levels of housekeeping mRNAs at different developmental ages. **A)** *Cav3.1* mRNA, **B)** *Cav3.2* mRNA and **C)** *CaV3.3* mRNA. Mean and s.e.m of four separate samples (arbitrary units).

5.8 Localisation of T-type calcium channels in dissociated SCG neurons

To complement the qPCR data of the above section, the localisation of T-type calcium channels (CACNA1G/Cav3.1, CACNA1H/Cav3.2 and CACNA1I/Cav3.3) was determined by immunocytochemistry in dissociated cultures of SCG neurons. P0 SCG neurons were grown overnight in the presence of 10 ng/ml NGF for 24 h. Neurons were positively identified by anti-β-III tubulin staining. Neurons were double labelled with anti-β-III tubulin and with specific antibodies for either CACNA1G/Cav3.1, CACNA1H/Cav3.2 or CACNA1I/Cav3.3. TO-PRO was used to stain the nucleus of cells (Fig.10). These experiments demonstrated that all three T-type calcium channels are expressed at the cell body. In addition, Cav3.2 and Cav3.3 are localised along the full extent of axons of P0 SCG neurons. Cells incubated with secondary antibody alone exhibited no background immunofluorescence.

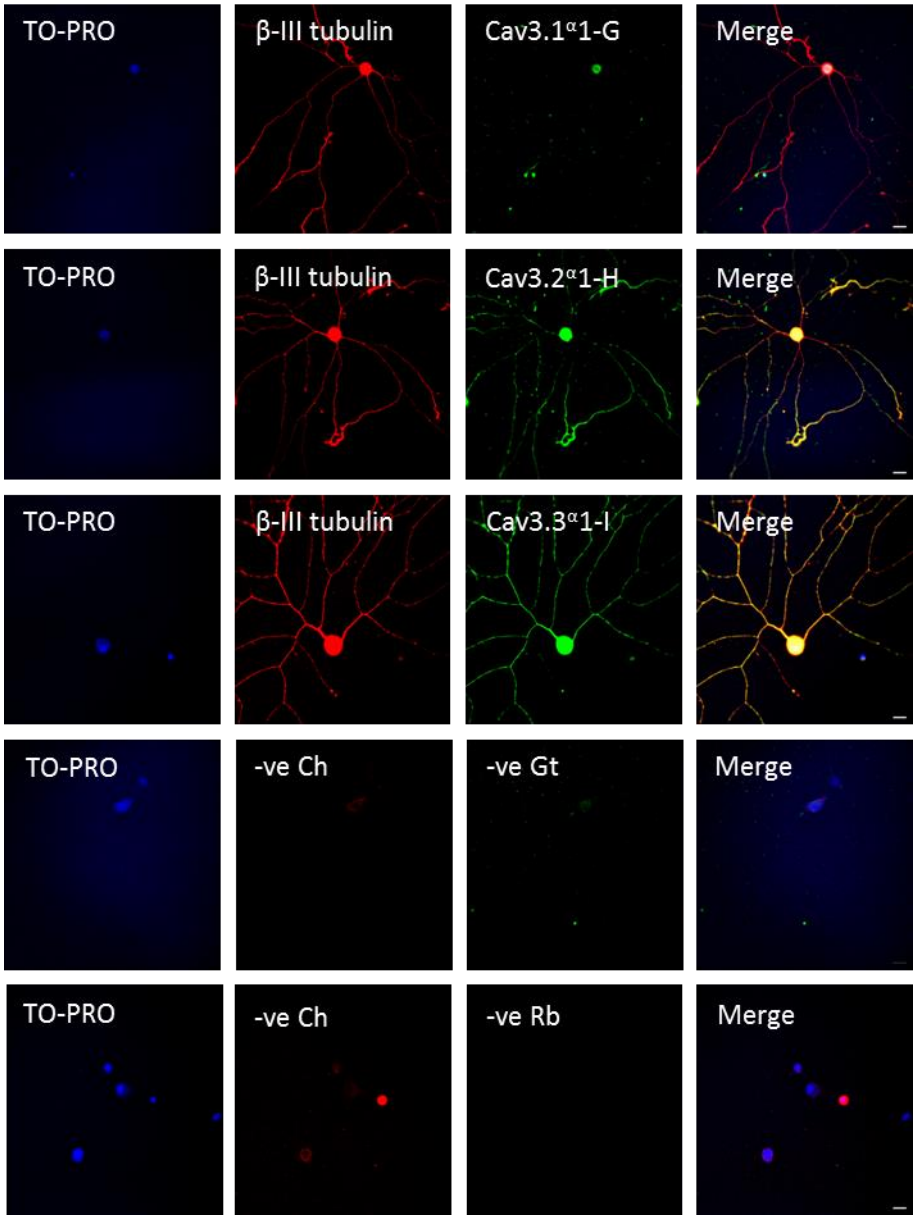

Figure 10: CACNA1G/Cav3.1, CACNA1H/Cav3.2 and CACNA1I/Cav3.3 are expressed by developing SCG neurons. Dissociated P0 SCG neurons were cultured overnight in the presence of 10 ng/ml NGF and stained the next day with specific antibodies for CACNA1G/Cav3.1, CACNA1H/Cav3.2 and CACNA1I/Cav3.3. The cultures were double labelled with anti-β-III tubulin to positively identify neurons. TO-PRO was used to identify the nucleus of cells. The two lower panels show cultures in which the primary antibodies were omitted from the staining protocol. Scale bar, 10µm, n=3.

5.9 Knockdown of T-type calcium channel genes by shRNA inhibits TNFR1-Fc enhanced sympathetic axonal growth and branching *in vitro*

The pharmacological studies presented above show that only T-type calcium channel blockers inhibit the growth enhancing effects of TNFR1-Fc on sympathetic neurons. In addition, all T-type calcium channels are expressed during development. For these reasons, I carried out studies to clarify which T-type calcium channel(s) mediates TNFR1-Fc induced neurite growth. shRNA was used to reduce the expression of Cav3.1, Cav3.2 or Cav3.3 channels in cultured P0 SCG neurons. shRNAs were cloned into the vector pGFP-V-RS, which drives expression of GFP and shRNA. For each T-type calcium channel, four different shRNA constructs were used (constructs A-D) separately to reduce channel expression. A scrambled shRNA sequence cloned into pGFP-V-RS (construct that does not target any gene) was used as a control. Individual dissociated suspensions of P0 SCG neurons were electroporated with individual shRNA constructs, plated and cultured overnight in the presence of 10 ng/ml NGF, either with or without 10 ng/ml TNFR1-Fc. The following day, GFP-positive neurons were imaged and images were subjected to Sholl analysis (data not shown) and neurite branching and length was quantified. All conditions were compared to control (scramble plus NGF) and compared between specific constructs with or without TNFR1-Fc.

For the most part, scramble plus TNFR1-Fc was the only condition to have a significant increase in neurite branching and length compared to scramble alone (Fig.11-13), with the exception of the length of neurites in Cav3.2 construct D transfected neurons in the presence of TNFR1-Fc (Fig.12) and the branching of Cav3.3 construct C transfected

neurons with and without TNFR1-Fc (Fig.13). The transfection of Cav3.1 construct A resulted in a reduction in neurite length and branching compared to controls in both the presence and absence of TNFR1-Fc, although the reduction in length was not statistically significant in the presence of TNFR1-Fc (Fig.11). Transfection of Cav3.2 construct C resulted in a significant decrease in neurite length in the presence of TNFR1-Fc when compared to the control (Fig.12).

The majority of shRNA constructs prevented TNFR1-Fc from enhancing neurite outgrowth and branching (Figs. 11-13). The only exception is the transfection of Cav3.3 construct A which failed to prevent an increase in neurite length in the presence of TNFR1-Fc (Fig.12). In addition, there was a significant decrease in neurite branching with the transfection of Cav3.1 construct D in the presence of TNFR1-Fc compared to those cells transfected with Cav3.1 construct D grown with NGF alone (Fig.11).

Together, the data in Figures 11, 12 and 13 reveals that reducing the expression of any of the T-type calcium channels inhibits TNFR1-Fc promoted neurite outgrowth from cultured P0 SCG neurons, suggesting that all three T-type calcium channels play a role in mediating the biological effects of TNF reverse signalling in SCG neurons. Refer to Table 2 for P-values.

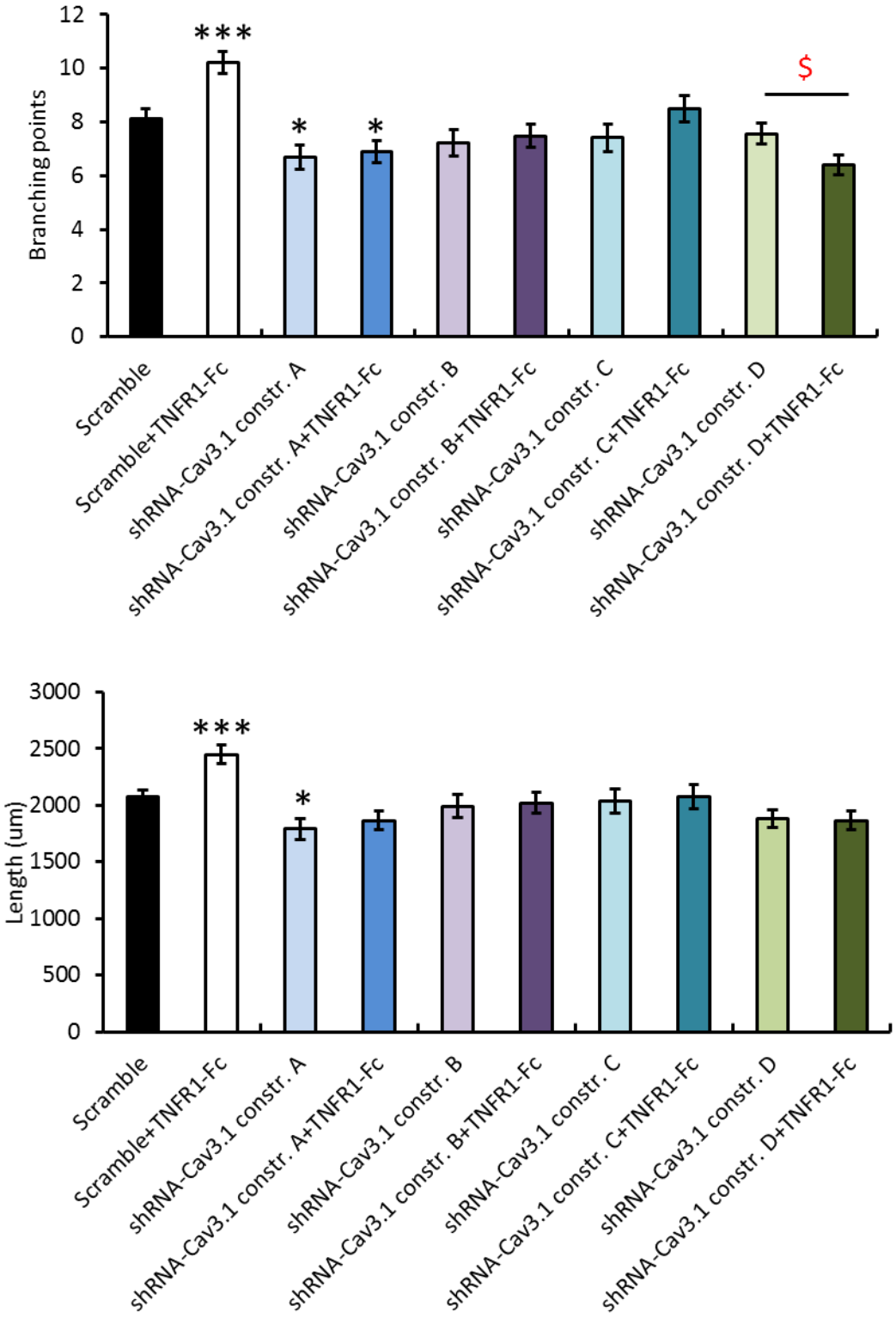

Figure 11, legend on following page.

Figure 11: CACNA1G/Cav3.1 knockdown in SCG neurons and its effect on neurite outgrowth. P0 SCG neurons were electroporated with either one of four shRNA constructs (A-D) for Cav3.1 or a control construct (scramble). Following transfection, neurons were cultured overnight in the presence of 10 ng/ml NGF, with or without 10 ng/ml TNFR1-Fc. Top panel shows mean number of branch points per neuron under each condition and lower panel shows mean neurite length per neuron under each condition. Statistical comparison with control, *** $p < 0.001$ and * $p < 0.05$. $ indicates significant difference ($p<0.05$) in number of neurite branch points between cultures transfected with the same construct, but cultured with or without TNFR1-Fc. Mean ± s.e.m of data from 3 separate experiments are plotted. More than 50 neurons were analysed per condition in each experiment; one-way ANOVA *post-hoc* Tuckey's HSD.

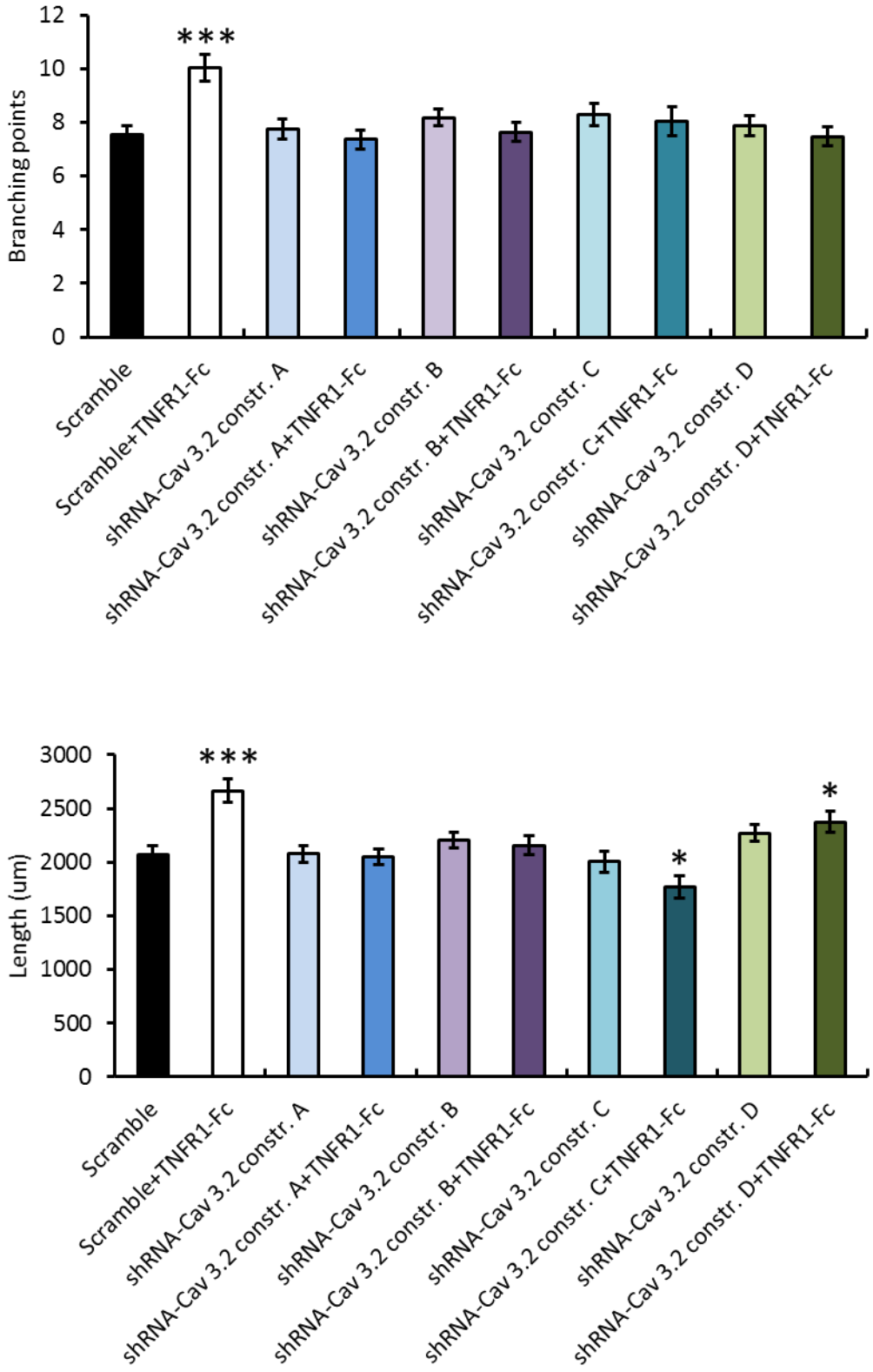

Figure 12, legend on following page.

Figure 12: CACNA1H/Cav3.2 knockdown in SCG neurons and its effect on neurite outgrowth. P0 SCG neurons were electroporated with either one of four shRNA constructs (A-D) for Cav3.2 or a control construct (scramble). Following transfection, neurons were cultured overnight in the presence of 10 ng/ml NGF, with or without 10 ng/ml TNFR1-Fc. Top panel shows mean number of branch points per neuron under each condition and lower panel shows mean neurite length per neuron under each condition. Statistical comparison with control, *** $p < 0.001$ and * $p < 0.05$. Mean ± s.e.m of data from 3 separate experiments are plotted. More than 50 neurons were analysed per condition in each experiment; one-way ANOVA *post-hoc* Tuckey's HSD.

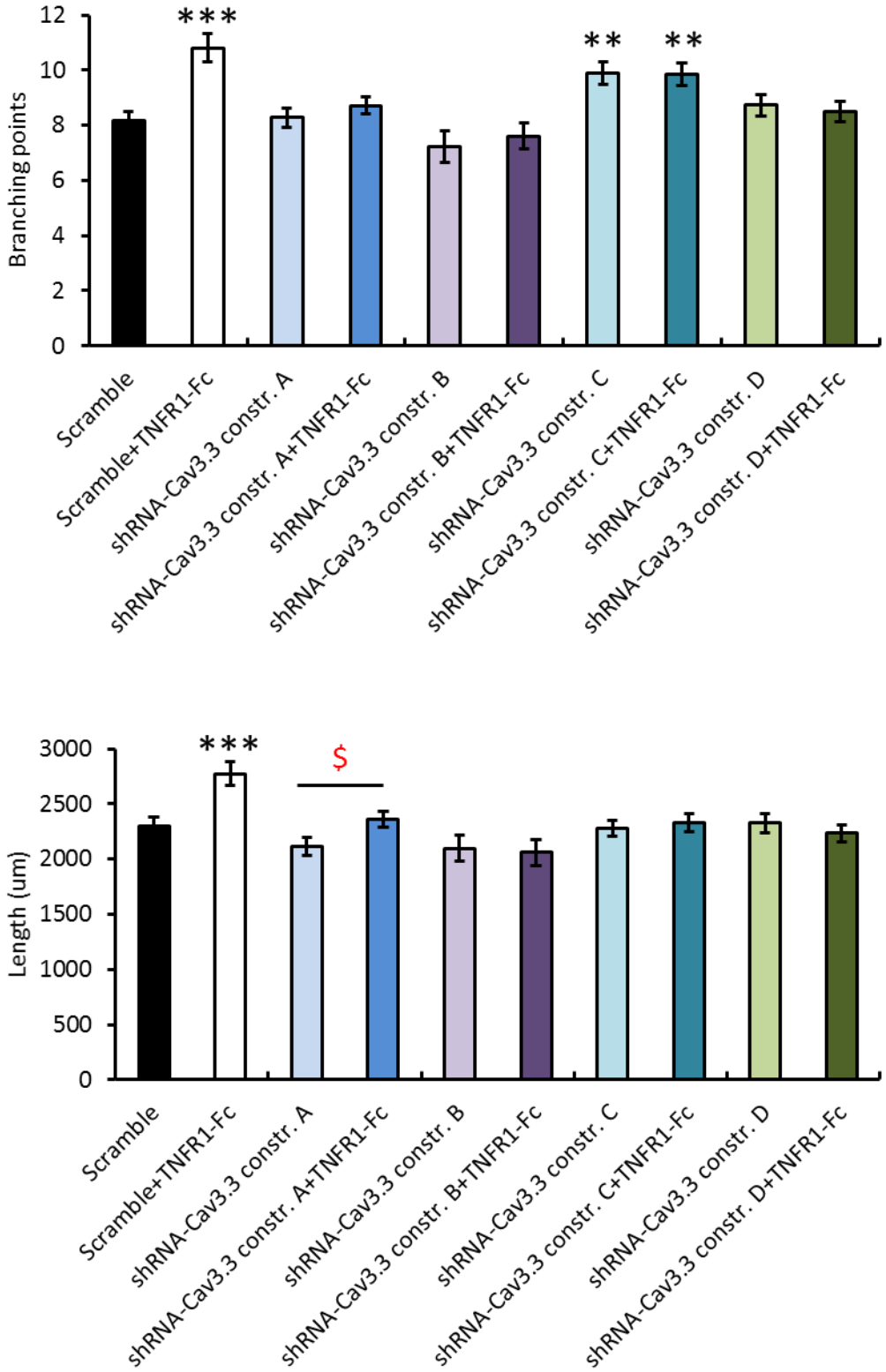

Figure 13, legend on following page.

Figure 13: CACNA1I/Cav3.3 knockdown in SCG neurons and its effect on neurite outgrowth. P0 SCG neurons were electroporated with either one of four shRNA constructs (A-D) for Cav3.3 or a control construct (scramble). Following transfection, neurons were cultured overnight in the presence of 10 ng/ml NGF, with or without 10 ng/ml TNFR1-Fc. Top panel shows mean number of branch points per neuron under each condition and lower panel shows mean neurite length per neuron under each condition. Statistical comparison with control, ***p<0.001 and **p<0.01. $ indicates significant difference (p<0.05) in neurite length between cultures transfected with the same construct, but cultured with or without TNFR1-Fc. Mean ± s.e.m of data from 3 separate experiments are plotted. More than 50 neurons were analysed per condition in each experiment; one-way ANOVA *post-hoc* Tuckey's HSD.

Table 2: P-values for Figures 11-13.

Branching, Condition	P-Value	Length, Condition	P-Value
Control (Cav3.1) – TNFR1-Fc	0.001	Control (Cav3.1) – TNFR1-Fc	<0.001
Control – Cav3.1 A	<0.05	Control – Cav3.1 A	<0.05
Control – Cav3.1 A +TNFR1-Fc	<0.05	Control – Cav3.1 A +TNFR1-Fc	NS
TNFR1-Fc – Cav3.1 A	<0.001	TNFR1-Fc – Cav3.1 A	<0.001
TNFR1-Fc – Cav3.1 A + TNFR1-Fc	<0.001	TNFR1-Fc – Cav3.1 A + TNFR1-Fc	<0.001
TNFR1-Fc – Cav3.1 B	<0.001	TNFR1-Fc – Cav3.1 B	<0.001
TNFR1-Fc – Cav3.1 B + TNFR1-Fc	<0.001	TNFR1-Fc – Cav3.1 B + TNFR1-Fc	<0.001
TNFR1-Fc – Cav3.1 C	<0.001	TNFR1-Fc – Cav3.1 C	<0.01
TNFR1-Fc – Cav3.1 C + TNFR1-Fc	<0.01	TNFR1-Fc – Cav3.1 C + TNFR1-Fc	<0.01
TNFR1-Fc – Cav3.1 D	<0.001	TNFR1-Fc – Cav3.1 D	<0.001
TNFR1-Fc – Cav3.1 D + TNFR1-Fc	<0.001	TNFR1-Fc – Cav3.1 D + TNFR1-Fc	<0.001
Cav3.1 D - Cav3.1 D + TNFR1-Fc	<0.05	Cav3.1 D - Cav3.1 D + TNFR1-Fc	NS
Control (Cav3.2) – TNFR1-Fc	<0.001	Control (Cav3.2) – TNFR1-Fc	<0.001
Control – Cav3.2 C + TNFR1-Fc	NS	Control – Cav3.2 C + TNFR1-Fc	<0.05
Control – Cav3.2 D + TNFR1-Fc	NS	Control – Cav3.2 D + TNFR1-Fc	<0.05
TNFR1-Fc – Cav3.2 A	<0.001	TNFR1-Fc – Cav3.2 A	<0.001
TNFR1-Fc – Cav3.2 A + TNFR1-Fc	<0.001	TNFR1-Fc – Cav3.2 A + TNFR1-Fc	<0.001
TNFR1-Fc – Cav3.2 B	<0.001	TNFR1-Fc – Cav3.2 B	0.001
TNFR1-Fc – Cav3.2 B + TNFR1-Fc	<0.001	TNFR1-Fc – Cav3.2 B + TNFR1-Fc	<0.001
TNFR1-Fc – Cav3.2 C	<0.01	TNFR1-Fc – Cav3.2 C	<0.001
TNFR1-Fc – Cav3.2 C + TNFR1-Fc	0.001	TNFR1-Fc – Cav3.2 C + TNFR1-Fc	<0.001
TNFR1-Fc – Cav3.2 D	<0.001	TNFR1-Fc – Cav3.2 D	<0.01
TNFR1-Fc – Cav3.2 D + TNFR1-Fc	<0.001	TNFR1-Fc – Cav3.2 D + TNFR1-Fc	<0.05
Control (Cav3.3) – TNFR1-Fc	<0.001	Control (Cav3.3) – TNFR1-Fc	<0.001
Control – Cav3.3 C	<0.01	Control – Cav3.3 C	NS
Control – Cav3.3 C + TNFR1-Fc	<0.01	Control – Cav3.3 C + TNFR1-Fc	NS
TNFR1-Fc – Cav3.3 A	<0.001	TNFR1-Fc – Cav3.3 A	<0.001
TNFR1-Fc – Cav3.3 A + TNFR1-Fc	<0.001	TNFR1-Fc – Cav3.3 A + TNFR1-Fc	<0.001
TNFR1-Fc – Cav3.3 B	<0.001	TNFR1-Fc – Cav3.3 B	<0.001
TNFR1-Fc – Cav3.3 B + TNFR1-Fc	<0.001	TNFR1-Fc – Cav3.3 B + TNFR1-Fc	<0.001
TNFR1-Fc – Cav3.3 C	NS	TNFR1-Fc – Cav3.3 C	<0.001
TNFR1-Fc – Cav3.3 C + TNFR1-Fc	NS	TNFR1-Fc – Cav3.3 C + TNFR1-Fc	<0.001
TNFR1-Fc – Cav3.3 D	<0.001	TNFR1-Fc – Cav3.3 D	<0.001
TNFR1-Fc – Cav3.3 D + TNFR1-Fc	<0.001	TNFR1-Fc – Cav3.3 D + TNFR1-Fc	<0.001
Cav3.3 A – Cav3.3 A + TNFR1-Fc	NS	Cav3.3 A – Cav3.3 A + TNFR1-Fc	<0.05

5.10 Discussion

In this chapter I provide evidence for the involvement of T-type calcium channels in mediating the axonal growth enhancing effects of TNF reverse signalling in developing sympathetic neurons. The initial indication that voltage-sensitive calcium channels are involved in mediated the growth enhancing effects of TNF reverse signalling came from the demonstration that dotarizine, a broad spectrum calcium channel blocker, eliminated the axon growth-promoting effects of TNFR1-Fc on SCG neurons. Experiments using pharmacological reagents that block different sub-types of calcium channels, narrowed this function down to T-type calcium channels. Whereas, reagents that block L, N, P/Q and R type channels had no significant effect on TNFR1-Fc-enhanced neurite growth, mibefradil, a T-type calcium channel blocker, completely eliminated the growth enhancing action of TNFR1-Fc. Accordingly, mibefradil prevented TNFR1-Fc-promoted elevation of cytosolic Ca^{2+}. Mibefradil is not completely specific for T-type channels, hence, I carried out additional experiments with potent and highly specific T-type calcium channel blockers that only became available very recently. Both TTA-A2 and TTA-P2 completely inhibited the neurite growth enhancing action of TNFR1-Fc on SCG neurons without affecting the survival of these neurons. Moreover, TTA-P2 blocked the axon growth promoting action of TNFR1-Fc in compartment cultures, suggesting that T-type channels are key local mediators of TNFR1-activated TNF reverse signalling on axon growth.

TNF reverse signalling has been shown to promote Ca^{2+} influx and rapid elevation of cytosolic Ca^{2+} in a macrophage cell line (Watts et al., 1999). However, the channels that mediate Ca^{2+} influx in these cells has not been determined. It would be interesting to

ascertain whether T-type calcium channels are universal participants in the cellular responses to TNF reverse signalling or have a unique role in neurons. An important question is how TNF reverse signalling opens T-type calcium channels. Depolarisation is the established mechanism by which these channels are opened. Very preliminary experiments, not included here, suggest that depolarisation accompanying the generation of action potentials is not involved, since TTX, a blocker of Na^+ channels, does not affect the ability of TNFR1-Fc to enhance neurite growth from cultured SCG neurons (L. Kisiswa, personal communication). To address this issue further, I have begun a collaboration with Annette Dolphin and Laurent Ferron of UCL, to ascertain whether any changes in membrane potential accompany Ca^{2+} influx, and to characterise the Ca^{2+} currents. However, from the small number of SCG neurons that have been patch-clamped to date, it is too early to draw conclusions. A further and intriguing possibility is that TNFR1-activated TNF reverse signalling opens T-type calcium channels by a voltage-independent mechanism. A variety of second messengers act on T-type channels to modulate their activity (Zhang et al., 2013). For this reason, it would be informative to see whether TNFR1-activated TNF reverse signalling induces post-translational changes in these channels.

The cytoplasmic domains of TNFSF members are highly conserved between species, however they tend to be extremely short (with the exception of FasL) and none possess enzymatic activity, suggesting the involvement of adaptor proteins in order to transduce downstream signals. Furthermore, six of the ten members of the TNFSF family known to reverse signal contain putative CKI binding motifs, mTNF among them (Watts et al., 1999). Phosphorylated amino acids on the intracellular domain of classical receptors are regularly used as docking sites for signalling complexes. Phosphorylation of amino acids

by CKI on the cytoplasmic domain of membrane-integrated TNFSF ligands could mimic this scenario and hence recruit adaptor proteins (Watts et al., 1999). With regards to mTNF, a study reported that it contains a serine at position 5 on the intracellular N-terminus that is constitutively phosphorylated by a CKI. Upon binding of soluble TNFR1 this serine becomes dephosphorylated and there is an increase in intracellular calcium (Watts et al., 1999). Therefore, it is possible that TNF-associated adaptor proteins cause post-translational modifications of T-type calcium channels, directly or indirectly, that open these channels by a novel mechanism that is independent of changes in membrane potential.

Consistent with the above findings, transcripts encoding T-type calcium channels were detected in the SCG during the period when sympathetic axons are ramifying in their targets. Transcripts for all three T-type calcium channel genes were detectable and had highest levels of expression during the period when TNFR1-activated TNF reverse signalling enhances sympathetic axon growth *in vitro*. Immunocytochemical localisation of the T-type calcium channel sub-types suggests that Cav3.2 and Cav3.3 are expressed on neuronal processes and cell bodies, whereas Cav3.1 expression is restricted to cell bodies. Given the results of compartment cultures, where blocking T-type calcium channels in the axon compartment inhibited TNFR1-Fc-enhanced axon growth, this would tend to suggest that Cav3.1 may not be involved in mediating TNFR1-Fc-enhanced axon growth. Yet, multiple shRNA´s directed to each T-type channel sub-type inhibited TNFR1-Fc-enhanced axon growth, suggesting that all three sub-types participate in mediating the effect of TNFR1-activated TNF reverse signalling on sympathetic axon growth. There are many possible explanations for this apparent discrepancy. First, immmunocytochemistry as employed here may not detect functionally relevant levels

of Cav3.1 on neurites. Second, the antibodies may not be specific. While no-primary antibody controls were negative, lack of staining on neurons lacking the relevant sub-type were not undertaken as we did not have access to the relevant knockout mice. Third, the localisation of sub-types *in vitro* may not reflect the situation *in vivo* and may change with time in culture, highlighting the need for immunohistochemical localisation *in vivo*. Fourth, because of limited time I was unable to confirm that the shRNAs specifically knockdown expression of the corresponding proteins. While scrambled sequence shRNA´s did not eliminate TNFR1-Fc-enhanced neurite growth, which provides some support for specificity, the use of shRNA is fraught with problems. The best approach would be to study neurons from mice that lack each T-type calcium channel sub-type, followed by studies of the sympathetic target field innervation phenotype of these mice. Indeed, mice deficient for each T-type calcium channel exist: Cav3.1 (Kim et al., 2001), Cav3.2 (Chen et al., 2003) and Cav3.3 (Lee et al., 2014). To date, there is no literature reporting the expression of T-type calcium channels by SCG neurons. The only autonomic ganglia known to functionally express T-type calcium channels are those of the rat major pelvic ganglia (Zhu et al., 1995, Lee et al., 2002). The results reported in this chapter highlight the importance of T-type calcium channels in mediating the growth enhancing effects of TNFR1-Fc on developing SCG sympathetic axons *in vitro*. Perhaps the lack of literature might be because the expression of these channels has not been studied in the context of sympathetic development.

We have made some progress in linking Ca^{2+} influx in sympathetic neurons to enhanced neurite growth (Kisiswa et al., 2013). Elevation of cytosolic Ca^{2+} that follows treating SCG neurons with TNFR1-Fc rapidly activates ERK1/ERK2 independently of NGF and activation of the latter is prevented by pre-treating the neurons with the intracellular

Ca^{2+} chelator BAPTA. Preventing ERK1/ERK2 activation by pharmacological inhibition of MEK1 and MEK2, the upstream activators of ERK1 and ERK2, prevents the enhanced neurite growth by TNFR1-Fc (Kisiswa et al., 2013). A link between ERK1/ERK2 activation and neurite growth is well established, in that NGF-promoted ERK1/ERK2 activation in PC12 cells and SCG neurons contributes to the neurite growth response (Gomez and Cohen, 1991, Thompson et al., 2004, Goold and Gordon-Weeks, 2005, O'Keeffe et al., 2008). TNF reverse signalling in monocytes has also been shown to promote ERK1/ERK2 activation (Kirchner et al., 2004a). Furthermore, the aforementioned study also reported that activation of ERK1/ERK2 was mediated by PKC (Kirchner et al., 2004a). Interestingly PKC can be activated by calcium influx (Takai et al., 1979). Together, this raises once again the question of whether calcium influx associated with TNF reverse signalling in the immune response is also mediated by T-type calcium channels. This is a possibility as T-type calcium channels are expressed by a variety of T-cell cell lines and macrophages (Gray et al., 2004, Yang et al., 2012). Although it is recognised that some membrane-integrated TNFSF members are able to act as receptors and are able to transduce signals (Watts et al., 1999, Eissner et al., 2004, Sun and Fink, 2007, Juhasz et al., 2013). To date, studies mostly describe changes in cellular responses, whereas the molecular mechanisms of signal transduction by reverse signalling are still poorly understood. Nonetheless some details have begun to emerge from studies of reverse signalling among members of the TNFSF in the immune system (Eissner et al., 2004). Reverse signalling by various TNFSF ligands converge on the modulation of ERK1/ERK2 or NF-κB.

While many questions remain unanswered, the results reported in this chapter support the idea that opening of T-type calcium channels is a key step in the molecular

mechanism by which TNFR1-activated TNF reverse signalling enhances sympathetic axon growth during the stage when these axons are ramifying within their target organs.

Chapter 6
TNF reverse signalling in developing sensory neurons *in vitro*

6.1 Introduction

In previous chapters I have provided evidence for the axon growth-enhancing effects of TNF reverse signalling in developing sympathetic neurons during the developmental period of final target innervation. In addition, via whole mount staining I have shown the physiological relevance of such findings in various target organs innervated by paravertebral sympathetic ganglia. However, is this process specific to developing sympathetic neurons or can TNF reverse signalling influence axonal growth from other kinds of neurons? To begin exploring this question, I studied the effect of TNF reverse signalling on two well-characterised, experimentally tractable populations of cranial sensory neurons, those of the trigeminal and nodose ganglia (Davies and Lumsden, 1990).

Trigeminal ganglion neurons depend on several neurotrophic factors for survival at different periods of their development. NGF, BDNF, NT-3 and MSP have been shown to promote survival of trigeminal neurons *in vitro* at different stages of development (Buchman and Davies, 1993, Forgie et al., 2000). At early embryonic ages, up to around E12, they are responsive to both BDNF and NT-3. After this period, there is a switch in survival dependence towards NGF. Around 80% of perinatal trigeminal neurons are responsive to NGF *in vitro* (Davies, 1988).

The main survival-promoting neurotrophic factor for developing nodose neurons in culture is BDNF (Lindsay et al., 1985). However, analysis of null mutant mice has revealed that BDNF, NT-3 and NT-4/5 are all necessary to support the survival of developing

nodose neurons *in vivo* (Farinas et al., 1994, Jones et al., 1994, Conover et al., 1995), with NT-3 and NT-4/5 being required early in nodose neuron development before the requirement for BDNF becomes established (Ringstedt et al., 1997). In addition, NGF supports the survival of a small sub-population of cultured nodose neurons between E11 and E14 (Forgie et al., 2000). In accordance with this, there is a small, but significant, reduction in the number of neurons in the nodose ganglia of late gestation NGF null-mutant embryos compared to wild type embryos (Forgie et al., 2000). The analysis of null mutant mice has also revealed that GDNF is required to support the survival of a sub-population of BDNF-responsive nodose neurons in the late embryonic period (Erickson et al., 2001).

In addition to their survival-promoting action, neurotrophins also play an important role in establishing correct target field innervation by sensory neurons (Davies, 2009). For example, mice overexpressing BDNF in epithelial target tissues of sensory neurons have an increase in peripheral innervation density (LeMaster et al., 1999). Double null mutants for BAX and BDNF have abnormal sensory innervation of peripheral tissues resulting from the growth of axons within tissues (Hellard et al., 2004). Overexpression experiments for NT-3 and *in vivo* studies of NT-3 null mice have linked NT-3 to both sensory and sympathetic axonal growth and guidance (Albers et al., 1996, Kuruvilla et al., 2004).

The preliminary data reported in this chapter suggests that TNFR1-activated TNF reverse signalling may play a role in enhancing sensory axonal growth and branching *in vitro* during development.

RESULTS

6.2 Trigeminal and nodose neurons respond to TNFR1-Fc during restricted periods of development

To test whether TNF reverse signalling influences axon growth from developing sensory neurons, dissociated cultures of trigeminal and nodose neurons sustained by 10 ng/ml NGF and BDNF, respectively, were grown for 24 h with and without 10 ng/ml TNFR1-Fc. The cultures were established over a range of ages (E16, E18 and P0), a period during which sensory axons are ramifying extensively in their peripheral target tissues. After 24 h, the neurons were stained with calcein-AM and the neurite arbors were subjected to Sholl analysis (Fig.1-2).

TNFR1-Fc enhanced neurotrophin-promoted neurite growth from both trigeminal and nodose neurons at particular ages. TNFR1-Fc promoted significant increases in total neurite branch point number and length from E16 trigeminal neurons (Fig.1B-C) and E18 nodose neurons (Fig.2B-C). Clear differences in the Sholl plots were also evident at these ages (Fig.1A and 2A). No significant differences in branching and length were observed with and without TNFR1-Fc in E18 and P0 trigeminal neuron cultures and in E16 and P0 nodose neuron cultures. Representative images of neurite arbors of E16 trigeminal and E18 nodose neurons grown with and without TNFR1-Fc are shown in Figs.1D and 2D.

A difference in morphology can be appreciated between trigeminal and nodose neurons in the representative images, this is due to the nature of the cultures. Trigeminal neurons tend to be longer and less branched both *in vitro* and *in vivo* compared to SCG and nodose neurons. On the other hand, nodose neurons tend to be smaller and have more complex neurite arbors compared both to SCG and trigeminal neurons.

These results indicate that TNF reverse signalling is capable of enhancing neurotrophin-promoted neurite growth from trigeminal and nodose neurons during circumscribed developmental windows.

Experiments were carried out at the ages when trigeminal and nodose neurons respond to TNFR1-Fc to ascertain whether this additionally affects survival. Neuron counts revealed that TNFR1-Fc did not affect the survival of trigeminal neurons at E16 and nodose neurons at E18, either in the presence of neurotrophic factors or in their absence (data not shown). This is in accordance with results in the developing SCG, where TNF reverse signalling does not promote P0 SCG neuronal survival.

To determine whether TNF reverse signalling influences sensory axon growth independently of neurotrophin-promoted axonal growth, E16 trigeminal and E18 nodose neurons were grown without neurotrophins, in the presence of 1 µg/ml of the broad-spectrum caspase inhibitor Q-VD-OPh, to prevent apoptosis in the absence of neurotrophins. The cultures were treated with either 10 ng/ml TNFR1-Fc or 10 ng/ml human Fc fragment (HFc) as control. After 24 h, the neurons were stained with calcein-AM and Sholl analysis was carried out and the neurite arbor branch point number and length were ascertained.

The neurite arbors of TNFR1-Fc-treated neurons were larger and more complex than those treated with HFc in terms of branch point number and length. However, these increases were only statistically significant in the case of trigeminal neurite arbor length. These preliminary results (because of limited time, only one repeat of these experiments was possible) raise the possibility that TNF reverse signalling, like in sympathetic

neurons, may enhance sensory neurite arbor growth independently of neurotrophins (Fig.3).

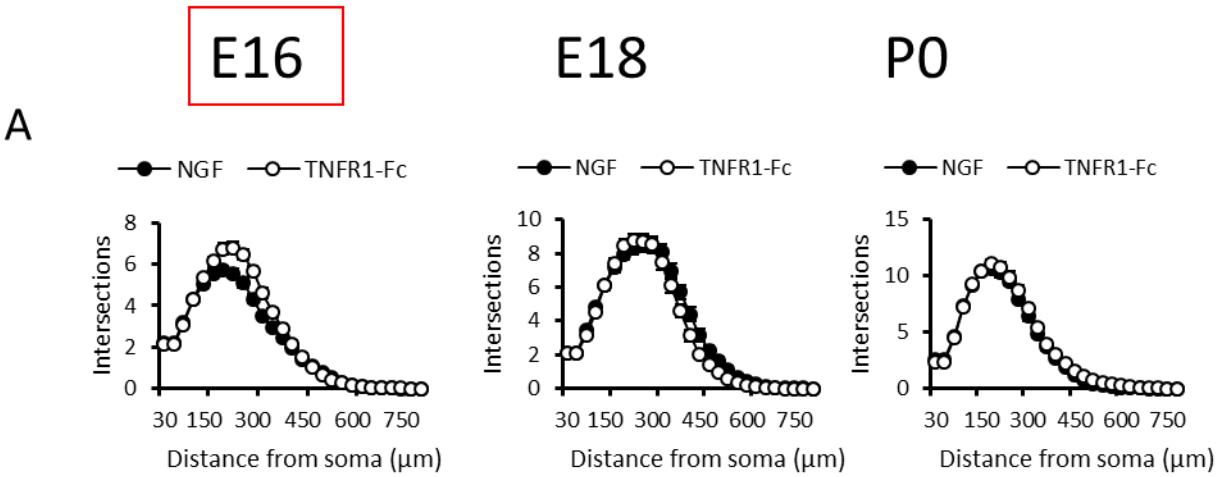
E16
E18
P0
A
NGF
TNFR1-Fc
Intersections
Distance from soma (µm)
30 150 300 450 600 750

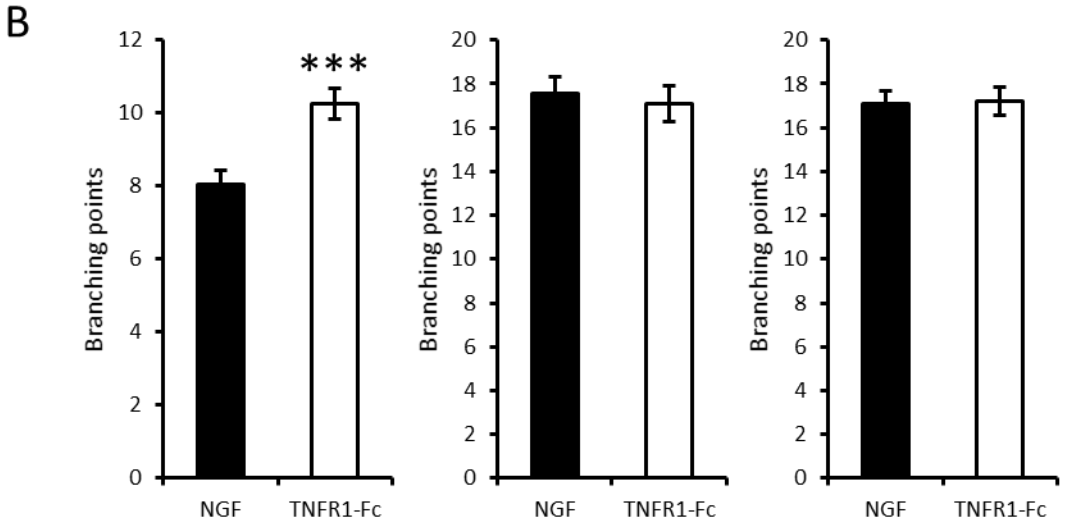
B
Branching points
***
NGF
TNFR1-Fc

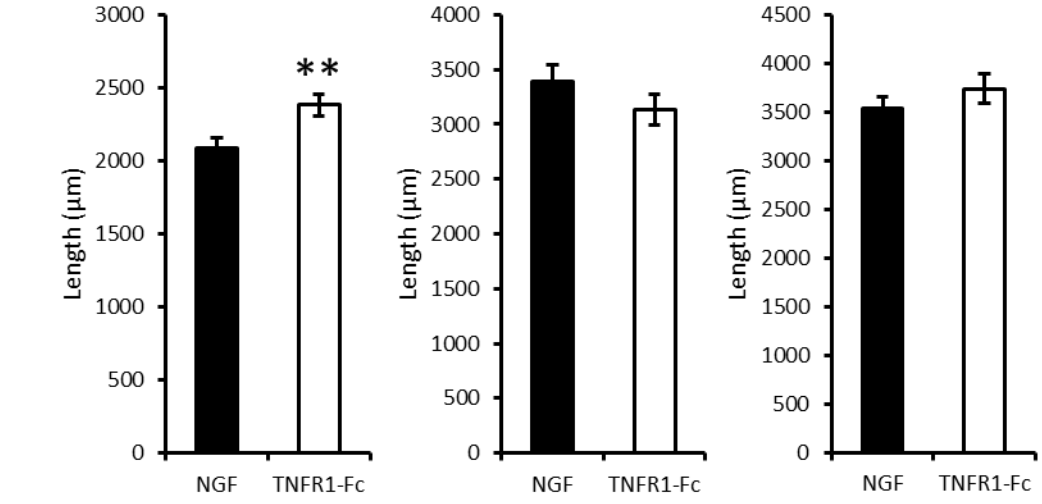
C
Length (µm)
**
NGF
TNFR1-Fc

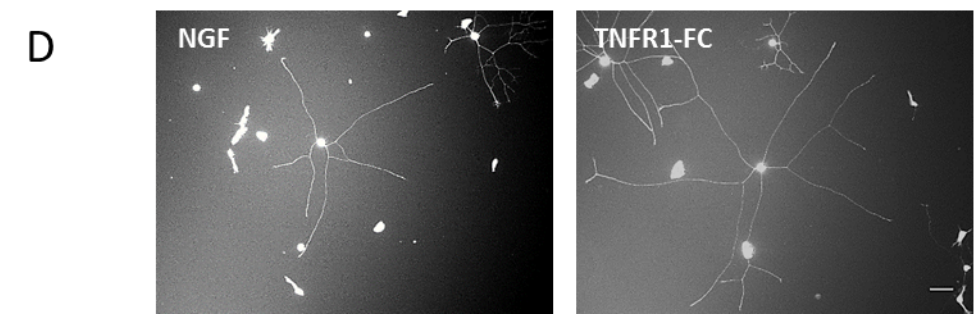
D
NGF
TNFR1-FC

Figure 1: TNF reverse signalling enhances trigeminal neuron axon growth at E16. Dissociated cultures of E16, E18 and P0 trigeminal neurons were grown overnight in the presence of either 10 ng/ml NGF alone or NGF plus 10 ng/ml TNFR1-Fc. **A)** Sholl profiles, **B)** branch point number and **C)** neurite length of the neurite arbors. **D)** Representative micrographs depicting the difference in morphology of E16 trigeminal neurons grown with NGF alone and NGF plus TNFR1-Fc. Scale bar, 20 µm. Mean ± s.e.m. of the data from 3 separate experiments are plotted. More than 50 neurons analysed per condition in each experiment; statistical comparison with control (NGF), ***p<0.001, **p<0.01, student T-test.

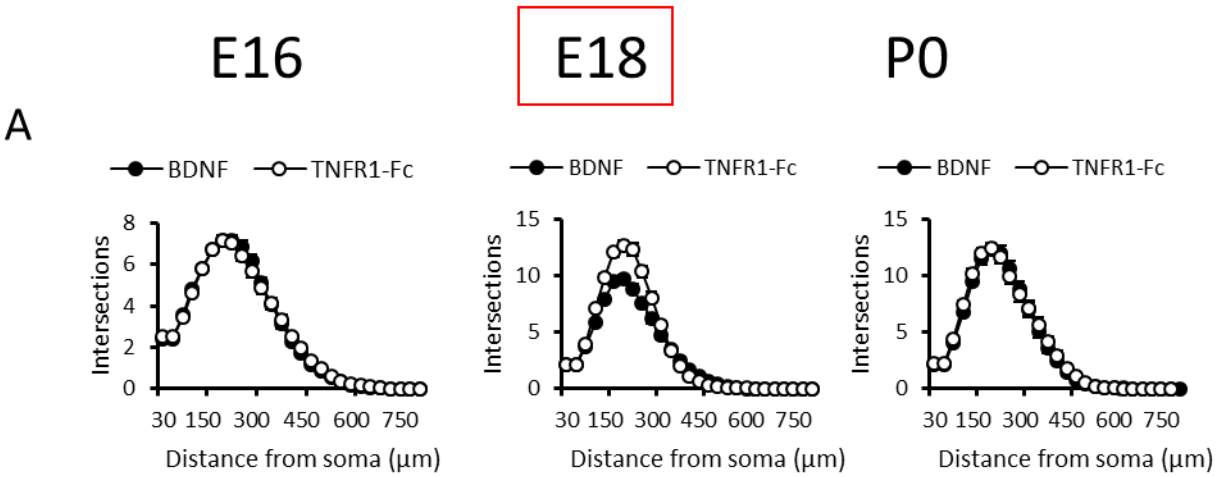
E16
E18
P0
A
BDNF
TNFR1-Fc
Intersections
Distance from soma (µm)
30 150 300 450 600 750

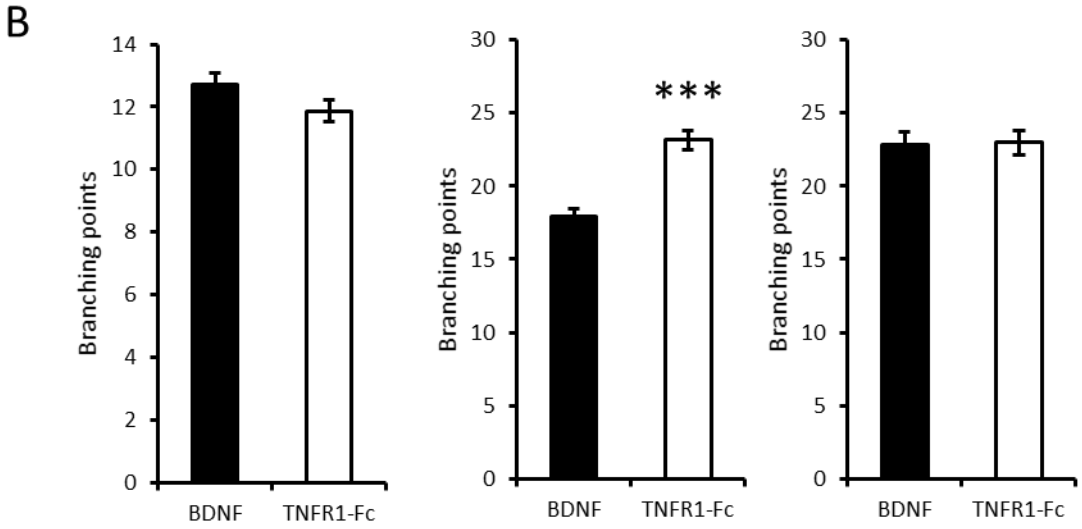
B
Branching points
BDNF
TNFR1-Fc
***

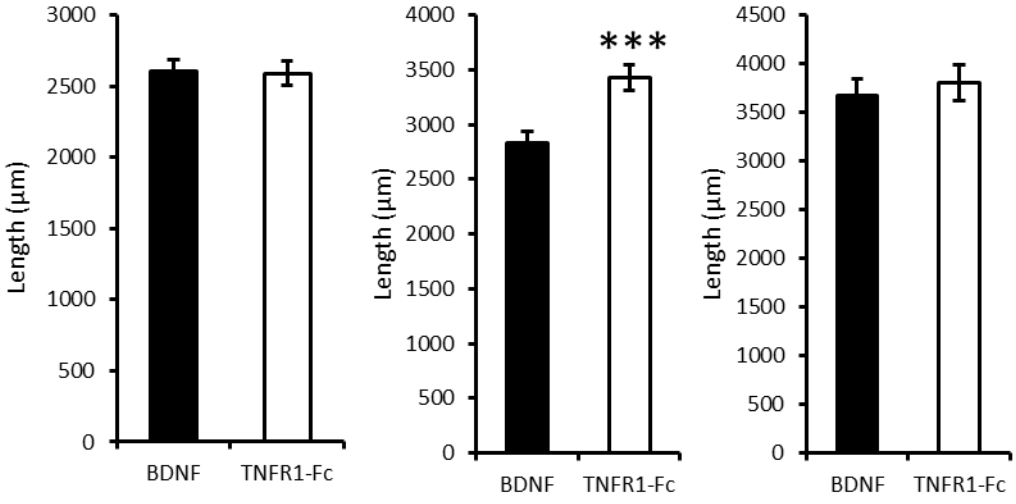
C
Length (µm)
BDNF
TNFR1-Fc
***

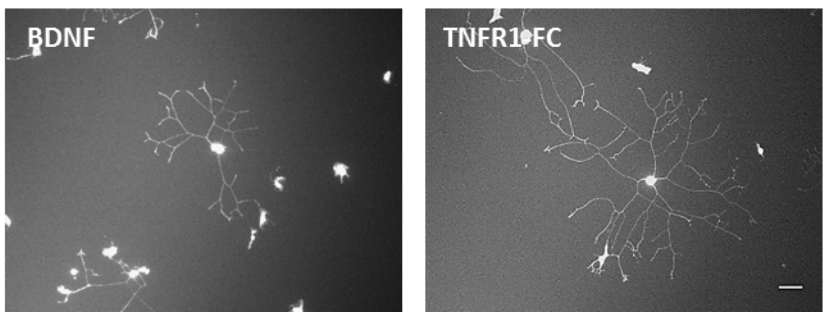
D
BDNF
TNFR1-FC

Figure 2: TNF reverse signalling enhances nodose neuron axon growth at E18. Dissociated cultures of E16, E18 and P0 nodose neurons were grown overnight in the presence of either 10 ng/ml NGF alone or NGF plus 10 ng/ml TNFR1-Fc. **A)** Sholl profiles, **B)** branch point number and **C)** neurite length of the neurite arbors. **D)** Representative micrographs depicting the difference in morphology of E18 nodose neurons grown with NGF alone and NGF plus TNFR1-Fc. Scale bar, 20 μm. Mean ± s.e.m. of the data from 3 separate experiments are plotted. More than 50 neurons analysed per condition in each experiment; statistical comparison with control (NGF), ***p<0.001, student T-test.

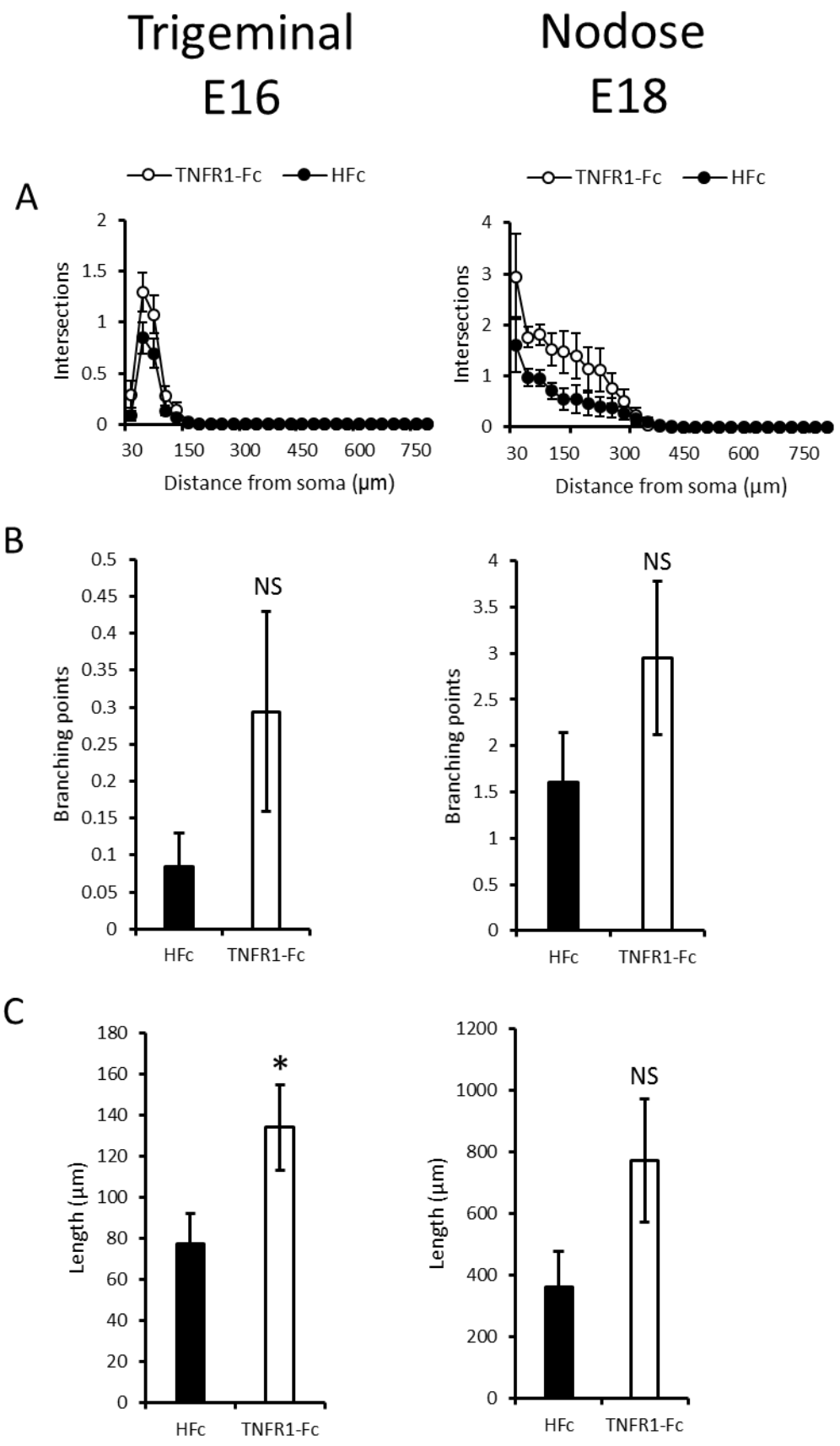

Figure 3, legend on following page.

Figure 3: TNF reverse signalling enhances axonal growth from cultured trigeminal and nodose neurons independently from neurotrophic factors. Dissociated cultures of E16 trigeminal and E18 nodose neurons were grown overnight in the presence of 1 µg/ml of the broad-spectrum caspase inhibitor Q-VD-OPh with either 10 ng/ml TNFR1-Fc or 10 ng/ml HFc. **A)** Sholl profiles, **B)** branch point number and **C)** neurite length of the neurite arbors. Mean ± s.e.m. of data from 1 experiment are plotted. More than 50 neurons imaged per condition; statistical comparison to control (HFc), *p<0.05, NS= not significant, student T-test.

6.3 Localisation of TNF and TNFR1 in trigeminal and nodose neurons

I used immunocytochemistry to ascertain the localisation of TNF and TNFR1 in dissociated cultures of E16 trigeminal and E18 nodose neurons. These neurons were grown overnight in the presence of NGF and BDNF, respectively, to sustain survival and promote axonal growth. The neurons were positively identified by β-III tubulin staining and labelled with either anti-TNF or anti-TNFR1. The nuclei were stained by TO-PRO. Like with SCG primary neuronal cultures, both trigeminal and nodose cultures contain non-neuronal cells, such as satellite glia cells. In addition, trigeminal cultures tend to have occasional fibroblasts due to the nature of the dissections. Cells incubated with secondary antibody alone exhibited no background immunofluorescence (Fig.4-5).

In E16 trigeminal neurons, strong TNF immunostaining was evident on cell bodies and along the full extent of axons. The cultures also contained some non-neural cells, most likely fibroblasts, which were also positive for TNF. However, while strong TNFR1 immunostaining was evident on cell bodies, the neurites were very weakly stained (Fig.4). This pattern of staining mirrors that observed in SCG neurons. In contrast, in E18 nodose neurons, TNF and TNFR1 immunostaining were clearly evident on both cell bodies and along the full extent of the neurites (Fig.5). The staining highlight once more

the difference in morphology of both these sensory neurons with each other and compared to SCG neurons.

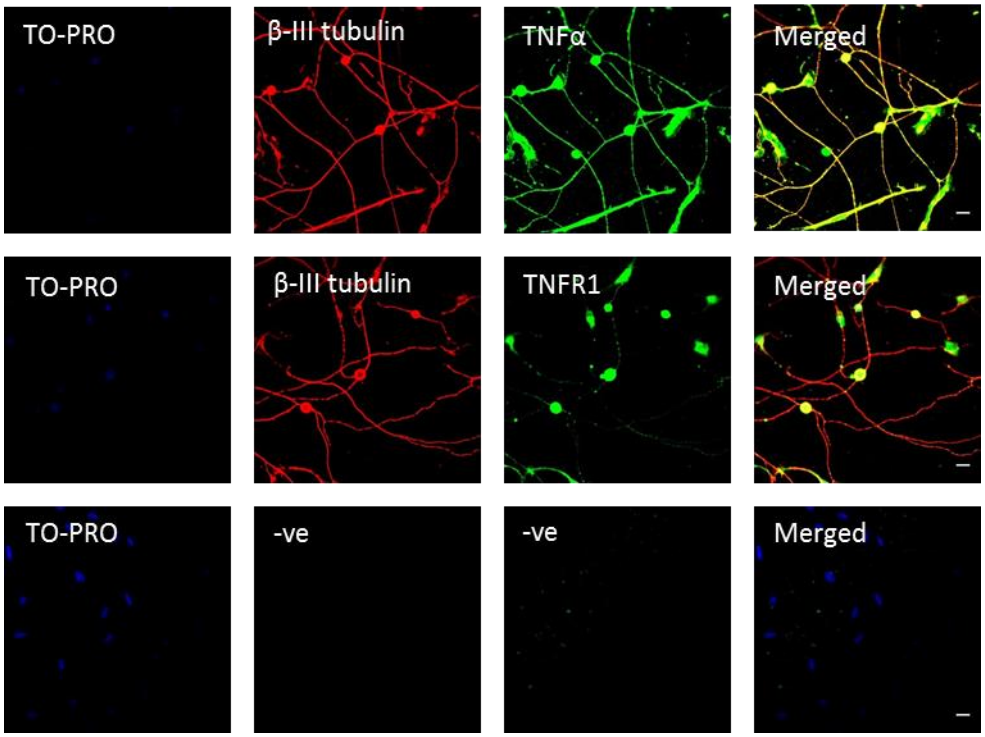

Figure 4: TNF and TNFR1 are expressed by E16 trigeminal neurons. Dissociated E16 trigeminal neurons were cultured overnight in the presence of 10 ng/ml NGF and stained the next day with specific antibodies for TNF and TNFR1. The cultures were double labelled with anti-β-III tubulin to positively identify neurons and TO-PRO was used to identify cell nuclei. The lower panels show cultures in which the primary antibodies were omitted from the staining protocol Scale bar, 20 µm.

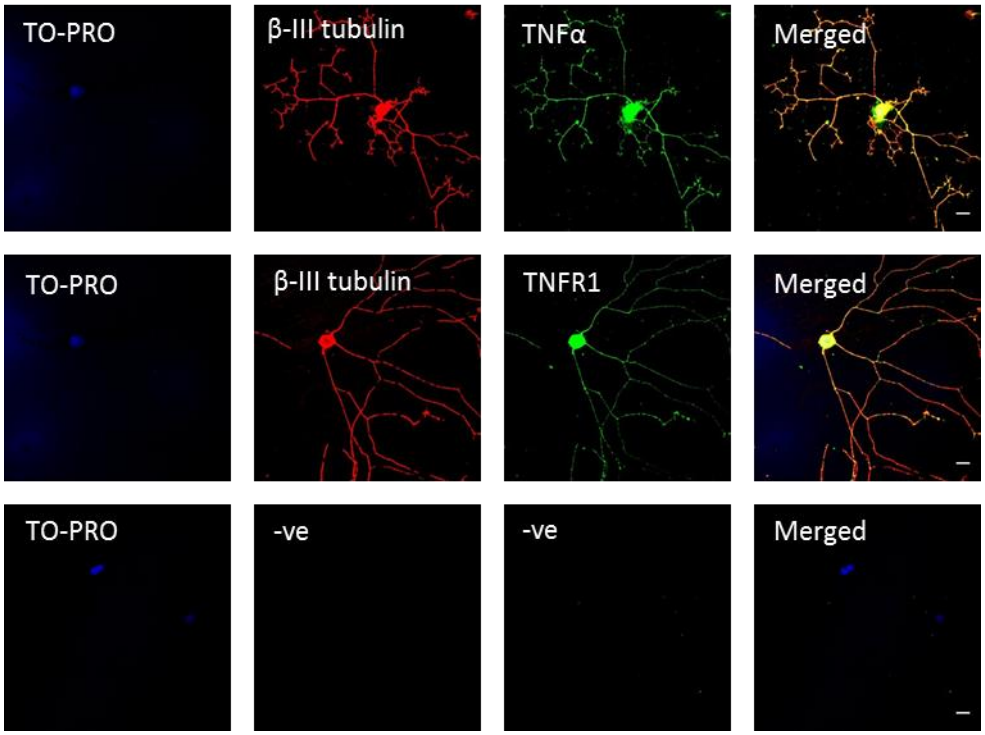

Figure 5: TNF and TNFR1 are expressed by E18 nodose neurons. Dissociated E18 nodose neurons were cultured overnight in the presence of 10 ng/ml BDNF and stained the next day with specific antibodies for TNF and TNFR1. The cultures were double labelled with anti-β-III tubulin to positively identify neurons and TO-PRO was used to identify cell nuclei. The lower panels show cultures in which the primary antibodies were omitted from the staining protocol. Scale bar, 20 µm.

6.4 Discussion

The preliminary data presented in this chapter suggest that TNF reverse signalling is able to enhance neurite growth and branching from both sensory neuron populations analysed (trigeminal and nodose) without affecting neuronal survival.

TNFR1-Fc induced significant increases in branching and length over narrow developmental windows for each neuron type. Trigeminal neurons only responded to TNFR1-Fc at E16 and nodose neurons only responded at E18. The ages when trigeminal and nodose neurons respond to TNFR1-Fc are different to those observed in SCG neurons, where neurons are responsive to TNFR1-Fc later in development, from P0 to P5. These differences may be related to the earlier development of sensory neurons, which are born earlier than SCG neurons and innervate and ramify in their targets before SCG neurons (Davies, 2003). Hence, if TNF reverse signalling is necessary for correct target innervation of sensory neurons it makes sense for sensory neurons to respond to TNFR1-Fc at earlier ages. In addition to enhancing the growth of trigeminal and nodose neurites, TNF reverse signalling has recently been reported to enhance NRTN-GFRα2-Ret-dependent neurite outgrowth from nonpeptidergic nociceptors in E14.5 DRG explant culture (Wheeler et al., 2014). The same study reported that these *in vitro* findings are physiologically relevant and seem to be required for the establishment of correct target innervation *in vivo.* Furthermore, TNF forward signalling also negatively regulated NGF-promoted neurite growth, differentiation and excitability of DRG peptidergic nociceptors from E14.5 up to P30 (Wheeler et al., 2014). These data together with our previous findings in sympathetic neurons suggest that TNF reverse signalling is widely involved in the development of the PNS. To further investigate this hypothesis,

an in-depth analysis of TNF reverse signalling should be carried out on cultures of trigeminal and nodose neurons from *Tnfα* and *Tnfrs1a* deficient mice to see if the growth enhancing effects are absent in *Tnfα* deficient neurons and that the addition of TNFR1-Fc still enhances axonal outgrowth in *Tnfrsf1*a deficient neurons. Furthermore, it would be important to investigate the innervation of trigeminal and nodose targets in $Tnf\alpha^{-/-}$ and $Tnfrs1a^{-/-}$ mice *in vivo*.

Trigeminal neurons arise from both the neural crest and the neurogenic trigeminal placode and nodose neurons arise from the third epibranchial neurogenic placode (Baker and Bronner-Fraser, 2001), this in contrast to sympathetic neurons which arise solely from neural crest cells. The neurite growth-enhancing effect of TNF reverse signalling therefore doesn't seem to be governed by the developmental origin of cells in terms of placode versus neural crest. Furthermore, TNF reverse signalling enhanced neurite growth is observed in the presence and absence of neurotrophins both in sensory and sympathetic neurons, hence, its effects on neurite growth are independent of neurotrophins. One could speculate that these are characteristics of a generalised mechanism for regulating axonal growth. This idea is consistent with work on other neuronal populations. In addition to the sympathetic and sensory neurons, other members within the Davies laboratory have examined the effects of TNF reverse signalling in cultured perinatal hippocampal neurons where it enhances axonal growth, but not dendritic growth (L. Kisiswa, personal communication). The addition of TNFR1-Fc to cortical neuron cultures also appears to enhance axonal growth (J.Ponce, personal communication). Taken together, these data raise the possibility that TNF mediated reverse signalling might be a widely used mechanism for enhancing axonal growth during development.

Immunolocalisation of TNF and TNFR1 on cultured neurons shows that in trigeminal neurons, TNF staining on neurites is intense, whereas TNFR1 staining is very weak. This is similar to what is observed in SCG neurons. For this reason, it would be interesting to study the immunolocalisation of TNFR1 and TNF in trigeminal targets to see if this parallels what is seen in SCG targets, where TNFR1 predominates, which is consistent with target-derived TNFR1 activating TNF reverse signalling on the innervating axons. In contrast, both TNFR1 and TNF are expressed with similar intensity along the neurites of cultured nodose neurons. This raises the possibility that TNF activated TNFR1 forward signalling in the processes of these neurons is also important for their development or that both forward and reverse signalling operate in these processes. Indeed, it has been shown that forward signalling and reverse signalling play a role during development of DRG nociceptors, where it has been shown that TNF and TNFR1 are co-expressed on the axons of these neurons (Wheeler et al., 2014). It would be informative to carry out studies of trigeminal and nodose neurons in compartment cultures to test the effects of TNF and TNFR1-Fc applied to either the soma or axons. Most importantly would be the analysis of trigeminal and nodose targets in *Tnfα* and *Tnfrsf1a* deficient mice, using markers for different kinds of sensory neurons.

Chapter 7
General Discussion

7.1 Findings

The main aim of my research was to investigate the role and molecular mechanism of action of TNF reverse signalling in sympathetic nervous system development and explore its wider role in the development of the peripheral nervous system. The data presented in this thesis, together with data of others of the Davies laboratory, reports for the first time the occurrence of TNF reverse signalling in the nervous system. TNF reverse signalling enhances the growth and branching of sympathetic axons at the stage when they are ramifying within their target fields without affecting neuronal survival. This is physiologically relevant and necessary for establishing correct sympathetic innervation of tissues innervated by the paravertebral sympathetic chain. TNF reverse signalling causes the opening of T-type calcium channels resulting in the influx of calcium, leading to ERK1 and ERK2 activation, which leads to enhanced axonal growth. Fig.1 depicts the time point at which TNF reverse signalling via TNFR1 comes into play during sympathetic development. A schematic drawing of the main findings of this thesis and the proposed working model is shown in Fig.2. Preliminary data additionally suggest that TNF reverse signalling is able to enhance axonal length and branching of the sensory axons of the trigeminal and nodose ganglia, suggesting that TNF reverse signalling may be a wide-spread mechanism for promoting axonal growth.

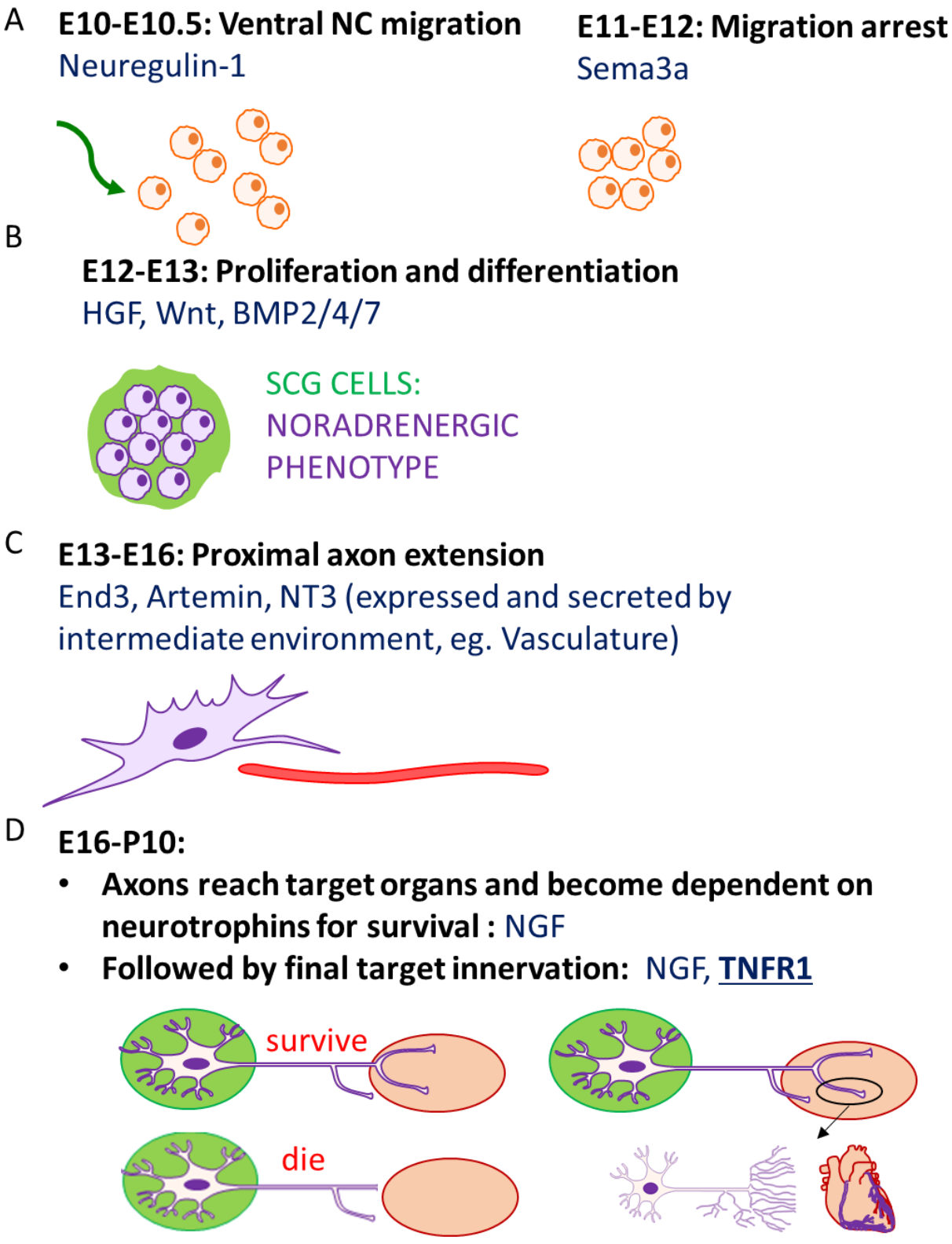

Figure 1: Summary timeline of sympathetic neuron development and the main factors involved .A-B) Early development. **C)** Proximal axon extension. **D)** Final target innervation. This thesis suggests a role for TNF reverse signalling via TNFR1 during final target innervation.

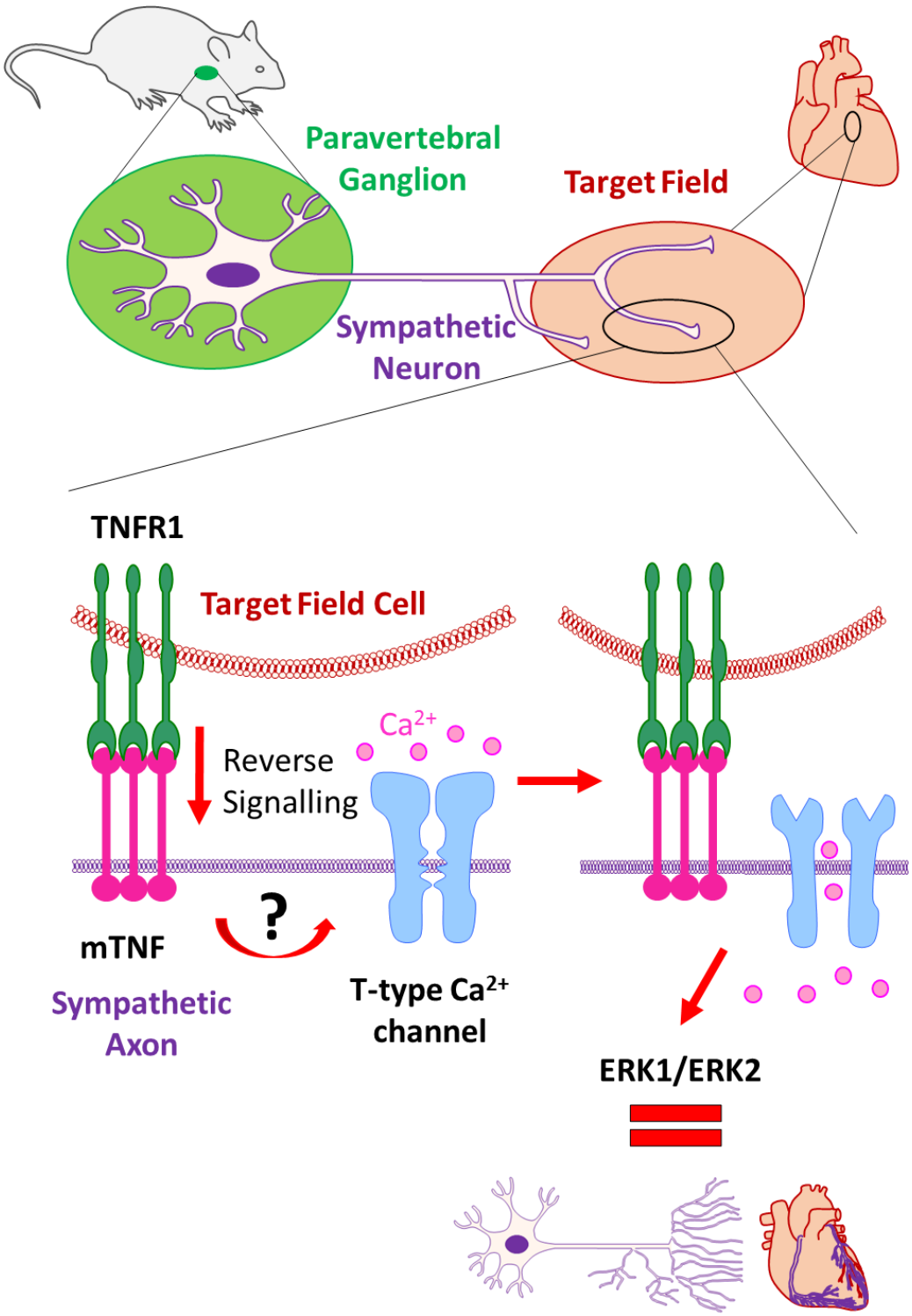

Figure 2: Working model for TNF reverse signalling during sympathetic development. Extending sympathetic neurons from paravertebral ganglia express TNF on their processes. Target fields express TNFR1. When processes are ramifying in their target organs, such as the heart, TNFR1 binds to membrane-integrated TNF, which transduces the signal via reverse signalling. This results in the opening of T-type calcium channels and entry of calcium into sympathetic neurons. Subsequently ERK1 and ERk2 are activated resulting in enhanced axonal growth within targets.

7.2 TNFSF in neuronal development

The discovery that TNF modulates axon growth by reverse signalling, not only adds to the growing body of evidence implicating members of the TNFSF in the regulation of axon growth in the developing nervous system, but also reveals an entirely new way to modulate axon growth. Previously, axon growth regulation by the TNFSF has been investigated and interpreted from the perspective of conventional forward signalling. Acting in this manner, several TNFSF members have been shown to be potent positive or negative regulators of axon growth. For example, whereas axon growth is enhanced by GITRL, FasL and APRIL (a proliferation-inducing ligand), it is inhibited by RANKL, LIGHT and TNF (Desbarats et al., 2003, Gutierrez et al., 2008, O'Keeffe et al., 2008, Gavalda et al., 2009, Gutierrez et al., 2013, Osorio et al., 2014). These TNFSF members, unlike neurotrophic factors, generally regulate axon growth without affecting neuronal survival and act over far shorter circumscribed developmental windows, than the extended period of development over which neurotrophic factors operate. Some of these TNFSF members exert their effects on neurons in a target-derived manner whereas others do so in an autocrine manner. In addition, they either modulate the axon growth response of neurons to neurotrophins or in some instances act independently of neurotrophins.

While most of this work has been carried out on sensory and sympathetic neurons of the developing peripheral nervous system, a limited number of studies has revealed that the TNFSF members exert effects on CNS neurons. For example, APRIL is able to enhance the growth of neonatal hippocampal pyramidal axons *in vitro* (Osorio et al., 2014) and similarly, TNFR1-activated reverse signalling only seems to enhance axonal length and

not dendritic growth in cortical and hippocampal cultures (L.Kisiswa and J.Ponce, personal communication). Paradoxically, CA1 and CA3 pyramidal neurons display less complex dendritic arborisation in TNF null mutant mice compared to wild type mice (Golan et al., 2004). While the addition of TNF to hippocampal neuron cultures leads to a reduction in neurite length and branching, which is in agreement with TNF forward signalling (Neumann et al., 2002). FasL, on the other hand, enhances dendritic and axonal branching points of hippocampal neurons (Zuliani et al., 2006). Together, this raises the possibility that the TNFSF regulates axon growth to refine connections not only in the PNS but also in the CNS.

Since we described TNF reverse signalling in developing sympathetic neurons (Kisiswa et al., 2013), TNF reverse signalling has been subsequently reported in developing DRG sensory neurons, where it also promotes axon growth (Wheeler et al., 2014). Interestingly, where reverse and forward TNF signalling has been shown to occur in the same class of neurons, these different signalling mechanisms have opposite effects on axon growth. In both sympathetic and sensory neurons, forward TNF signalling inhibits the axon growth promoting effects of neurotrophins, whereas reverse signalling enhances axon growth (Gutierrez et al., 2008, Kisiswa et al., 2013, Nolan et al., 2014, Wheeler et al., 2014). Additionally, it seems that the balance between forward and reverse signalling in PNS development aids in differentiating between target field innervation of different cell types or organ function: be it peptidergic versus nonpeptidergic nociceptors (Wheeler et al., 2014), intrinsic differences between paravertebral versus prevertebral neurons and hematopoietic versus non hematopoietic target organs (Chapter 4). This has a parallel in the immune system, where one signalling pathway (be it forward or reverse) will attenuate the immune

response while its counterpart will intensify it (Juhasz et al., 2013). In both the developing nervous system and the immune system, it seems that the balance between forward and reverse signalling enables TNF to exert a multitude of effects, at times with opposing outcomes, thereby widening the breadth of its actions, hence, exemplifying the concept of signal recycling. In future work it will be informative to clarify the factors that shift the balance between forward and reverse signalling.

Very recently, CD40-activated CD40L reverse signalling has been shown to enhance NGF-promoted axon growth from perinatal sympathetic neurons with no effect on neuronal survival. However, it does not promote axon growth in the absence of NGF (McWilliams et al., 2015). In contrast to TNF reverse signalling, which acts in a target-derived manner, CD40L reverse signalling operates by an autocrine mechanism. NGF negatively regulates the expression of CD40L and CD40, hence, this axon growth promoting autocrine signalling only operates at low concentrations of NGF. As a consequence, deficiencies in sympathetic innervation in CD40-deficient mice are restricted to tissues that express low levels of NGF. This reveals how the differential regulation of an autocrine loop, affecting axon growth within a population of neurons, can modulate the innervation of a specific set of targets.

The above work has elucidated that superimposed upon the signals provided by neurotrophins, which regulate neuronal survival and axon growth, there is a diverse set of signals, provided by the TNF superfamily, that additionally regulate axon growth in a variety of ways. Why has this additional set of signals been recruited to regulate innervation during the course of evolution? The increasing complexity of the nervous system throughout vertebrate evolution has undoubtedly necessitated the proliferation

of signals for its development. The diverse actions of multiple members of the TNFSF on developing neurons, together with the ability of several members of this superfamily to engage in forward and reverse signalling, adds a level of complexity that makes them well placed for refining the complexity of neural connections.

Moreover, there are reasons to suppose that extracellular signals with the characteristics of neurotrophins require additional signalling molecules to refine neural connectivity. Due to the fact that neurotrophins sustain both neuronal survival and promote axon growth and branching, if they were the only factors regulating innervation, one would predict a fixed relationship between the number of neurons innervating a tissue and axon growth and branching within that tissue. Therefore, the small number of neurons sustained by tissues that express low levels of neurotrophins would have proportionally stunted terminal axon branches, whereas the larger number of neurons innervating high neurotrophin expressing tissues would have proportionally larger axon ramification within the tissue. Hence, having an additional set of signals, such as the TNFSF that regulate axon growth and branching without affecting survival, enables the size of axon terminal arbors to be regulated independently of survival. Thereby, allowing greater control over axon growth and ramification in different tissues.

7.3 Concluding remarks

The findings reported in this thesis add to the exciting and growing field of research that places TNFSF members as regulators of neural development. Furthermore, it highlights the importance of reverse signalling in this process, which adds to the multiple and diverse ways the TNFSF influences neural development. Moreover, it raises many

interesting questions. Such as what are the molecular details of the mechanism of TNF reverse signalling and to what extent these are similar in the immune response. As well as, the extent to which TNFSF reverse signalling is employed in neural development and the factors that govern the balance between forward and reverse signalling in neural development.

References

AGGARWAL, B. B. 2003. Signalling pathways of the TNF superfamily: a double-edged sword. *Nat Rev Immunol,* 3**,** 745-56.

AIRAKSINEN, M. S. & SAARMA, M. 2002. The GDNF family: signalling, biological functions and therapeutic value. *Nat Rev Neurosci,* 3**,** 383-94.

ALBERS, K. M., PERRONE, T. N., GOODNESS, T. P., JONES, M. E., GREEN, M. A. & DAVIS, B. M. 1996. Cutaneous overexpression of NT-3 increases sensory and sympathetic neuron number and enhances touch dome and hair follicle innervation. *Journal of Cell Biology,* 134**,** 487-497.

ALBERS, K. M., WRIGHT, D. E. & DAVIS, B. M. 1994. Overexpression of Nerve Growth-Factor in Epidermis of Transgenic Mice Causes Hypertrophy of the Peripheral Nervous-System. *Journal of Neuroscience,* 14**,** 1422-1432.

ANDRES, R., FORGIE, A., WYATT, S., CHEN, Q., DE SAUVAGE, F. J. & DAVIES, A. M. 2001. Multiple effects of artemin on sympathetic neurone generation, survival and growth. *Development,* 128**,** 3685-95.

ANGELETTI, R. H. & BRADSHAW, R. A. 1971. Nerve Growth Factor from Mouse Submaxillary Gland: Amino Acid Sequence. *Proceedings of the National Academy of Sciences of the United States of America,* 68**,** 2417-2420.

BAKER, C. V. H. & BRONNER-FRASER, M. 2001. Vertebrate Cranial Placodes I. Embryonic Induction. *Developmental Biology,* 232**,** 1-61.

BALOH, R. H., TANSEY, M. G., LAMPE, P. A., FAHRNER, T. J., ENOMOTO, H., SIMBURGER, K. S., LEITNER, M. L., ARAKI, T., JOHNSON JR, E. M. & MILBRANDT, J. 1998. Artemin, a Novel Member of the GDNF Ligand Family, Supports Peripheral and Central Neurons and Signals through the GFRα3–RET Receptor Complex. *Neuron,* 21**,** 1291-1302.

BARDE, Y. A., EDGAR, D. & THOENEN, H. 1982. Purification of a new neurotrophic factor from mammalian brain. *EMBO J,* 1**,** 549-53.

BARKER, V., MIDDLETON, G., DAVEY, F. & DAVIES, A. M. 2001. TNFalpha contributes to the death of NGF-dependent neurons during development. *Nat Neurosci,* 4**,** 1194-8.

BAUER, S., KERR, B. J. & PATTERSON, P. H. 2007. The neuropoietic cytokine family in development, plasticity, disease and injury. *Nature Reviews Neuroscience,* 8**,** 221-232.

BELLIVEAU, D. J., KRIVKO, I., KOHN, J., LACHANCE, C., POZNIAK, C., RUSAKOV, D., KAPLAN, D. & MILLER, F. D. 1997. NGF and Neurotrophin-3 Both Activate TrkA on Sympathetic Neurons but Differentially Regulate Survival and Neuritogenesis. *The Journal of Cell Biology,* 136**,** 375-388.

BERGER, E. A. & SHOOTER, E. M. 1977. Evidence for pro-β-nerve growth factor, a biosynthetic precursor to β-nerve growth factor. *Proceedings of the National Academy of Sciences of the United States of America,* 74**,** 3647-3651.

BIBEL, M. & BARDE, Y. A. 2000. Neurotrophins: key regulators of cell fate and cell shape in the vertebrate nervous system. *Genes Dev,* 14**,** 2919-37.

BLACK, R. A., RAUCH, C. T., KOZLOSKY, C. J., PESCHON, J. J., SLACK, J. L., WOLFSON, M. F., CASTNER, B. J., STOCKING, K. L., REDDY, P., SRINIVASAN, S., NELSON, N., BOIANI, N., SCHOOLEY, K. A., GERHART, M., DAVIS, R., FITZNER, J. N., JOHNSON, R. S., PAXTON, R. J., MARCH, C. J. & CERRETTI, D. P. 1997. A metalloproteinase disintegrin that releases tumour-necrosis factor-[alpha] from cells. *Nature,* 385**,** 729-733.

BODMER, D., LEVINE-WILKINSON, S., RICHMOND, A., HIRSH, S. & KURUVILLA, R. 2009. Wnt5a mediates nerve growth factor-dependent axonal branching and growth in developing sympathetic neurons. *J Neurosci,* 29**,** 7569-81.

BODMER, J. L., SCHNEIDER, P. & TSCHOPP, J. 2002. The molecular architecture of the TNF superfamily. *Trends Biochem Sci,* 27**,** 19-26.

BRADSHAW, R. A., MURRAY-RUST, J., IBÁÑEZ, C. F., MCDONALD, N. Q., LAPATTO, R. & BLUNDELL, T. L. 1994. Nerve growth factor: structure/function relationships. *Protein Science : A Publication of the Protein Society,* 3**,** 1901-1913.

BRITSCH, S., LI, L., KIRCHHOFF, S., THEURING, F., BRINKMANN, V., BIRCHMEIER, C. & RIETHMACHER, D. 1998. The ErbB2 and ErbB3 receptors and their ligand, neuregulin-1,

are essential for development of the sympathetic nervous system. *Genes & Development,* 12**,** 1825-1836.

BRUNO, M. A. & CUELLO, A. C. 2006. Activity-dependent release of precursor nerve growth factor, conversion to mature nerve growth factor, and its degradation by a protease cascade. *Proceedings of the National Academy of Sciences,* 103**,** 6735-6740.

BUCHMAN, V. L. & DAVIES, A. M. 1993. Different neurotrophins are expressed and act in a developmental sequence to promote the survival of embryonic sensory neurons. *Development,* 118**,** 989-1001.

CABAL-HIERRO, L. & LAZO, P. S. 2012. Signal transduction by tumor necrosis factor receptors. *Cellular Signalling,* 24**,** 1297-1305.

CAMPENOT, R. B. 1987. Local control of neurite sprouting in cultured sympathetic neurons by nerve growth factor. *Brain Res,* 465**,** 293-301.

CAMPENOT, R. B. & MACINNIS, B. L. 2004. Retrograde transport of neurotrophins: Fact and function. *Journal of Neurobiology,* 58**,** 217-229.

CARLSON, S. L., FELTEN, D. L., LIVNAT, S. & FELTEN, S. Y. 1987. Noradrenergic sympathetic innervation of the spleen: V. Acute drug-induced depletion of lymphocytes in the target fields of innervation results in redistribution of noradrenergic fibers but maintenance of compartmentation. *J Neurosci Res,* 18**,** 64-9, 130-1.

CARROLL, S. L., BYER, S. J., DORSEY, D. A., WATSON, M. A. & SCHMIDT, R. E. 2004. Ganglion-specific patterns of diabetes-modulated gene expression are established in prevertebral and paravertebral sympathetic ganglia prior to the development of neuroaxonal dystrophy. *J Neuropathol Exp Neurol,* 63**,** 1144-54.

CARSWELL, E. A., OLD, L. J., KASSEL, R. L., GREEN, S., FIORE, N. & WILLIAMSON, B. 1975. An endotoxin-induced serum factor that causes necrosis of tumors. *Proceedings of the National Academy of Sciences of the United States of America,* 72**,** 3666-3670.

CHAO, M. V. 2003. Neurotrophins and their receptors: a convergence point for many signalling pathways. *Nat Rev Neurosci,* 4**,** 299-309.

CHEN, C.-C., LAMPING, K. G., NUNO, D. W., BARRESI, R., PROUTY, S. J., LAVOIE, J. L., CRIBBS, L. L., ENGLAND, S. K., SIGMUND, C. D., WEISS, R. M., WILLIAMSON, R. A., HILL, J. A. & CAMPBELL, K. P. 2003. Abnormal Coronary Function in Mice Deficient in α1H T-type Ca2+ Channels. *Science,* 302**,** 1416-1418.

CHEN, Y., ZENG, J., CEN, L., WANG, X., YAO, G., WANG, W., QI, W. & KONG, K. 2009. Multiple roles of the p75 neurotrophin receptor in the nervous system. *J Int Med Res,* 37**,** 281-8.

CHEVENDRA, V. & WEAVER, L. C. 1991. Distribution of splenic, mesenteric and renal neurons in sympathetic ganglia in rats. *J Auton Nerv Syst,* 33**,** 47-53.

CHUNG, J. Y., PARK, Y. C., YE, H. & WU, H. 2002. All TRAFs are not created equal: common and distinct molecular mechanisms of TRAF-mediated signal transduction. *J Cell Sci,* 115**,** 679-88.

CLAPHAM, D. E. 2007. Calcium signaling. *Cell,* 131**,** 1047-58.

COHEN, J. & WILKIN, G. P. 1995. *Neural Cell Culture: A Practical Approach*, IRL Press.

COHEN, S., LEVI-MONTALCINI, R. & HAMBURGER, V. 1954. A Nerve Growth-Stimulating Factor Isolated from Sarcom as 37 and 180. *Proc Natl Acad Sci U S A,* 40**,** 1014-8.

CONOVER, J. C., ERICKSON, J. T., KATZ, D. M., BIANCHI, L. M., POUEYMIROU, W. T., MCCLAIN, J., PAN, L., HELGREN, M., IP, N. Y., BOLAND, P. & ET AL. 1995. Neuronal deficits, not involving motor neurons, in mice lacking BDNF and/or NT4. *Nature,* 375**,** 235-8.

CROWLEY, C., SPENCER, S. D., NISHIMURA, M. C., CHEN, K. S., PITTS-MEEK, S., ARMANINI, M. P., LING, L. H., MCMAHON, S. B., SHELTON, D. L., LEVINSON, A. D. & ET AL. 1994. Mice lacking nerve growth factor display perinatal loss of sensory and sympathetic neurons yet develop basal forebrain cholinergic neurons. *Cell,* 76**,** 1001-11.

CUNHA, C., BRAMBILLA, R. & THOMAS, K. L. 2010. A simple role for BDNF in learning and memory? *Frontiers in Molecular Neuroscience,* 3.

CZABOTAR, P. E., LESSENE, G., STRASSER, A. & ADAMS, J. M. 2014. Control of apoptosis by the BCL-2 protein family: implications for physiology and therapy. *Nat Rev Mol Cell Biol,* 15**,** 49-63.

DAVIES, A. M. 1988. The trigeminal system: an advantageous experimental model for studying neuronal development. *Development,* 103 Suppl**,** 175-83.

DAVIES, A. M. 1989. Intrinsic differences in the growth rate of early nerve fibres related to target distance. *Nature,* 337**,** 553-5.

DAVIES, A. M. 1994a. Intrinsic programmes of growth and survival in developing vertebrate neurons. *Trends Neurosci,* 17**,** 195-9.

DAVIES, A. M. 1994b. Neurotrophic factors. Switching neurotrophin dependence. *Curr Biol,* 4**,** 273-6.

DAVIES, A. M. 1996. The neurotrophic hypothesis: where does it stand? *Philos Trans R Soc Lond B Biol Sci,* 351**,** 389-94.

DAVIES, A. M. 1997. Neurotrophin switching: where does it stand? *Curr Opin Neurobiol,* 7**,** 110-8.

DAVIES, A. M. 2000. Neurotrophins: neurotrophic modulation of neurite growth. *Curr Biol,* 10**,** R198-200.

DAVIES, A. M. 2003. Regulation of neuronal survival and death by extracellular signals during development. *The EMBO Journal,* 22**,** 2537-2545.

DAVIES, A. M. 2009. Extracellular signals regulating sympathetic neuron survival and target innervation during development. *Autonomic Neuroscience,* 151**,** 39-45.

DAVIES, A. M., LEE, K. F. & JAENISCH, R. 1993. p75-deficient trigeminal sensory neurons have an altered response to NGF but not to other neurotrophins. *Neuron,* 11**,** 565-74.

DAVIES, A. M. & LUMSDEN, A. 1990. Ontogeny of the somatosensory system: origins and early development of primary sensory neurons. *Annu Rev Neurosci,* 13**,** 61-73.

DAVIS, C. & KANNAN, M. S. 1987. Sympathetic innervation of human tracheal and bronchial smooth muscle. *Respir Physiol,* 68**,** 53-61.

DEHAL, N. S., DEKABAN, G. A., KRASSIOUKOV, A. V., PICARD, F. J. & WEAVER, L. C. 1993. Identification of renal sympathetic preganglionic neurons in hamsters using transsynaptic transport of herpes simplex type 1 virus. *Neuroscience,* 56**,** 227-40.

DESBARATS, J., BIRGE, R. B., MIMOUNI-RONGY, M., WEINSTEIN, D. E., PALERME, J. S. & NEWELL, M. K. 2003. Fas engagement induces neurite growth through ERK activation and p35 upregulation. *Nature Cell Biology,* 5**,** 118-125.

DICKSON, B. J. 2002. Molecular Mechanisms of Axon Guidance. *Science,* 298**,** 1959-1964.

DOTTORI, M., GROSS, M. K., LABOSKY, P. & GOULDING, M. 2001. The winged-helix transcription factor Foxd3 suppresses interneuron differentiation and promotes neural crest cell fate. *Development,* 128**,** 4127-38.

DOUARIN, N. L. & KALCHEIM, C. 1999. *The Neural Crest*, Cambridge University Press.

DUPIN, E., CREUZET, S. & LE DOUARIN, N. M. 2006. The contribution of the neural crest to the vertebrate body. *Adv Exp Med Biol,* 589**,** 96-119.

EDWARDS, R. H., RUTTER, W. J. & HANAHAN, D. 1989. Directed Expression of Ngf to Pancreatic Beta-Cells in Transgenic Mice Leads to Selective Hyperinnervation of the Islets. *Cell,* 58**,** 161-170.

EISSNER, G., KIRCHNER, S., LINDNER, H., KOLCH, W., JANOSCH, P., GRELL, M., SCHEURICH, P., ANDREESEN, R. & HOLLER, E. 2000. Reverse signaling through transmembrane TNF confers resistance to lipopolysaccharide in human monocytes and macrophages. *J Immunol,* 164**,** 6193-8.

EISSNER, G., KOLCH, W. & SCHEURICH, P. 2004. Ligands working as receptors: reverse signaling by members of the TNF superfamily enhance the plasticity of the immune system. *Cytokine & Growth Factor Reviews,* 15**,** 353-366.

ELDREDGE, L. C., GAO, X. M., QUACH, D. H., LI, L., HAN, X., LOMASNEY, J. & TOURTELLOTTE, W. G. 2008. Abnormal sympathetic nervous system development and physiological dysautonomia in Egr3-deficient mice. *Development,* 135**,** 2949-57.

ELFVIN, L. G., LINDH, B. & HOKFELT, T. 1993. The chemical neuroanatomy of sympathetic ganglia. *Annu Rev Neurosci,* 16**,** 471-507.

ELMORE, S. 2007. Apoptosis: a review of programmed cell death. *Toxicol Pathol,* 35**,** 495-516.

ENOMOTO, H., CRAWFORD, P. A., GORODINSKY, A., HEUCKEROTH, R. O., JOHNSON, E. M., JR. & MILBRANDT, J. 2001. RET signaling is essential for migration, axonal growth and axon guidance of developing sympathetic neurons. *Development,* 128**,** 3963-74.

ERICKSON, J. T., BROSENITSCH, T. A. & KATZ, D. M. 2001. Brain-derived neurotrophic factor and glial cell line-derived neurotrophic factor are required simultaneously for survival of dopaminergic primary sensory neurons in vivo. *Journal of Neuroscience,* 21**,** 581-9.

ERNSBERGER, U., EDGAR, D. & ROHRER, H. 1989. The survival of early chick sympathetic neurons in vitro is dependent on a suitable substrate but independent of NGF. *Developmental Biology,* 135**,** 250-262.

ERNSBERGER, U., PATZKE, H., TISSIER-SETA, J. P., REH, T., GORIDIS, C. & ROHRER, H. 1995. The expression of tyrosine hydroxylase and the transcription factors cPhox-2 and Cash-1: evidence for distinct inductive steps in the differentiation of chick sympathetic precursor cells. *Mechanisms of Development,* 52**,** 125-136.

FAGAN, A. M., ZHANG, H., LANDIS, S., SMEYNE, R. J., SILOS-SANTIAGO, I. & BARBACID, M. 1996. TrkA, but not TrkC, receptors are essential for survival of sympathetic neurons in vivo. *Journal of Neuroscience,* 16**,** 6208-18.

FARINAS, I., JONES, K. R., BACKUS, C., WANG, X. Y. & REICHARDT, L. F. 1994. Severe sensory and sympathetic deficits in mice lacking neurotrophin-3. *Nature,* 369**,** 658-61.

FEINBERG, T. E. & MALLATT, J. 2013. The evolutionary and genetic origins of consciousness in the Cambrian Period over 500 million years ago. *Front Psychol,* 4**,** 667.

FENG, X. 2005. Regulatory roles and molecular signaling of TNF family members in osteoclasts. *Gene,* 350**,** 1-13.

FERGUSON, M., RYAN, G. B. & BELL, C. 1986. Localization of sympathetic and sensory neurons innervating the rat kidney. *J Auton Nerv Syst,* 16**,** 279-88.

FERRAN, C., DAUTRY, F., MERITE, S., SHEEHAN, K., SCHREIBER, R., GRAU, G., BACH, J. F. & CHATENOUD, L. 1994. Anti-tumor necrosis factor modulates anti-CD3-triggered T cell cytokine gene expression in vivo. *J Clin Invest,* 93**,** 2189-96.

FERREIRA, J. N. & HOFFMAN, M. P. 2013. Interactions between developing nerves and salivary glands. *Organogenesis,* 9**,** 199-205.

FIORE, M., ANGELUCCI, F., ALLEVA, E., BRANCHI, I., PROBERT, L. & ALOE, L. 2000. Learning performances, brain NGF distribution and NPY levels in transgenic mice expressing TNF-alpha. *Behavioural Brain Research,* 112**,** 165-175.

FITZGERALD, M. J. T., GRUENER, G. & MTUI, E. 2012. *Clinical neuroanatomy and neuroscience* [Online]. [Edinburgh?]: Saunders/Elsevier. Available: http://www.clinicalkey.com/dura/browse/bookChapter/3-s2.0-C20090601896.

FLATMARK, T. 2000. Catecholamine biosynthesis and physiological regulation in neuroendocrine cells. *Acta Physiol Scand,* 168**,** 1-17.

FORGIE, A., KUEHNEL, F., WYATT, S. & DAVIES, A. M. 2000. In vivo survival requirement of a subset of nodose ganglion neurons for nerve growth factor. *European Journal of Neuroscience,* 12**,** 670-676.

FORGIE, A., WYATT, S., CORRELL, P. H. & DAVIES, A. M. 2003. Macrophage stimulating protein is a target-derived neurotrophic factor for developing sensory and sympathetic neurons. *Development,* 130**,** 995-1002.

FRADE, J. M. & BARDE, Y.-A. 1998. Nerve growth factor: two receptors, multiple functions. *BioEssays,* 20**,** 137-145.

FRANCIS, N., FARINAS, I., BRENNAN, C., RIVAS-PLATA, K., BACKUS, C., REICHARDT, L. & LANDIS, S. 1999. NT-3, like NGF, is required for survival of sympathetic neurons, but not their precursors. *Dev Biol,* 210**,** 411-27.

FRANCIS, N. J. & LANDIS, S. C. 1999. Cellular and molecular determinants of sympathetic neuron development. *Annual Review of Neuroscience,* 22**,** 541-566.

GANS, C. & NORTHCUTT, R. G. 1983. Neural crest and the origin of vertebrates: a new head. *Science,* 220**,** 268-73.

GATTONE, V. H., 2ND, MARFURT, C. F. & DALLIE, S. 1986. Extrinsic innervation of the rat kidney: a retrograde tracing study. *Am J Physiol,* 250**,** F189-96.

GAVALDA, N., GUTIERREZ, H. & DAVIES, A. M. 2009. Developmental regulation of sensory neurite growth by the tumor necrosis factor superfamily member LIGHT. *Journal of Neuroscience,* 29**,** 1599-607.

GIBBINS, I. L. 1991. Vasomotor, pilomotor and secretomotor neurons distinguished by size and neuropeptide content in superior cervical ganglia of mice. *J Auton Nerv Syst,* 34**,** 171-83.

GIBSON, D. A. & MA, L. 2011. Developmental regulation of axon branching in the vertebrate nervous system. *Development,* 138**,** 183-95.

GILBERT, S. F. 2006. *Developmental biology,* Sunderland, Mass., Sinauer Associates Publishers.

GLEBOVA, N. O. & GINTY, D. D. 2004. Heterogeneous requirement of NGF for sympathetic target innervation in vivo. *J Neurosci,* 24**,** 743-51.

GLEBOVA, N. O. & GINTY, D. D. 2005. Growth and survival signals controlling sympathetic nervous system development. *Annu Rev Neurosci,* 28**,** 191-222.

GOLAN, H., LEVAV, T., MENDELSOHN, A. & HULEIHEL, M. 2004. Involvement of tumor necrosis factor alpha in hippocampal development and function. *Cereb Cortex,* 14**,** 97-105.

GOMEZ, N. & COHEN, P. 1991. Dissection of the Protein-Kinase Cascade by Which Nerve Growth-Factor Activates Map Kinases. *Nature,* 353**,** 170-173.

GOOLD, R. G. & GORDON-WEEKS, P. R. 2005. The MAP kinase pathway is upstream of the activation of GSK3beta that enables it to phosphorylate MAP1B and contributes to the stimulation of axon growth. *Mol Cell Neurosci,* 28**,** 524-34.

GRAY, L. S., PEREZ-REYES, E., GAMORRA, J. C., HAVERSTICK, D. M., SHATTOCK, M., MCLATCHIE, L., HARPER, J., BROOKS, G., HEADY, T. & MACDONALD, T. L. 2004. The role of voltage gated T-type Ca2+ channel isoforms in mediating “capacitative” Ca2+ entry in cancer cells. *Cell Calcium,* 36**,** 489-497.

GRELL, M. 1995. Tumor necrosis factor (TNF) receptors in cellular signaling of soluble and membrane-expressed TNF. *J Inflamm,* 47**,** 8-17.

GROVES, A. K., GEORGE, K. M., TISSIER-SETA, J. P., ENGEL, J. D., BRUNET, J. F. & ANDERSON, D. J. 1995. Differential regulation of transcription factor gene expression and phenotypic markers in developing sympathetic neurons. *Development,* 121**,** 887-901.

GUILLEMOT, F. & JOYNER, A. L. 1993. Dynamic expression of the murine Achaete-Scute homologue Mash-1 in the developing nervous system. *Mechanisms of Development,* 42**,** 171-185.

GUTIERREZ, H. & DAVIES, A. M. 2007. A fast and accurate procedure for deriving the Sholl profile in quantitative studies of neuronal morphology. *J Neurosci Methods,* 163**,** 24-30.

GUTIERREZ, H., KISISWA, L., O'KEEFFE, G. W., SMITHEN, M. J., WYATT, S. & DAVIES, A. M. 2013. Regulation of neurite growth by tumour necrosis superfamily member RANKL. *Open Biol,* 3**,** 120150.

GUTIERREZ, H., O'KEEFFE, G. W., GAVALDA, N., GALLAGHER, D. & DAVIES, A. M. 2008. Nuclear factor kappa B signaling either stimulates or inhibits neurite growth depending on the phosphorylation status of p65/RelA. *Journal of Neuroscience,* 28**,** 8246-56.

HALL, B. K. 2000. The neural crest as a fourth germ layer and vertebrates as quadroblastic not triploblastic. *Evolution & Development,* 2**,** 3-5.

HAMBURGER, V. & YIP, J. W. 1984. Reduction of experimentally induced neuronal death in spinal ganglia of the chick embryo by nerve growth factor. *J Neurosci,* 4**,** 767-74.

HARASHIMA, S., HORIUCHI, T., HATTA, N., MORITA, C., HIGUCHI, M., SAWABE, T., TSUKAMOTO, H., TAHIRA, T., HAYASHI, K., FUJITA, S. & NIHO, Y. 2001. Outside-to-inside signal through the membrane TNF-alpha induces E-selectin (CD62E) expression on activated human CD4+ T cells. *J Immunol,* 166**,** 130-6.

HEHLGANS, T. & PFEFFER, K. 2005. The intriguing biology of the tumour necrosis factor/tumour necrosis factor receptor superfamily: players, rules and the games. *Immunology,* 115**,** 1-20.

HELLARD, D., BROSENITSCH, T., FRITZSCH, B. & KATZ, D. M. 2004. Cranial sensory neuron development in the absence of brain-derived neurotrophic factor in BDNF/Bax double null mice. *Dev Biol,* 275**,** 34-43.

HEUMANN, R., KORSCHING, S., SCOTT, J. & THOENEN, H. 1984. Relationship between levels of nerve growth factor (NGF) and its messenger RNA in sympathetic ganglia and peripheral target tissues. *EMBO J,* 3**,** 3183-9.

HIGUCHI, M., NAGASAWA, K., HORIUCHI, T., OIKE, M., ITO, Y., YASUKAWA, M. & NIHO, Y. 1997. Membrane tumor necrosis factor-alpha (TNF-alpha) expressed on HTLV-I-infected T cells mediates a costimulatory signal for B cell activation--characterization of membrane TNF-alpha. *Clin Immunol Immunopathol,* 82**,** 133-40.

HONMA, Y., ARAKI, T., GIANINO, S., BRUCE, A., HEUCKEROTH, R. O., JOHNSON JR, E. M. & MILBRANDT, J. 2002. Artemin Is a Vascular-Derived Neurotropic Factor for Developing Sympathetic Neurons. *Neuron,* 35**,** 267-282.

HORIUCHI, T., MITOMA, H., HARASHIMA, S., TSUKAMOTO, H. & SHIMODA, T. 2010. Transmembrane TNF-alpha: structure, function and interaction with anti-TNF agents. *Rheumatology (Oxford),* 49**,** 1215-28.

HOWARD, L., WYATT, S., NAGAPPAN, G. & DAVIES, A. M. 2013. ProNGF promotes neurite growth from a subset of NGF-dependent neurons by a p75NTR-dependent mechanism. *Development,* 140**,** 2108-17.

HOWARD, M. J. 2005. Mechanisms and perspectives on differentiation of autonomic neurons. *Dev Biol,* 277**,** 271-86.

HUANG, E. J. & REICHARDT, L. F. 2001. Neurotrophins: roles in neuronal development and function. *Annu Rev Neurosci,* 24**,** 677-736.

IFTINCA, M. C. 2011. Neuronal T-type calcium channels: what's new? Iftinca: T-type channel regulation. *J Med Life,* 4**,** 126-38.

IFTINCA, M. C. & ZAMPONI, G. W. 2009. Regulation of neuronal T-type calcium channels. *Trends Pharmacol Sci,* 30**,** 32-40.

JANIG, W. & MCLACHLAN, E. M. 1992. Characteristics of function-specific pathways in the sympathetic nervous system. *Trends Neurosci,* 15**,** 475-81.

JAVOIS, L. C. 1994. *Immunocytochemical Methods and Protocols*, Humana Press.

JOHNS, E. J., KOPP, U. C. & DIBONA, G. F. 2011. Neural control of renal function. *Compr Physiol,* 1**,** 731-67.

JOHNSON, E. M., JR., GORIN, P. D., BRANDEIS, L. D. & PEARSON, J. 1980. Dorsal root ganglion neurons are destroyed by exposure in utero to maternal antibody to nerve growth factor. *Science,* 210**,** 916-8.

JOHNSTON, M. V., RUTKOWSKI, J. L., WAINER, B. H., LONG, J. B. & MOBLEY, W. C. 1987. Ngf Effects on Developing Forebrain Cholinergic Neurons Are Regionally Specific. *Neurochemical Research,* 12**,** 985-994.

JONES, K. R., FARINAS, I., BACKUS, C. & REICHARDT, L. F. 1994. Targeted Disruption of the Bdnf Gene Perturbs Brain and Sensory Neuron Development but Not Motor-Neuron Development. *Cell,* 76**,** 989-999.

JUHASZ, K., BUZAS, K. & DUDA, E. 2013. Importance of reverse signaling of the TNF superfamily in immune regulation. *Expert Review of Clinical Immunology,* 9**,** 335-348.

KANDEL, E. R., SCHWARTZ, J. H. & JESSELL, T. M. 2000. *Principles of neural science,* New York, McGraw-Hill, Health Professions Division.

KAPLAN, D. R. & STEPHENS, R. M. 1994. Neurotrophin signal transduction by the Trk receptor. *J Neurobiol,* 25**,** 1404-17.

KAPPERS, J. A. 1960. The development, topographical relations and innervation of the epiphysis cerebri in the albino rat. *Z Zellforsch Mikrosk Anat,* 52**,** 163-215.

KAWASAKI, T., BEKKU, Y., SUTO, F., KITSUKAWA, T., TANIGUCHI, M., NAGATSU, I., NAGATSU, T., ITOH, K., YAGI, T. & FUJISAWA, H. 2002. Requirement of neuropilin 1-mediated Sema3A signals in patterning of the sympathetic nervous system. *Development,* 129**,** 671-80.

KIM, D., SONG, I., KEUM, S., LEE, T., JEONG, M. J., KIM, S. S., MCENERY, M. W. & SHIN, H. S. 2001. Lack of the burst firing of thalamocortical relay neurons and resistance to absence seizures in mice lacking alpha(1G) T-type Ca(2+) channels. *Neuron,* 31**,** 35-45.

KIMURA, K., IEDA, M. & FUKUDA, K. 2012. Development, maturation, and transdifferentiation of cardiac sympathetic nerves. *Circ Res,* 110**,** 325-36.

KIRCHNER, S., BOLDT, S., KOLCH, W., HAFFNER, S., KAZAK, S., JANOSCH, P., HOLLER, E., ANDREESEN, R. & EISSNER, G. 2004a. LPS resistance in monocytic cells caused by reverse signaling through transmembrane TNF (mTNF) is mediated by the MAPK/ERK pathway. *Journal of Leukocyte Biology,* 75**,** 324-331.

KIRCHNER, S., HOLLER, E., HAFFNER, S., ANDREESEN, R. & EISSNER, G. 2004b. Effect of different tumor necrosis factor (TNF) reactive agents on reverse signaling of membrane integrated TNF in monocytes. *Cytokine,* 28**,** 67-74.

KISISWA, L., OSORIO, C., ERICE, C., VIZARD, T., WYATT, S. & DAVIES, A. M. 2013. TNFalpha reverse signaling promotes sympathetic axon growth and target innervation. *Nat Neurosci,* 16**,** 865-73.

KLABUNDE, R. E. 2005. *Cardiovascular Pharmacology Concepts* [Online]. Available: http://www.cvpharmacology.com/autonomic_ganglia [Accessed 16.08.2015 2015].

KLEIN, R., LAMBALLE, F., BRYANT, S. & BARBACID, M. 1992. The trkB tyrosine protein kinase is a receptor for neurotrophin-4. *Neuron,* 8**,** 947-56.

KLEIN, R., SMEYNE, R. J., WURST, W., LONG, L. K., AUERBACH, B. A., JOYNER, A. L. & BARBACID, M. 1993. Targeted disruption of the trkB neurotrophin receptor gene results in nervous system lesions and neonatal death. *Cell,* 75**,** 113-22.

KNOLL, B., WEINL, C., NORDHEIM, A. & BONHOEFFER, F. 2007. Stripe assay to examine axonal guidance and cell migration. *Nature Protocols,* 2**,** 1216-1224.

KOLODKIN, A. L. & TESSIER-LAVIGNE, M. 2011. Mechanisms and molecules of neuronal wiring: a primer. *Cold Spring Harb Perspect Biol,* 3.

KORNER, H., COOK, M., RIMINTON, D. S., LEMCKERT, F. A., HOEK, R. M., LEDERMANN, B., KONTGEN, F., FAZEKAS DE ST GROTH, B. & SEDGWICK, J. D. 1997. Distinct roles for lymphotoxin-alpha and tumor necrosis factor in organogenesis and spatial organization of lymphoid tissue. *Eur J Immunol,* 27**,** 2600-9.

KORSCHING, S., AUBURGER, G., HEUMANN, R., SCOTT, J. & THOENEN, H. 1985. Levels of nerve growth factor and its mRNA in the central nervous system of the rat correlate with cholinergic innervation. *EMBO J,* 4**,** 1389-93.

KOTZBAUER, P. T., LAMPE, P. A., ESTUS, S., MILBRANDT, J. & JOHNSON JR, E. M. 1994. Postnatal development of survival responsiveness in rat sympathetic neurons to leukemia inhibitory factor and ciliary neurotrophic factor. *Neuron,* 12**,** 763-773.

KRAUS, R. L., LI, Y., GREGAN, Y., GOTTER, A. L., UEBELE, V. N., FOX, S. V., DORAN, S. M., BARROW, J. C., YANG, Z. Q., REGER, T. S., KOBLAN, K. S. & RENGER, J. J. 2010. In vitro characterization of T-type calcium channel antagonist TTA-A2 and in vivo effects on arousal in mice. *J Pharmacol Exp Ther,* 335**,** 409-17.

KUMMER, W., FISCHER, A., KURKOWSKI, R. & HEYM, C. 1992. The sensory and sympathetic innervation of guinea-pig lung and trachea as studied by retrograde neuronal tracing and double-labelling immunohistochemistry. *Neuroscience,* 49**,** 715-37.

KURUVILLA, R., ZWEIFEL, L. S., GLEBOVA, N. O., LONZE, B. E., VALDEZ, G., YE, H. & GINTY, D. D. 2004. A neurotrophin signaling cascade coordinates sympathetic neuron development through differential control of TrkA trafficking and retrograde signaling. *Cell,* 118**,** 243-55.

LAMBALLE, F., KLEIN, R. & BARBACID, M. 1991. trkC, a new member of the trk family of tyrosine protein kinases, is a receptor for neurotrophin-3. *Cell,* 66**,** 967-79.

LAMBERT, R., BESSAÏH, T., CRUNELLI, V. & LERESCHE, N. 2014. The many faces of T-type calcium channels. *Pflügers Archiv - European Journal of Physiology,* 466**,** 415-423.

LAMPE, R. A., DEFEO, P. A., DAVISON, M. D., YOUNG, J., HERMAN, J. L., SPREEN, R. C., HORN, M. B., MANGANO, T. J. & KEITH, R. A. 1993. Isolation and pharmacological characterization of omega-grammotoxin SIA, a novel peptide inhibitor of neuronal voltage-sensitive calcium channel responses. *Mol Pharmacol,* 44**,** 451-60.

LEE, J.-H., KIM, E.-G., PARK, B.-G., KIM, K.-H., CHA, S.-K., KONG, I. D., LEE, J.-W. & JEONG, S.-W. 2002. Identification of T-Type α1H Ca2+ Channels (Cav3.2) in Major Pelvic Ganglion Neurons. *Journal of Neurophysiology,* 87**,** 2844-2850.

LEE, S. E., LEE, J., LATCHOUMANE, C., LEE, B., OH, S.-J., SAUD, Z. A., PARK, C., SUN, N., CHEONG, E., CHEN, C.-C., CHOI, E.-J., LEE, C. J. & SHIN, H.-S. 2014. Rebound burst firing in the reticular thalamus is not essential for pharmacological absence seizures in mice. *Proceedings of the National Academy of Sciences,* 111**,** 11828-11833.

LEMASTER, A. M., KRIMM, R. F., DAVIS, B. M., NOEL, T., FORBES, M. E., JOHNSON, J. E. & ALBERS, K. M. 1999. Overexpression of brain-derived neurotrophic factor enhances sensory innervation and selectively increases neuron number. *Journal of Neuroscience,* 19**,** 5919-31.

LEVI-MONTALCINI, R. 1987. The nerve growth factor 35 years later. *Science,* 237**,** 1154-62.

LEVI-MONTALCINI, R. & ANGELETTI, P. U. 1968. Nerve growth factor. *Physiol Rev,* 48**,** 534-69.

LEWIN, G. R. & BARDE, Y. A. 1996. Physiology of the neurotrophins. *Annu Rev Neurosci,* 19**,** 289-317.

LINDSAY, R. M., BARDE, Y. A., DAVIES, A. M. & ROHRER, H. 1985. Differences and similarities in the neurotrophic growth factor requirements of sensory neurons derived from neural crest and neural placode. *J Cell Sci Suppl,* 3**,** 115-29.

LOWERY, L. A. & VAN VACTOR, D. 2009. The trip of the tip: understanding the growth cone machinery. *Nat Rev Mol Cell Biol,* 10**,** 332-43.

LUEBKE, J. I. & WRIGHT, L. L. 1992. Characterization of superior cervical ganglion neurons that project to the submandibular glands, the eyes, and the pineal gland in rats. *Brain Research,* 589**,** 1-14.

MADDEN, K. S., BELLINGER, D. L., FELTEN, S. Y., SNYDER, E., MAIDA, M. E. & FELTEN, D. L. 1997. Alterations in sympathetic innervation of thymus and spleen in aged mice. *Mech Ageing Dev,* 94**,** 165-75.

MAINA, F., HILTON, M. C., ANDRES, R., WYATT, S., KLEIN, R. & DAVIES, A. M. 1998. Multiple roles for hepatocyte growth factor in sympathetic neuron development. *Neuron,* 20**,** 835-46.

MAINA, F. & KLEIN, R. 1999. Hepatocyte growth factor, a versatile signal for developing neurons. *Nat Neurosci,* 2**,** 213-7.

MAKITA, T., SUCOV, H. M., GARIEPY, C. E., YANAGISAWA, M. & GINTY, D. D. 2008. Endothelins are vascular-derived axonal guidance cues for developing sympathetic neurons. *Nature,* 452**,** 759-763.

MARMIGERE, F. & ERNFORS, P. 2007. Specification and connectivity of neuronal subtypes in the sensory lineage. *Nat Rev Neurosci,* 8**,** 114-127.

MASSIE, B. M. 1997. Mibefradil: a selective T-type calcium antagonist. *Am J Cardiol,* 80**,** 23I-32I.

MCDONALD, N. Q., LAPATTO, R., MURRAYRUST, J., GUNNING, J., WLODAWER, A. & BLUNDELL, T. L. 1991. New-Protein Fold Revealed by a 2.3-a Resolution Crystal-Structure of Nerve Growth-Factor. *Nature,* 354**,** 411-414.

MCWILLIAMS, T. G., HOWARD, L., WYATT, S. & DAVIES, A. M. 2015. Regulation of Autocrine Signaling in Subsets of Sympathetic Neurons Has Regional Effects on Tissue Innervation. *Cell Reports,* 10**,** 1443-1449.

MEHRKE, G., ZONG, X. G., FLOCKERZI, V. & HOFMANN, F. 1994. The Ca++-Channel Blocker Ro-40-5967 Blocks Differently T-Type and L-Type Ca++ Channels. *Journal of Pharmacology and Experimental Therapeutics,* 271**,** 1483-1488.

MICROFLUIDICS, X. 2009. *About Xona Microfluidics* [Online]. Available: http://www.xonamicrofluidics.com/about.html [Accessed 24.04.15 2015].

MIDDLETON, G. & DAVIES, A. M. 2001. Populations of NGF-dependent neurones differ in their requirement for BAX to undergo apoptosis in the absence of NGF/TrkA signalling in vivo. *Development,* 128**,** 4715-28.

MOLLER, M. & BAERES, F. M. 2002. The anatomy and innervation of the mammalian pineal gland. *Cell Tissue Res,* 309**,** 139-50.

MOLLER, M., RAVAULT, J. P. & COZZI, B. 1996. The chemical neuroanatomy of the mammalian pineal gland: neuropeptides. *Neurochem Int,* 28**,** 23-33.

MOSS, M. L., JIN, S. L. C., MILLA, M. E., BURKHART, W., CARTER, H. L., CHEN, W.-J., CLAY, W. C., DIDSBURY, J. R., HASSLER, D., HOFFMAN, C. R., KOST, T. A., LAMBERT, M. H., LEESNITZER, M. A., MCCAULEY, P., MCGEEHAN, G., MITCHELL, J., MOYER, M., PAHEL, G., ROCQUE, W., OVERTON, L. K., SCHOENEN, F., SEATON, T., SU, J.-L., WARNER, J., WILLARD, D. & BECHERER, J. D. 1997. Cloning of a disintegrin metalloproteinase that processes precursor tumour-necrosis factor-[alpha]. *Nature,* 385**,** 733-736.

MOWLA, S. J., FARHADI, H. F., PAREEK, S., ATWAL, J. K., MORRIS, S. J., SEIDAH, N. G. & MURPHY, R. A. 2001. Biosynthesis and post-translational processing of the precursor to brain-derived neurotrophic factor. *J Biol Chem,* 276**,** 12660-6.

MYERS, D. G. 2013. *Psychology,* New York, Worth Publishers.

NANCE, D. M. & SANDERS, V. M. 2007. Autonomic innervation and regulation of the immune system (1987-2007). *Brain Behav Immun,* 21**,** 736-45.

NEUMANN, H., SCHWEIGREITER, R., YAMASHITA, T., ROSENKRANZ, K., WEKERLE, H. & BARDE, Y. A. 2002. Tumor necrosis factor inhibits neurite outgrowth and branching of hippocampal neurons by a rho-dependent mechanism. *Journal of Neuroscience,* 22**,** 854-62.

NEWCOMB, R., SZOKE, B., PALMA, A., WANG, G., CHEN, X., HOPKINS, W., CONG, R., MILLER, J., URGE, L., TARCZY-HORNOCH, K., LOO, J. A., DOOLEY, D. J., NADASDI, L., TSIEN, R. W., LEMOS, J. & MILJANICH, G. 1998. Selective peptide antagonist of the class E calcium channel from the venom of the tarantula Hysterocrates gigas. *Biochemistry,* 37**,** 15353-62.

NIKOLETOPOULOU, V., LICKERT, H., FRADE, J. M., RENCUREL, C., GIALLONARDO, P., ZHANG, L., BIBEL, M. & BARDE, Y. A. 2010. Neurotrophin receptors TrkA and TrkC cause neuronal death whereas TrkB does not. *Nature,* 467**,** 59-63.

NOLAN, A. M., COLLINS, L. M., WYATT, S. L., GUTIERREZ, H. & O'KEEFFE, G. W. 2014. The neurite growth inhibitory effects of soluble TNFα on developing sympathetic neurons are dependent on developmental age. *Differentiation,* 88**,** 124-130.

O'KEEFFE, G. W., GUTIERREZ, H., PANDOLFI, P. P., RICCARDI, C. & DAVIES, A. M. 2008. NGF-promoted axon growth and target innervation requires GITRL-GITR signaling. *Nat Neurosci,* 11**,** 135-42.

OPPENHEIM, R. W. 1991. Cell death during development of the nervous system. *Annu Rev Neurosci,* 14**,** 453-501.

OSORIO, C., CHACON, P. J., WHITE, M., KISISWA, L., WYATT, S., RODRIGUEZ-TEBAR, A. & DAVIES, A. M. 2014. Selective regulation of axonal growth from developing hippocampal neurons by tumor necrosis factor superfamily member APRIL. *Mol Cell Neurosci,* 59**,** 24-36.

OSTERRIEDER, W. & HOLCK, M. 1989. In vitro pharmacologic profile of Ro 40-5967, a novel Ca2+ channel blocker with potent vasodilator but weak inotropic action. *J Cardiovasc Pharmacol,* 13**,** 754-9.

PACHNIS, V., MANKOO, B. & COSTANTINI, F. 1993. Expression of the c-ret proto-oncogene during mouse embryogenesis. *Development,* 119**,** 1005-17.

PACK, R. J., AL-UGAILY, L. H. & WIDDICOMBE, J. G. 1984. The innervation of the trachea and extrapulmonary bronchi of the mouse. *Cell Tissue Res,* 238**,** 61-8.

PARDINI, B. J., LUND, D. D. & SCHMID, P. G. 1989. Organization of the sympathetic postganglionic innervation of the rat heart. *J Auton Nerv Syst,* 28**,** 193-201.

PARK, K. M. & BOWERS, W. J. 2010. Tumor necrosis factor-alpha mediated signaling in neuronal homeostasis and dysfunction. *Cell Signal,* 22**,** 977-83.

PASPARAKIS, M., ALEXOPOULOU, L., EPISKOPOU, V. & KOLLIAS, G. 1996. Immune and inflammatory responses in TNF alpha-deficient mice: a critical requirement for TNF alpha in the formation of primary B cell follicles, follicular dendritic cell networks and germinal centers, and in the maturation of the humoral immune response. *J Exp Med,* 184**,** 1397-411.

PATEL, T. D., JACKMAN, A., RICE, F. L., KUCERA, J. & SNIDER, W. D. 2000. Development of sensory neurons in the absence of NGF/TrkA signaling in vivo. *Neuron,* 25**,** 345-57.

PEREZ-REYES, E. 2003. Molecular physiology of low-voltage-activated t-type calcium channels. *Physiol Rev,* 83**,** 117-61.

PESCHON, J. J., TORRANCE, D. S., STOCKING, K. L., GLACCUM, M. B., OTTEN, C., WILLIS, C. R., CHARRIER, K., MORRISSEY, P. J., WARE, C. B. & MOHLER, K. M. 1998. TNF receptor-deficient mice reveal divergent roles for p55 and p75 in several models of inflammation. *J Immunol,* 160**,** 943-52.

PUIMEGE, L., LIBERT, C. & VAN HAUWERMEIREN, F. 2014. Regulation and dysregulation of tumor necrosis factor receptor-1. *Cytokine Growth Factor Rev*.

PURVES, D. 2008. *Neuroscience,* Sunderland, Mass., Sinauer.

PURVES, D., SNIDER, W. D. & VOYVODIC, J. T. 1988. Trophic regulation of nerve cell morphology and innervation in the autonomic nervous system. *Nature,* 336**,** 123-8.

QUINSON, N., ROBBINS, H. L., CLARK, M. J. & FURNESS, J. B. 2001. Locations and innervation of cell bodies of sympathetic neurons projecting to the gastrointestinal tract in the rat. *Arch Histol Cytol,* 64**,** 281-94.

REICHARDT, L. F. 2006. Neurotrophin-regulated signalling pathways. *Philos Trans R Soc Lond B Biol Sci,* 361**,** 1545-64.

REISSMANN, E., ERNSBERGER, U., FRANCIS-WEST, P. H., RUEGER, D., BRICKELL, P. M. & ROHRER, H. 1996. Involvement of bone morphogenetic protein-4 and bone morphogenetic protein-7 in the differentiation of the adrenergic phenotype in developing sympathetic neurons. *Development,* 122**,** 2079-88.

RINGSTEDT, T., KUCERA, J., LENDAHL, U., ERNFORS, P. & IBANEZ, C. F. 1997. Limb proprioceptive deficits without neuronal loss in transgenic mice overexpressing neurotrophin-3 in the developing nervous system. *Development,* 124**,** 2603-13.

RODRIGUEZ-TEBAR, A., DECHANT, G. & BARDE, Y.-A. 1990. Binding of brain-derived neurotrophic factor to the nerve growth factor receptor. *Neuron,* 4**,** 487-492.

ROHRER, H. 2011. Transcriptional control of differentiation and neurogenesis in autonomic ganglia. *Eur J Neurosci,* 34**,** 1563-73.

RONN, L. C., RALETS, I., HARTZ, B. P., BECH, M., BEREZIN, A., BEREZIN, V., MOLLER, A. & BOCK, E. 2000. A simple procedure for quantification of neurite outgrowth based on stereological principles. *J Neurosci Methods,* 100**,** 25-32.

ROTHE, J., LESSLAUER, W., LOTSCHER, H., LANG, Y., KOEBEL, P., KONTGEN, F., ALTHAGE, A., ZINKERNAGEL, R., STEINMETZ, M. & BLUETHMANN, H. 1993. Mice lacking the tumour necrosis factor receptor 1 are resistant to TNF-mediated toxicity but highly susceptible to infection by Listeria monocytogenes. *Nature,* 364**,** 798-802.

RUBIN, E. 1985. Development of the rat superior cervical ganglion: ganglion cell maturation. *J Neurosci,* 5**,** 673-84.

RUULS, S. R., HOEK, R. M., NGO, V. N., MCNEIL, T., LUCIAN, L. A., JANATPOUR, M. J., KÖRNER, H., SCHEERENS, H., HESSEL, E. M., CYSTER, J. G., MCEVOY, L. M. & SEDGWICK, J. D. 2001. Membrane-Bound TNF Supports Secondary Lymphoid Organ Structure but Is Subservient to Secreted TNF in Driving Autoimmune Inflammation. *Immunity,* 15**,** 533-543.

SCARISBRICK, I. A., JONES, E. G. & ISACKSON, P. J. 1993. Coexpression of mRNAs for NGF, BDNF, and NT-3 in the cardiovascular system of the pre- and postnatal rat. *J Neurosci,* 13**,** 875-93.

SEIDAH, N. G., BENJANNET, S., PAREEK, S., SAVARIA, D., HAMELIN, J., GOULET, B., LALIBERTE, J., LAZURE, C., CHRETIEN, M. & MURPHY, R. A. 1996. Cellular processing of the nerve growth factor precursor by the mammalian pro-protein convertases. *Biochem J,* 314 (Pt 3)**,** 951-60.

SEJNOWSKI, T. J. 1982. Peptidergic synaptic transmission in sympathetic ganglia. *Fed Proc,* 41**,** 2923-8.

SHAH, N. M., GROVES, A. K. & ANDERSON, D. J. 1996. Alternative Neural Crest Cell Fates Are Instructively Promoted by TGFβ Superfamily Members. *Cell,* 85**,** 331-343.

SHIELDS, R. W., JR. 1993. Functional anatomy of the autonomic nervous system. *J Clin Neurophysiol,* 10**,** 2-13.

SHOLL, D. A. 1953. Dendritic organization in the neurons of the visual and motor cortices of the cat. *J Anat,* 87**,** 387-406.

SIMOES-COSTA, M. & BRONNER, M. E. 2015. Establishing neural crest identity: a gene regulatory recipe. *Development,* 142**,** 242-57.

SITE, SWENSON, R., CATLIN, B., LYONS, J. & MEDICAL, D. 2008. *Chapter 27: The esophagus, stomach and intestines* [Online]. Available: https://www.dartmouth.edu/~humananatomy/part_5/chapter_27.html.

SKAPER, S. D. 2012. The neurotrophin family of neurotrophic factors: an overview. *Methods Mol Biol,* 846**,** 1-12.

SMEYNE, R. J., KLEIN, R., SCHNAPP, A., LONG, L. K., BRYANT, S., LEWIN, A., LIRA, S. A. & BARBACID, M. 1994. Severe sensory and sympathetic neuropathies in mice carrying a disrupted Trk/NGF receptor gene. *Nature,* 368**,** 246-9.

SMITH, C. A., FARRAH, T. & GOODWIN, R. G. 1994. The TNF receptor superfamily of cellular and viral proteins: activation, costimulation, and death. *Cell,* 76**,** 959-62.

SMITH, R. V. & SATCHELL, D. G. 1985. Extrinsic pathways of the adrenergic innervation of the guinea-pig trachealis muscle. *J Auton Nerv Syst,* 14**,** 61-73.

SMITH, R. V. & SATCHELL, D. G. 1986. Determination of extrinsic pathways of adrenergic nerves to the guinea-pig trachealis muscle using surgical denervation and organ-bath pharmacology. *Agents Actions,* 19**,** 48-54.

SOPPET, D., ESCANDON, E., MARAGOS, J., MIDDLEMAS, D. S., REID, S. W., BLAIR, J., BURTON, L. E., STANTON, B. R., KAPLAN, D. R., HUNTER, T., NIKOLICS, K. & PARADA, L. F. 1991. The neurotrophic factors brain-derived neurotrophic factor and neurotrophin-3 are ligands for the trkB tyrosine kinase receptor. *Cell,* 65**,** 895-903.

SOUTHARD-SMITH, E. M., KOS, L. & PAVAN, W. J. 1998. Sox10 mutation disrupts neural crest development in Dom Hirschsprung mouse model. *Nat Genet,* 18**,** 60-4.

SQUINTO, S. P., STITT, T. N., ALDRICH, T. H., DAVIS, S., BIANCO, S. M., RADZIEJEWSKI, C., GLASS, D. J., MASIAKOWSKI, P., FURTH, M. E., VALENZUELA, D. M. & ET AL. 1991. trkB encodes a functional receptor for brain-derived neurotrophic factor and neurotrophin-3 but not nerve growth factor. *Cell,* 65**,** 885-93.

SUN, M. & FINK, P. J. 2007. A new class of reverse signaling costimulators belongs to the TNF family. *J Immunol,* 179**,** 4307-12.

SZURSZEWSKI, J. H. 1981. Physiology of mammalian prevertebral ganglia. *Annu Rev Physiol,* 43**,** 53-68.

TAIT, S. W. G. & GREEN, D. R. 2010. Mitochondria and cell death: outer membrane permeabilization and beyond. *Nat Rev Mol Cell Biol,* 11**,** 621-632.

TAKAI, Y., KISHIMOTO, A., IWASA, Y., KAWAHARA, Y., MORI, T. & NISHIZUKA, Y. 1979. Calcium-dependent activation of a multifunctional protein kinase by membrane phospholipids. *Journal of Biological Chemistry,* 254**,** 3692-3695.

TAKEI, Y. & LASKEY, R. 2008. Tumor necrosis factor alpha regulates responses to nerve growth factor, promoting neural cell survival but suppressing differentiation of neuroblastoma cells. *Mol Biol Cell,* 19**,** 855-64.

TAKEUCHI, K., PARK, E., LEE, C., KIM, J., TAKAHASHI, H., SWARTZ, K. & SHIMADA, I. 2002. Solution structure of omega-grammotoxin SIA, a gating modifier of P/Q and N-type Ca(2+) channel. *J Mol Biol,* 321**,** 517-26.

TANSEY, M. G. & SZYMKOWSKI, D. E. 2009. The TNF superfamily in 2009: new pathways, new indications, and new drugs. *Drug Discov Today,* 14**,** 1082-8.

TEJERINA, T., CHULIA, T. & GONZALEZ, P. 1993. Effects of dotarizine on 45Ca2+ movements and contractile responses in vascular smooth muscle. *Eur J Pharmacol,* 239**,** 75-81.

TENG, K. K., FELICE, S., KIM, T. & HEMPSTEAD, B. L. 2010. Understanding proneurotrophin actions: Recent advances and challenges. *Dev Neurobiol,* 70**,** 350-9.

TERAMOTO, T., KUWADA, M., NIIDOME, T., SAWADA, K., NISHIZAWA, Y. & KATAYAMA, K. 1993. A Novel Peptide from Funnel-Web Spider Venom, Omega-Aga-Tk, Selectively Blocks P-Type Calcium Channels. *Biochemical and Biophysical Research Communications,* 196**,** 134-140.

TESSAROLLO, L. 1998. Pleiotropic functions of neurotrophins in development. *Cytokine Growth Factor Rev,* 9**,** 125-37.

THOENEN, H. 2000. Neurotrophins and activity-dependent plasticity. *Prog Brain Res,* 128**,** 183-91.

THOENEN, H. & BARDE, Y. A. 1980. Physiology of nerve growth factor. *Physiol Rev,* 60**,** 1284-335.

THOMPSON, J., DOLCET, X., HILTON, M., TOLCOS, M. & DAVIES, A. M. 2004. HGF promotes survival and growth of maturing sympathetic neurons by PI-3 kinase- and MAP kinase-dependent mechanisms. *Mol Cell Neurosci,* 27**,** 441-52.

TIVERON, M. C., HIRSCH, M. R. & BRUNET, J. F. 1996. The expression pattern of the transcription factor Phox2 delineates synaptic pathways of the autonomic nervous system. *J Neurosci,* 16**,** 7649-60.

TRUDRUNG, P., FURNESS, J. B., POMPOLO, S. & MESSENGER, J. P. 1994. Locations and chemistries of sympathetic nerve cells that project to the gastrointestinal tract and spleen. *Arch Histol Cytol,* 57**,** 139-50.

TWOHIG, J. P., CUFF, S. M., YONG, A. A. & WANG, E. C. 2011. The role of tumor necrosis factor receptor superfamily members in mammalian brain development, function and homeostasis. *Rev Neurosci,* 22**,** 509-33.

ULTSCH, M. H., WIESMANN, C., SIMMONS, L. C., HENRICH, J., YANG, M., REILLY, D., BASS, S. H. & DE VOS, A. M. 1999. Crystal structures of the neurotrophin-binding domain of TrkA, TrkB and TrkC1. *Journal of Molecular Biology,* 290**,** 149-159.

VATER, W., SCHLOSSM.K, STOEPEL, K., HOFFMEIS.F, KRONEBER.G, PULS, W., KALLER, H., OBERDORF, A. & MENG, K. 1972. Pharmacology of 4-(2'-Nitrophenyl)-2,6-Dimethyl-3,5-Dicarbomethoxy-1,4-Dihydropyridine(Nifedipine, Bay a 1040). *Arzneimittel-Forschung,* 22**,** 1-&.

VAUX, D. L. & KORSMEYER, S. J. 1999. Cell death in development. *Cell,* 96**,** 245-54.

VILLARROYA, M., GANDIA, L., LARA, B., ALBILLOS, A., LOPEZ, M. G. & GARCIA, A. G. 1995. Dotarizine Versus Flunarizine as Calcium-Antagonists in Chromaffin Cells. *British Journal of Pharmacology,* 114**,** 369-376.

VIZARD, T. N., O'KEEFFE, G. W., GUTIERREZ, H., KOS, C. H., RICCARDI, D. & DAVIES, A. M. 2008. Regulation of axonal and dendritic growth by the extracellular calcium-sensing receptor. *Nat Neurosci,* 11**,** 285-91.

VOGEL, K. S. & DAVIES, A. M. 1991. The Duration of Neurotrophic Factor Independence in Early Sensory Neurons Is Matched to the Time Course of Target Field Innervation. *Neuron,* 7**,** 819-830.

VUDATTU, N. K., HOLLER, E., EWING, P., SCHULZ, U., HAFFNER, S., BURGER, V., KIRCHNER, S., ANDREESEN, R. & EISSNER, G. 2005. Reverse signalling of membrane-integrated

tumour necrosis factor differentially regulates alloresponses of CD4+ and CD8+ T cells against human microvascular endothelial cells. *Immunology,* 115**,** 536-43.

WAETZIG, G. H., ROSENSTIEL, P., ARLT, A., TILL, A., BRAUTIGAM, K., SCHAFER, H., ROSE-JOHN, S., SEEGERT, D. & SCHREIBER, S. 2005. Soluble tumor necrosis factor (TNF) receptor-1 induces apoptosis via reverse TNF signaling and autocrine transforming growth factor-beta1. *FASEB J,* 19**,** 91-3.

WATTS, A. D., HUNT, N. H., WANIGASEKARA, Y., BLOOMFIELD, G., WALLACH, D., ROUFOGALIS, B. D. & CHAUDHRI, G. 1999. A casein kinase I motif present in the cytoplasmic domain of members of the tumour necrosis factor ligand family is implicated in 'reverse signalling'. *EMBO J,* 18**,** 2119-26.

WESTPHAL, H. & THEILER, K. 2014. *The House Mouse: Atlas of Embryonic Development*, Springer Berlin Heidelberg.

WHEELER, M. A., HEFFNER, D. L., KIM, S., ESPY, S. M., SPANO, A. J., CLELAND, C. L. & DEPPMANN, C. D. 2014. TNF-alpha/TNFR1 signaling is required for the development and function of primary nociceptors. *Neuron,* 82**,** 587-602.

WHITE, F. A., KELLER-PECK, C. R., KNUDSON, C. M., KORSMEYER, S. J. & SNIDER, W. D. 1998. Widespread elimination of naturally occurring neuronal death in Bax-deficient mice. *J Neurosci,* 18**,** 1428-39.

WIESMANN, C., ULTSCH, M. H., BASS, S. H. & DE VOS, A. M. 1999. Crystal structure of nerve growth factor in complex with the ligand-binding domain of the TrkA receptor. *Nature,* 401**,** 184-188.

WRIGHT, L. L. & LUEBKE, J. I. 1989. Somatostatin-, vasoactive intestinal polypeptide- and neuropeptide Y-like immunoreactivity in eye- and submandibular gland-projecting sympathetic neurons. *Brain Research,* 494**,** 267-275.

WYATT, S. & DAVIES, A. M. 1995. Regulation of nerve growth factor receptor gene expression in sympathetic neurons during development. *The Journal of Cell Biology,* 130**,** 1435-1446.

WYATT, S., PINON, L. G., ERNFORS, P. & DAVIES, A. M. 1997. Sympathetic neuron survival and TrkA expression in NT3-deficient mouse embryos. *EMBO J,* 16**,** 3115-23.

XIN, L., WANG, J., ZHANG, H., SHI, W., YU, M., LI, Q., JIANG, X., GONG, F., GARDNER, K., LI, Q. Q. & LI, Z. 2006. Dual regulation of soluble tumor necrosis factor-alpha induced activation of human monocytic cells via modulating transmembrane TNF-alpha-mediated 'reverse signaling'. *Int J Mol Med,* 18**,** 885-92.

YAN, H., NEWGREEN, D. F. & YOUNG, H. M. 2003. Developmental changes in neurite outgrowth responses of dorsal root and sympathetic ganglia to GDNF, neurturin, and artemin. *Developmental Dynamics,* 227**,** 395-401.

YANG, L., LINDHOLM, K., KONISHI, Y., LI, R. & SHEN, Y. 2002. Target depletion of distinct tumor necrosis factor receptor subtypes reveals hippocampal neuron death and survival through different signal transduction pathways. *J Neurosci,* 22**,** 3025-32.

YANG, Y.-T. T., WHITEMAN, M. & GIESEG, S. P. 2012. HOCl causes necrotic cell death in human monocyte derived macrophages through calcium dependent calpain activation. *Biochimica et Biophysica Acta (BBA) - Molecular Cell Research,* 1823**,** 420-429.

YE, H., KURUVILLA, R., ZWEIFEL, L. S. & GINTY, D. D. 2003. Evidence in Support of Signaling Endosome-Based Retrograde Survival of Sympathetic Neurons. *Neuron,* 39**,** 57-68.

YU, M., SHI, W., ZHANG, J., NIU, L., CHEN, Q., YAN, D., LIU, T., JING, W., JIANG, X., WEI, F., YIN, B., ZHANG, W., LI, Q. & LI, Z. 2009. Influence of reverse signaling via membrane TNF-alpha on cytotoxicity of NK92 cells. *Eur J Cell Biol,* 88**,** 181-91.

YUAN, J. & YANKNER, B. A. 2000. Apoptosis in the nervous system. *Nature,* 407**,** 802-9.

ZHANG, Y., JIANG, X., SNUTCH, T. P. & TAO, J. 2013. Modulation of low-voltage-activated T-type Ca2 + channels. *Biochimica et Biophysica Acta (BBA) - Biomembranes,* 1828**,** 1550-1559.

ZHAO, L., CHEN, J., LIU, L., GAO, J., GUO, B. & ZHU, B. 2015. Essential role of TNF-alpha in development of spleen fibroblastic reticular cells. *Cell Immunol,* 293**,** 130-6.

ZHU, Y., ZBORAN, E. L. & IKEDA, S. R. 1995. Phenotype-specific expression of T-type calcium channels in neurons of the major pelvic ganglion of the adult male rat. *J Physiol,* 489 (Pt 2)**,** 363-75.

ZIGMOND, M. J. 1999. *Fundamental neuroscience,* San Diego, Academic Press.

ZULIANI, C., KLEBER, S., KLUSSMANN, S., WENGER, T., KENZELMANN, M., SCHREGLMANN, N., MARTINEZ, A., DEL RIO, J. A., SORIANO, E., VODRAZKA, P., KUNER, R., GROENE, H. J., HERR, I., KRAMMER, P. H. & MARTIN-VILLALBA, A. 2006. Control of neuronal branching by the death receptor CD95 (Fas/Apo-1). *Cell Death Differ,* 13**,** 31-40.

ZWEIFEL, L. S., KURUVILLA, R. & GINTY, D. D. 2005. Functions and mechanisms of retrograde neurotrophin signalling. *Nat Rev Neurosci,* 6**,** 615-625.

Appendices

APPENDIX I

PCR protocols:

Tnfα

Primers:

Tnfα common foward: 5'- CTC TTC TGT CTA CTG AAC -3'

Tnfα WT reverse: 5'- TTT ATC TCT TGC TTA TCC -3'

Tnfα KO reverse: 5'- TTC TAT CGC CTT CTT GAC -3'

Estimated band size: WT=320 bp

KO=398 bp

PCR reaction (Paq5000 Hotstart DNA Polymerase, Agilent Technologies):

Buffer 10x 2.5 µl

dNTPs 0.2 µl

Tnfα common foward 0.5 µl

Tnfα WT reverse 1 µl

Tnfα KO reverse 0.25 µl

Paq5000 enzyme 0.4 µl

Nuclease free water 18.15 µl

Reaction mix: 2 µl of DNA + 23 µl of PCR mix

PCR Program:

Step 1: 95˚C 2 min

Step 2: 95˚C 30 sec

Step 3: 50˚C 30 sec

Step 4: 72˚C 30 sec

Step 5: 72˚C 3min

Cycle 2 to 4: 40x

Tnfrsf1a

Primers:

Tnfrs1a common foward: 5'- GGC TGC AGT CCA CGC ACT GG -3'

Tnfrs1a WT reverse: 5'- TGT GAA AAG GGC ACC TTT ACG GC -3'

Tnfrs1a KO reverse: 5'- ATT CGC CAA TGA CAA TGA CAA GAC GCT GG -3'

Estimated band size: WT=470 bp

KO=300 bp

PCR reaction (Paq5000 Hotstart DNA Polymerase, Agilent Technologies):

Buffer 10x 2.5 µl

dNTPs 0.25 µl

Tnfα common foward 0.6 µl

Tnfα WT reverse 0.6 µl

Tnfα KO reverse 0.6 µl

Paq5000 enzyme 0.25 µl

Nuclease free water 18.2 µl

Reaction mix: 2 µl of DNA + 23 µl of PCR mix

PCR Program:

Step 1: 95˚C 2 min

Step 2: 95˚C 30 sec

Step 3: 58˚C 1 min

Step 4: 72˚C 1 min

Step 5: 72˚C 3min

Cycle 2 to 4: 40x

mTNF

Primers:

mTNF foward: 5'- GTC TGT CTT AAC TAA CCT -3'

mTNF reverse: 5'- GTA TGA GAT AGC AAA TCG -3'

Estimated band size: WT=814 bp

mutant=920 bp

PCR reaction (Paq5000 Hotstart DNA Polymerase, Agilent Technologies):

Buffer 10x 2.5 µl

dNTPs 0.25 µl

mTNF foward 0.75 µl

mTNF reverse 0.75 µl

Paq5000 enzyme 0.25 µl

Nuclease free water 18.5 µl

Reaction mix: 2 µl of DNA + 23 µl of PCR mix

PCR Program:

Step 1: 95˚C 2 min

Step 2: 95˚C 30 sec

Step 3: 58˚C 30 sec

Step 4: 72˚C 1 min

Step 5: 72˚C 3min

Cycle 2 to 4: 38x

APPENDIX II

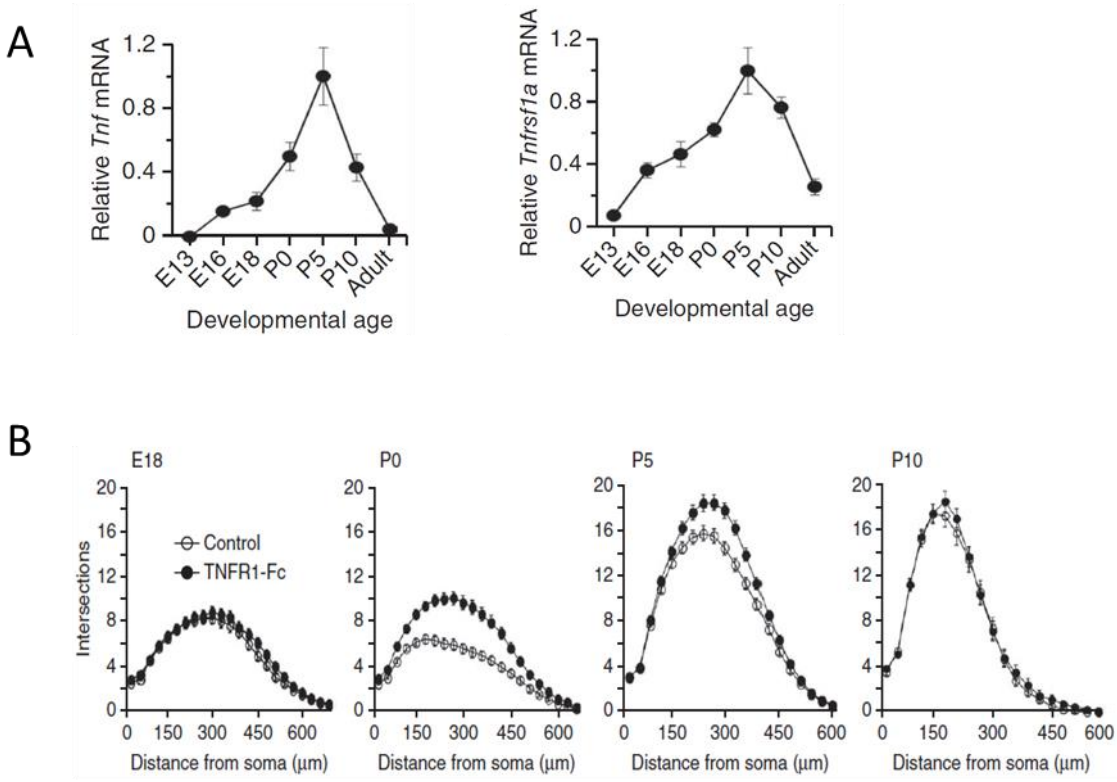

Figure 1: A) Expression of *Tnfα* and *Tnfsr1a* mRNA in the SCG at different developmental time points. mRNA amounts relative to the geometric mean of reference mRNAs for glyceraldehyde phosphate dehydrogenase and succinate dehydrogenase in SCG at indicated ages. Data are normalized to 1.0 at the peak of expression of *Tnfα* and *Tnfrsf1a* mRNAs at P5 (mean ± s.e.m. of data from three separate sets of ganglia at each age). **B) TNF mediated reverse signalling in the SCG at different developmental ages.** Sholl plots of the neurite arbors of E18, P0, P5 and P10 SCG neurons cultured for 24 h with 10 ng ml–1 TNFR1-Fc or without it (control) in presence of 10 ng ml–1 NGF. * All images and figure legends extracted from (Kisiswa et al., 2013).

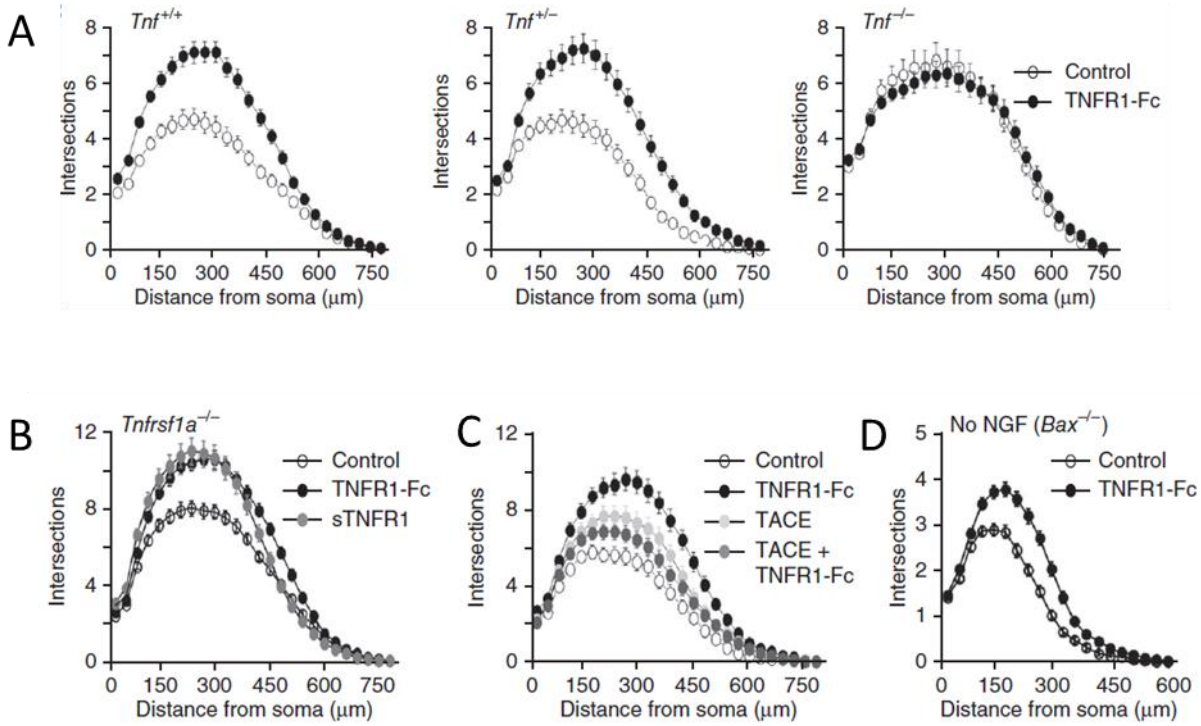

Figure 2: A) TNF reverse signalling in TNF KO mice. Sholl plots of neurons from P0 *Tnfα*$^{+/+}$, *Tnfα*$^{+/–}$ and *Tnfα*$^{–/–}$ littermates cultured for 24 h with NGF alone (control, *n* = 150) or NGF plus TNFR1-Fc (*n* = 150). **B) TNF reverse signalling in TNFR1 KO mice.** Sholl plots of neurons from *Tnfrsf1*a$^{–/–}$ mice grown for 24 h with either NGF alone (control, n = 150) or NGF plus TNFR1-Fc (n = 150) or NGF plus sTNFR1 (n = 150). **C) TNF reverse signalling in the presence of TACE.** Sholl plots of neurons of P0 CD1+ wild-type mice cultured for 24 h with either NGF alone (control, n = 234) or NGF plus TNFR1-Fc (n = 243), 200 ng ml–1 TACE (n = 247) and TNFR1-Fc plus TACE (n = 248). **D) TNF reverse signalling withought NGF.** Sholl plots of the neurite arbors of neurons from Bax$^{–/–}$ mice grown for 24 h in the presence (n = 174) or absence (n = 196) of TNFR1-Fc in medium lacking NGF. Mean ± s.e.m. of data from three experiments. * All images and figure legends extracted from (Kisiswa et al., 2013).

APPENDIX III

A

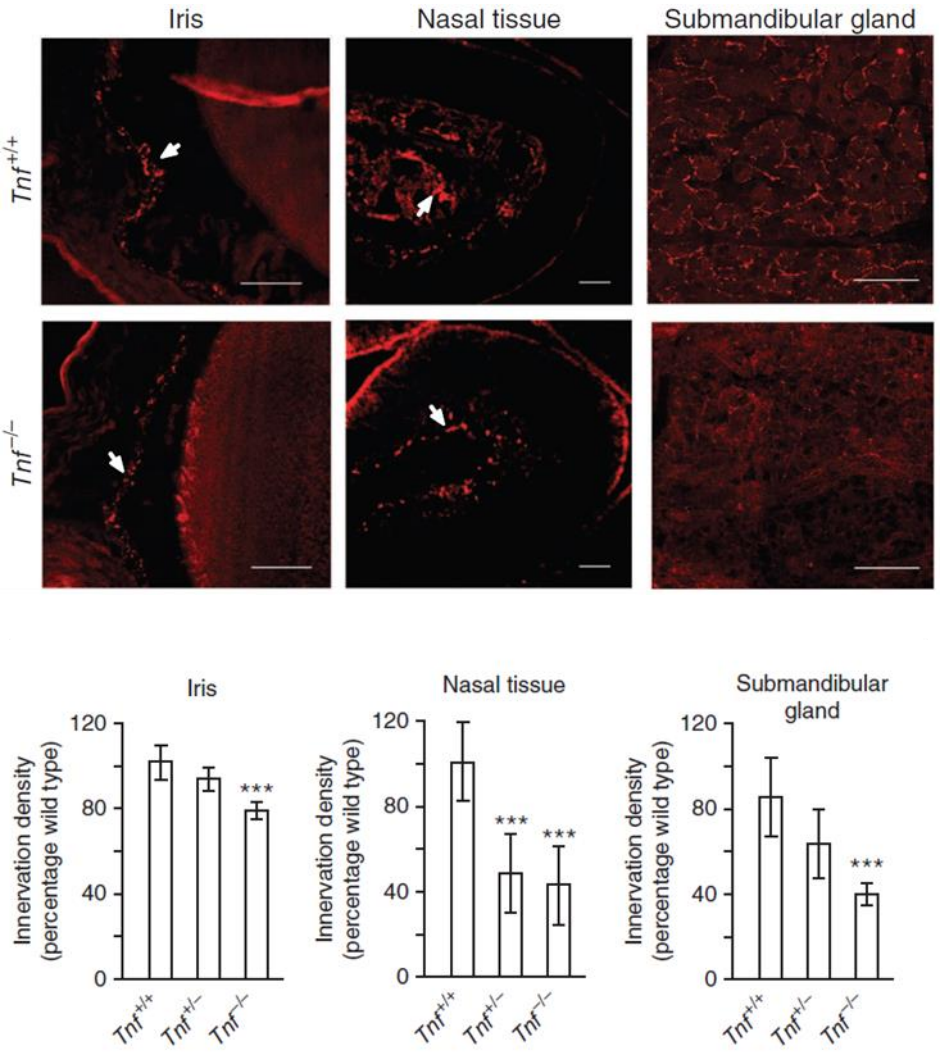

B

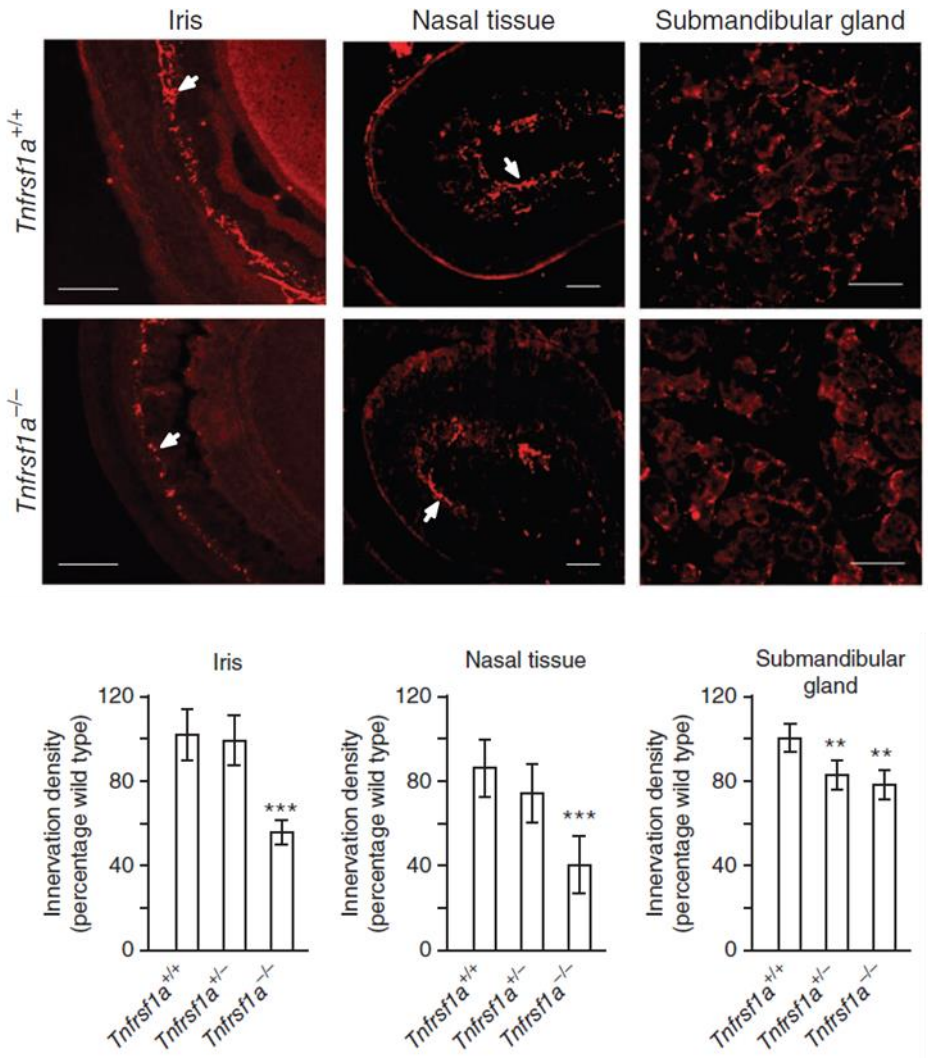

Figure 1, legend on following page.

Figure 1: Sympathetic innervation densities of SCG target organs from *Tnfα* and *Tnfrs1a* deficient mice calculated by TH immunofluorescence intensity. A) Representative micrographs of sections of the iris, nasal turbinate tissue and submandibular gland parenchyma of P10 *Tnfα*$^{+/+}$ and *Tnfα*$^{-/-}$ mice labeled with anti–tyrosine hydroxylase (TH) (images were selected from 78 *Tnfα*$^{+/+}$ and 124 *Tnf–/–* iris images, 59 *Tnfα*$^{+/+}$ and 75 *Tnfα*$^{-/-}$ nasal turbinate tissue images and 135 *Tnfα*$^{+/+}$ and 86 *Tnfα*$^{-/-}$ submandibular gland images). Arrows indicate the major location of TH-positive fibers: in the part of the section passing through the iris and the central core of connective tissue of a nasal turbinate where blood vessels and sympathetic fibers are concentrated. Scale bars, 100 µm. Graphs show relative TH immunofluorescence in the iris, nasal turbinate tissue and submandibular gland of P10 *Tnfα*$^{+/+}$, *Tnfα*$^{+/-}$ and *Tnfα*$^{-/-}$ mice expressed as a percentage of the mean immunofluorescence in *Tnfα*$^{+/+}$ mice. **B)** Representative micrographs of sections of the iris, nasal turbinate tissue and submandibular gland parenchyma of P10 *Tnfrsf1a*$^{+/+}$ and *Tnfrsf1a*$^{-/-}$ mice labeled with anti-tyrosine hydroxylase (images were selected from 453 *Tnfrsf1a*$^{+/+}$ and 324 *Tnfrsf1a*$^{-/-}$ iris images, 73 *Tnfrsf1a*$^{+/+}$ and 71 *Tnfrsf1a*$^{-/-}$ nasal turbinate tissue images and 141 *Tnfrsf1a*$^{+/+}$ and 122 *Tnfrsf1a*$^{-/-}$ submandibular gland images). Scale bars, 100 µm. Graphs show relative tyrosine hydroxylase immunofluorescence in the iris, nasal turbinate tissue and submandibular gland of P10 *Tnfrsf1a*$^{+/+}$, *Tnfrsf1a*$^{+/-}$ and *Tnfrsf1a*$^{-/-}$ mice expressed as a percentage of the mean immunofluorescence in P10 *Tnfrsf1a*$^{+/+}$ mice. Mean ± s.e.m. of data from 5 *Tnfα*$^{+/+}$mice, 6 *Tnfα*$^{+/-}$ mice, 7 *Tnfα*$^{-/-}$ mice, 7 *Tnfrsf1a*$^{+/+}$ mice, 6 *Tnfrsf1a*$^{+/-}$ mice and 6 *Tnfrsf1a*$^{-/-}$ mice (**P < 0.01 and ***P < 0.001 compared to control, Fisher's *post hoc* test).*All images and figure legends extracted from (Kisiswa et al., 2013).

APPENDIX IV

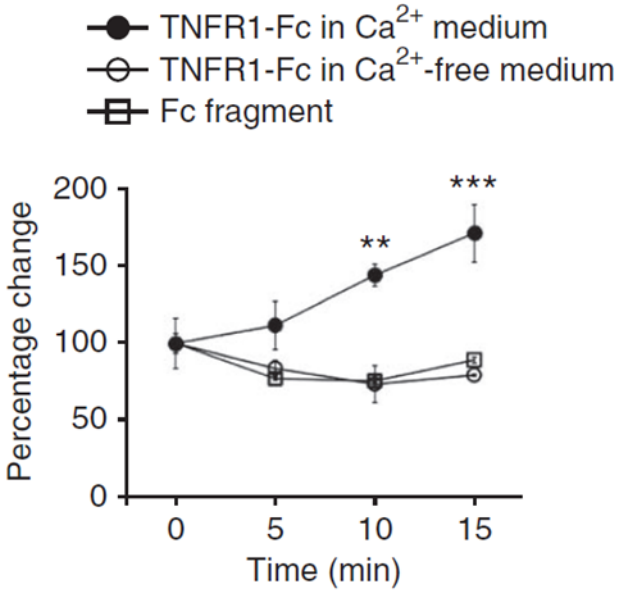

Figure 1: TNFR1-Fc causes influx of intracellular Ca^{2+}. Change in cytosolic free-Ca2+ after addition of either Fc fragment or TNFR1-Fc in either Ca2+-free medium or medium containing 1.2 mM Ca2+ (mean ± s.e.m. of three experiments, >20 neurons imaged per condition per experiment). * All images and figure legends extracted from (Kisiswa et al., 2013).

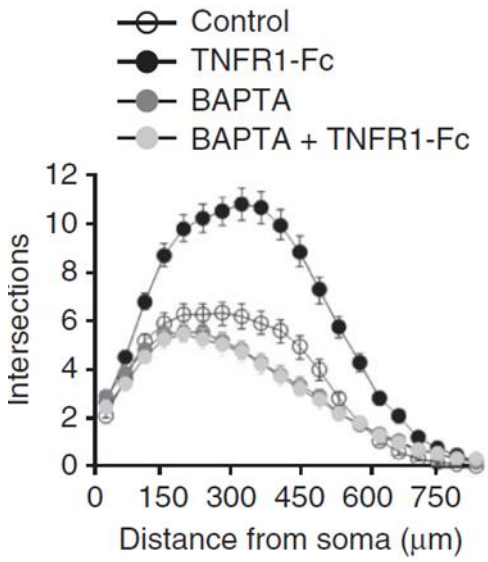

Figure 2: Bapta inhibits the growth promoting effects of TNFR1-Fc. Sholl profiles of P0 SCG neurons cultured for 24 h with either NGF (control) or NGF plus 1 µM BAPTA-AM, TNFR1-Fc or BAPTA-AM plus TNFR1-Fc (mean ± s.e.m., >150 neurons per condition from three independent experiments). * All images and figure legends extracted from (Kisiswa et al., 2013).